A Biorefinery Approach to Short Chain Olefins from Plant Oils by a Multicatalytic Sequence Comprising Olefin Metathesis

Dissertation zur Erlangung des

akademischen Grades eines

Doktors der Naturwissenschaften (Dr. rer. nat.)

vorgelegt von

Stefanie de Roo

an der

Mathematische-Naturwissenschaftliche Sektion

Fachbereich Chemie

Konstanz, 2023

Tag der mündlichen Prüfung: 21.07.2023

1. Referent/Referentin: Prof. Dr. Stefan Mecking

2. Referent/Referentin: Prof. Dr. Peter Kroth

Die vorliegende Dissertation entstand in der Zeit von Dezember 2018 bis Oktober 2022 unter der Leitung von Herrn Prof. Dr. Stefan Mecking am Fachbereich Chemie der Universität Konstanz.

DANKSAGUNG / ACKNOWLEDGEMENT

Mein größter Dank gilt Prof. Dr. Stefan Mecking für die Aufnahme in seine Arbeitsgruppe und die hervorragende Betreuung dieser Arbeit. Danke für das Anvertrauen dieses spannenden und vielseitigen Themas und für das stetige Interesse an meiner Arbeit.

Ich danke Prof. Dr. Peter Kroth für die Übernahme des Zweitgutachtens sowie Prof. Dr. Alexander Wittemann für die Übernahme des Prüfungsvorsitzes.

Der Arbeitsgruppe Kroth möchte ich für die Hilfsbereitschaft und das Bereitstellen von Materialen für die Algenkultivierung bedanken. Des Weiteren möchte ich mich bei Natalie Schunck bedanken, welche mir die praktische Kultivierung und Ernte von Mikroalgen nähergebracht hat.

Bei Natalie möchte ich mich auch für die vielen hilfreichen Diskussionen zum Thema „Renewables“ bedanken wie auch für die stetige Hilfsbereitschaft und ihr offenes Ohr bei jeglichen Problemen.

Ganz besonders möchte ich Felix Einsiedler für die enge Zusammenarbeit im Rahmen dieses Projekts danken, vor allem für die amüsante Zeit im Labor, viele wertvolle Diskussionen und die ???-Sessions.

Danke auch an meine Mitarbeiterpraktikanten, HiWis und Masterstudenten für ihre Mitarbeit auf diesem Thema, ihr Engagement und die konstruktiven Diskussionen: Felix Schoder, Levin Elser, Denis Corales und Lara Holderied.

Ich danke auch unserem Mädels Büro für die super entspannte Atmosphäre, die unterhaltsamen Schwätzchen und Kaffeepausen in der Sonne. Danke Anne, Natalie und Nina.

Für das Ermöglichen eines reibungslosen Laboralltags gilt ein dickes Dankeschön Robin Kirsten, Dr. Inigo Göttker-Schnetmann und Lars Bolk. Gisela Berner danke ich auch für die Hilfe bei der Bewältigung verschiedenster administrativer Hürden.

Allen ehemaligen und aktuellen Mitgliedern der AG Mecking danke ich für die tolle Arbeitsatmosphäre, die Zusammenarbeit und die lustige Zeit.

Des Weiteren bedanke ich mich bei allen die diese Arbeit oder Teile davon Korrektur gelesen haben: Felix Einsiedler, Natalie Schunck und Dr. Tjaard de Roo.

Ein Dank geht auch an die KoRS-CB für die lehrreichen Weiterbildungen, Workshops und Retreats.

Meinen Freunden aus Konstanz danke ich für die schöne Zeit während des gesamten Studiums und der Promotion. Danke Lisa und Steffi für die Kochabende und die entspannte Zeit am See. Bei Larissa möchte ich mich für die zahlreichen Rückenmassagen bedanken, die mich nach einem schlechten Tag gerettet haben.

Meiner Familie danke ich für die jahrelange Unterstützung und Zuspruch während der gesamten Zeit an der Uni. Besonders möchte ich mich auch bei Tjaard bedanken, der mir während meiner gesamten Promotion den Rücken gestärkt hat und immer für mich da ist. Zuletzt danke ich unserer Tochter Janna die mir den Endspurt mit ihrem Lächeln versüßt hat.

PUBLICATIONS & COMMUNICATIONS

Journal Publications

- Witt, T.; Häußler, M.; Kulpa, S.; Mecking, S., Chain Multiplication of Fatty Acids to Precise Telechelic Polyethylene. *Angew. Chem. Int. Ed.* **2017,** *56* (26), 7589-7594.

Publications related to this work

- de Roo, S., Einsiedler, F., Mecking, S., Catalytic Biorefining of Natural Oils to Basic Olefinic Building Blocks of Proven Chemical Valorization Schemes *Angew. Chem. Int. Ed.* **2023**, 62, e202219222.

Poster Presentations

- Kulpa, S.; Schunck, N.; Mecking S.
  at the 10th Workshop on Fats and Oils as Renewable Feedstock for the Chemical Industry, Karlsruhe, Germany, March 2019.
  "Immobilized Olefin Metathesis Catalysts for the Conversion of renewable Raw Materials"
- Kulpa, S.; Zimmerer, J.; Kroth, P.; Mecking S.
  at the ISOM23 - International Symposium on Olefin Metathesis and Related Chemistry, Barcelona, Spain, July 2019.
  "Immobilized Olefin Metathesis Catalysts for the Conversion of renewable Raw Materials"

- Kulpa, S.; Mecking S.
  at the KoRS-CB Retreat, Gülstein, Germany, August 2019.
  "Immobilized Olefin Metathesis Catalysts for the Conversion of renewable Raw Materials"

- De Roo, S.; Einsiedler, F.; Mecking S.
  at the KoRS-CB Retreat, Gülstein, Germany, August 2021.
  Biorefining of Microalgae Lipids to Industrial Key Chemicals by Integration of Extraction and Tandem Catalysis

ZUSAMMENFASSUNG / ABSTRACT

Der weltweite Bedarf an erdölbasierenden Produkten wie Spezialchemikalien und Polymeren hat in den letzten Jahrzehnten stetig zugenommen. Erneuerbare Rohstoffe erlangten dadurch als Alternative zu Erdöl an Bedeutung. Besonders die in vielen nachwachsenden Rohstoffen enthaltenen ungesättigten Fettsäuren eignen sich wegen ihres chemischen Aufbaus aus langen Kohlenwasserstoffketten, Carboxylgruppen und mindestens einer Doppelbindung für eine katalytische Aufwertung zu industriell relevanten Intermediaten. Nutzpflanzen wie Sonnenblumen, Soja und Raps spielen als Lipidquelle für erneuerbare Chemikalien eine große Rolle, da diese bereits etablierte Kultivierungs- und Extraktionsmethoden aufweisen. Besonders interessant ist auch die Verwendung von Mikroalgen als erneuerbarer Rohstoff, welche gegenüber den traditionellen Lipidquellen Vorteile aufweisen. Sie können sowohl in Salz- als auch in Brackwasser kultiviert werden, weshalb keine großen landwirtschaftlichen Nutzflächen benötigt werden und die Kultivierung somit nicht mit der Lebensmittelindustrie konkurriert. Des Weiteren weisen sie hohe Wachstumsraten auf und erreichen Ölanteile von bis zu 70 % des Trockengewichts.

Bisher lag der Fokus der Forschung auf der Umwandlung von Pflanzen- und Algenölen zu Biodiesel. Dieses Konzept der Defunktionalisierung der Fettsäuren zu Kohlenwasserstoffen schöpft allerdings nicht das ganze Potential der einzigartigen Strukturen der Fettsäuren aus, weshalb eine katalytische Aufwertung zu relevanten Intermediaten wünschenswert ist. Während sich die Umsetzung von nachwachsenden Rohstoffen zu Aromaten bereits in einem fortgeschrittenen Entwicklungsstand befindet, stellt die direkte Umwandlung zu industriell relevanten olefinischen Produkten noch eine Herausforderung dar. Insbesondere kurzkettige lineare α-Olefine sind von Interesse, da sie vielgefragte chemische Grundbausteine für die Synthese von Waschmitteln, Weichmachern, Schmiermitteln als auch von verschiedenen Polymeren darstellen. Deren industrielle Produktion wird mittels des erdölbasierenden „Shell Higher Olefin Process“ ermöglicht und weist eine jährliche Produktionskapazität von über einer Millionen Tonnen auf. In Hinblick auf ein erdölunabhängiges Verfahren, ist die Entwicklung einer alternativen Syntheseroute für α-Olefine, welche auf erneuerbaren Rohstoffen basiert, von großem Interesse.

Im Rahmen dieser Arbeit wird ein neuartiges Bioraffinerie Konzept vorgestellt, welches erneuerbare Pflanzen- und Mikrolagenöle zu kurzkettigen α - Olefinen als auch zu terminal ungesättigten Estern (C_3 bis C_{10}) umwandelt. Dies wurde in $scCO_2$ als umweltfreundliches Medium mittels einer katalytischen Reaktionssequenz aus Ethenolyse – Doppelbindungsisomerisierung – Ethenolyse bewerkstelligt und sowohl in einer halbkontinuierlichen Betriebsweise als auch im Fließbetrieb untersucht.

Da eine ausreichende Löslichkeit von Fettsäuren in $scCO_2$ nur bei hohen CO_2 Dichten und damit hohen Drücken gegeben ist, wurde für die Umsetzung des halbkontinuierlichen Prozesses mit homogenen Katalysatoren eine hierfür konstruierte Hochdruck-Anlage verwendet (Abbildung 1).

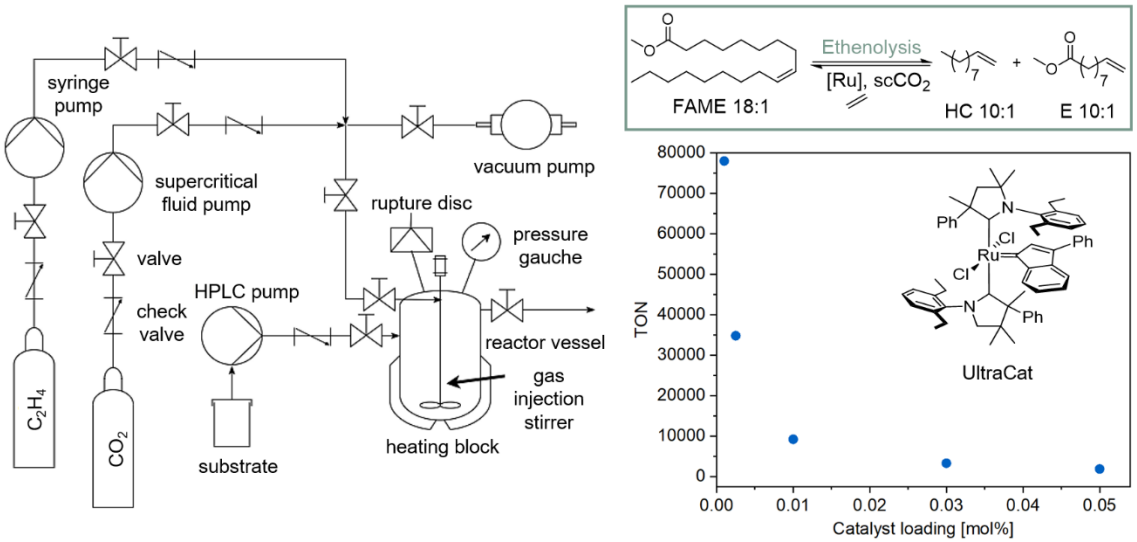

Abbildung 1. Ethenolyse von verestertem Sonnenblumenöl mit hohem Methyloleat-Gehalt (HOSO) in überkritischen CO_2 unter Verwendung von UC in einer halbkontinuierlichen Reaktoranlage.

Durch die kontrollierte Zugabe von Katalysator-Lösungen und Additiven unter CO_2-Druck wurde die gewünschte katalytische Reaktionssequenz in einer Eintopfreaktion ermöglicht. Diese Arbeit fokussiert sich auf die Analyse und Optimierung der Ethenolyse-Reaktionen des Bioraffinerie-Ansatzes. Erste Untersuchungen wurden daher in einer separaten Ethenolyse-Reaktion in $scCO_2$ von verestertem Sonnenblumenöl mit hohem Methyloleat-Gehalt (HOSO, FAME 18:1) als Modelsubstrat durchgeführt. Dabei zeigte sich durch das Testen verschiedener Katalysatoren, dass der Ruthenium-basierte Metathese-Katalysator „UltraCat“ (UC) bei einer Katalysatorbeladung von 10 ppm mit einer Umsatzzahl von 78 000 bemerkenswert hohe Aktivitäten wie auch Selektivitäten von über 97 % in der Ethenolyse aufweist. Dies deutete auf eine gute Löslichkeit des UC Katalysators in überkritischem CO_2 hin.

In weiteren Untersuchungen wurde deutlich, dass sowohl der Palladium-basierte Isomerisierungskatalysator als auch das für dessen Aktivierung benötigte Methanol einen negativen Einfluss auf die Ethenolyse-Aktivität hat. Dennoch konnten durch die Verwendung von minimal benötigten Methanol Mengen als auch durch Erhöhung der Katalysatorbeladung des UC, hohe Umsätze und Selektivitäten über 90 % erzielt werden. Damit wurde die Eignung des UC Katalysators für den Einsatz im Rahmen des Bioraffinerie-Konzepts nachgewiesen.

Basierend auf den Ergebnissen der einzelnen Ethenolyse Experimente wurde die Umsetzung von verestertem HOSO mit Hilfe des neuen Tandem-Verfahrens analysiert. Unter optimierten Bedingungen konnte eine erfolgreiche Umwandlung der Fettsäuren zu gewünschten kurzkettigen α-Olefinen und ungesättigten Estern erzielt werden. Hierbei wurden hohe Umsätze und Selektivitäten über 90 % in beiden Ethenolyse Schritten erzielt als auch eine Isomerisierung der primären Ethenolyse Produkte bis nahe dem Gleichgewicht (*Abbildung 2*).

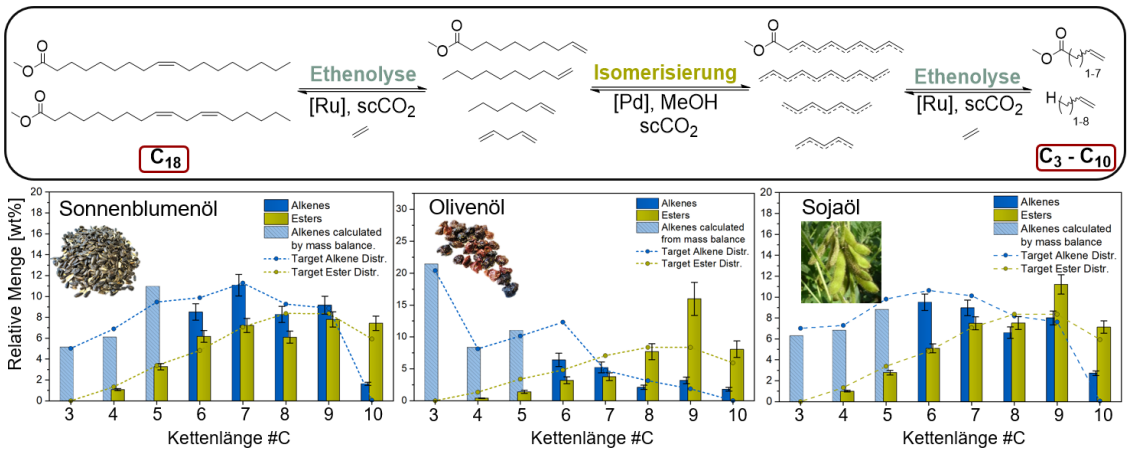

Substrate	1. Ethenolyse			2. Ethenolyse			
	Umsatz [%]		Selektivität [%]	Umsatz [%]		Selektivität für Produkte <C_{10} [%]	Selektivität für terminale Produkte [%]
Sonnenblumenöl	FAME 18:1	97	97	HC 10:1 E 10:1	96 91	97	92
Olivenöl	FAME 18:1/2/3	96	99	HC 10:1 E 10:1	86 83	97	95
Sojaöl	FAME 18:1/2/3	98	99	HC 10:1 E 10:1	90 85	97	97

Abbildung 2. Konzept und Ergebnisse des katalytischen Bioraffinerie-Ansatzes für verschiedene erneuerbare Öle.

Dies spiegelt sich in der erhaltenen Produktverteilung wider, welche vergleichbar mit einer theoretisch berechneten Verteilung ist. Bemerkenswert sind vor allem die hohen erzielten Selektivitäten für Produkte mit Kettenlängen <C_{10} von über 97 % als auch für terminale Produkte von bis zu 92 %. Hervorzuheben ist, dass die Verwendung von

$scCO_2$ im Vergleich zu organischen Lösungsmitteln wie MeOH eine Erhöhung der Selektivität für terminale Produkte aufweist, da eine simultane isomerisierende Ethenolyse in $scCO_2$ stärker unterdrückt wird. Dies stellt im Hinblick auf dieses Verfahren ein Schlüsselfaktor für den Erhalt von industriell relevanten α -Olefinen dar.

Des Weiteren zeigte die Anwendung des Konzepts auf andere Pflanzenöle mit höheren Anteilen an mehrfachungesättigten Fettsäuren, wie Olivenöl und Sojaöl, deren erfolgreiche katalytische Umwandlung zu den gewünschten Produkten. Dabei wurden hohe Selektivitäten für terminale Produkte der Kettenlängen C_3 bis C_{10} von über 95 % erhalten. Allerdings wurde auch eine leichte Verschiebung der Produktverteilung zu höheren Kettenlängen als Folge einer Verlangsamung der Doppelbindungsisomerisierung beobachtet. Grund hierfür sind die in großen Anteilen enthaltenen mehrfachungesättigten Fettsäuren, welche durch Koordination an den Isomerisierungs-Katalysator die Doppelbindungsisomerisierung behindern können.

Außerdem wurde die Robustheit des Verfahrens gegenüber Verunreinigungen durch die Verwendung von Altöl analysiert, indem HOSO mehrfach für das Frittieren von Pommes verwendet und anschließend im katalytischen Bioraffinerieprozess umgesetzt wurde. Neben einer leicht verringerten Aktivität in der Ethenolyse, welche vermutlich auf die Anwesenheit von Verunreinigungen zurückzuführen ist, wurde dennoch die zu erwartende Produktverteilung mit hohen Selektivitäten für die gewünschten terminalen Produkte von 94 % erzielt.

Das Bioraffinerie Verfahren wurde auch erfolgreich auf Öle angewendet, welche direkt aus den jeweiligen Lipidquellen (Sonnenblumenkerne, Oliven) mittels $scCO_2$ extrahiert wurden. Die erhaltenen Ergebnisse sind vergleichbar zu denen der kommerziell erhältlichen Öle. Die Verwendung von $scCO_2$ als Extraktionsmedium bietet den Vorteil einer hohen Lipidselektivität des Extrakts und ermöglicht dessen katalytische Umsetzung ohne aufwendige Aufarbeitung. Dies ist im Besonderen relevant für Mikroalgenbiomasse, da spezielle Mikrolagenöle mit hohen Anteilen an ungesättigten Fettsäuren nur schwer kommerziell zugänglich sind. Für die Aufwertung von Mikrolagenöl wurde die einzellige Kieselalge *Phaeodactylum tricornutum* als Lipidquelle verwendet, da diese eine hohe Robustheit als auch hohe Anteile an ungesättigten Fettsäuren aufweist. Das mittels überkritischem CO_2 extrahierte Mikroalgenöl wies vergleichbare Fettsäurezusammensetzungen zu

Literaturwerten auf. Auch hier konnte das veresterte Mikroalgenöl in der konsekutiven Ethenolyse und Isomerisierung mit hohen Selektivitäten von über 90 % zu den gewünschten terminalen Produkten umgesetzt werden (*Abbildung 3*).

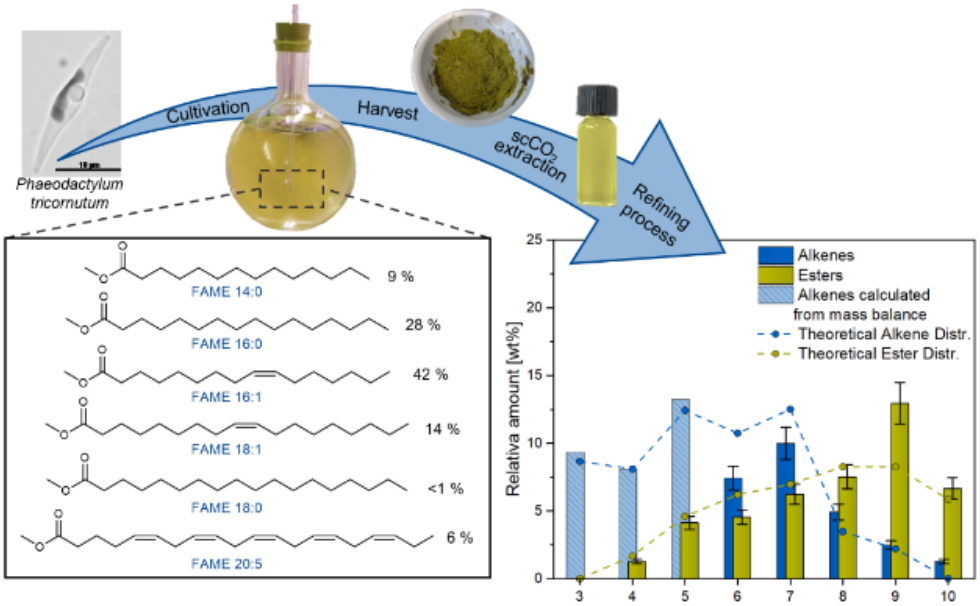

Abbildung 3. Aufwertung von Mikroalgen-Biomasse mittels überkritischer CO_2-Extraktion und des katalytischen Bioraffinerie Verfahrens.[146]

Dabei weisen die verwendeten Katalysatoren eine gute Kompatibilität mit dem Mehrstoffgemisch auf, welches neben Fettsäuren auch andere organische Strukturen wie Pigmente enthält. Die Anwendung des neuen Bioraffinerie Ansatzes auf verschiedene erneuerbare Pflanzen- und Mikroalgenöle konnte somit eindrücklich veranschaulicht werden.

Anschließend sollte das Bioraffinerie Konzept in einem kontinuierlichen Fließbetrieb untersucht werden. Dies stellt für eine industrielle Anwendung eine kosteneffizientere Methode gegenüber der chargenweisen Produktion dar. Geträgerte homogene Katalysatoren ermöglichen die Realisierung einer solchen Fließreaktion und bringen weitere Vorteile mit sich wie die simple Abtrennung der Produktmischung vom Katalysator als auch dessen Recycling. Im Rahmen dieser Arbeit wurde ein literaturbekannter immobilisierter Hoveyda-Grubbs Katalysator verwendet, welcher mittels eines Triethoxysilan-Linkers kovalent an Silikamaterialien angebunden ist.

Dessen Aktivität und Stabilität wurde zunächst in der Selbstmetathese von Methyloleat unter Fließbetrieb untersucht. Dabei zeigte sich eine gute Stabilität und hohe Aktivität des Katalysators in Ethylacetat mit konstanten Gleichgewichtsumsätzen von 50 % über einen Zeitraum von bis zu 10 h (*Abbildung 4*).

Dies wurde auch im umweltfreundlichen Medium überkritischem Kohlenstoffdioxid beobachtet. Die mittels induktiv gekoppelter Plasma-Emissionsspektroskopie (ICP-OES) analysierten Produkt-Mischungen wiesen außerdem in beiden Medien nur geringe Mengen an Ruthenium auf, was auf eine stabile kovalente Anbindung des Katalysators an das Trägermaterial hindeutet. Damit konnte die Eignung des verwendeten immobilisierten Metathese Katalysators für die Selbstmetathese unter kontinuierlichem Fließbetrieb verdeutlicht werden.

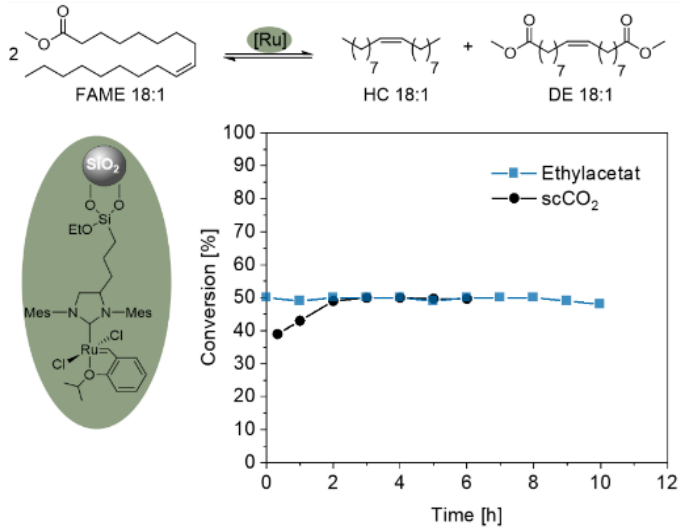

Abbildung 4. Selbst-Metathese von Methyloleat im kontinuierlichen Fließbetrieb in Ethylacetat und überkritischem CO_2 als Reaktionsmedium

In der kontinuierlichen Ethenolyse wurden unter optimierten Bedingungen maximale Umsätze von 80 % und Selektivitäten für Ethenolyse Produkte von 80 % erreicht. Im Vergleich zur Selbstmetathese wies der Katalysator jedoch eine verringerte Stabilität auf, welche vermutlich auf Katalysatordeaktivierug zurückzuführen ist. Dies ist ein bekanntes Problem bei der Kreuzmetathese mit Ethen, da hierbei instabile Ruthenium-Methylidene-Spezies entstehen, welche unerwünschte Nebenreaktionen eingehen können.

Dieses Verhalten wurde auch im sequenziellen Verfahren von Ethenolyse-Isomerisierung-Ethenolyse im kontinuierlichen Fließbetrieb beobachtet, weshalb die erwünschte Produktverteilung nur teilweise erzielt werden konnte. Hierbei wurden hauptsächlich die primären Ethenolyse und Selbstmetathese Produkte gebildet als auch Produkte längerer Ketten von bis zu C_{27}. Um ein robusteres Verfahren zu erzielen könnte die Verwendung von Ruthenium-Katalysatoren mit stabileren zyklischen amino-alkyl (CAAC)- Liganden von Vorteil sein. Diese weisen wie im

halbkontinuierlichen Chargenbetreib zu beobachten war höhere Aktivitäten in Anwesenheit von Ethen auf. Allerdings stellt dessen Synthese für eine mögliche kovalente Anbindung an Silikamaterialien noch eine große Herausforderung und wurde bisher noch nicht publiziert.

TABLE OF CONTENTS

DANKSAGUNG / ACKNOWLEDGEMENT I

PUBLICATIONS & COMMUNICATIONS III

ZUSAMMENFASSUNG / ABSTRACT IV

TABLE OF CONTENTS XI

I ANNOTATIONS XV

1 GENERAL INTRODUCTION 1

1.1 Lipids as Renewable Feedstock 2

1.1.1 Plant oils 3

1.1.2 Microalgae oil 6

1.2 Olefin Metathesis by Molecular Catalysts 11

1.2.1 Homogeneous Olefin Metathesis Catalysts 13

1.2.2 Combination of Olefin Metathesis and Double Bond Isomerization 17

1.2.3 Immobilized Olefin Metathesis Catalysts 21

1.3 Supercritical Carbon Dioxide 28

1.3.1 Supercritical Carbon Dioxide as Extraction Medium of Renewable Lipids 29

1.3.2 Supercritical Carbon Dioxide as Reaction Medium for Olefin Metathesis 31

2 SCOPE OF THE THESIS 34

3 BATCH SOLUTION PROCESS FOR COMBINED ETHENOLYSIS AND ISOMERIZATION 36

3.1 Introduction 36

3.2 Results and Discussion 39

3.2.1 Construction of the Reactor Set-up 39

3.2.2 Ethenolysis of Transesterified Sunflower Oil in $scCO_2$ 43

3.2.3 Impact of Alcohols and Ethylene Pressures on the Catalyst Performance in $scCO_2$ 48

3.2.4 Influence of ethylene pressures on the ethenolysis performance 50
3.2.5 Catalyst-Catalyst interactions 51
3.2.6 Multicatalytic Sequential Conversion of Renewable Oils 55
3.2.7 Extraction and catalysis of renewable feedstocks 74
3.3 Conclusion 83
3.4 Experimental Section 87
3.4.1 Nuclear Magnetic Resonance – NMR 87
3.4.2 Gas Chromatography – GC 87
3.4.3 General Considerations 89
3.4.4 High Pressure Equipment 89
3.4.5 Cultivation and Harvesting of Microalgae 90
3.4.6 Extraction of Lipids 91
3.4.7 General Procedure for Ethenolysis in $scCO_2$ 92
3.4.8 General Procedure for Isomerizing Ethenolysis in $scCO_2$ 92
3.4.9 General Procedure for the Multicatalytic Sequential Catalysis of Ethenolysis - Isomerization - Ethenolysis in $scCO_2$ 93
3.4.10 General Procedure for Frying of Potato Chips 93
4 FLOW SYSTEM FOR CONSECUTIVE ETHENOLYSIS AND ISOMERIZATION 94
4.1 Introduction 94
4.2 Results and Discussion 96
4.2.1 Synthesis of the Immobilized Olefin Metathesis Catalyst 96
4.2.2 Continuous Flow Self-metathesis of Methyl Oleate in Organic Solvents 98
4.2.3 Continuous Flow Self-metathesis of Methyl Oleate in $scCO_2$ 106
4.2.4 Continuous Flow Ethenolysis of Methyl Oleate 110
4.2.5 Sequential Conversion of Methyl Oleate under Continuous Flow Mode 120
4.3 Conclusion 126
4.4 Materials and Methods 129

4.4.1 Nuclear Magnetic Resonance – NMR 129
4.4.2 Gas Chromatography – GC 130
4.4.3 High Pressure Equipment 130
4.4.4 Synthesis of Triethoxysilyl-Functionalized Catalyst 20 131
4.4.5 Synthesis of N^1,N^2-Dimesitylethane-1,2-diimine (3) 131
4.4.6 Synthesis of N^1,N^2-Dimesitylpentene-1,2-diamine (4) 131
4.4.7 Synthesis of 4-allyl-1,3-Dimesityldihydroimidazolium chloride (5) 132
4.4.8 Synthesis of 1,3–Dimesityl-4-(3-triethoxysilyl)propyl)-dihydro-imida- zolium chloride (6) 133
4.4.9 Synthesis of [$RuCl_2$ (1,3-dimesityl-4-(3-triethoxy silyl) propyl)-dihydro-imidazol-2-ylidene) (=CH–*o*-^{i}PrO–Ph)] (8) 134
4.4.10 Synthesis of Hybrid Silica Material HGII-SiO_2 135
4.4.11 Continuous flow self-metathesis in organic solvents 136
4.4.12 Continuous flow self-metathesis in $scCO_2$ 136
4.4.13 Continuous flow Ethenolysis in $scCO_2$ 136
4.4.14 Split test 137
4.4.15 Multicatalytic Sequential Continuous flow Process in CO_2 137
5 CONCLUSIVE SUMMARY 138
6 APPENDIX 145
7 REFERENCES 152

I ANNOTATIONS

Abbreviations

Abbreviations of the 'International System of Units' (SI-Units), chemical formulas, and abbreviations of chemical groups (Me, Et, etc.) according to the IUPAC (International Union of Pure and Applied Chemistry) nomenclature are not listed.

Equipment and Methods

GC	Gas chromatography
ICP-OES	Inductively coupled plasma optical emission spectroscopy
NMR	Nuclear magnetic resonance

NMR Spectroscopy

δ	Chemical shift in ppm
d	Doublet
dd	Doublet of doublets
hept	Heptet/septet
$^{n}J_{XY}$	Coupling constant of atom X and Y over n bonds
m	Multiplet
ppm	Parts per million
q	Quartet
quin	Quintet
s	Singlet
t	Triplet

Compounds

$CHCl_3$	Chloroform
CO_2	Carbon dioxide
DCM	dichloromethane
dtbpx	1,2-bis{(di-*tert*-butylphosphino)methyl}benzene
DE 18:1	Dimethyl 9-octadecenedioate
EtOH	Ethanol
E 4:1	Methyl 3-butenoate
E 5 :1	Methyl 4-pentenoate
E 6:1	Methyl 5-hexenoate
E 7:1	Methyl 6-heptenoate
E 8:1	Methyl 7-octenoate
E 9:1	Methyl 8-nonenoate
E 10:1	Methyl 9-decenoate
FAME 14:0	Myristic acid methyl ester
FAME 16:0	Palmitic acid methyl ester
FAME 16:1	Palmitoleic acid methyl ester
FAME 18:0	Stearic acid methyl ester
FAME 18:1	Oleic acid methyl ester
FAME 18:2	Methyl linoleate
FAME 18:3	Methyl linolenate
FAME 20:5	Eicosapentaenoic acid methyl ester
HC 3:1	Propylene
HC4:1	1-Butene
HC5:1	2-Pentene
HC5:2	1,4-Pentadiene
HC 6:1	1-Hexene
HC7:1	1-Hepten
HC 8:1	1-Octene

HC 9:1	2-Nonene
HC 10:1	1-Decene
HC 18:1	9-Octadecene
HGI	Hoveyda Grubbs 1st generation catalyst
HGII	Hoveyda Grubbs 2nd generation catalyst
HUC	Hoveyda type UltraCat
HOSO	High oleic sunflower oil
MO	Methyl oleate
MeOH	Methanol
$scCO_2$	Supercritical carbon dioxide
TfOH	Trifluoromethanesulfonic acid
TsOH	p-Toluenesulfonic acid
UC	UltraCat

Other Abbreviations

a.u.	Arbitrary unit
cat.	Catalyst(s)
CAAC	Cyclic alkyl amino carbene
conv.	Conversion
EPDM	Ethylene-propylene-diene-rubber
equiv.	Equivalent(s)
FID	Flame ionization detector
h	Hour(s)
HPLC	High performance liquid chromatography
IS	Internal standard
min	Minute(s)
pdb	Per double bond
PTFE	Polytetrafluorethylen
rt	Room temperature

selec.	Selectivity
SFE	Supercritical fluid extraction
TON	Turnover number = (mol of products) · (mol of catalyst precursor)$^{-1}$
vs	Versus
wt%	Percentage by weight

1 General Introduction

The use of renewable resources is one of the cornerstones of green chemistry as they serve as promising alternative to fossil feedstocks. Alongside this benefit, the unique molecular structures and functional groups found in renewable sugars, lipids or proteins, offer access to new types of intermediates and materials with different or even superior properties compared to traditional fossil feedstock-based products. Fats and oils of vegetable are to date one of the most important renewable feedstocks of the chemical industry which is why this work is focused on lipids as renewable resource.

Lipids can be found in various feedstocks, including for instance crop plants, nuts as well as aquatic organisms such as algae. Plant oils contain up to 55 % of lipids and provide the advantage of already existing production and extraction processes allowing for a straightforward utilization. On the contrary, algae biomass does not compete with the food industry as it can be cultivated on non-arable land in fresh, brackish or sea water. Moreover, cultivation can be performed on a large scale in a relatively short period leading to lipid contents of up to 70 % of their dry weight.

Starting from plant and microalgae oil, the production of biofuel by defunctionalization of the lipids to a mixture of hydrocarbons was investigated in academia as well as in industry.[1,2] However, this defunctionaliztion process does not exploit the full potential of the chemical structure of these microalgae lipids. Opposed to that, a more targeted catalytic transformation to industrial key intermediates allows access to much broader and higher value applications than biofuels. Short chain linear α-olefins represent one important key intermediate for the chemical industry as they serve among other things for the production of various polymers, lubricants and surfactants. Moreover, the demand for mid-chain dicarboxylic acids such as adipic, sebacic and azelaic acid is due to their use for nylon production, for instance, high. Industrially, the synthesis of those intermediates is provided by petroleum-based procedures such as the Shell Higher Olefin Process which produces α-olefins from ethylene in one million tons per year. To replace such petroleum-based processes, novel biorefinery approaches, where sustainable biomass is processed into desired intermediates, are required.

1.1 Lipids as Renewable Feedstock

In ages of depleting fossil raw materials, required in high amounts for refinery processes in the chemical industry, renewable feedstocks have gained importance as a replacement and extension. In general, a renewable resource can be naturally replenished at a rate comparable to its rate of consumption. Food crops, agricultural waste as well as algal biomass rank among the most significant renewable feedstocks (Figure 1.1). The idea to use these renewable biomasses to extract constituents such as proteins, lipids and carbohydrates has long been applied. The complex chemical structures were used with limited chemical modification for the paper, surfactant or food industry. Opposed to that, the interest in biorefinery processes, where proteins, lipids or carbohydrates from renewable feedstocks are converted into various chemical building blocks that can be used for the production of industrial relevant products, has only increased in the last decades and is still one of the most important challenges chemists face today. Especially lipids, consisting of glycerol, phosphates or sugars and fatty acids are a promising renewable raw material for such a biorefinery. They contain a long hydrocarbon fatty acid chain with an acid and double bond functionality allowing for the synthesis of highly relevant industrial intermediates such as olefins, diacids and other hydrocarbons.

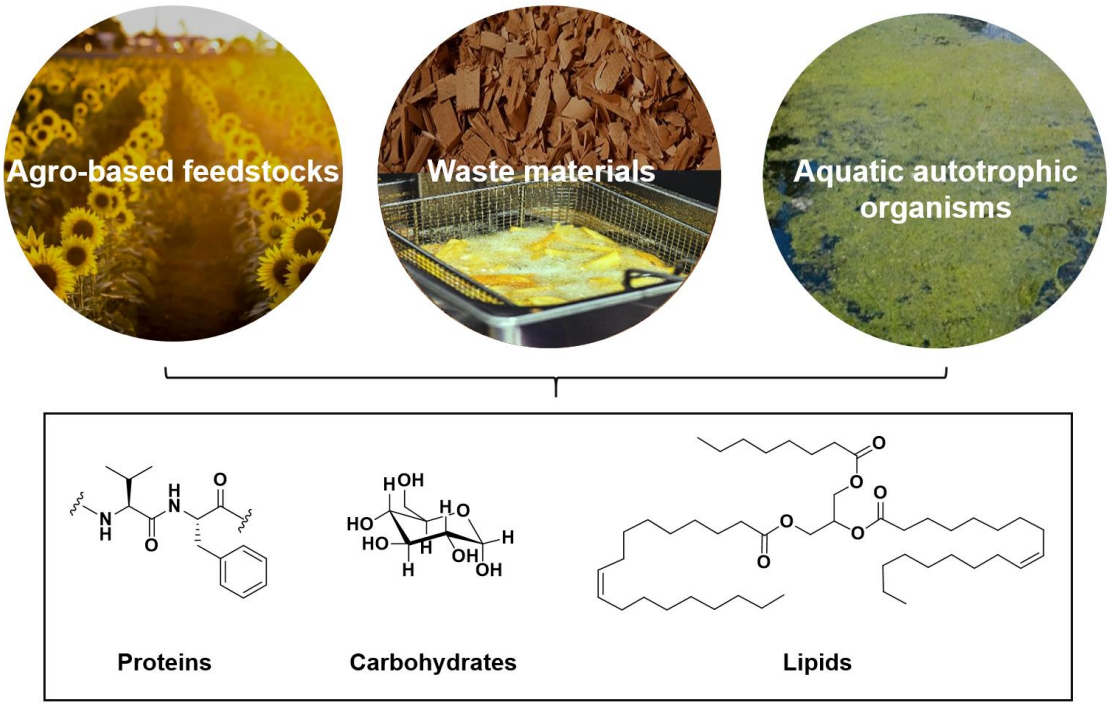

Figure 1.1. Main substance classes found in various biomasses.

1.1.1 Plant oils

In 2021, around 640 million tons of oilseeds were consumed globally, whereby the major proportions of 61 % and 31 % served as animal feed and for the food industry, respectively. Around 10 % were used for industrial purposes such as in cosmetics, laundry detergents, biofuels, paints and lubricants.[3] Thus, this so called first generation feedstocks are among the most important renewable sources of lipids for the commercial production of chemicals.[4,5] Their main advantage over other lipid sources are already established extraction and production routes including machinery and quality standards. For chemical transformation schemes of these plant oils, their production values, oil contents and fatty acid composition play an important role. Biodiesel for instance, accounting for half of the chemicals derived from plant oils, is mainly produced from palm, soybean and rapeseed oil, as these plant oils show the highest global production values.[3] In addition, oilseeds differ in their oil content. Compared to the other mentioned oils, sunflower seeds exhibit with 55 % the highest oil content, making it also an attractive renewable lipid source (Figure 1.2).

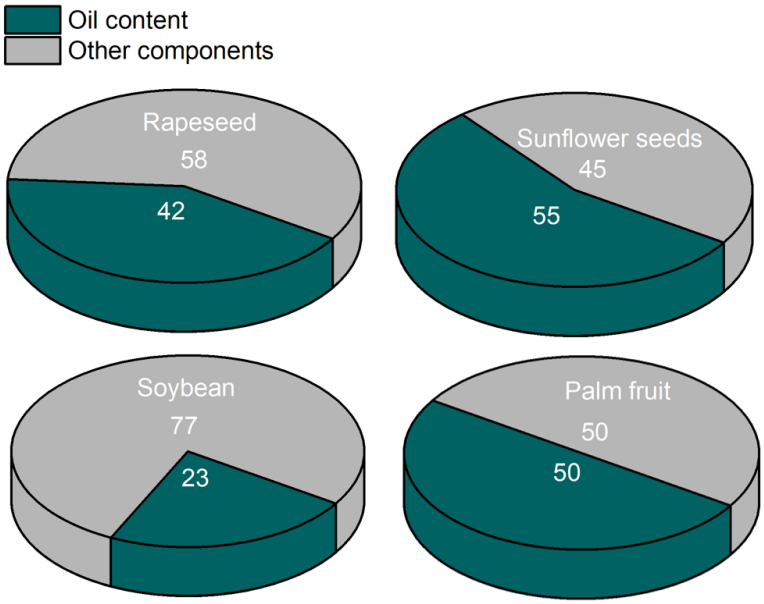

Figure 1.2 Oil content of various plant oils. Shown values are extracted from a published report on global market supply 2020/2021.

Conventionally, the oil is extracted from oilseeds by mechanical extraction such as hydraulic pressing. Besides this method, solvent extraction has been widely used due to economical and practical concerns. In addition, the utilization of supercritical carbon dioxide ($scCO_2$) emerged recently in as green lipid extraction medium (see chapter 1.3.1)

Especially, the fatty acid composition can be a further essential parameter for suited chemical transformation schemes as specific functionalization reactions such as isomerizing alkoxycarbonylation[4] and olefin metathesis[5] require unsaturated fatty acids which are present in variable amounts in various plant oils (Figure 1.3, Table 1.1).[6]

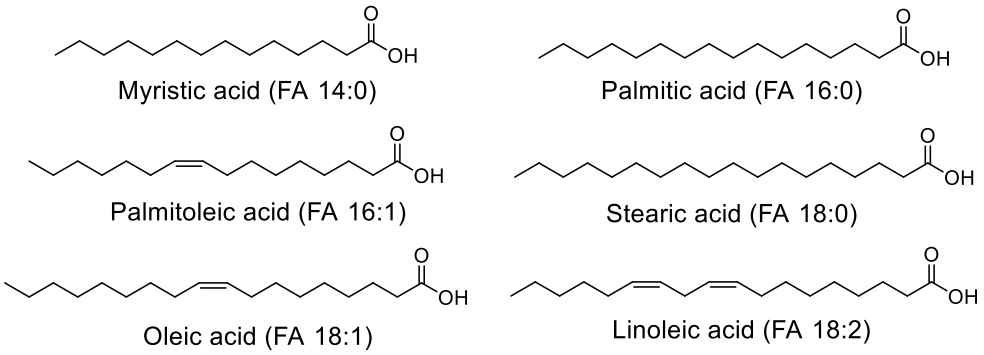

Figure 1.3 Fatty acids present in plant oils. Fatty acids are commonly abbreviated by 18:1 and 18:2 for example, corresponding to 18 carbon atoms and the number of double bonds.

Table 1.1 Most abundant fatty acids in various plant oils.[6]

Plant oil	Myristic acid	Palmitic acid	Stearic acid	Palmitoleic acid	Oleic acid	Linoleic acid
Rapeseed	-	4.5 ± 0.03	3.3 ± 0.07	-	65.7 ± 0.32	19.6 ± 0.34
Sunflower	-	5.5 ± 0.2	4.2 ± 0.1	-	26.2 ± 0.6	64.89 ± 7.3
Soybean	-	12.2 ± 0.1	6.5 ± 0.0	0.1 ± 0.0	29.1 ± 0.0	46.8 ± 0.3
Palm fruit	1.6 ± 0.1	39.6 ± 5.4	5.4 ± 2.1	-	42.9 ± 6.9	8.9 ± 1.3

For industrial purposes, plant oils serve so far mainly for the production of biofuels. A chemical valorization into value added intermediates could, however, further broaden the application of these renewable feedstocks. This can be accomplished for example by cleavage reactions of the fatty acids to various target products. Industrial examples are ozonolysis and catalytic oxidation, yielding mid-chain α,ω-dicarboxylic acids and derivatives.[7] Especially ozonolysis has an industrial relevance for the synthesis of azelaic acid and pelargonic acid, representing desired monomers for the production of polymers and plasticizers. Another catalytic reaction facilitating the biorefinery of plant oils is olefin metathesis. The company Elevance, for instance, converts palm, soybean and rapeseed oil into industrial relevant olefins, unsaturated esters and diesters by means of butenolysis and self-metathesis on an industrial scale (Figure 1.4 a).[8]

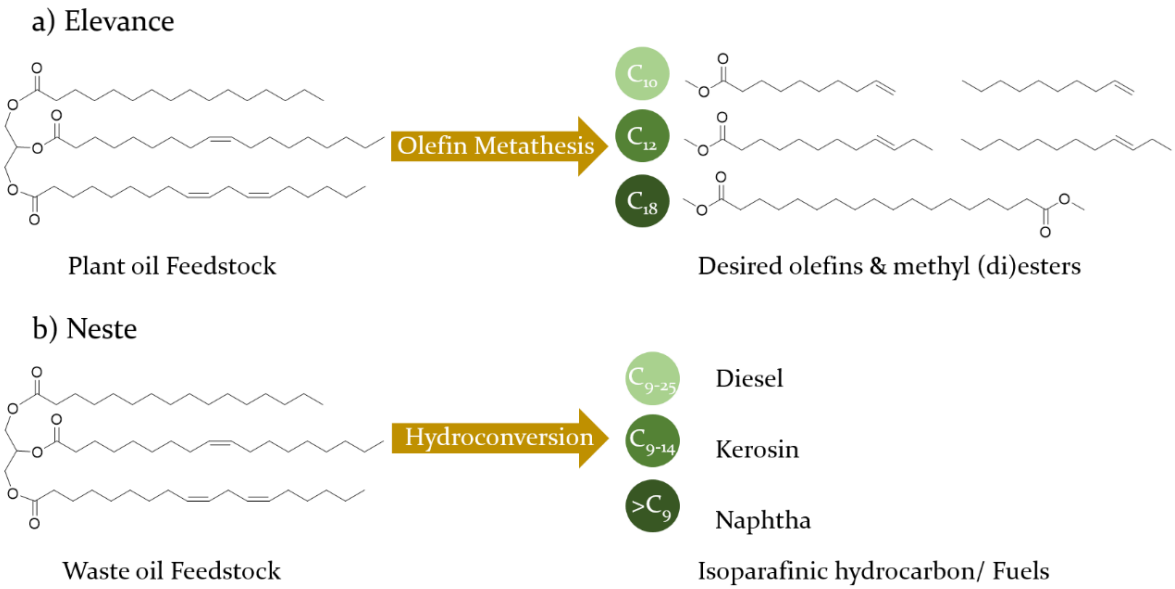

Figure 1.4 Industrial processes to convert renewable lipids into relevant building blocks.[8]

Despite the established industrial use of plant oils for the synthesis of valuable renewable intermediates, the use of food crops also entails disadvantages. Competition with the food production, contribution to water shortages and the destruction of the world's forests diminishes its potential.[9] In contrast to food crops, second generation feedstocks including agricultural waste materials such as nonedible oils and forest residues, address some of these drawbacks as they are produced within existing process routes and do not generate environmental problems regarding agricultural areas and competition with food production. Moreover, the emission intensive disposal of used oils is prevented. This is why suitable techniques for their conversion into relevant chemical building blocks are sought-after. The company Neste, for instance, established technologies to transform waste materials including residue fats and oils by hydrotreating into renewable hydrocarbons on an industrial scale (Figure 1.4 b).[10] These renewable hydrocarbons not only allow for the production of renewable diesel but also of various plastics.

1.1.2 Microalgae oil

Recently, so called third generation feedstocks emerged as lipid source which are photoautotrophic unicellular organisms like microalgae. They count to the most promising renewable raw materials, as they can be cultivated in a wide range of aquatic habitats including rivers, lakes and even wastewater and tolerate a wide range of temperatures and ph values, enabling their worldwide growth.[11] Thus, the usage of microalgae as feedstock does not compromise food supplies, rainforests or arable land. Moreover, they show remarkably high growth rates since they may double their biomass within 24 hours, resulting in higher yields per area compared to plant oils.[2] Microalgae strains produce significant amounts of lipids serving partly as membrane lipids enclosing the cell but mainly as energy storage.[12, 13] Especially the latter can correspond to a lipid content of up to 50 % of dry weight.[2] Moreover, an easy genetic modification is possible allowing for a further increase of the lipid content to up to 70 wt%.[14,15] In addition to other commonly occurring fatty acids in plant oils, microalgae exhibit fatty acids with unusual chain lengths and a high degree of unsaturation not found in significant amounts in nature elsewhere. The polyunsaturated fatty acids eicosapentaenoic acid (EPA, FA 20:5) and docosahexaenoic acid (FA 22:6) represent two prominent examples (Figure 1.5).

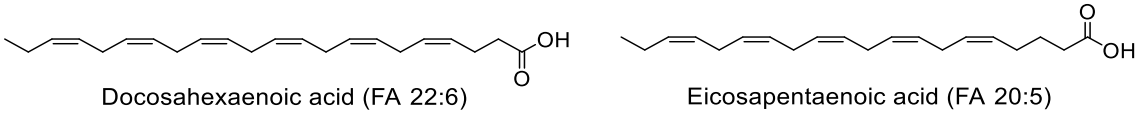

Figure 1.5 Chemical structure of polyunsaturated fatty acids in microalgae.

Due to these benefits, utilization as renewable feedstock seems promising. Since the 1950s, research on the production of biofuels from microalgae was conducted which resulted in production trails of several thousand tons.[16] Nevertheless, due to limitations regarding algae growth and energy-intensive downstream processes including harvesting and extraction of the microalgae as well as isolation of the lipids, biofuels and chemical intermediates based on algae are not yet commercially available.[17,18] Current approaches focus on the usage of microalgae feedstock for their transformation into high-value chemicals as its valorization represents a more sustainable concept with broader applications. The synthesis of desired building blocks for the chemical industry can be performed as well as the production of otherwise poorly accessible intermediates from renewable resources. Due to the presence of unique fatty acids this concept also allows for the synthesis of novel chemical building blocks and materials with new properties.

1.1.2.1 Phaeodactylum tricornutum

Besides other microalgae species, *Phaeodactylum tricornutum* has recently emerged as a potential microalgae lipid source. This marine diatom is an ecologically significant, poly-morphological and unicellular microalgae which is well-known and used to study physiological and biochemical processes. This is due to their flexibility in growth conditions, a short doubling time and its photoautotrophism. In addition, this marine diatom grows in salt water, preventing the competition with freshwater sources which makes it more commercially attractive. Furthermore, high lipid contents of up to 57 % of their dry weight can be reached under optimum conditions and remarkably high amounts of unsaturated fatty acids are produced, allowing for a chemical transformation (Table 1.2).[2,15]

Table 1.2 Composition of fatty acids extracted from Phaeodactylum tricornutum.[19, 20]

Fatty acid	Fatty acid ratio [mol%]
FA 14:0	9 – 11
FA 16:0	13 - 25
FA 16:1	29-47
FA 18:0	<1
FA 18:1	4 - 8
FA 20:5	10 - 30
FA 22:6	1 - 3

The average degree of unsaturation in the lipids can be influenced by a change in growth conditions including light conditions, temperatures, pH value, CO_2 concentration and nutrient supply as well as by genetic engineering.[21,22,23] The latter is facilitated due to its completely sequenced genome.[24] This is why *Phaeodactylum tricornutum* represents a promising renewable lipid source for catalytic valorization and was used in this work.

1.1.2.2 From microalgae Cultivation *via* Extraction to Chemical Modifications

To obtain a final industrially relevant product from microalgae, several technical processes are necessary including cultivation, harvest, extraction and a final chemical modification (Scheme 1.1).

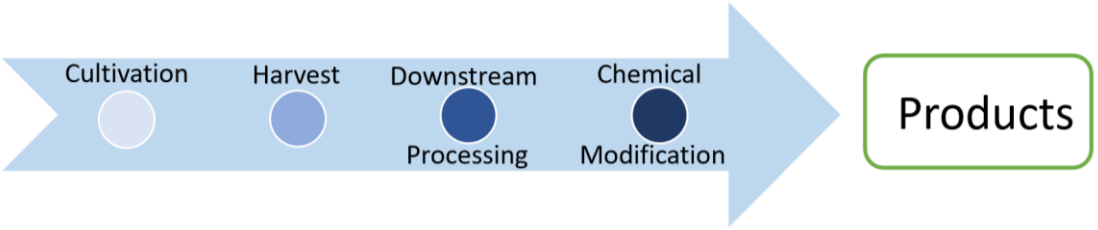

Scheme 1.1 General scheme of the production of chemicals from microalgae.

The cultivation of microalgae is the most time-intensive step but also the most important in terms of receiving high lipid contents. The lipid productivity, representing the combined effects of oil content and biomass production of microalgae, is known to be dependent on the cultivation conditions.[25]

Due to the high flexibility of microalgae, they can be grown under photoautotrophic conditions[26,27], using sunlight as energy source and CO_2 as carbon source, mixotrophically with different energy and carbon sources or under heterotrophic conditions, where a carbon source is added in dark fermenters. Heterotrophic[28] and mixotrophic cultivation of suitable algae species reach higher cell concentrations compared to autotrophic cultivation due to an easy availability of carbon sources. Nevertheless, phototrophic cultivation is the most commonly used cultivation condition [26, 27] as from a sustainable point of view, only CO_2 from the atmosphere is utilized to form chemical energy through photosynthesis[28], preventing the use of other costly carbon sources. In contrast, heterotrophic cultivation does not fully exploit the potential of microalgae as it is still dependent of arable land.[29,30] This is the reason why this chapter will focus on photoautotrophically cultivated microalgae.

In general, the autotrophic growth of microalgae can be performed in batch or continuous operations.[18] On a large industrial scale, they are cultivated in open cultivation systems or closed photobioreactors. Open ponds show the advantage of lower operating costs, whereas photobioreactors benefit from higher productivity and biomass concentration and show lower risk of contamination.[30,31] On a laboratory scale, their cultivation in flasks provides a simple procedure.

The subsequent harvesting of the microalgae cells and the extraction of the contained lipids count to the most cost-intensive steps. The low cell concentration on autotrophic algae cultures, ranging from 0.1 to 8 g dry weight L^{-1} and requiring the removal of high amounts of water, is one reason.[32] Moreover, due to their small cell diameter of 5 to 50 µm, separation from the aqueous media is hampered.[33] The use of continuous centrifugation decreases the overall harvesting costs. Subsequent lipid extraction from the microalgae biomass can be performed by several methods. The most common extraction procedure includes the use of organic solvents as described by Folch *et* al. in 1951 and Bligh and Dyer in 1959, where a biphasic solvent system of $CHCl_3$/MeOH/H_2O is applied.[34,35] As the lipids enrich in the chloroform phase and proteins and carbohydrates are contained in the water phase, a separation is possible. Due to the addition of water, drying of the microalgae is not required, facilitating the overall downstream process. Moreover, to overcome the drawback of a thick cell wall, impeding the extraction of the lipids from the lipid droplets, pre-treatment by cell disruptions such as autoclaving, bead-beating, ultra-sonication was found to enhance extraction efficiency.[14,36,37] However, as the use of these organic solvent mixtures comes along with a negative impact on human health and environment, alternative extraction mediums are desired. Extraction of lipids by means of supercritical carbon dioxide ($scCO_2$) was developed showing several advantages over organic solvents (see chapter 1.3.1). [38,39,40]

As discussed before, current efforts to use microalgae feedstocks in industrial processes mainly focus on the production of biofuels as well as the use of the incorporated ω-3 fatty acids as health supplements.[41] On the contrary, literature on the chemical functionalization of microalgae lipids into valuable industrial intermediates are rare. Our group reported on the isomerizing methoxycarbonylation of extracted microalgae oil from the diatom *Phaeodactylum tricornutum*.[42] With the catalyst precursor [Pd(dtbpx)$(OTf)_2$], the monounsaturated fatty acids were converted in the presence of CO and MeOH into a mixture of linear 1,17- and 1,19-diesters in high purity, whereas present polyunsaturated fatty acids (FAME 20:5) resulted in a broad product spectrum. Remarkably, the catalyst was active in the presence of various organic components such as chlorophylls, carotenoids and carbohydrates, extracted from the cells present in the crude oil. By polycondensation of these intermediates with corresponding diols the access to novel polyesters-17/19.17/19 was possible, showing desired high melting and crystallization temperatures comparable to polyethylene. Moreover, saturated diesters with chain lengths of C_{17} and C_{19} could be produced by CO free alkoxycarbonylation of monounsaturated fatty acids from microalgae

oil.[43] A simultaneous extraction and conversion was accomplished by the use of methanol in combination with formates instead of CO.

To overcome the problem of an unselective transformation of polyunsaturated fatty acid eicosapentaenoic acid (FA 20:5) by isomerizing alkoxycarbonylation, a selective dual catalysis one-pot approach was established.[44] *Via* selective heterogeneous hydrogenation on Pd/γ-Al_2O_3 and homogeneous carbonylation with the [(dtbpx)PdH(L)]$^+$catalyst, FA 20:5 is hydrogenated to up to 80% to the monounsaturated fatty acid 20:1 and subsequently functionalized to the desired 1,21-diester. This approach can be also applied to crude microalgae oil containing a mixture of mono and polyunsaturated fatty acids.

The transformation of microalgae oil by olefin metathesis was further investigated recently in our group. A procedure for the catalytic upgrading of the five-fold unsaturated fatty acid FA 20:5 to among others benzene *via* olefin metathesis and catalytic hydrogenation was developed.[43] In addition, short-chain unsaturated fatty acid methyl esters and mono- and dienes were produced in a high selectivity by butenolysis of microalgae oil. In a further isomerizing alkoxycarbonylation, value added linear mid-chain (di-)carboxylic acid esters could be accessed. The simultaneous extraction and transformation of microalgae lipids by cross metathesis in $scCO_2$ was also shown. In this case, mid-chain olefinic and unsaturated ester products were obtained (see chapter 1.3.2).

1.2 Olefin Metathesis by Molecular Catalysts

Olefin metathesis belongs to the most important reaction in organic synthesis and allows among others for the transformation of oleo chemical feedstocks.[45,5] The high significance of this reaction is also reflected in its utilization for industrial processes. The Phillips triolefin process was the first industrial process developed at Phillips Petroleum Co. in the 1960s, providing access to ethylene and 2-butene by olefin metathesis of propylene using a heterogeneous WO_3/SiO_2 catalyst. Nowadays, the process is performed for the production of propylene from ethylene and 2-butene. Further, the Shell Higher Olefin Process (SHOP) represents a further prominent example which uses an olefin metathesis reaction in combination with oligomerization and double bond isomerization to produce linear olefins on a large industrial scale (see chapter 1.2.3.1).

The first alkene metathesis was observed in 1956 by Eleuterio and co-workers during the polymerization of propylene using a tungsten catalyst.[46] The concept of a transalkylidenation reaction was first reported in 1967 by Calderon *et* al., describing a transition metal catalyzed reaction in which an exchange of alkylidene moieties between alkenes takes place (Scheme 1.2).

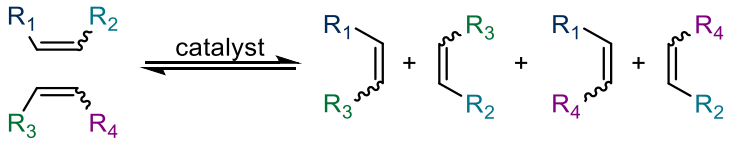

Scheme 1.2 General principle of olefin metathesis of unsymmetrically substituted olefins.

A few years later, Hérisson and Chauvin proposed a mechanism for the olefin metathesis that is still widely accepted today.[47] The concept comprises an initial step where an olefinic substrate reacts with the catalyst precursor to form an active metal carbene complex (Scheme 1.3, left side). In a subsequent [2+2] cycloaddition with another olefin, a metallacyclobutane intermediate is formed which can undergo a cycloreversion to the original species or to a new alkene and alkylidene species.

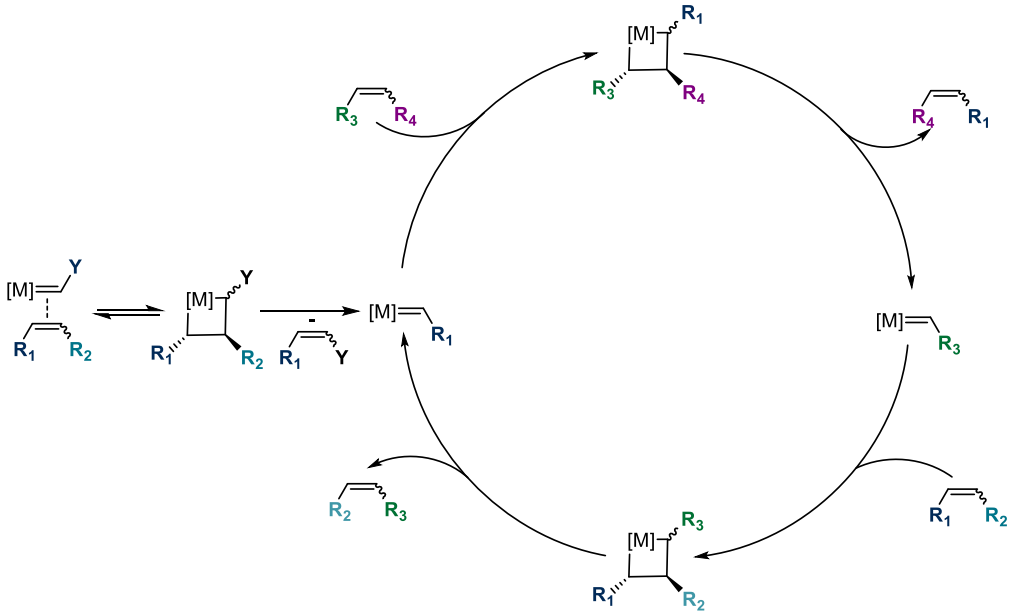

Scheme 1.3 Catalytic cycle of cross metathesis proposed by Chauvin.

With the development of a wide range of catalysts (see chapter 1.2.1), various types of olefin metathesis reactions are realized providing access to a broad spectrum of unsaturated compounds and finding applications in organic and polymer chemistry. In general, they can be divided in self-metathesis (Scheme 1.4 a), where two identical olefins react, and in cross-metathesis (CM) describing the metathesis with two different olefins (Scheme 1.4 b).

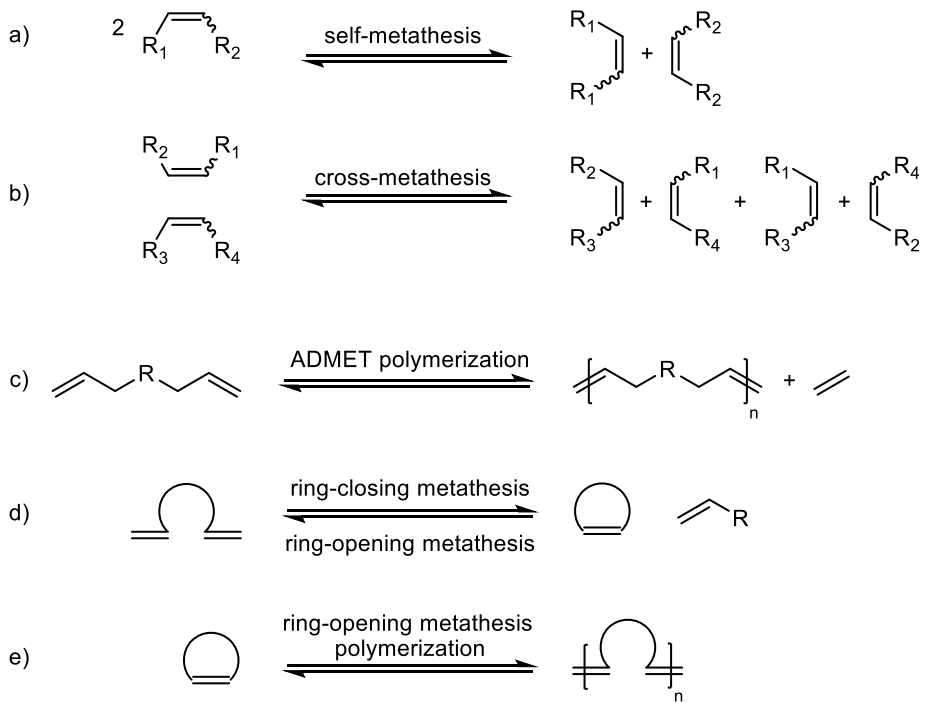

Scheme 1.4 Various types of olefin metathesis.

Furthermore, intramolecular reactions are possible when the substrate bears more than one double bond. In this case, acyclic diene metathesis polymerization (ADMET, Scheme 1.4 c) and ring closing metathesis (RCM) can be performed (Scheme 1.4 d). The back reaction is called ring-opening metathesis (ROM). A special type of ring-opening metathesis is the ring-opening metathesis polymerization (ROMP, Scheme 1.4 e), leading to polymers.

1.2.1 Homogeneous Olefin Metathesis Catalysts

First early metathesis catalysts were developed between 1950 and 1990, consisting of a catalytically active transition metal compound and a metal alkyl such as tungsten hexachloride with tetramethyl tin (WCl_6/ $SnMe_4$).[48] These catalytic systems showed a high selectivity for the desired products. However, they reached only low catalyst turnover numbers (TON), impeding a high catalyst performance. On the contrary, well-defined homogeneous tungsten and molybdenum as well as ruthenium catalysts, developed by Schrock[49] and Grubbs[50], respectively, showed higher functional-group tolerance and catalytic activities (Figure 1.6). Schrock carbene metal complexes were found to have high activities especially for sterically demanding olefins, whereas ruthenium-based catalysts (Figure 1.6 GI and GII) show a higher tolerance towards water, oxygen and various functional groups.

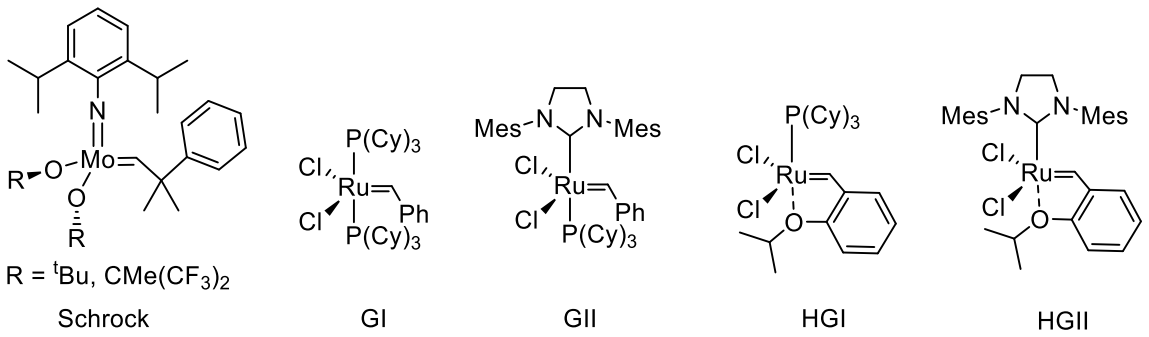

Figure 1.6 Schrock-type and Grubbs-type olefin metathesis catalysts. S: Schrock type catalyst bearing different residues. GI: Grubbs 1st generation catalyst, GII: Grubbs 2nd generation catalyst, HGI: Hoveyda-Grubbs 1st generation catalyst, HGII: Hoveyda-Grubbs 2nd generation catalyst. Cy = cyclohexyl, Ph=phenyl, Mes=mesitylene.[49,50]

Grubbs and co-worker developed more active and stable ruthenium catalyst, containing ortho-isopropoxyphenylmethylene chelate ligands. Substitution of a phosphine ligand of the Grubbs 1st generation catalyst with an N-Heterocyclic Carbene (NHC) ligand gave the Grubbs 2nd generation catalyst, showing an enhanced reactivity as well as functional group

tolerance while maintaining the thermal stability. Furthermore, the introduction of an ortho-isopropoxyphenylmethylene chelate ligand led to the so called Hoveyda-Grubbs 1st and 2nd generation catalysts, possessing an even higher stability towards moister and air and revealing lower initiation rates.[51] The enhanced performance is the reason why these Ru-based catalysts are widely used in literature for various applications and is especially relevant for the transformation of renewable feedstocks such as fatty acids.[5]

1.2.1.1 Olefin Metathesis of Unsaturated Fatty Acids

In 1972, Boelhouwer and co-workers reported on the first olefin metathesis of unsaturated fatty acid derivatives using $WCl_6/SnMe_4$ as catalyst.[48] This ill-defined catalytic system reached the thermodynamic equilibrium in the self-metathesis of methyl oleate after 24 h at high catalyst loadings of 3 mol% (Scheme 1.5).

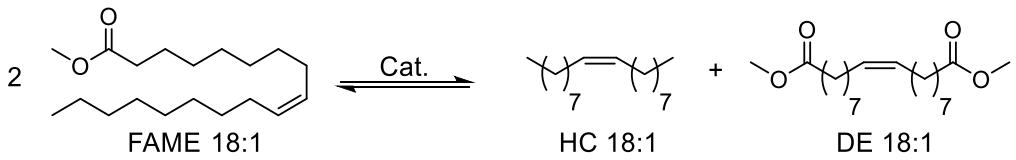

Scheme 1.5 Equilibrium reaction of the self-metathesis of methyl oleate.

In contrast, the development of the well-defined Grubbs and Hoveyda Grubbs 2nd generation catalyst enhanced the catalytic productivity significantly for this type of reactions. As reported by Dinger *et* al., with 1 ppm of GII as catalyst, turnover numbers of 440 000 were reached in the self-metathesis of methyl oleate.[52] In addition, with these catalytic systems cross-metathesis with various types of olefins, including acrylates[53], acrylonitrile[54,55] or ethylene[56], are possible. Unless a product can be removed selectively from the reaction, the self-metathesis of unsaturated fatty acids lacks a driving force, yielding an equilibrium mixture with only 50 % products. Foglia *et* al. described a solution to this problem by performing the reaction in bulk to precipitate the diacids.[57] This pushes the equilibrium towards the desired products leading to a conversion of 80 %.

Aside self-metathesis of fatty acids, cross-metathesis represents a field of current interest as it gives access to a wider range of possible products. In particular, ethenolysis, describing the cross-metathesis with ethylene, is one of the most prominent examples, providing the synthesis of α-olefins and terminal unsaturated esters. In case of methyl oleate (FAME 18:1), 1-decen (HC 10:1) and methyl 9-decenoate (E 10:1) are formed (Scheme 1.6). These products

are valuable intermediates for the chemical industry and serve for the production of fuels, lubricants, surfactants and polymers, for instance.[58,59]

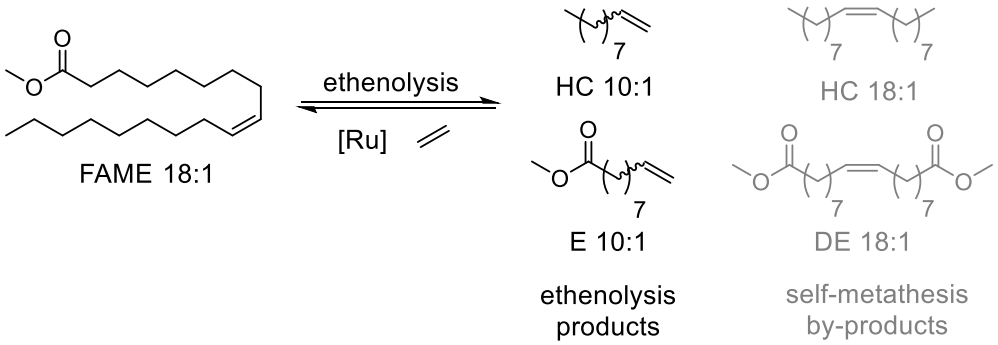

Scheme 1.6 Ethenolysis of methyl oleate (FAME 18:1).

In ethenolysis there is a trade-off between selectivity and productivity, representing a major challenge. High ethylene pressures provide high selectivities for ethenolysis products over competing self-metathesis products, but the use of high ethylene concentrations promote unproductive ethylene self-metathesis, resulting in a decreased catalytic productivity (Scheme 1.7).[5] A main limiting factor in the cross metathesis of fatty acids with ethylene is the formation of unstable methylidene complexes [$L_nRu{=}CH_2$], showing a higher propensity for irreversible deactivation reactions.[60,61]

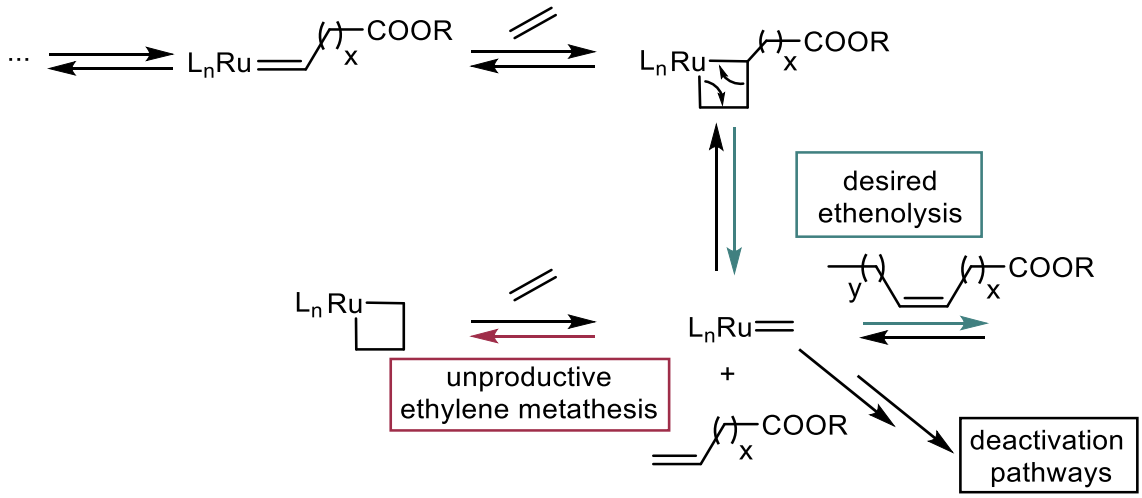

Scheme 1.7 Simplified scheme of unproductive ethylene metathesis.[5]

Ethenolysis of methyl oleate was reported using well-defined homogeneous ruthenium based as well as molybdenum-based catalysts. While molybdenum complexes reported by Schrock *et* al. reached TONs of up to 5000[62], Grubbs and Hoveyda-Grubbs catalysts showed TONs of 600 to 8000.[63] As TONs of > 50 000 are quoted to be prerequisite for processes of economic interest, catalysts with sufficiently high performances were desired.[60] With the

development of complexes bearing cyclic alkyl amino carbene ligands (CAAC), as reported by Schrodi *et* al., TONs of 35 000 were reached (Figure 1.7, HUC).[56] Increasing the purity of ethylene from 99.9 % to 99.995 %, also enhanced catalyst performance for CAAC-HGII[59,64] as well as for other catalysts such as the commercial available UltraCat were observed (Figure 1.7, UC). Here, TONs in a range of 74 000 to 180 000 were yielded, providing an efficient transformation of methyl oleate in an ethenolysis reaction.

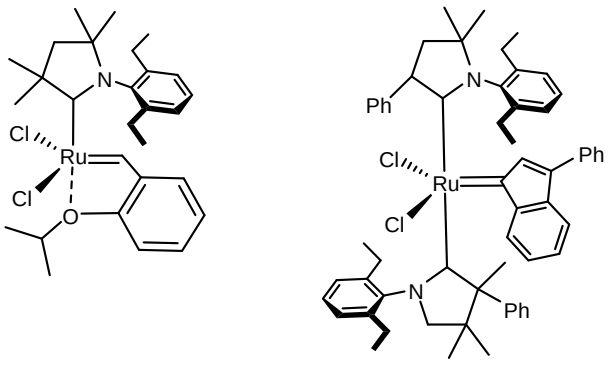

HUC **UC**

Figure 1.7 Olefin metathesis catalysts HUC (Hoveyda UltraCat) and UC (UltraCat) bearing cyclic alkyl amino carbene ligands. Ph=phenyl.

In academia, further research was conducted in the field of olefin metathesis for the upgrading of plant oils. Dixneuf *et* al. reported on the cross-metathesis of fatty acids with acrylonitrile to get access to α,ω -bifunctional products that can be further transformed *via* reduction into valuable monomers such as linear aminoesters, amicoacids and aminoalcohols (Figure 1.8 A).[65,66] In addition, cross metathesis with acrylates[67] as well as allyl chloride[68] was investigated resulting in α,ω –difunctional monomers (Figure 1.8 B). These monomers can be further functionalized and used for the synthesis of polyesters, nylon materials and detergents.[69] Our group established the synthesis of ultra-long-chain α,ω-diesters from plant-oil derived oleic acid *via* a "chain doubling" strategy (Figure 1.8 C). With a sequence of self-metathesis, dynamic catalytic isomerization crystallization and a further self-metathesis, unsaturated diesters with chain lengths of C_{32} can be reached. They serve as monomer for the production of polyesters possessing desired high melting points.[70]

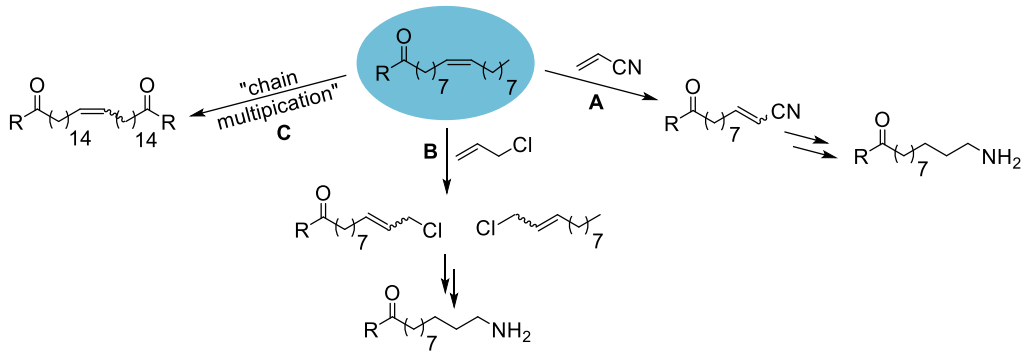

Figure 1.8 Catalytic upgrading of plant oil based fatty acids such as methyl oleate (R= Me, FAME 18:1) to value-added intermediates.

1.2.2 Combination of Olefin Metathesis and Double Bond Isomerization

As discussed before, olefin metathesis is a powerful synthetic concept in organic synthesis and opens new industrial routes to important petrochemicals, polymers as well as specialty chemicals. Already existing industrial processes, applying olefin metathesis are for instance the Phillips triolefin process for the production of propylene as mentioned earlier and the synthesis of polynorbornene *via* ring-opening metathesis polymerization of 2-norbornene (bicyclo[2.2.1]-2-heptene).[71] Moreover, the transformation of renewable unsaturated fatty acids to relevant olefins and unsaturated (di)esters is performed by butenolysis on an industrial scale in the Elevance biorefinery process (see chapter 1.1.1).[72] Even broader product spectra can be provided by combining olefin metathesis with other valuable catalytic reactions in a one-pod process, involving multiple catalytic transformations followed by a single workup stage. In literature, most examples show a combination of metathesis with (de)hydrogenation or double bond isomerization.[73,74,75] Especially when olefins or unsaturated esters are used as monomers, the involvement of a double bond isomerization allows for a broadening or adjustment of the original product spectrum. The latter is for instance used in the prominent Shell Higher Olefin Process (SHOP).

1.2.2.1 Shell Higher Olefin Process

The Shell Higher Olefin Process was developed in 1968 to convert ethylene to α-olefins and represents due to its high production values one of the most remarkable industrial chemical processes.[76] Linear α-olefins are an important class of industrially relevant intermediates. Whereas light linear α-olefins (<C_{10}) are especially used as co-monomers for the production of polyethylene and plasticizer, olefins with longer chain lengths of C_{10} to C_{18} serve as precursor for the synthesis of lubricants, coatings and surfactants. Their synthesis is accomplished in the SHOP by ethylene oligomerization in the presence of a nickel catalyst, leading to a mixture of even-numbered α-olefins with a Flory-Schultz distribution. By the utilization of a catalyst soluble in polar solvents, a convenient way of catalyst recycling is enabled as the olefins formed are immiscible in the solvent. α-olefins with chain lengths in the rage of C_{12}-C_{18} are recovered from the process by distillation and represent the main products.

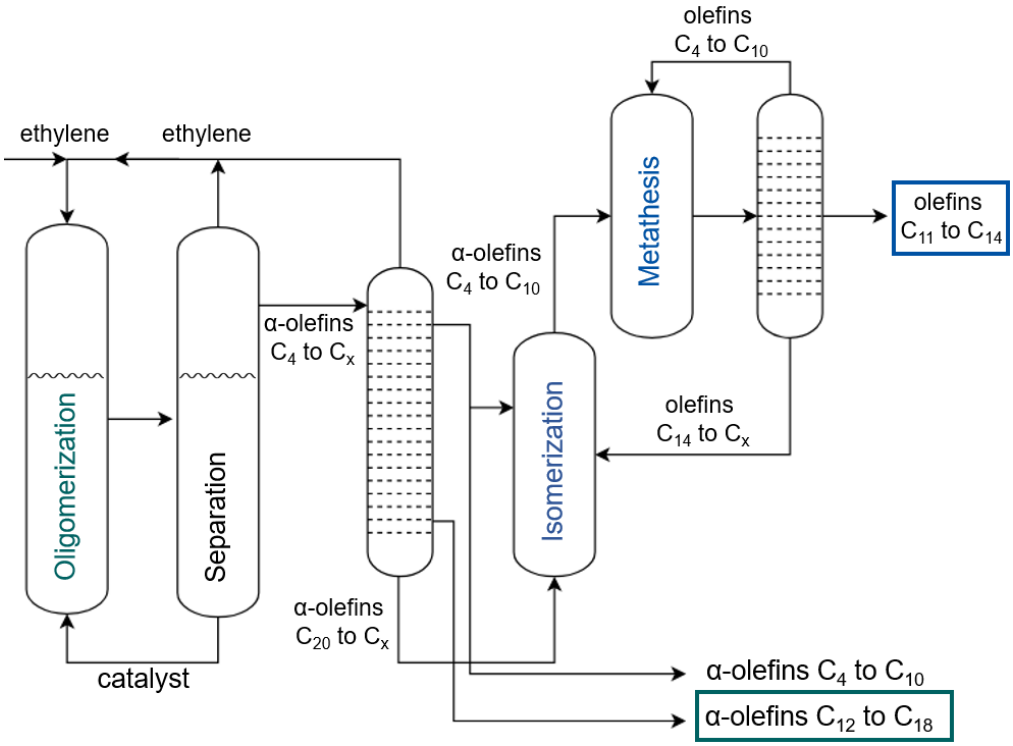

Figure 1.9 Schematic drawing of the set-up of the Shell Higher Olefin Process.

Other α-olefins having no big market (partially C_4-C_{10} and >C_{20}) are recombined, isomerized and exposed to metathesis giving internal olefins with both odd and even numbers with a desired chain length of C_{11} to C_{14}. They are used for the synthesis of detergent alcohols and alkylates.[77] Here, with the procedure of an isomerization and metathesis, a considerable adjustment in output is possible to suit market demands.

1.2.2.2 One-Pot Approaches of Olefin Metathesis and Isomerization

As demonstrated in the SHOP, a combined process of olefin metathesis and isomerization can be applied to transform a product mixture with a wide range of chain lengths to a more narrowed distribution. On the contrary, a one-pot metathesis/isomerization approach also allows for the extension of a product scope, such as to olefin blends.[78,79,80]

In general, double bond isomerization is one of the unwanted side reactions occurring during olefin metathesis. For Grubbs-type metathesis catalysts, for instance, isomerization is observed and caused by a ruthenium hydride species, formed upon decomposition of the catalyst. Unintended double-bond isomerization during metathesis was first described by Porri *et* al. in 1975 (Scheme 1.8).[81] Using a bimetallic iridium/silver catalyst an olefin mixture was formed during the metathesis polymerization of olefins rather than the expected polyolefins. Grubbs *et* al. used this observation to steer the isomerization/metathesis process in a targeted way. With the same Ir/Ag catalyst system at high loadings, 1-ocatadecene is converted into a wide range of olefins as well as methyl oleate into a mixture of olefins, unsaturated monoesters and α,ω-diesters.[82]

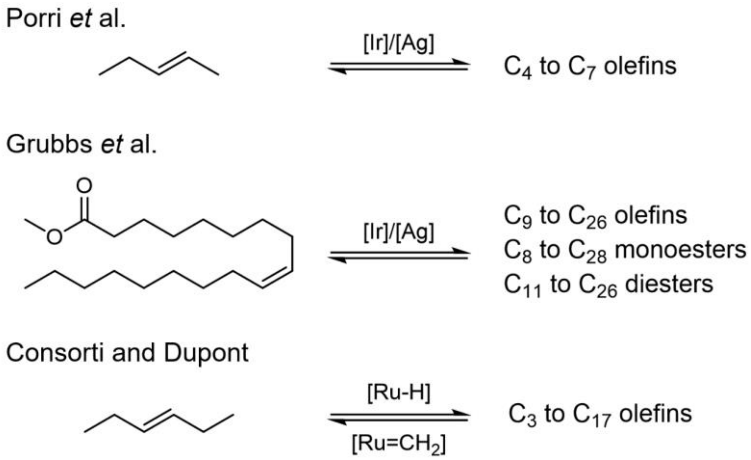

Scheme 1.8 Isomerizing metathesis of olefins and fatty acids described in literature.

Nevertheless, as the conversion remained even at high catalyst loadings incomplete and was far from equilibrium, a more efficient synthetic concept was desired. This was accomplished by the use of bimetallic systems comprising of highly active metathesis catalysts and an additional isomerization catalyst.

Consorti and Dupont published an isomerizing metathesis of 3-hexene using a modified HGII metathesis catalyst with a ruthenium hydride isomerization catalyst in ionic liquids.[83] Here the isomerization to metathesis ratio was increased, as compared to the polar metathesis catalyst the isomerization catalyst as well as the olefins were preferentially

present in the non-polar organic phase. Within this procedure a successful simultaneous isomerizing metathesis was proven resulting in an olefin mixture with carbon atoms of up to C_{17}.

Gooßen *et* al. demonstrated the conversion of 3-hexene into a similar product distribution within a shorter period of time by means of a Pd-dimer isomerization catalyst $[Pd(m\text{-}Br)(^tBu_3P)]_2$ and the GII catalyst.[79] With this highly active bimetallic system even allylic esters were converted.[84] The application of a combined isomerization and metathesis is especially useful for the transformation of renewable fatty acids into a wide product range, since their chain length is prescribed by nature which limits the possible product scope. Thus, Gooßen *et* al. further investigated the isomerizing self-metathesis of oleic acid into a defined distributions of unsaturated compounds with chain lengths of up to C_{32} (Figure 1.10, above).[79]

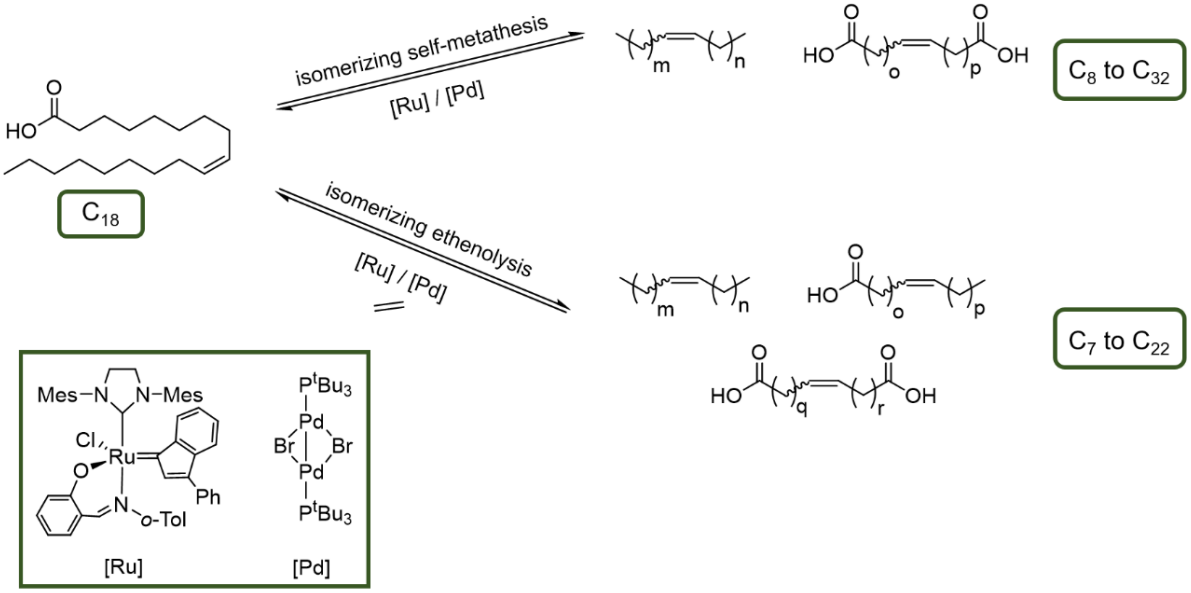

Figure 1.10 Isomerizing olefin metathesis of oleic acid described by Gooßen et al.

Moreover, the isomerizing cross-metathesis of oleic acid with ethylene was demonstrated (Figure 1.10, below). Whereas the ethenolysis resulted in blends of olefins and unsaturated esters with chain lengths below 22 carbon atoms, cross metathesis with trans-3-hexenedioic acid gave a mixture of olefins, monocarboxylates and α,ω-dicarboxylates with a lower mean chain length compared to isomerizing self-metathesis.

Recently, the same group published a procedure to get access to biofuel from rapeseed oil esters by isomerizing metathesis. With the use of a ternary catalyst system comprising of the $[Pd(m\text{-}Br)(^tBu_3P)]_2$ isomerization catalyst and two ruthenium based metathesis catalysts, rapeseed oil esters were converted in a constant stream of ethylene gas by an

isomerizing ethenolysis to a defined olefin, monoester, and diester blend.[85] The obtained product blend showed an evenly rising boiling point curve, meeting the EN 590 specifications for modern (petro)diesel engines.

1.2.3 Immobilized Olefin Metathesis Catalysts

Olefin metathesis reactions using homogeneous catalysts discussed before show a broad application in organic synthesis in the pharmaceutical[86,87] and polymer industry[88,89] as well as for the synthesis of challenging natural products.[90] The main benefits are a high reactivity and selectivity. However, with respect to industrial applications, homogeneous synthesis reaches its limits, since it comes along with hampered catalyst recycling and separation from the product mixture, especially required for pharmaceutical applications.

As opposed to this, molecular catalysts immobilized on a solid support can overcome these restrictions. They provide a facile separation by filtration from the product mixture and provide an easy recovery and reuse of the catalyst. Alongside these advantages, supported catalysts enable the performance of high through–put techniques such as continuous flow processes. From an industrial point of view, such processes are interesting due to low catalyst wastage, facile automation, good reproducibility and less maintenance costs.[91] Thus, a lot of effort was made to synthesize and analyze immobilized molecular olefin metathesis catalysts. As the Hoveyda-Grubbs 2nd generation catalyst is a well-studied catalytic system, shows high activity and selectivities and has a high tolerance towards functional groups, this chapter mainly discusses the utilization of HGII for immobilization purposes.

As a solid support, various materials were investigated including ion exchange[92] and Merrifield resins[93], polyethylene glycol and other polymers[94] as well as silica materials[95,96]. Silica materials, in particular, are of special interest due to their thermal, chemical and mechanical stability and high surface areas.[97,98] Hence, they represent a versatile support for the immobilization of HGII. In general, different types of silica materials were used such as amorphous or crystalline forms with porous, irregular and regular tridimensional framework of silicon and oxygen with varying pore sizes, pore volumes and surface areas. Mesoporous silica materials, showing pore diameters in a range of 2 to 50 nm are of particular importance as they come along with high surface areas and allow immobilization of the catalyst inside the pores, possibly increasing and prolonging activities.[99] Examples of

mesoporous silica used for immobilization purposes are SBA-15[100,101], MCM-41[102], KIT-5[103] and non-ordered mesoporous silica gel[104] (Table 1.3).

Table 1.3 Structural characteristics of various mesoporous silica materials used for the immobilization of HGII.

Silica material	Pore architecture	Pore size [nm]	Surface area [m²/g]
Silica gel (Merck grade 7734)	Non-ordered	6	600
SBA-15[100,101]	Hexagonal	4.7-30	690-1040
MCM-41[102]	Hexagonal	2-6.5	845
KIT-5[103]	Cubic	7	1054

SBA: Santa Barbara Amorphous type material, MCM: Mobil Crystalline Material

1.2.3.1 Immobilization Approaches on Silica

The immobilization of HGII onto silica materials can be performed by covalent and non-covalent interactions. The first immobilization of HGII was reported in 2008 by Van Berlo *et* al. where the immobilization was achieved by physical interactions, prevailing between the catalyst and silanol groups of the used silica pellets.[105] In addition, other mesoporous silica materials were used for such non-covalent linkage, including SBA-1[106] , MCM-41[107] and SBA-15[108]. Even though they revealed good activities in RCM and CM of several substrates and provide a simple immobilization procedure as no time intensive catalyst modification is necessary, non-covalent immobilization shows an increased tendency for catalyst leaching processes, especially in polar solvents such as toluene and dichloromethane.[105] This hampers the recycling of the catalyst and its use in continuous flow processes.

Opposed to that, covalent linkage of a modified HGII catalyst precursor provides a stable interaction between the silica materials and minimizes catalyst leaching. Thus, synthesis routes to modified homogeneous HGII catalyst that allow for the covalent bonding onto silica materials were developed. In literature, three possible anchoring approaches are reported involving the linkage *via* the NHC ligand, exchange of the halogen ligands or the linkage *via* the alkylidene ligand (Figure 1.11).

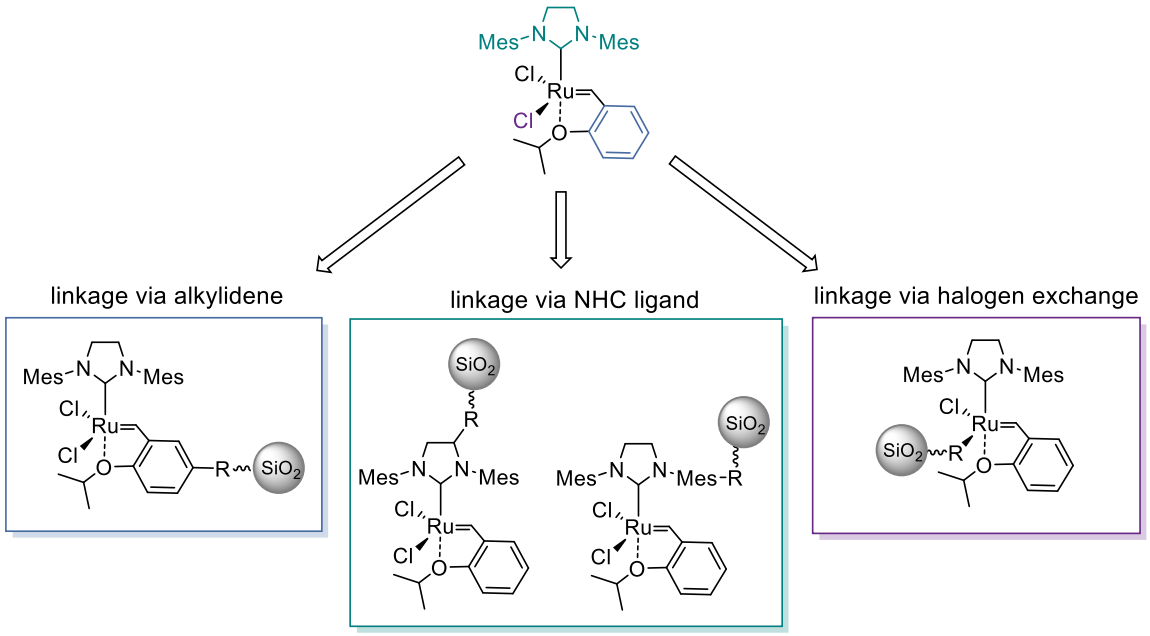

Figure 1.11 Described approaches for a covalent immobilization of Hoveyda Grubbs 2nd generation catalyst onto silica materials. R = organic residue, Mes = mesitylene.

With regard to a straight-forward synthesis route, immobilization *via* the chelating benzylidene ligand is the most common strategy as described by Hoveyda and co-workers[109], Blechert *et* al.[110] and Moreau and co-workers[111]. They reported on an easy reuse and recycling of the supported catalysts. Nevertheless, these catalytic systems are prone to leach since the benzylidene ligand dissociates during the catalytic cycle.[112,113] This impedes its utilization for continuous flow reactions.

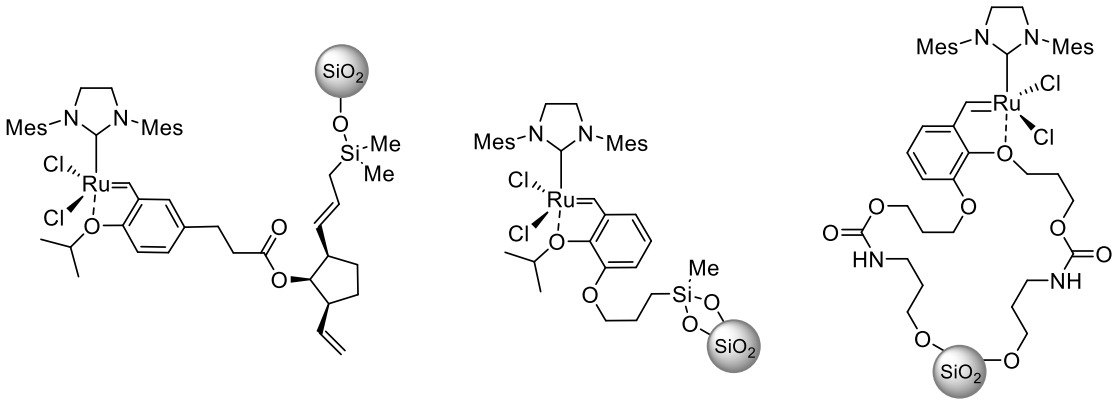

Figure 1.12 Hoveyda Grubbs 2nd generation catalyst immobilized onto silica via the benzylidene ligand. Me = Methyl group, Mes = Mesitylene.[109,110,111]

Covalent linkage *via* halogen exchange is another possible immobilization strategy as reported by Marciniec *et* al.[114] and Balcar *et* al[115]. This was facilitated by attachment to silica *via* Si-O-R bonds as well as *via* fluorinated silver (I) carboxylates (Figure 1.13), respectively. These catalysts revealed a high performance in RCM. However, the exchanged ligands were found to be labile leading to bimetallic deactivation pathways.

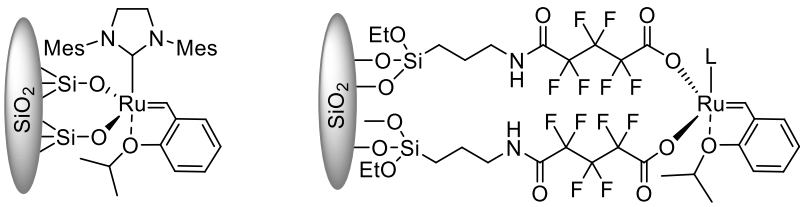

Figure 1.13 Published Hoveyda Grubbs 2nd generation catalyst immobilized onto silica materials via halogen exchange. L= NHC ligand. Mes= mesitylene.[114,115]

Even though immobilization *via* the NHC ligand represents the most demanding strategy in terms of synthetic effort, it is the most promising approach due to the strong coordination of the NHC ligand to the ruthenium center, making it the most substitutionally inert ligand.[116] Several synthetic pathways to covalently linked HGII catalysts by modification of the NHC ligand were published (Figure 1.14).[104]

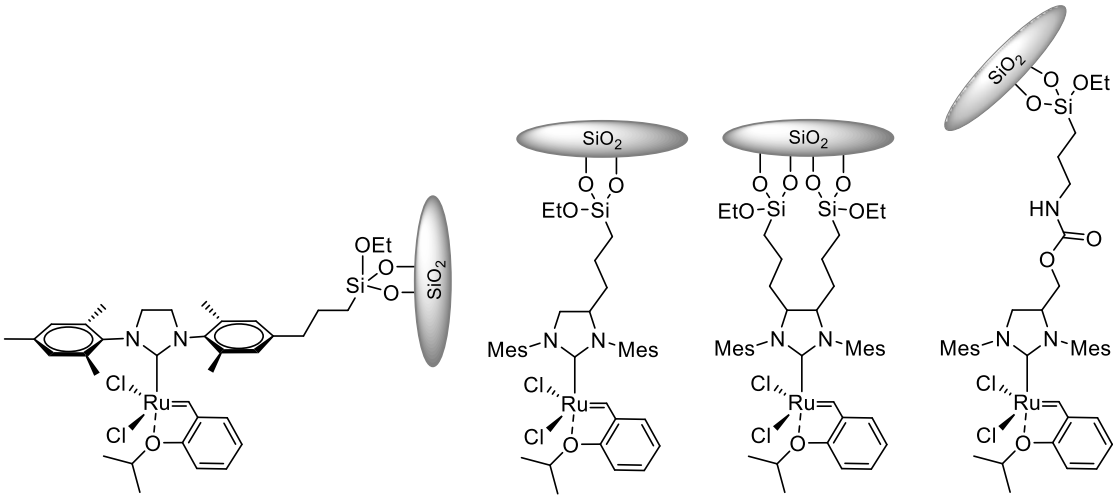

Figure 1.14 Published Hoveyda Grubbs 2nd generation catalyst immobilized onto silica materials via the NHC ligand. Mes= mesitylene.[104,116-118]

Grubbs and co-workers reported the synthesis of an HGII catalyst bearing a triethoxysilyl-group at the mesitylene or the imidazole moiety (Figure 1.14). A higher catalytic activity was observed for catalyst precursor modified at the imidazole moiety, as the linkage *via* the mesitylene ring probably causes interactions between the silica material and the active ruthenium center, thereby inhibiting a fast metathesis reaction. Mongé-Marcet *et* al.

reported on an immobilization of a disilylated HGII catalyst onto silica by co-gelification, leading to controllable catalyst loadings.[117] In addition, they prepared a hybrid silica material by linking a monosilyated HGII catalyst to mesoporous SBA-15 silica (Figure 1.14)[118]. All these described catalysts showed a good performance in the RCM of different dienes even when the catalyst was recycled for at least three times.

The procedures mentioned so far involve all the synthesis of a modified Ru-based catalyst precursor which is grafted onto silica material by condensation or co-gelification. On the contrary, Copéret and co-workers described a strategy where a functionalized mesoporous silica material was prepared containing regularly distributed NHC-moieties that can be further converted with GI catalyst precursor to give the corresponding Ru-NHC derivatives covalently bonded on the silica material (Scheme 1.9).[119] These catalysts showed a high catalytic activity in the self-metathesis of ethyl oleate.

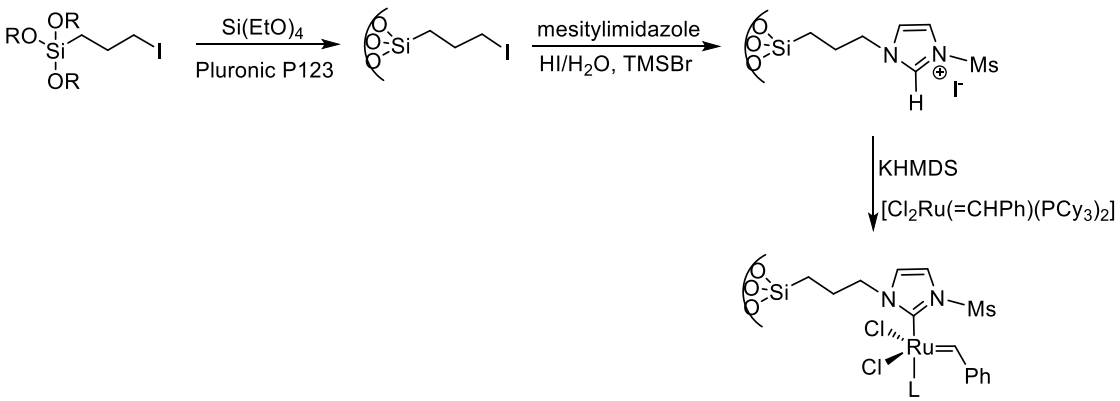

Scheme 1.9 Preparation strategy for immobilized olefin metathesis catalyst on mesoporous silica materials reported by Copéret and co-workers. Ph=phenyl, Mes= mesitylene. [119]

With the development of immobilized Hoveyda-Grubbs catalysts, the transformation of substrates such as fatty acids is also possible in a continuous flow process. This opens the possibility for industrial applications.

1.2.3.2 Use of Immobilized Olefin Metathesis Catalysts for the Conversion of Unsaturated Fatty Acids

In contrast to homogeneous catalysts, immobilized catalysts are only rarely used for the conversion of renewable lipids and fatty acids. Zelin *et* al. describe the preparation of a non-covalently bonded HGII catalyst precursor on silica by impregnation. With high catalyst loadings of 1 mol% they obtained an equilibrium conversion of 50 % in the self-metathesis of methyl oleate.[120] The same group reported on the ethenolysis of methyl oleate using the same catalytic system.[121] At a catalyst loading of 4 mol% and an ethylene pressure of 1.25 bar, conversions of up to 82 % with selectivities for ethenolysis products of 77 % were reached. For both reactions, methyl oleate conversion rates were found to be low compared to the homogeneous catalyst. However, ruthenium leaching was negligible indicating a sufficient anchoring of the catalyst.

The performance of self-metathesis of methyl oleate by means of an immobilized catalyst was also described by Bek *et* al. (Scheme 1.10). [115] They modified mesoporous SBA-15 silica material with a phosphine linker enabling the covalent attachment of a Grubbs 2nd generation catalyst by ligand exchange. In this case, equilibrium conversion was reached after 2 h using 0.4 mol% of the immobilized catalyst.

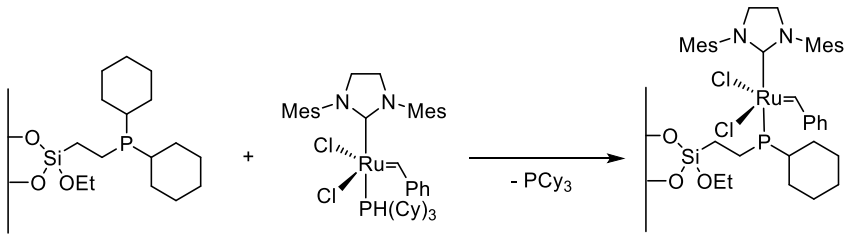

Scheme 1.10 Immobilized Grubbs 2nd generation catalyst for the self-metathesis of methyl oleate. Cy= cyclohexyl, Ph=phenyl, Mes= mesitylene. [115]

Another supported olefin metathesis catalyst that was studied in the self-metathesis of methyl oleate was reported by Cabrera *et* al., where HGII type catalysts adsorbed onto silica material were applied (Figure 1.15).[122] In contrast to Zelin and Bek, the catalyst was used for continuous flow applications, showing an equilibrium conversion of around 30 % over 420 min in cyclohexane. Even though a TON of 2475 was reached, a relatively high ruthenium leaching of 12 to 19 % was observed. This hints at an insufficient strong binding of the catalyst precursor to the solid support.

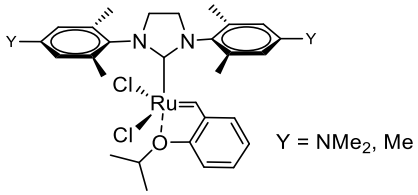

Figure 1.15 Olefin metathesis catalyst precursor that was immobilized by adsorption onto silica support.[122]

1.3 Supercritical Carbon Dioxide

In 1822, Baron Charles Cagniard de la Tour first described the critical point of different substances. Beyond a specific temperature and pressure, the densities of the liquid and gaseous phases of a specific substance become equal and the distinction between them disappears, leading to a single supercritical fluid phase.[123] In this supercritical phase, a liquid-like density is observed resulting in a comparable solvent strength to that of a liquid. At the same time, a gas-like viscosity and surface tension are observable, enabling greater penetration into porous solids. By changing the pressure and temperature, the properties of the supercritical phase can be tuned towards a more gas-like or liquid-like behavior.

Especially supercritical carbon dioxide is a widely used supercritical medium due to its chemical and physical properties such as a non-flammability and no toxicity, relatively low cost and moderate critical constants (31°C, 73,8 bar, Figure 1.16).[124]

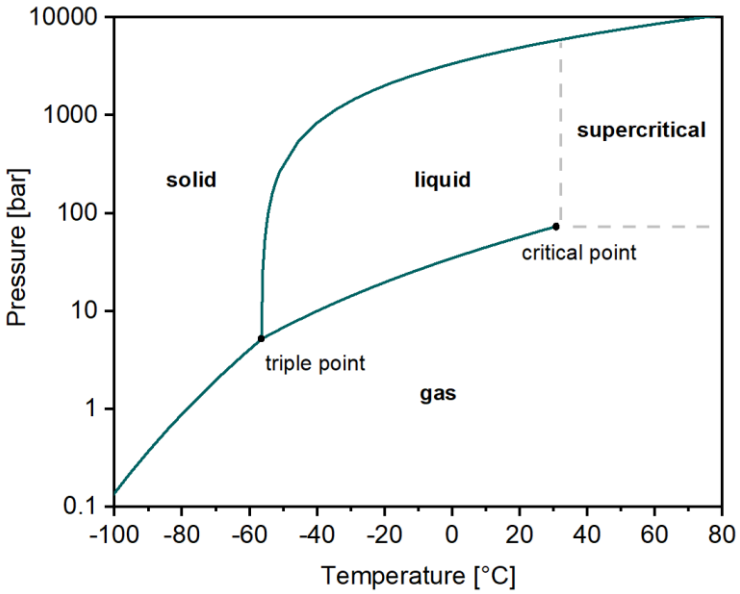

Figure 1.16. Phase diagram of carbon dioxide.[124]

Furthermore, it is inert to a wide range of chemicals and shows a good heat transport capacity. Even though it is a greenhouse gas, it does not intensify the greenhouse effect when it is withdrawn from the environment to use it in a process and subsequently again released to the environment. Regarding these properties, $scCO_2$ is an attractive and green alternative to organic solvents. Thus, in the recent decades there has been a high amount of attention paid to the use of supercritical liquids as extraction, chromatography and reaction medium.

1.3.1 Supercritical Carbon Dioxide as Extraction Medium of Renewable Lipids

Various natural compounds including vitamins, natural pigments, oils and aromas show a good solubility in $scCO_2$.[125,126] Thus, one of the most widely used application of $scCO_2$ is the extraction of worthwhile products from natural resources. Total CO_2 consumption in supercritical extraction processes is estimated to approximately 30 000 and 35 000 tons in 2012. Worldwide, over 100 facilities are estimated to use dense CO_2 for extraction and purification purposes. Since the 1970s, large-scale commercial plants using $scCO_2$ extraction have been in operation in the food, pharmaceutical and textile industries.[127] Decaffeination of coffee was one of the first processes commercialized using supercritical CO_2. Besides this process, supercritical fluid extraction was used to refine cooking oil and recover flavors from spices, hops[128] and other plant materials[129]. Furthermore, extraction and purification of food supplements and active ingredients for pharmaceuticals is performed.

Traditional extraction methods involve the utilization of organic solvents, where the separation of the desired compound is accomplished by its dissolution in the organic solvent, enabling a separation from the solid residue. To isolate the pure compound, a tedious removal of the solvent under high temperatures or low pressures is necessary. In contrast, the usage of $scCO_2$ facilitates the complete removal of the solvent from the product just by depressurization. Due to the mild critical parameters of CO_2, low process temperatures can be applied, leading to a higher compound stability during the process. As the solubility is depending on the density and dielectric constant of CO_2, which themselves is depending on the used pressures and temperatures, process parameters can be easily tuned. This allows for a higher selectivity in the extraction process.[130,131] A main disadvantage of $scCO_2$ extraction are the high investment costs compared to conventional methods. However, as solvent residues in the product can be avoided and meet legal limitation laws for human and animal applications, this drawback is balanced out. Thus, $scCO_2$ extraction is a suitable alternative to organic solvent extraction, serving already in industrial applications.

In recent times, extraction of essential oils by $scCO_2$ gained in importance, since increasingly stringent environmental regulations in the nutrition and health sector let to the need for clean extraction technologies.[132] In this context, extraction of oils from several natural biomasses were studied, including crop plants such as sunflower, soybean and rapeseed, nuts as well as fruits. To reach maximum extraction yields, reaction parameters such as

temperature, pressure and extraction time were tuned. These studies revealed that higher pressures have a positive effect on the extraction yield, as the solubility of lipids in $scCO_2$ increases with the pressure. On the contrary, temperature shows a more complex behavior. At pressures close to the critical point, temperature increase reveals a negative effect whereas at higher pressures elevated temperatures enhanced the extraction yield.[133,134] In addition, other reaction parameters such as flow rates, the extractor set-up and the use of co-solvents can highly influence the extraction performance.

Next to plant oils and fruits, microalgae oil extraction attracted the attention mostly in context of biofuel production.[135,136] In this case, reported optimized parameters vary widely as different algae strains, cultivation conditions and cell disruption pre-treatments make an additional contribution to the extraction performance.[137,138,139] Extraction of the herein used microalgae strain *Phaeodactylum triconutum* was reported only scarcely. Tommasi *et* al. reported on the extraction by dimethyl carbonate and $scCO_2$ using deep eutectic solvents.[137] They demonstrated that a significant improvement in extraction efficiency from 1 to 7 wt% of the dry weight can be reached when the microalgae cells were pretreated with deep eutectic solvents and microwave, as the cell wall is destroyed. Recently, our group published an enhanced extraction of *Phaeodactylum tricornutum in* $scCO_2$ by using high temperatures, pressures as well as ultra-sonication as pretreatment.[140] Under these conditions a maximum lipid yield of 25 wt% was reached with lower amounts of pigments compared to the Folch extraction method (2.5 % *vs.* 1 %). This demonstrates that $scCO_2$ can be used as an efficient extraction method for lipids.

1.3.2 Supercritical Carbon Dioxide as Reaction Medium for Olefin Metathesis

Supercritical CO_2 has been applied as reaction medium in several industrial relevant reactions, including hydroformylation, hydrogenation, polymerization and alkylation. In contrast, olefin metathesis in $scCO_2$ is not widely explored yet. The first olefin metathesis, performed in condensed CO_2 as reaction medium was published in 1996 by Mistele *et* al.[141] They demonstrated a ROMP of norbonene using $[Ru(H_2O)_6(tos)_2]$ as catalytic system, which yielded molecular weights comparable to those obtained in organic solvent systems. Furthermore, he observed that by the addition of methanol, resulting in an improved solubility of the initiator, the cis/trans ratio of the polymer can be controlled.

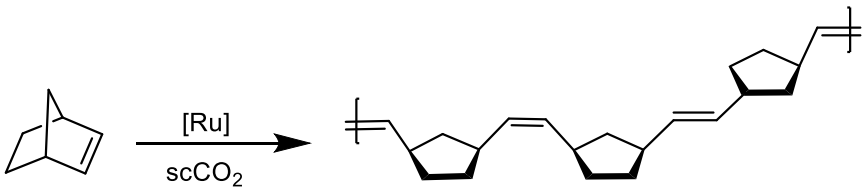

Scheme 1.11 Ring closing metathesis polymerization of norbonene in $scCO_2$.

Fürstner *et* al. described a higher activity in ROMP of norbonene when well-defined GI and GII catalysts were used.[142] Their efficiency was similar to that in chlorinated organic solvents. Cassidy and co-workers showed that the microstructure of polynorbonenes arising from ROMP can be adjusted with ruthenium and molybdenum catalyst by the polarity of the reaction medium. Upon addition of methanol, THF or DMSO, he observed for ruthenium metathesis catalysts a high trans/cis ratio, whereas molybdenum catalyst showed a reversed behavior.

Next to ROMP, RCM in $scCO_2$ of several dienes with ruthenium and molybdenum catalysts was analyzed by Fürstner and Murruzzu *et* al.[143,144] This enabled the synthesis of biologically active products such as Karahanaenone and Oxazolidinylpiperidine, used as olfactory substance and precursor of glycosidase inhibitor, respectively. In addition, an influence of the CO_2 density on the competition between intra und intermolecular reactions was monitored. By applying high densities, intramolecular RCM is favored whereas lower densities resulted in intermolecular acyclic diene metathesis (ADMET). Thus by adjusting the CO_2 density, the reaction could be controlled towards oligomers or medium size rings.

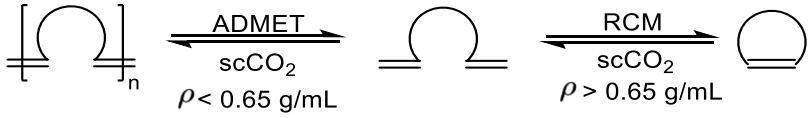

Scheme 1.12 Influence of CO_2 density on the competition between ADMET and RCM.

A further profit of the utilization of $scCO_2$ instead of organic solvents can be found in the acido-basic properties of CO_2. Whereas in organic solvents, RCM of substrates containing amino groups is often inhibited, a temporary protection group formed in $scCO_2$, facilitates the reaction. [142, 143]

Besides ROMP and RCM, only little research has been conducted in the field of cross metathesis in $scCO_2$. Song *et* al. reported on the ethenolysis of ethyl oleate using 1 mol% of GI (Scheme 1.13).[145] He revealed at 35 °C and 80 bar a high equilibrium conversion of around 90 % in $scCO_2$ as products were well dissolved in CO_2 in contrast to the substrate ethyl oleate. At higher pressures, products and substrate were in the same phase which is why a slower metathesis was observed.

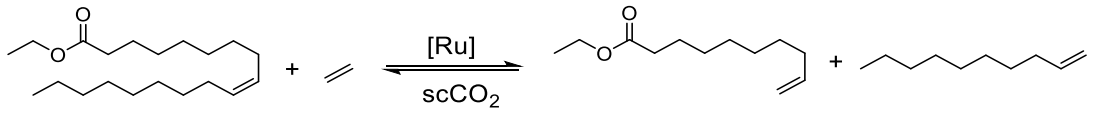

Scheme 1.13 Ethenolysis of ethyl oleate in $scCO_2$.

The catalytic upgrading of microalgae lipids by ethenolysis and butenolysis in $scCO_2$ was recently elaborated in our group (Figure 1.17).[140] The use of 0.5 mol% of HGI in the cross metathesis with ethylene as well as butylene yielded the desired mid-chain olefins and unsaturated esters. Under optimum conditions of 45 °C and 300 bar CO_2 both reactions proceeded with conversions and selectivities for the desired products of over 80 %. In addition, a simultaneous extraction and ethenolysis as well as butenolysis, respectively, was successfully performed. Compared to the separate extraction and catalysis procedure, lower conversions were observed, which was stated to be caused by slower extraction in the batch reactor compared to continuous flow extraction of the lipids.

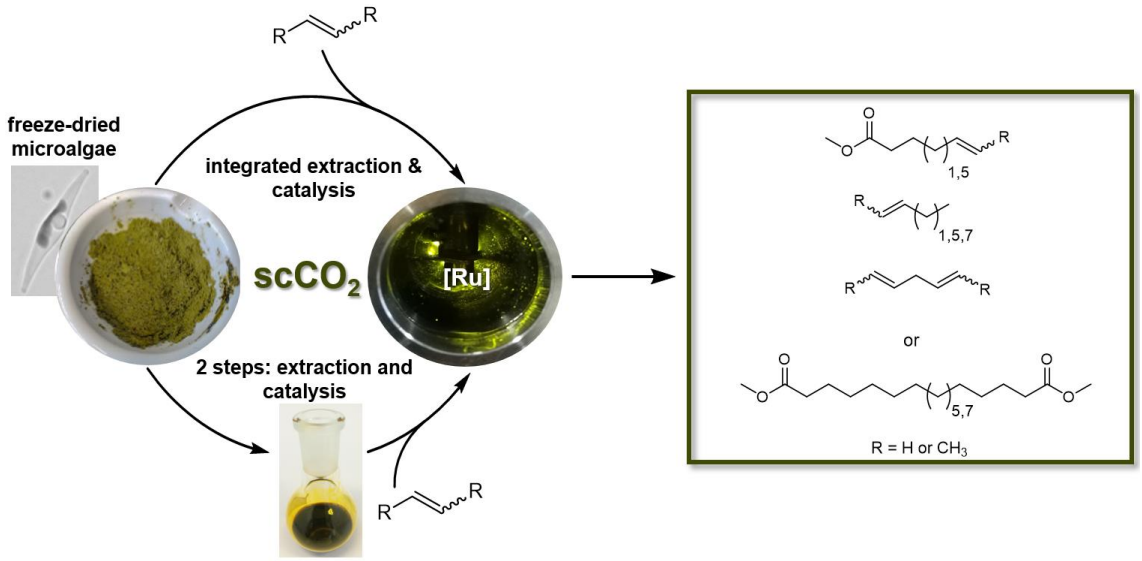

Figure 1.17 Extraction and catalytic valorization of microalgae oil by ethenolysis and butenolysis in $scCO_2$.[140]

2 Scope of the Thesis

As an alternative to today's fossil feedstock-based refineries, a biorefining of renewable feedstocks has been intensively discussed. Yet, a biorefining concept that provides suitable building blocks in a direct fashion is lacking. Rather, renewable feedstocks are defunctionalized to replace fossil-based naphtha feedstocks in a petrochemical refinery, or carbohydrate-based platform chemicals like 5-hydroxymethylfurfural with a limited scope of follow-up chemistry are pursued.[146]

The scope of this thesis comprises the implementation of a new biorefinery concept, allowing for the catalytic transformation of renewable plant oils to essential building blocks such as short chain α-olefins and terminal unsaturated esters. Based on a catalytic sequence of ethenolysis, double bond isomerization and subsequent ethenolysis, the fatty acid chains are shortened to valuable chemical building blocks in the C_3 to C_{10} regime. They represent desired intermediates as most industrial relevant products which are based on these building blocks provide already established industrial processes. In particular, they serve as monomers for the production of much sought-after polymer, surfactant and lubricants.

To simplify the overall process starting from the biomass, the extraction of the plant oils and their catalytic biorefining were performed in supercritical carbon dioxide ($scCO_2$) as extraction and reaction medium. With respect to an environmentally friendly and cost-efficient process, $scCO_2$ represents a promising medium. The solubility of plant oils in $scCO_2$ is known to be increased at high CO_2 densities and thus at high pressures. To this end, customized high pressure reactor set-ups were constructed for their catalytic upgrading.

The biorefinery approach was investigated in a one-pot solution process for various renewable feedstocks including oil crops, microalgae biomass and waste oil by means of homogeneous catalysis. In this work, studies were focused on the optimization of the ethenolysis reaction in $scCO_2$ towards high conversions and selectivities for ethenolysis products, especially in the presence of isomerization catalyst and its required activation solvent methanol, as this forms the basis for a successful transformation in the multicatalytic sequential concept.

Relating to industrial applications, continuous flow processes show several advantages over batch reactions, including cost-efficient separation, recycling and reuse of the catalyst. For this reason, the utilization of an immobilized Hoveyda-Grubbs olefin metathesis catalysts was investigated in the self-metathesis and ethenolysis of fatty acids in organic solvents as well as in $scCO_2$ in a continuous flow mode. Ultimately, a sequence of ethenolysis-isomerization-ethenolysis was performed and reaction conditions screened to allow for the implementation of the biorefinery approach in a high-throughput technique.

3 Batch Solution Process for Combined Ethenolysis and Isomerization

3.1 Introduction

Olefins and aromatics form the basis for a wide range of sought-after products such as plastics, electronics, coatings and textiles. So far, they are mainly gained from crude oil. However, with the depletion of petrochemical resources, the production of chemicals from renewable resources is the solution to become independent from crude oil. Routes to aromatics from various renewable feedstocks are at an advanced stage of development, however, the production of olefin products is still challenging. Fatty acid methyl esters (FAME) have, due to their long hydrocarbon chain and ester functionalization, a high potential for a transformation into olefins and (di)esters. They can be found in several renewable raw materials including plant oils, waste oils and non-food crops as well as microalgae. In 2021, around 200 million tons of plant oils were produced worldwide whereby approximately 20 % of it was used for non-food applications.[3] The production of surfactants, lubricants, personal care products and biofuels from plant oils such as palm, sunflower and soybean oil is already established in the industry.[147] Here, the fatty acids are used without or only after minor chemical modifications such as a transesterification reactions. As opposed to that, there are only few industrial examples where plant oils are converted into platform chemicals such as olefins and dicarboxylic acids. One example is the conversion of plant oils to long-chain olefins, unsaturated esters and diesters by means of olefin metathesis, which is performed by the company Elevance on an industrial scale. On the other side, the company Neste established technologies to transform waste materials including residue fats and oils by hydroconversion into renewable long chain isoparaffinic hydrocarbons. These renewable hydrocarbons cover the long chain olefin segment which allow not only for the production of renewable fuels but also of various plastics.[8,10]

However, these procedures do not provide short chain linear alpha olefins, which are produced in one million tons per year by the petroleum-based Shell Higher Olefin Process (SHOP), underlining the high industrial demand. Moreover, the synthesis of short- to mid-chain diacids (C_3 to C_{11}) plays an important role for the polymer industry. Short chain diacids (up to C_6) are produced on a large scale but mainly by petrochemical routes until today. Mid-chain diacids including C_9 and C_{10} diacids, are synthesized from renewable oils, although the established industrial synthesis routes are tedious or bear technical and safety challenges such as in ozonolysis.

Yet, an industrial biorefinery concept that provides suitable linear short chain building blocks in a direct fashion to enable the production of a wide range of chemicals and materials by already established technical processes, is lacking. Ethenolysis is a powerful reaction to upgrade fatty acids to terminal α-olefinic and ester products. However, it leads due to the prescribed structure of fatty acids in nature, to a narrow product distribution which consists mainly of mid- and long-chain products. Gooßen *et al.* described an isomerizing ethenolysis of methyl oleate that allows for a broadening of the product distribution and provides next to the long-chain segments (up to C_{18}) also short-chain products.

In this chapter, a biorefining concept is described that specifically targets short chain α-olefins and unsaturated esters in the C_3 to C_{10} regime, as most products and intermediates today are based on these building blocks. This allows for the utilization of already established industrial processes for their further transformation (Figure 3.1). To this end, an initial ethenolysis step can half the chain length, with subsequent further sequential isomerization and ethenolysis to the final desired products. As an environmentally benign reaction medium supercritical carbon dioxide ($scCO_2$) is employed. This can also simplify the overall biomass to product process as $scCO_2$ is particularly well suited to selectively extract lipids from biomass, and the extraction solution may be fed to the catalytic conversions without the need for changing solvents and other work-up.

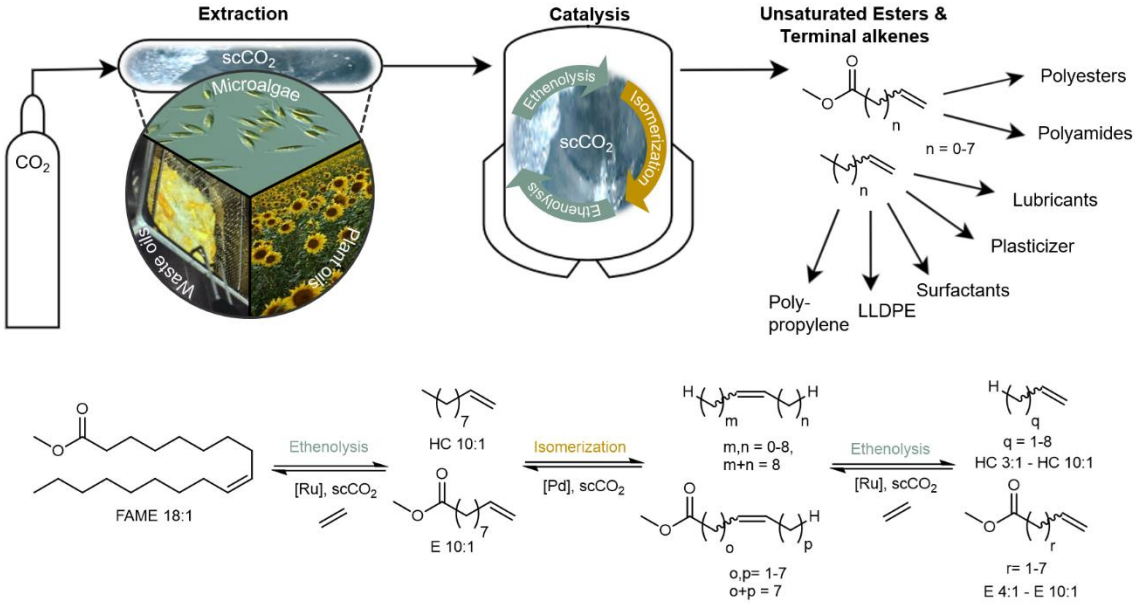

Figure 3.1 Schematic representation of the three-step catalytic biorefinery batch process towards short chain 1-olefins and unsaturated esters, shown exemplary for methyl oleate.[146]

3.2 Results and Discussion

3.2.1 Construction of the Reactor Set-up

To implement the desired biorefinery approach in supercritical carbon dioxide ($scCO_2$), a suited reactor set-up is required. The solubility of fatty acids is reported to be increased in $scCO_2$ when its density comes close to 1 g mL^{-1}.[148] In order to reach a high carbon dioxide density at required reaction temperatures of 50-85 °C, to ensure a sufficient catalytic activity in the ethenolysis of fatty acids, high pressures between 250 and 500 bar are necessary. For this purpose, a high-pressure semi-batch reactor set-up was constructed (Figure 3.2).

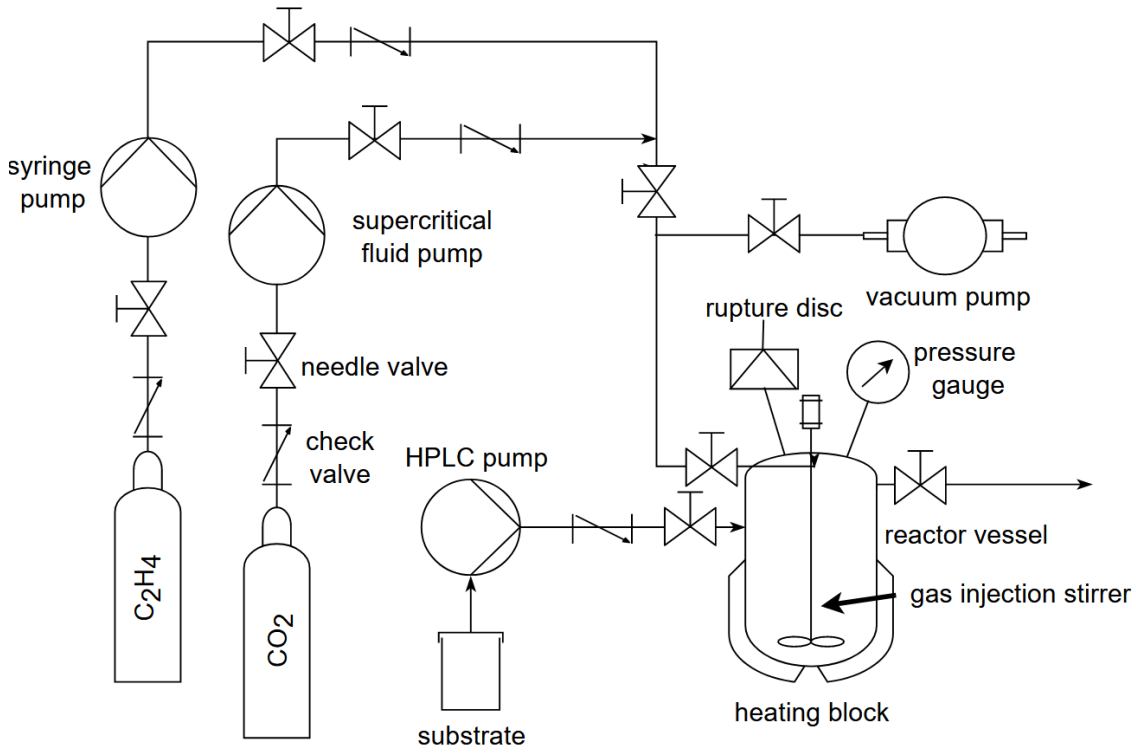

Figure 3.2 Technical drawing of the reactor set-up designed for a consecutive reaction of ethenolysis - isomerization – ethenolysis.[146]

As a reaction chamber, a 100 mL stainless steel vessel with three fixed needle valves that resist pressures up to 700 bar was chosen. The inside pressure is monitored over the whole process by a digital pressure gauche. A rupture disc opens at 700 bar to prevent over pressurization. A heating block is used to allow for a precise temperature control of the inlet temperature which is further equipped with water cooling enabling for a rapid cooling of the reaction mixture when necessary. Three needle vales are connected to the reactor vessel *via* different connecting types (Figure 3.3). Needle valve 1 is directly connected to the interior space of the vessel and serves as inlet for the catalyst solutions which are pumped against

the inlet pressure of the reactor by a high-performance liquid chromatography (HPLC) pump. In contrast to a simple batch reactor this enables the addition of catalyst solutions and additives during the course of the reaction. Therefore, a dissolving of the substrate in CO_2 and ethylene can take place prior to the addition of the catalyst, enabling a faster initial reaction. In addition, various catalysts can be added over the course of the reaction allowing for a sequence of catalytic reactions.

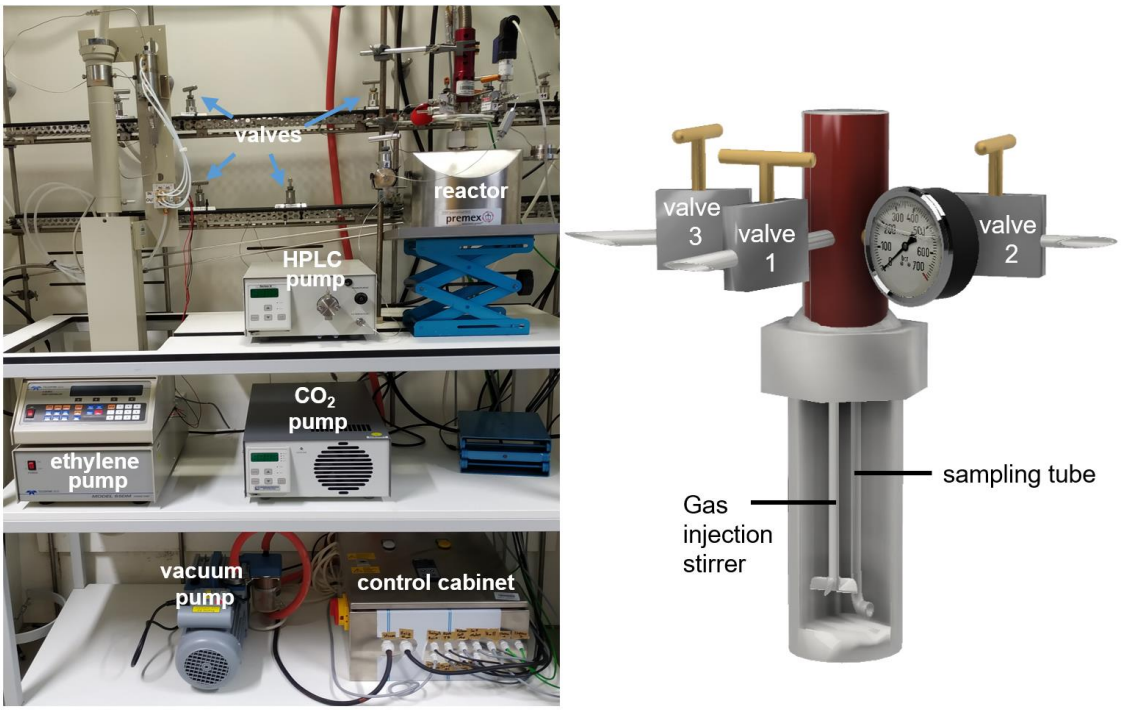

Figure 3.3 Picture of the designed reactor set-up which is connected to a control cabinet (left) and scheme of the reactor vessel with the connected valves (right). [146]

Needle valve 2 serves as outlet of the reaction mixture, being connected inside the vessel to a sampling tube that provides a simple and homogenous sampling of the supercritical mixture. Valve 3 is connected to a gas injection stirrer. Apart from stirring, it enables the evacuation of the reaction vessel and, compared to a head-space pressurization, shows an increased velocity of the gas flow, leading to a faster mixing of the media. In detail, CO_2 pressures are built up by a high-pressure supercritical fluid pump and ethylene is delivered by a high-pressure syringe pump that allows the dosing of ethylene at pressures of up to 700 bar. A cooling jacket is installed at the cylinder to prevent an uncontrolled ethylene polymerization due to temperature increase while compression. The installed pumps, the stirrer as well as the heating block and the pressure gauche are connected to a control cabinet which enables a remote access of the components by the program Lab-vision®. In detail, a programmed sequence of commands was prepared that automatically controlled pressures, temperatures and flow rates of the connected reactor parts making the process

more efficient and safer (Figure 3.4 a). The process data are collected over the whole reaction time, enabling the analysis of pressure and temperature changes over the course of the reaction (Figure 3.4 b).

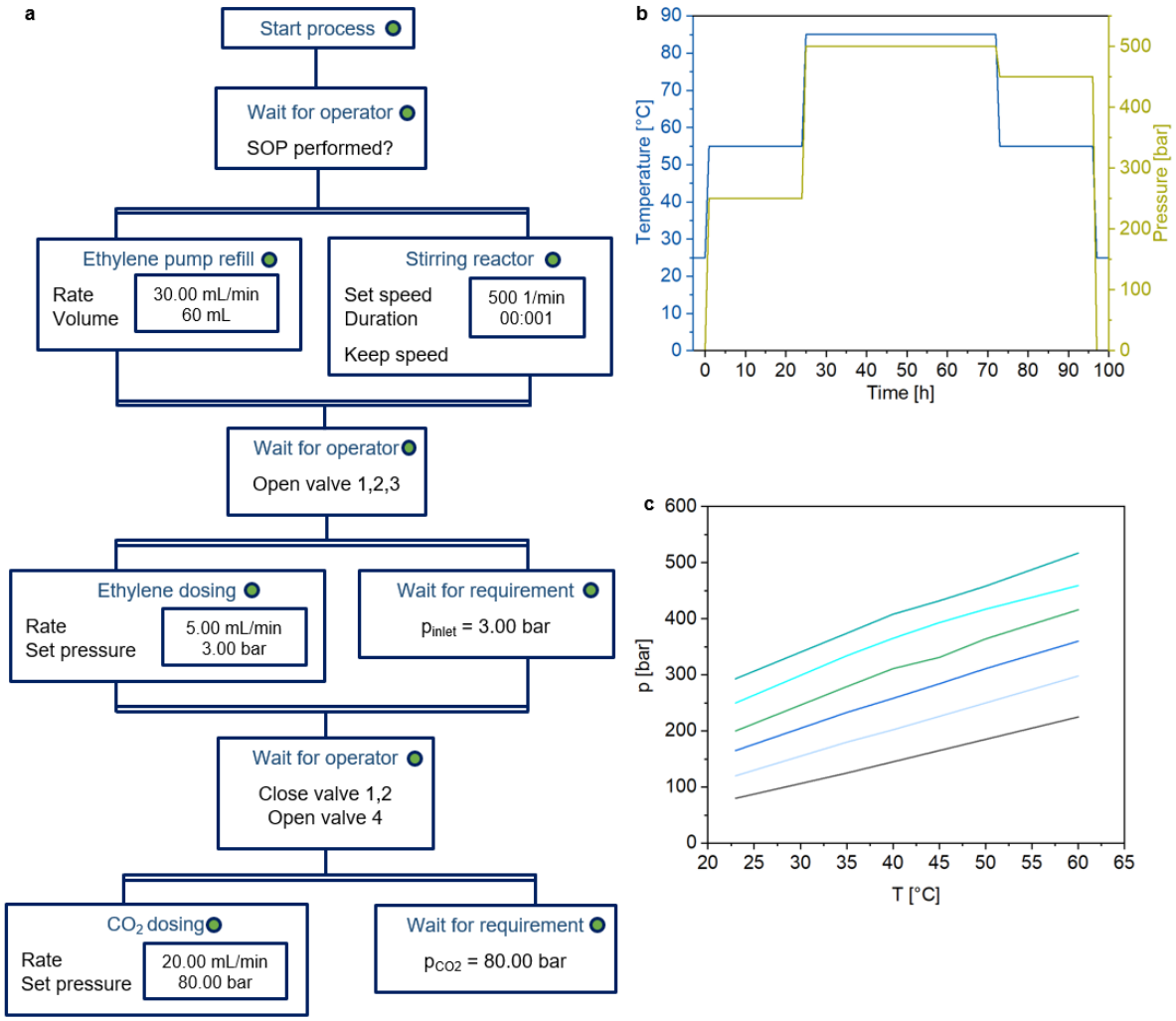

Figure 3.4 a, row of commands which are automatically performed by the Labvision program. b, example of temperature and pressure developments during a reaction procedure in the built reactor vessel. c, temperature – pressure curves of carbon dioxide in the 100 mL reaction vessel. [146]

Before a catalytic reaction was performed using the new reactor set-up, the pressure behavior of carbon dioxide at different temperatures was analyzed (Figure 3.4 c). The vessel was pressurized with a defined CO_2 pressure at a specific temperature. While increasing the temperature over time, the inlet pressure was measured yielding temperature-pressure curves. These serve for the prediction of end pressures at specific temperatures, preventing the built up of too high pressures.

Several sealing ring materials were tested for their resistance to a CO_2 ethylene mixture including fluorinated rubber (FKM), ethylene-propylene-diene-rubber (EPDM) as well as polytetrafluorethylen (PTFE) (Figure 3.5). Whereas PFTE is too stiff to allow for an appropriate sealing of the reaction vessel and the check valves, FKM did not resist the CO_2 ethylene product mixture leading to the formation of fine cracks and subsequent pressure loss. In contrast, EPDM has a good chemical resistance as well as a high tightness even after up to 20 cycles. Therefore, all further catalytic reactions were performed using EPDM as sealing material.

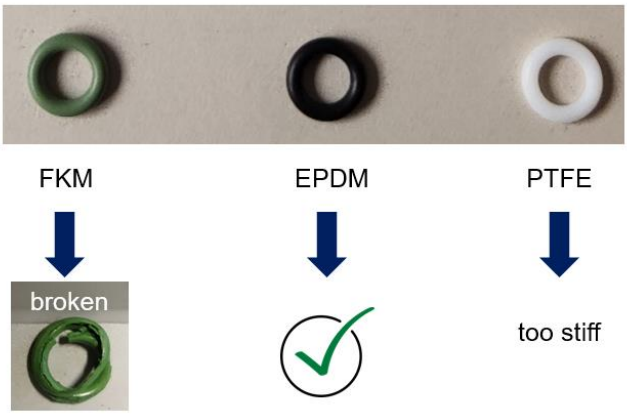

Figure 3.6 Tested sealing materials for a CO_2/ ethylene mixture.

3.2.2 Ethenolysis of Transesterified Sunflower Oil in $scCO_2$

The targeted multicatalytic sequential approach, comprising of catalytic ethenolysis and double bond isomerization, allows for the transformation of renewable fatty acids to a broad spectrum of industrial relevant building blocks such as α-olefins and precursors for diacids. To provide a robust process, suitable conditions in $scCO_2$ for both catalytic reactions need to be found. This work focusses on the investigation of the ethenolysis steps. The fatty acid methyl oleate (FAME 18:1) is a common model substrate for renewable fatty acids since it is present in various plant and microalgae oils. For the analysis of a single ethenolysis in $scCO_2$, transesterified high oleic sunflower oil (HOSO) from DAKO AG was used as it represents a simple model renewable feedstock with a main content of 92.5 % for the mono unsaturated fatty acid methyl oleate and only small amounts of the saturated fatty acids methyl palmitoleate (FAME 16:0) and methyl stearate (FAME 18:0, Figure 3.8).

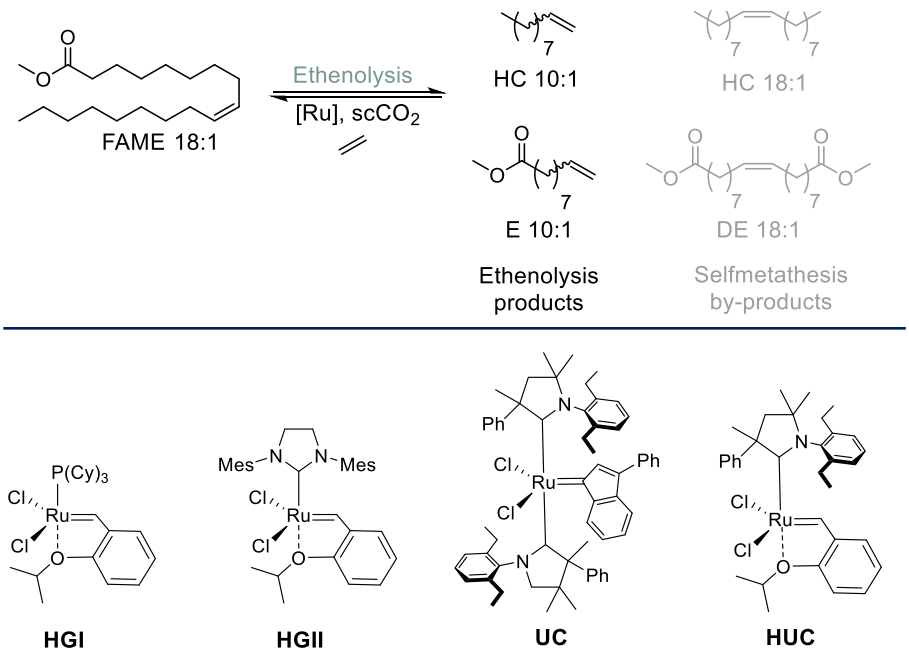

Figure 3.7 Reaction scheme of an ethenolysis reaction of methyl oleate with possible self-metathesis by-product formation (top). Chemical structure of the Hoveyda Grubbs 1st generation catalyst (HGI), Hoveyda Grubbs 2nd generation catalyst (HGII), the UltraCat (UC) and the Hoveyda type UltraCat (HUC) (bottom).

The catalytic upgrading of methyl oleate to methyl 9-decenoate (E 10:1) and 1-decene (HC 10:1) *via* ethenolysis was recently demonstrated in $scCO_2$.[20] It was shown that the Hoveyda Grubbs 1st generation catalyst (HGI, Figure 3.7) dissolves in $scCO_2$ and allows the transformation of methyl oleate into the desired ethenolysis products with conversions of up to 88 % and selectivities for the ethenolysis products of up to >99 % after 6 h.

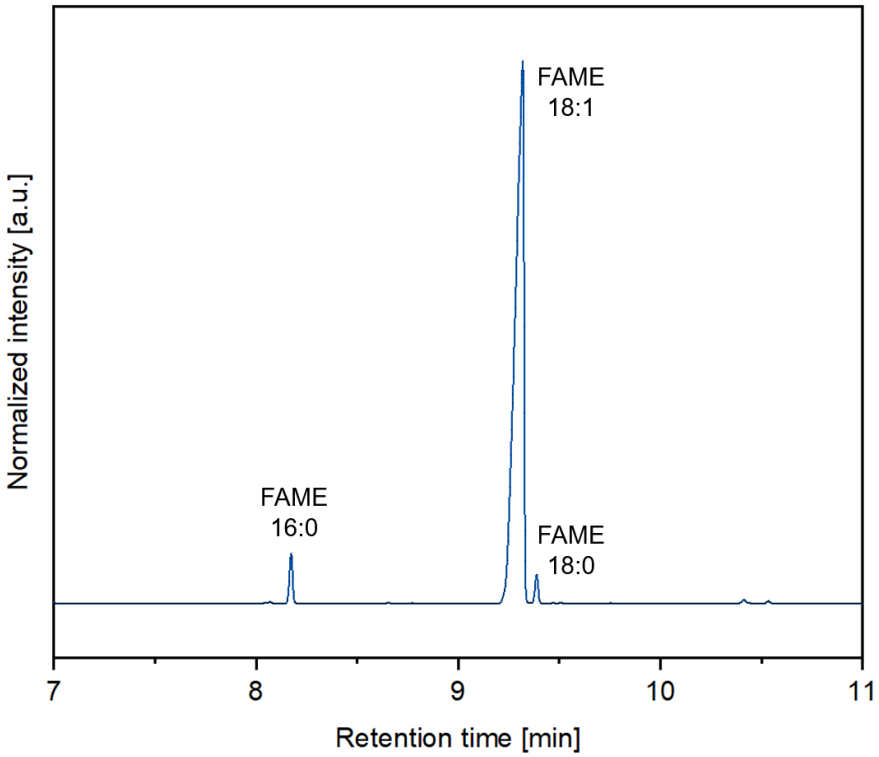

Figure 3.8 Gas chromatogram of transesterified high oleic sunflower oil showing a fatty acid methyl ester mixture of methyl palmitoleate (FAME 16:0), methyl stearate (FAME 18:0) and methyl oleate (FAME 18:1).

The highest achieved catalytic productivity, which is reflected in the turnover number (TON), was calculated to 650 using the catalyst under the described conditions. Since a biorefinery concept is pursued that is competitive with regard to effort and sustainability, lower catalyst loadings as well as higher TONs are desired. In literature, the Hoveyda Grubbs 2nd generation catalyst (HGII) as well as the Ru-based catalysts bearing cyclic alkyl amino carbene ligands (CAAC) such as the UltraCat (UC) and Hoveyda type analogue (HUC), feature good productivities in the neat ethenolysis of methyl oleate. Especially UC and HUC are known to be highly active, as investigations revealed that the presence of the cyclic alkyl amino carbene ligand suppresses β-elimination of the unsubstituted ruthenium-acyclobutane formed by the reaction of the reactive catalyst with ethylene.[149] To find the best suited catalytic system in $scCO_2$, all four catalysts were screened for their catalyst performance and selectivity in the ethenolysis of HOSO (Table 3.1).

Table 3.1. Screening of the catalytic activity in the ethenolysis of HOSO in $scCO_2$.

Entry	Cat.	mol% [cat]	Conv. [%]*	Selec. [%]†	TON
1	HGI	0.5	70	99	140
2	HGII	0.5	92	99	186
3	HUC	0.5	91	99	182
4	UC	0.5	90	99	180
5	HGII	0.05	49	79	980
6	UC	0.05	82	99	1640
7	HUC	0.05	80	99	1600

Reaction conditions: 2 mL of HOSO, 20 bar ethylene, p_{tot} at 45 °C = 450 bar, 6 mL of DCM, 2 h, ρ_{CO_2} = 0.955 g/ml, * determined by gas chromatography, † with respect to ethenolysis products.

First, 0.5 mol% of catalyst, 20 bar of ethylene and a total pressure of 450 bar CO_2 at 55 °C were employed for all four catalysts respectively (Table 3.1, entry 1-4). To compare the initial performance of the catalysts, the conversions were calculated after 2 h *via* gas chromatography (GC). With the use of $scCO_2$ as solvent, the HGII, UC and HUC catalysts show with conversions between 90 and 92 % (Table 1, entry 2, 3, 4) higher performances than the HGI catalyst with a conversion of only 70 % (Table 3.1, entry 1). This is also reflected in higher TON for HGII (186), UC (180) and HUC (182) (HGI catalyst 140). Since the HGII, UC and HUC catalysts feature a similar catalytic productivity and selectivity, lower catalyst loadings of 0.05 mol% for these catalysts were applied. The two catalysts, bearing CAAC ligands reveal a higher catalyst performance than the HGII catalyst. Whereas UC and the HUC catalyst reached after 2 h a conversion of around 80 % and a selectivity of 99 %, the HGII catalyst only resulted in a conversion of 49 % as well as a low selectivity for ethenolysis products of 79 %. Moreover, their high performance indicates a sufficient solubility in $scCO_2$. Even though a TON of 1640 could be reached under these conditions, higher productivities are desired to realize a competitive and sustainable bio refinery approach. Thus, reaction conditions for UC were optimized in terms of catalyst loading, ethylene pressure, reaction temperature and reaction time. (Table 3.2).

Table 3.2 Catalyst Performance of UC at different reaction conditions.

Entry	mol% [cat]	T [°C]	$p_{ethylen}$ [bar]	t [h]	Conv. [%]*	Selec. [%]†	TON
1	0.05	45	20	2	82	99	1640
2	0.05	55	10	4	92	98	1840
3	0.03	55	10	4	96	98	3266
4	0.01	55	10	4	92	96	9200
5	25 ppm	55	10	4	87	97	34 800
6	10 ppm	55	10	4	25	98	25 000
7	10 ppm	55	10 ‡	4	78	97	78 000
8	10 ppm §	55	10 ‡	4	5	98	5000

Reaction conditions: 2 mL of HOSO, 20 bar ethylene, p_{tot} at T = 450 bar, 6 mL of DCM, ρ_{CO_2} = 0.955 g/ml, * determined by gas chromatography, † with respect to ethenolysis products, ‡ high purity ethylene 4.5, § HUC was used.

Since UC exhibits a comparable high initiation temperature of 40 °C, the reaction temperature was increased to 55 °C and the reaction time was extended to 4 h to ensure a complete reaction (Table 3.2, entry 2). Under these conditions an enhanced conversion of 92 % with a steady selectivity of 98 % as well as an increased TON of 1840 was observed. A further decrease of the catalyst amount to 0.03 and 0.01 mol% showed conversions and selectivities in the same range, thus increased TONs of up to 9200. Even lowering the catalyst loadings to 25 ppm resulted in high conversions and selectivities of 87 % and 97 %, respectively. Moreover, an elevated TON of up to 34 800 could be achieved with 25 ppm (Table 3.2, entry 5). Under the used conditions, we assume that the catalyst/DCM solution forms one phase with the $scCO_2$. The increased productivity upon reduction of the catalyst loadings is in accordance with observations published by Grubbs, Fogg and others.[149] Investigations of Fogg and co-workers revealed that by lowering the catalyst loading, bimolecular decomposition pathways can be suppressed and thus an enhanced productivity is achieved.[13] However, lower catalyst loadings of 10 ppm led to a diminished productivity of 25000. Grubbs and co-workers could show that the use of ethylene with a higher purity of 99.995 % in contrast to 99.95 % resulted in a 1.5 times increased TON in the ethenolysis of methyl oleate.[59] Within this work, we could demonstrate that the use of purer ethylene (99.995 %) led at a catalyst loading of 10 ppm to a further increased catalytic productivity of 78000 in $scCO_2$ (Table 3.2, entry 7, Figure 3.9). This is to our knowledge the highest observed TON so far for the ethenolysis of methyl oleate in $scCO_2$. As a comparison, the reported neat

ethenolysis of methyl oleate using 10 ppm of UC, 15 bar of ethylene (4.5) at 50 °C, TONs of 60 000 were reported with the UC catalyst, illustrating a comparable performance.[150]

HUC was also tested under the optimized conditions developed with UC. As only a conversion of 5 % was reached, the use of HUC was not further pursued (Table 3.2, entry 7 & 8).

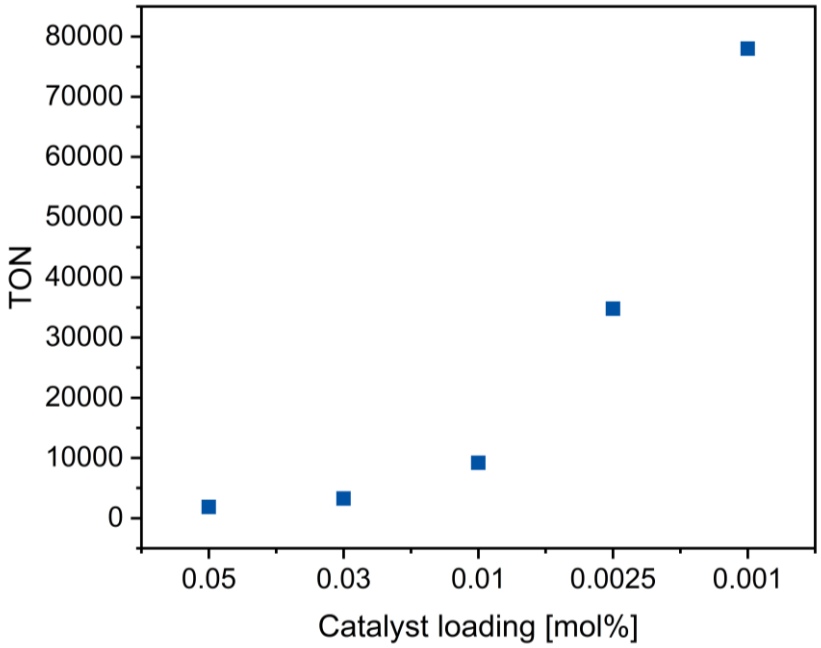

Figure 3.9. Achieved TONs in correlation with catalyst loadings.

Whereas conversions and selectivities seem to be comparable when the ethenolysis reaction with UC is performed in $scCO_2$ or in neat substrates, their reaction profiles differ over time. The initial catalytic activity in $scCO_2$ is relatively low compared to the ethenolysis reaction in neat substrates (Figure 3.10). Ethenolysis under neat conditions shows a conversion of 87 % after 30 min, in $scCO_2$ a conversion of only 21 % was reached. This lower conversions in $scCO_2$ might be due to a lower solubility of the catalyst decelerating the reaction. This trend continues in the further reaction process, as without CO_2 the equilibrium conversion is already reached after 120 min, in $scCO_2$ on the contrary it takes 240 min to end up in equilibrium.

Apart from solvent free conditions, reducing handling costs, the use of other green solvents is of industrial interest. Compressed CO_2 represents a cost-efficient, non-flammable and nontoxic medium. In addition, it serves as extraction medium, allowing for a straight-

forward process of a combined extraction and transformation of fatty acids. Thus, longer reaction times that might be required when using $scCO_2$ are reasonable.

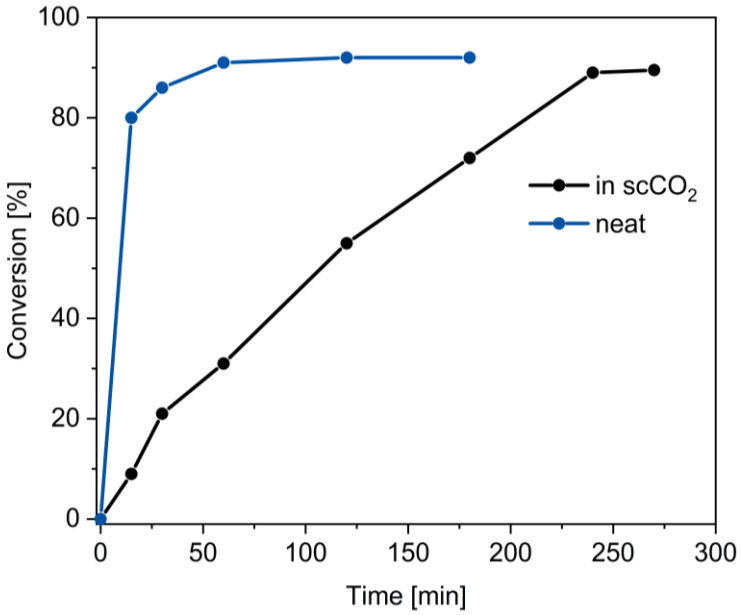

Figure 3.10. Reaction profiles for the ethenolysis of transesterified HOSO with and without CO_2. Reaction conditions: 6 mL transesterified HOSO, 0.03 mol% UC, 10 bar ethylene, 55 °C, p_{tot} = 450 bar when CO_2 is used as reaction medium.

3.2.3 Impact of Alcohols and Ethylene Pressures on the Catalyst Performance in $scCO_2$

For the pursued multicatalytic sequential biorefinery approach an additional isomerization catalyst is necessary. In previous work the catalytic system [(dtbpx)Pd(OTf)$_2$] showed to be active in the isomerizing alkoxycarbonylation with $scCO_2$ as reaction medium.[20] Thus, it was investigated in the double bond isomerization of olefins and unsaturated esters in $scCO_2$. These experiments were conducted by Felix Einsiedler as part of a joined research project.[151]

With respect to a combined reaction, several reaction parameters for both catalytic reactions need to be considered. This work focus on the ethenolysis reaction. On the one side, the [Pd] catalyst precursor requires an alcohol source to form a Pd-H species that enables the conversion of olefins and unsaturated esters into their double bond isomers.[152] Since it is known that alcohols can have a negative impact on the ethenolysis reaction, the ethenolysis productivity was analysed in the presence of methanol and ethanol.[153] For this purpose, 0.5 mL of the alcohols were added to the reaction mixture, respectively, and conversions, selectivities as well as TONs were compared (Table 3.3).

Table 3.3. Influence of co-solvent on the catalytic activity.

Entry	Co-solvent	Conv. [%]*	Selec. [%]†	TON
1	6 mL DCM	92	96	9200
2	5.5 mL DCM +0.5 mL MeOH	64	96	6400
3	5.5 mL DCM +0.5 mL EtOH	48	97	4800
4	5.9 mL DCM +0.1 mL MeOH	77	98	7800

Reaction conditions: 2 mL of HOSO, 0.01 mol% **UC**, 10 bar ethylene, T=55°C, 4 h, p_{tot}=450 bar, ρ_{CO_2} = 0.955 g/ml, * determined by gas chromatography, † with respect to ethenolysis products.

Whereas the reaction in a CO_2 /DCM mixture led to a high conversion of 92 %, the addition of MeOH as well as of EtOH resulted in a reduction to 64 % (TON 6400) and 48 % (TON 4800, Figure 3.11, Table 3.3, entry 2 & 3), respectively. In addition, ethanol appears to have a higher negative impact on the catalytic productivity. In contrast to that, the addition of alcohols had no effect on the selectivity which is high in all cases with values between 96 % and 98 %. Thus, for a combined ethenolysis and isomerization MeOH was the co-solvent of choice.

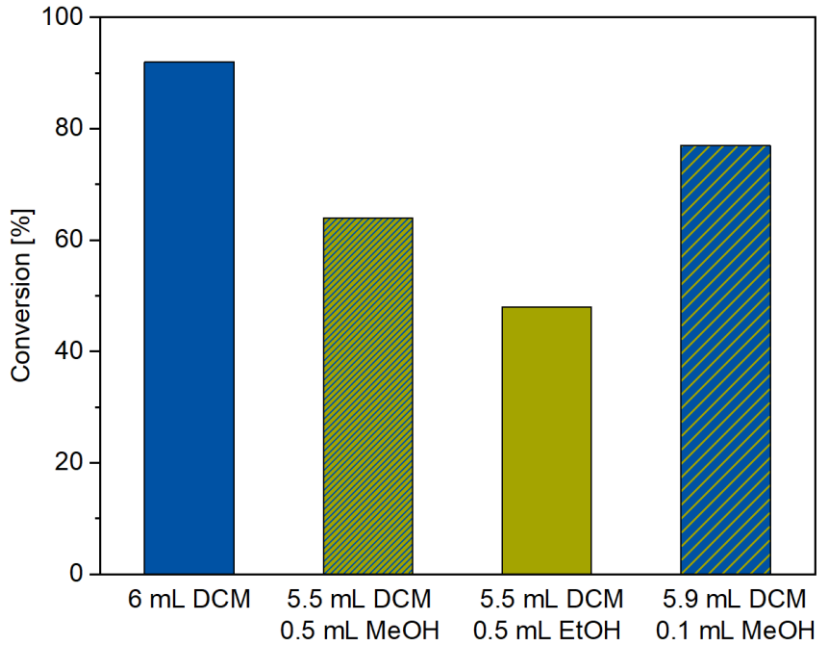

Figure 3.11. Influence of alcohols on the ethenolysis performance of HOSO in $scCO_2$. Reaction conditions: 2 mL of HOSO, 0.01 mol% UC, 10 bar ethylene, T=55 °C, 4 h.

The minimum amount of alcohol that is needed for an effective Pd-H formation, while simultaneously keeping the negative impact of methanol to a minimum, was optimized. This was found to be 0.1 mL of MeOH, which led to an ethenolysis of HOSO, with 0.01 mol% of **UC** after 4 h, to a conversion of 77 % and a selectivity of 98 %. In addition, the use of higher catalyst loadings of 0.06 mol% and longer reaction times of 6 h enhanced the conversions to over 90 %, providing a good catalyst performance in a consecutive isomerization and ethenolysis.

3.2.4 Influence of ethylene pressures on the ethenolysis performance

It could be demonstrated that the presence of 10 bar ethylene pressure during the double bond isomerization led to a reduced productivity of the isomerization catalyst.[151] This reflects the preferred unproductive coordination and addition of ethylene to the active Pd-H species, slowing down the double bond isomerization of the substrates. To ensure a sufficient isomerization in the combined reaction sequence, ethylene amounts need to be minimized during the first ethenolysis step. Thus, the efficiency of the ethenolysis reaction at lower ethylene pressures was examined (Table 3.4).

Table 3.4 Influence of ethylene pressures on the catalytic activity.

Entry	Cat. Loading [mol%]	$p_{C_2H_2}$ [bar]	Time [h]	Con. [%]*	Selec. [%]†
1	0.03	10	4	96	98
2	0.03	5	4	96	98
3	0.03	3	4	87	94
4	0.06	3‡	6	98	97

Reaction conditions: 2 mL of HOSO, T= 55 °C, p_{tot}= 450 bar, 6 mL of DCM, ρ_{CO_2} = 0.955 g/ml, * determined by gas chromatography, † with respect to ethenolysis products, ‡ p_{tot}= 250 bar.

A reduction of the ethylene pressure from 10 to 5 bar revealed no change in conversion and selectivity (Table 3.4, entry 1 & 2). In contrast to that, a further decrease of the ethylene pressure to 3 bar resulted in a decreased conversion and selectivity of 87 % and 94 %, respectively. With the use of reduced ethylene amounts a deceleration of the ethenolysis reaction can be assumed, requiring longer reaction times. Nevertheless, higher catalyst loadings of 0.06 mol% and a longer reaction time of 6 h led to high conversions of 98 % even at low ethylene pressure of 3 bar.

3.2.5 Catalyst-Catalyst interactions

In a simultaneous isomerizing ethenolysis, not only reactants and additives such as ethylene and alcohols are important parameters that need to be analyzed to enhance the catalytic performance, but also the interaction between the two catalysts. To get a closer look into this, an ethenolysis reaction was performed in the presence of the double bond isomerization precursor [(dtbpx)Pd(OTf)$_2$] (Figure 3.12). To impede catalyst activation and hence an isomerization of the fatty acids, the reaction was carried out without MeOH. Different catalyst rations of UC to [(dtbpx)Pd(OTf)$_2$] were applied. The conversions and selectivities, calculated by GC, indicated that the presence of higher amounts of the isomerization catalyst diminish the performance of UC in the ethenolysis reaction (Table 3.5, Figure 3.12).

Table 3.5. Influence of the isomerization catalyst [(dtbpx)Pd(OTf)$_2$] on the catalytic activity of the ethenolysis catalyst UC.

Entry	UC [mol%]	[(dtbpx)Pd(OTf)$_2$] [mol%]	$p_{ethylen}$ [bar]	Conv. [%]*	Selec. [%]†
1	0.03	0.00	10	96	98
2	0.05	0.03	10	80	90
3	0.03	0.03	10	66	77
4	0.03	0.05	10	10	97

Reaction conditions: 2 mL of HOSO, 6 mL of DCM, $V_{reactor}$= 100 mL, T=55 °C, 4 h, ρ_{CO_2} = 0.955 g/ml, * determined by gas chromatography, † with respect to ethenolysis products.

The ethenolysis performed without [(dtbpx)Pd(OTf)$_2$] reached a conversion of 96 % and a selectivity of 98 %. A ratio of 0.03 mol% of [Pd] to 0.05 mol% of UC led to a reduced conversion and selectivity of 80 and 90 %, respectively (Table 3.5, entry 1,2). The trend for decreased conversions and selectivities was further observed when the relative amount of [(dtbpx)Pd(OTf)$_2$] to UC was increased. Using the same catalyst ratio, a conversion of 66 % and a selectivity of 77 % was observed, respectively (Table 3.5, entry 3). Even higher amounts of [(dtbpx)Pd(OTf)$_2$] of 0.05 mol% led to a conversion of 10 % (Table 3.5, entry 4, Figure 3). These observations clearly show a negative impact of the isomerization catalyst precursor on the catalyst performance of UC in the ethenolysis reaction.

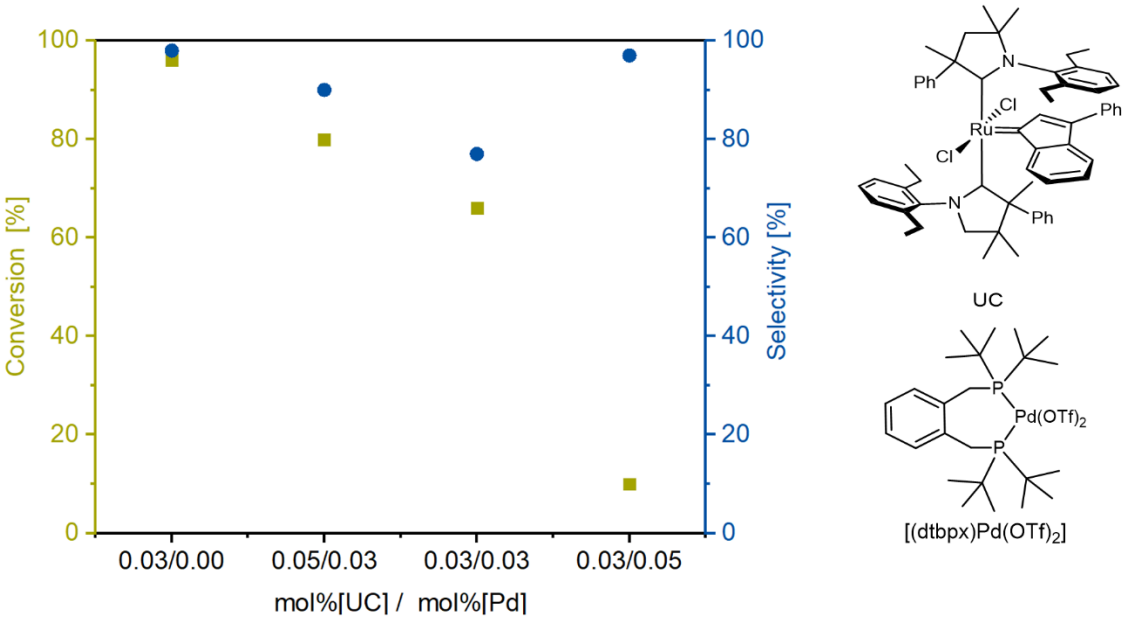

Figure 3.12. Influence of different catalyst ratios of UC and [(dtbpx)Pd(OTf)$_2$] on the conversion and selectivity of the ethenolysis of methyl oleate.

To analyze this behavior for the active isomerization species, a consecutive isomerizing ethenolysis was performed (Scheme 3.1). In this case, the ethenolysis activity is not only affected by the active Pd- catalyst but also by the MeOH activator.

Scheme 3.1. Consecutive isomerizing ethenolysis of methyl oleate.

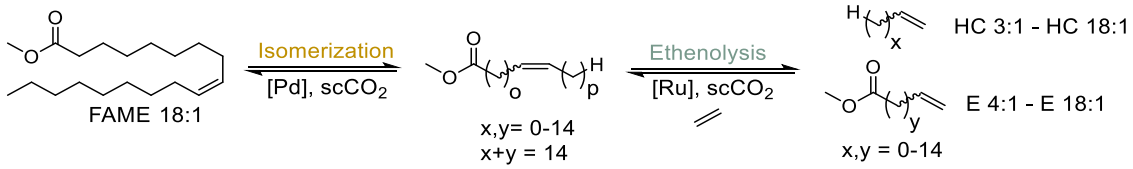

The product mixture obtained with the use of 0.5 mol% of [(dtbpx)Pd(OTf)$_2$] for the isomerization and 0.3 mol% of UC for the ethenolysis, was analyzed by GC (Figure 3.13). Even though olefin and unsaturated ester products with chain lengths up to C_{18} were observed, the conversion for the ethenolysis was relatively low with 60 %. Hence, the active Pd-catalyst also has a negative impact on the ethenolysis performance. Compared to the reaction without MeOH activator (Table 3.5, entry 4), higher conversions were reached. This might be due to the use of higher total amounts for both catalysts in the isomerizing ethenolysis reaction (0.5 mol% of [(dtbpx)Pd(OTf)$_2$] and 0.3 mol% of UC), leading to a diminished negative effect of [(dtbpx)Pd(OTf)$_2$] on the ethenolysis reaction. As observed for the ethenolysis in the presence of [(dtbpx)Pd(OTf)$_2$] without MeOH activator, the change of the catalyst ratio to 1:1 (0.3 mol%) resulted also in an increased isomerizing ethenolysis conversion of 90 %. In conclusion, the last two steps of the sequential reaction

require higher total amounts of [(dtbpx)Pd(OTf)$_2$] and UC in a ratio of at least 1:1 to reach a sufficient ethenolysis performance.

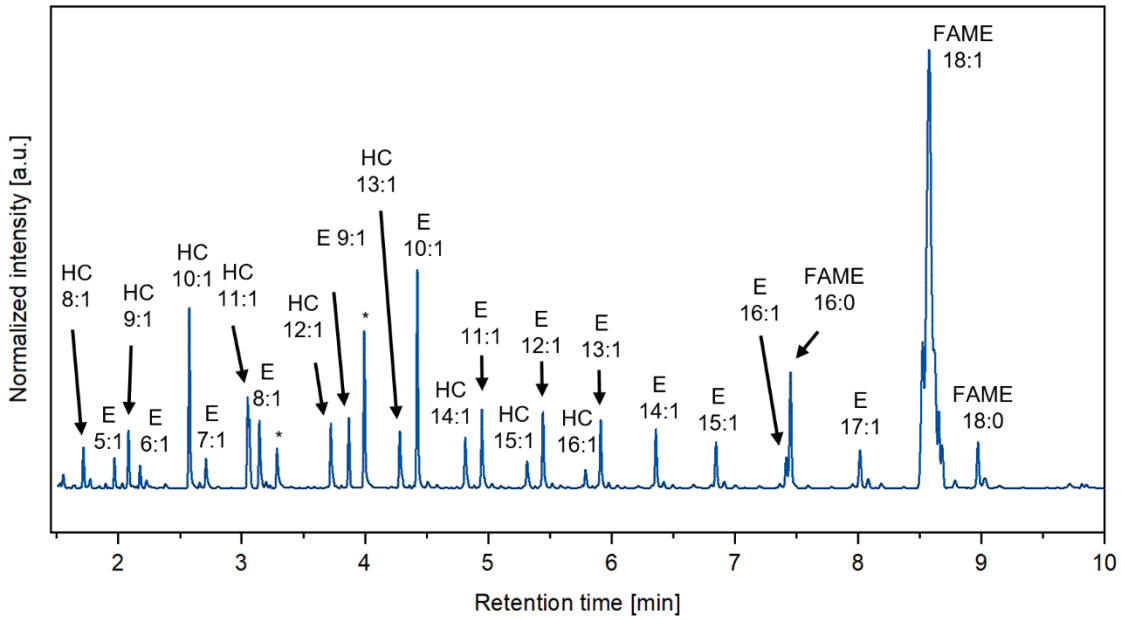

Figure 3.13. Gas chromatogram of consecutive isomerization and ethenolysis reactions of transesterified HOSO. *Corresponds to ethyl vinyl ether signals. Reaction conditions: (1) isomerization: 6 mmol HOSO, 0.5 mol% of [Pd], 0.5 mL of MeOH, 5.5 mL of DCM, 55 °C, 350 bar, 1.5 h, (2) ethenolysis: 0.3 mol% of UC, 10 bar ethylene, 6 mL of DCM, 55 °C, 450 bar, 4 h.

To get a closer insight into the catalyst interactions, NMR experiments were conducted by analyzing a mixture of 9.4 µmol of UC and [(dtbpx)Pd(OTf)$_2$] in CD_2Cl_2. To monitor a change in the catalyst structure which could be associated with a diminished performance, the ^{1}H NMR signals of pure UC catalyst were compared to the catalyst mixture (Figure 3.14). In the aromatic region of the ^{1}H NMR spectrum of the UC catalyst, several signals can be assigned to protons of the indylidene ligand (Figure 3.14, bottom). For the catalyst mixture, already after 10 minutes, these signals disappear and new signals are formed between 7.9 and 8.8 ppm (Figure 3.14, center). The newly formed signals cannot be assigned to the original UC or the Pd- catalyst (Figure 3.14, top & bottom). This indicates a change in the chemical structure of the ruthenium complex and probably is the reason for a decreased catalytic activity.

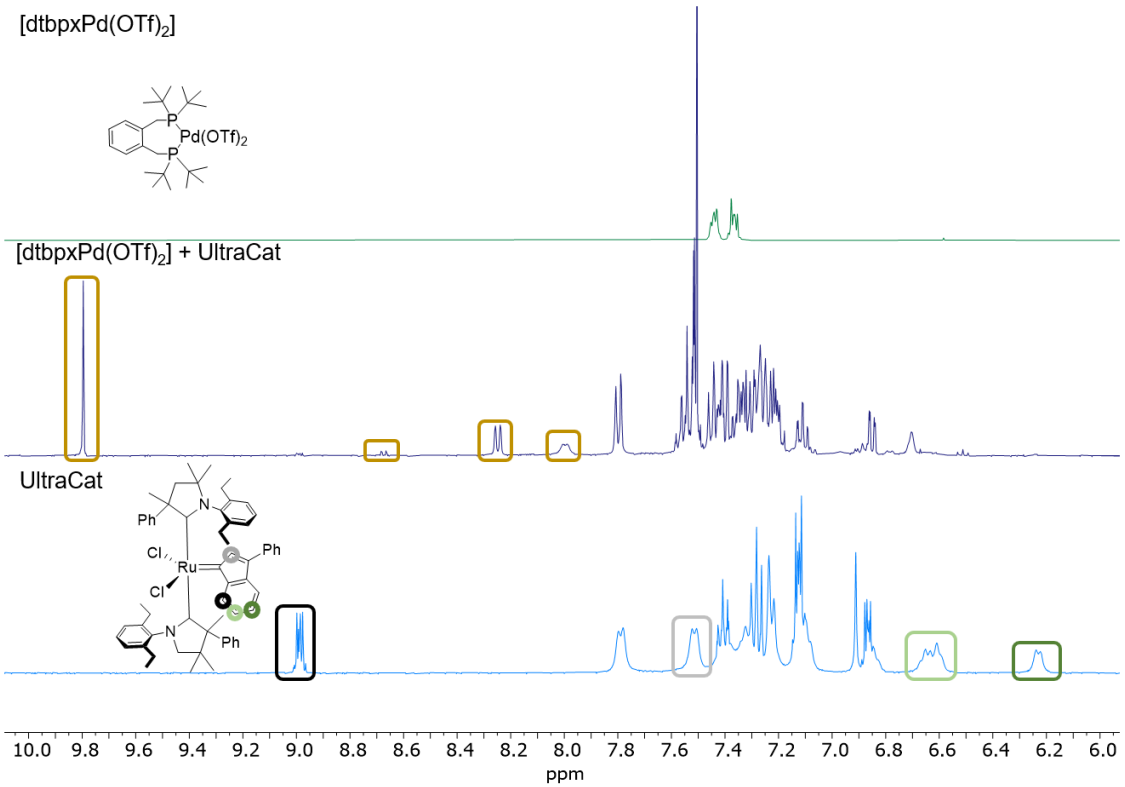

Figure 3.14. ^{1}H NMR spectrum (400 MHz, 25°C, CD_2Cl_2) of the isomerization catalyst [(dtbpx)Pd(OTf)$_2$] (top), a mixture of 9.4 µmol of UC and [(dtbpx)Pd(OTf)$_2$] (center) and of UC (bottom).

Within these experiment, a more detailed analysis of the change in chemical structure of both complexes was not possible, nevertheless the findings reflect the negative impact of [(dtbpx)Pd(OTf)$_2$] on the performance of the ethenolysis catalyst UC.

3.2.6 Multicatalytic Sequential Conversion of Renewable Oils

Please note that the performance and analysis of all isomerization experiments in the multicatalytic sequential process were performed by Felix Einsiedler within his thesis.[151] All collected data from the multicatalytic sequential concept were analyzed in cooperation with Felix Einsiedler.

3.2.6.1 High Oleic Sunflower Oil

Since especially short chain alpha olefins and esters play a major role in the chemical industry, a shift of the obtained products from the isomerizing ethenolysis to shorter chain lengths of $<C_{10}$ is desired (Figure 3.15 a). The here proposed multicatalytic sequential approach, comprising of an ethenolysis, followed by an isomerization and a second ethenolysis reaction, allows for the synthesis of such short chain compounds. As HOSO mainly consists of a single unsaturated fatty acid (Figure 3.15 b, bottom), allowing for an easy analysis of the product distribution, it was used as a reference compound for the three-step multicatalytic sequential concept. Prior to use, it was transesterified to enable a direct detection of the ester and olefin products by GC and purified by distillation to exclude any side effect due to impurities. Reaction conditions were chosen based on the findings from single ethenolysis and consecutive isomerizing ethenolysis reactions. Thus, the primary ethenolysis was performed on the one side with a low ethylene pressure of 3 bar to enable a sufficient isomerization and on the other side with increased catalyst amounts of 0.06 mol% to still reach high ethenolysis conversions under these low ethylene pressures. For the isomerization, a low MeOH amount of 0.1 mL was used to prevent deactivation of UC in the second ethenolysis as well as lower catalyst loadings of $[(dtbpx)Pd(OTf)_2]$ compared to UC in order to minimize the negative effect of $[(dtbpx)Pd(OTf)_2]$ on the ethenolysis performance. Under these conditions, the primary ethenolysis resulted in a conversion of methyl oleate of 90 % with a selectivity for the desired ethenolysis products 1-decene (HC 10:1) and decen-9-oate (E 10:1) of 96 % (Figure 3.15 b, center). However, after double bond isomerization and second ethenolysis, only low amounts of the expected terminal unsaturated esters and olefins with chain lengths $<C_{10}$ were observed by GC (Figure 3.15 b, top). The comparison of the isomer distribution obtained in $scCO_2$ under these reaction

conditions with equilibrium isomer distributions from reference experiments at 55°C in MeOH/DCM showed an incomplete isomerization in $scCO_2$ (Figure 3.15 c, d).

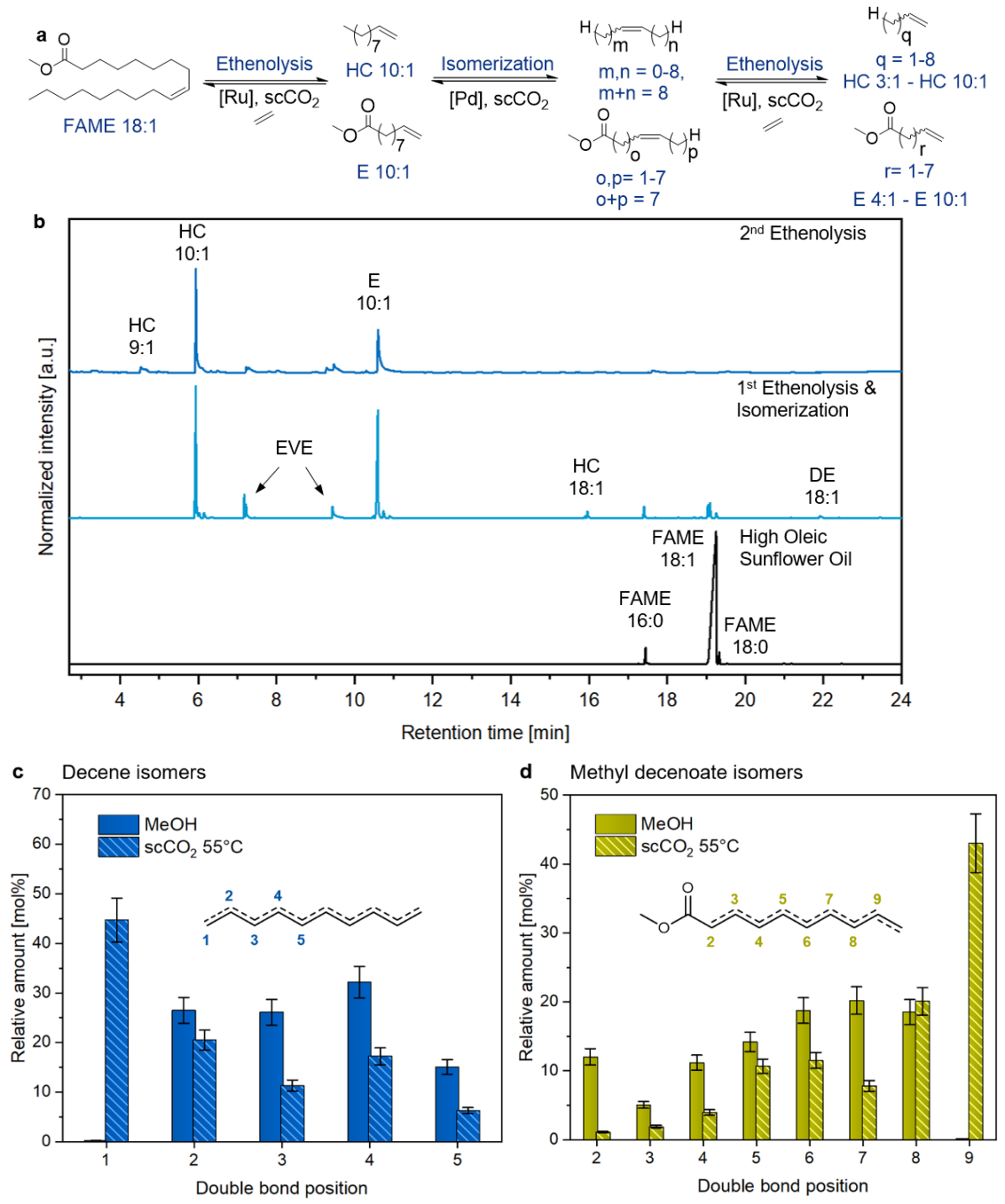

Figure 3.15 a, Chemical equation for the presented tandem approach of HOSO. b, Gas chromatogram of HOSO (bottom), the product mixture after the 1st ethenolysis and the isomerization reaction (center) as well as after the 2nd ethenolysis reaction (top). Conditions: 3 mmol HOSO, 0.06 mol% of UC, 6 mL of DCM, 55 °C, 250 bar, 3 bar ethylene, 6 h; isomerization 0.2 mol% of $[(dtbpx)Pd(OTf)_2]$ per double bond (pdb), 0.1 mL of MeOH, 5.9 mL of DCM, 55 °C, 3 bar Ethylene, 350 bar, 16 h; ethenolysis: 0.3 mol% of UC pdb, 6 mL of DCM, 55 °C, 450 bar, 6 h . Isomer distribution of c) decene and d) methyl decenoate in MeOH and $scCO_2$. [146, 151]

Thus high amounts of terminal unsaturated isomers were still present, preventing a full conversion in the second ethenolysis to shorter products. Next to this limitation in the second ethenolysis, the general ethenolysis performance was with conversions of 13 % and 17 % for HC 10:1 and E 10:1 low, yielding only minor amounts of products with chain length $<C_{10}$.

To reach an isomer distribution close to equilibrium as well as high ethenolysis conversions, the reaction temperature during isomerization was increased from 55 °C to 85 °C and additional 10 bar of ethylene were added for the second ethenolysis step. This resulted in ethenolysis conversions of 95 % with a selectivity for ethenolysis products of 98 %. After the second ethenolysis, a product mixture of esters and olefins with chain lengths $<C_{10}$ were detected by GC (Figure 3.16, bottom) indicating an isomerization that was closer to equilibrium. Nevertheless, as high relative amounts for the terminal isomer of decene and methyl decenoate were observed, the isomerization equilibrium was still not reached.

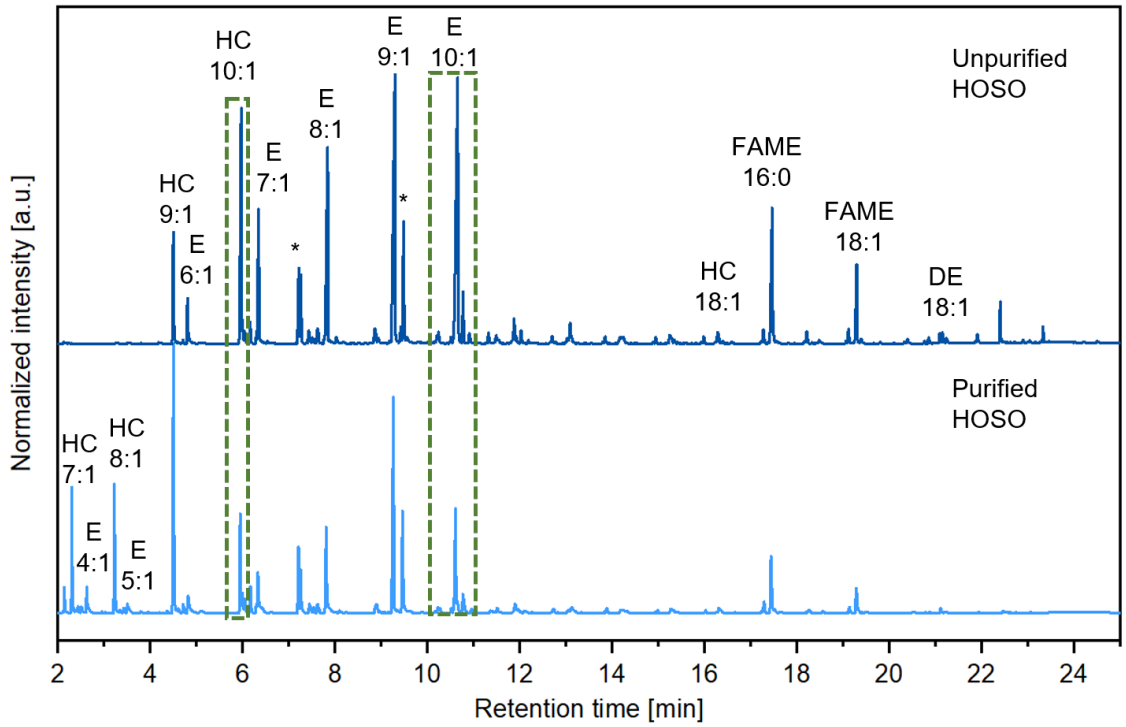

Figure 3.16. Gas chromatogram of the product mixture after sequential catalysis of purified HOSO (bottom) and purified HOSO (top). *corresponds to EVE signals.
Conditions: ethenolysis: 3 mmol HOSO, 0.06 mol% of UC, 6 mL of DCM, 55 °C, p_{tot}= 250 bar, 3 bar ethylene pressure, 6 h; isomerization: 0.2 mol% of [(dtbpx)Pd(OTf)$_2$] pdb, 0.1 mL of MeOH, 5.9 mL of DCM, 85 °C, 3 bar ethylene pressure, p_{tot}= 350 bar, 16 h; ethenolysis: 0.3 mol% of UC pdb, 6 mL of DCM, 55 °C, p_{tot}= 450 bar, +15 bar ethylene pressure, 6 h.

This resulted in an incomplete conversion in the subsequent ethenolysis of 84 % for HC 10:1 and 82 % for E 10:1. As the here presented concept should be applied to several unpurified renewable oils, the multicatalytic sequential process was further optimized for HOSO that was not purified by distillation. To initially analyze the impact of the present impurities in the oil on the catalyst performance, the process was repeated with unpurified HOSO using the same reaction conditions (*Figure 3.16*, top). For the primary ethenolysis, a comparable high conversion and selectivity of 97 %, respectively, was obtained. This was also the case for the second ethenolysis with a conversion of 84 % for HC 10:1 and 79 % for E 10:1. These results indicate that the present impurities in the oil have no notable negative effect on the ethenolysis performance. However, isomerization did not reach an isomer distribution that was close to equilibrium (Appendix Table 6.3).[151] To enhance the isomerization performance, the reaction was repeated with higher amounts of Pd-catalyst (0.4 mol% per double bond) and expanded reaction times of 48 h. To prevent a negative impact on the ethenolysis activity, the catalyst loading and the reaction time was also increased for the second ethenolysis to 0.4 mol% and 24 h, respectively.

To allow for the analysis of the full spectrum of formed products including all low boiling olefins (HC 3:1 to HC 6:1) the sampling procedure as well as the GC measuring method were optimized. By means of dry ice, a DCM/EVE solution was cooled to capture as high amounts of low boiling products as possible from the $scCO_2$ product mixture. For the detection of the short chain products by GC, liquid CO_2 was used to cool down the GC oven to 7 °C and slower heating rates were applied to enable signal separation. With this procedure, it was possible to detect all desired α-olefins (HC 3:1-HC 10:1) and terminal unsaturated esters (E 3:1-E 10:1) by GC (Figure 3.17).

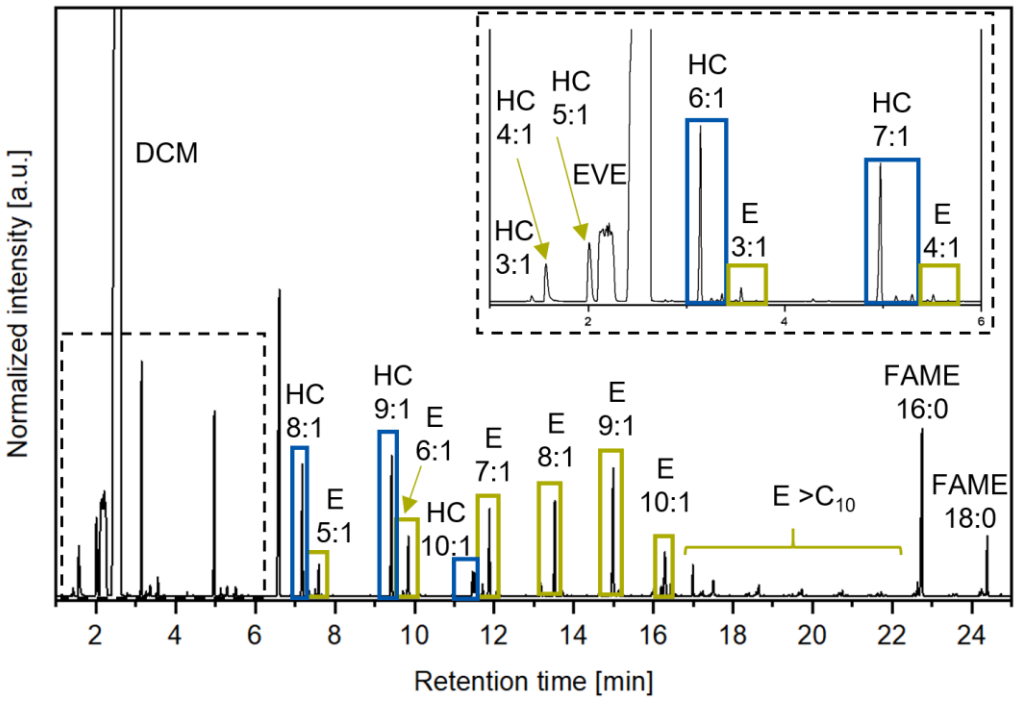

Figure 3.17. Gas chromatogram of the obtained product mixture (HC 3:1 to HC 10:1 corresponds to alkenes and E 3:1 to E 10:1 to esters) starting from transesterified HOSO, EVE corresponds to ethyl vinyl ether. Conditions: ethenolysis: 3 mmol HOSO, 0.06 mol% of UC, 6 mL of DCM, 55 °C, p_{tot}= 250 bar, 3 bar ethylene pressure , 6 h; isomerization: 0.4 mol% of [(dtbpx)Pd(OTf)$_2$] pdb, 0.1 mL of MeOH, 5.9 mL of DCM, 85 °C, p_{tot}=350 bar, 48 h; ethenolysis: 0.4 mol% of UC pdb, 6 mL of DCM, 55 °C, p_{tot}= 450 bar, +15 bar ethylene pressure, 24 h.

Even though the optimized sampling of the reaction mixture enabled the detection of all products, losses of low boiling olefins propylene to pentene (HC 3:1 to HC 5:1) are inevitable which hampers their quantitative detection. Therefore, a reference experiment was performed. The reactor vessel was pressurized with 4 bar of a standard gas mixture containing 3 mol% of the low boiling olefins HC 5:1, HC 4:1 and HC 3:1. Moreover, 3 mol% of higher boiling olefin HC 9:1 was added as reference and the reactor was pressurized with carbon dioxide to the typical reaction pressures used in the multicatalytic sequential procedure. Subsequently, the olefin mixture was collected by the described sampling procedure. With the assumption that higher boiling olefin HC 9:1 is fully collected and detected by GC measurements, the average relative loss of the light olefins was calculated. From this reference experiment, it can be concluded that around 40 % of HC 5:1 is detected by GC and only 17 % and 3 % of HC 4:1 and HC 3:1, respectively (Figure 3.18, dashed blue bars). Detected amounts of HC 3:1 to HC 5:1 in the performed multicatalytic sequential catalysis experiments showed comparable results (Figure 3.18, dark blue bars).

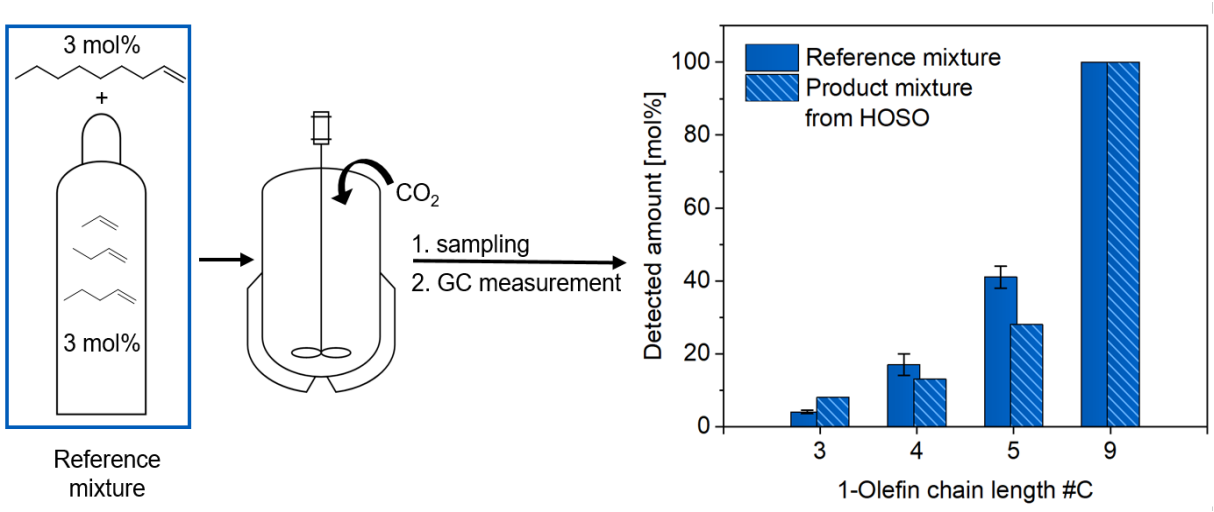

Figure 3.18. Reference experiment illustrating the partial loss of low boiling olefins HC 3:1 to HC 5:1 upon depressurization of the reaction mixture in the sampling process. [146]

Thus, to visualize the actual product distribution of the approach, the total amounts of low boiling olefins HC 3:1 to HC 5:1 were calculated by mass balance. For this purpose, the actual isomer distribution present in the multicatalytic sequential process mixture was determined by ^{13}C NMR analysis after isomerization. After a theoretical ethenolysis (taking the actual conversion of the second ethenolysis into account), all olefin amounts were back calculated (Figure 3.19 a,b). The validity of this procedure is confirmed as calculated and experimentally observed amounts of HC 6:1 to HC 10:1 (Figure 3.19 b right diagram) are matching. This underlines the determined values for HC 3:1 to HC 5:1 are reasonable and allows for the visualization of the product distribution obtained from the multicatalytic sequential experiments.

To evaluate the obtained product distributions, theoretical distributions from complete and fully selective ethenolysis steps, and ideal isomerization to equilibrium were calculated. This calculation assumed a complete ethenolysis of the equilibrium isomer distribution of decene and methyl decenoate obtained by exhaustive isomerization in MeOH (Figure 3.19 c).

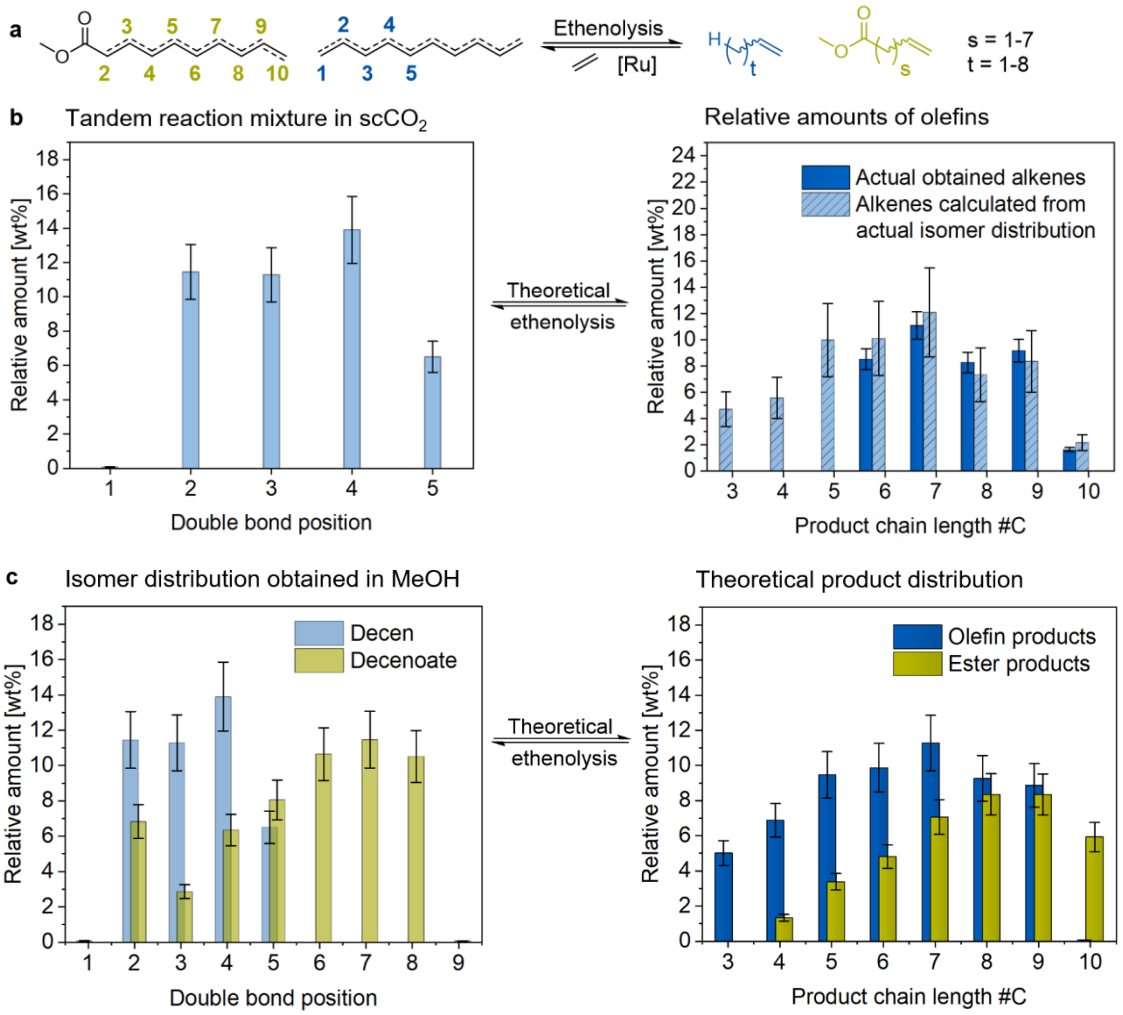

Figure 3.19. a, Ethenolysis of isomerized decene and methyl decenoate resulting in the formation of olefins and unsaturated esters with chain length of C_3 to C_{10}. b, The actual decene isomer distribution obtained in the tandem process of HOSO after isomerization was determined by ^{13}C NMR (left diagram). A subsequent theoretical ethenolysis gives the theoretical observed amounts for all alkenes (right diagram, light blue bars). c, starting from the equilibrium isomer ratios of decene and methyl decenoate in MeOH (left diagram), a theoretical complete ethenolysis of the isomers yields the theoretical product distribution for the starting material HOSO (right diagram).[146]

However, reference experiments with 0.4 mol% of UC showed in the ethenolysis of the α,β-methyl decenoate isomer to E 3:1 and HC 9:1 (Figure 3.20 a) only low conversions of 38 % even after 24 h (*Figure 3.20* a). In addition, negligible amounts of methyl acrylate E 3:1 in the product mixture were detected by GC after multicatalytic sequential catalysis. Thus, for the calculation of the theoretical product distribution, the conversion of the α,β-methyl decenoate isomer in the ethenolysis was neglected, yielding higher theoretical amount for E 10:1 of around 6 wt%. For a comparison of the theoretical product distribution with the actual obtained distribution from the multicatalytic sequential process, the theoretical distribution was depicted as points with dashed lines (Figure 3.20).

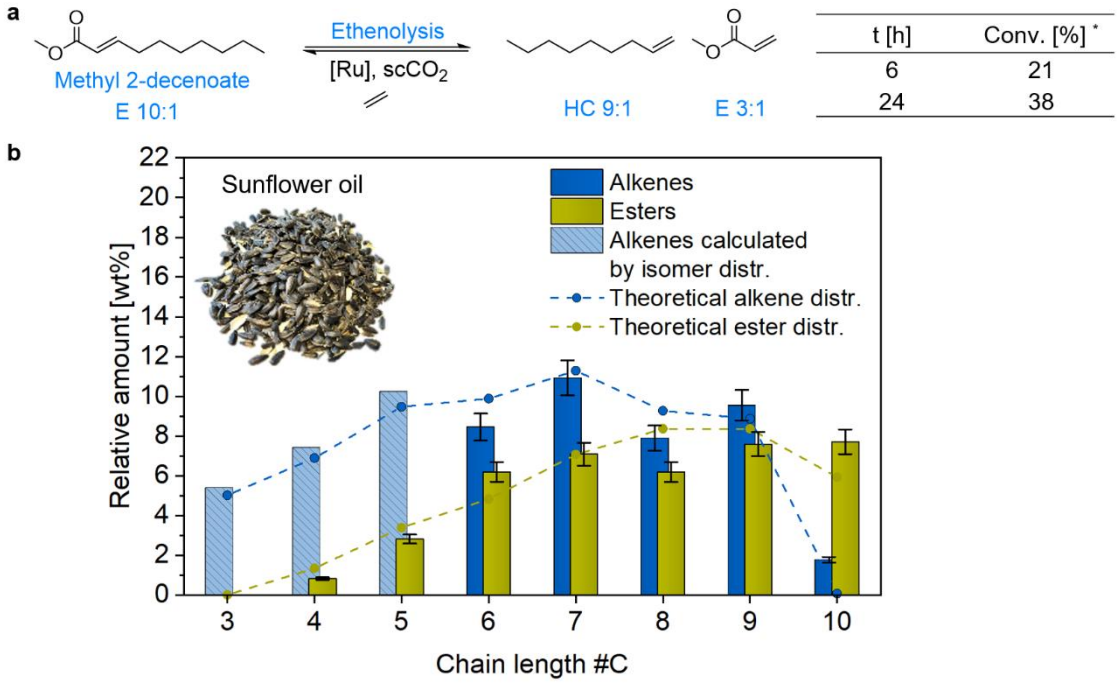

Figure 3.20. a, Ethenolysis of Methyl 2-decenoate. Reaction conditions: 0.4 mol% UC, 15 bar ethylene, 55 °C, 24 h. * determined by GC b, Obtained product distribution for alkenes (blue) and unsaturated esters (yellow) after tandem catalysis starting from high oleic sunflower oil. Dashed lines represent the theoretical product distribution. Conditions: ethenolysis: 3 mmol substrate, 0.06 mol% of UC, 6 mL of DCM, 55 °C, p_{tot}= 250 bar, 3 bar ethylene pressure, 6 h; isomerization: 0.4 mol% of [(dtbpx)Pd(OTf)$_2$] pdb, 0.1 mL of MeOH, 5.9 mL of DCM, 85 °C, p_{tot}= 350 bar, 48 h; ethenolysis: 0.4 mol% of UC pdb, 6 mL of DCM, 55 °C, p_{tot}= 450 bar, +15 bar ethylene, 24 h.

A comparison of both distributions showed that relative product amounts obtained from the multicatalytic sequential process (Figure 3.20 b, blue and yellow bars) fit to the theoretical product distribution (Figure 3.20 b, dashed line) for methyl esters E 4:1 to E 10:1 and olefins HC 3:1 to HC 10:1. The first ethenolysis resulted in a conversion of 97 % leading to a high selectivity for products <C_{10} with a value of 97 % (Figure 3.21 a). In addition, the higher catalyst loadings and the extended reaction times in the second ethenolysis led to an enhanced conversion of HC 10:1 and E10:1 of 96 % and 91 %, respectively. This was also the case for the double bond isomerization, reaching an isomer distribution that was close to equilibrium (Appendix Table 6.3).[151]. Moreover, the good correlation between the observed and target distribution indicates that no simultaneous isomerizing ethenolysis, hence no shortening of longer products is observed. This is further emphasized by a high selectivity for terminal alkenes and unsaturated esters of 92 % (Figure 3.21 a).

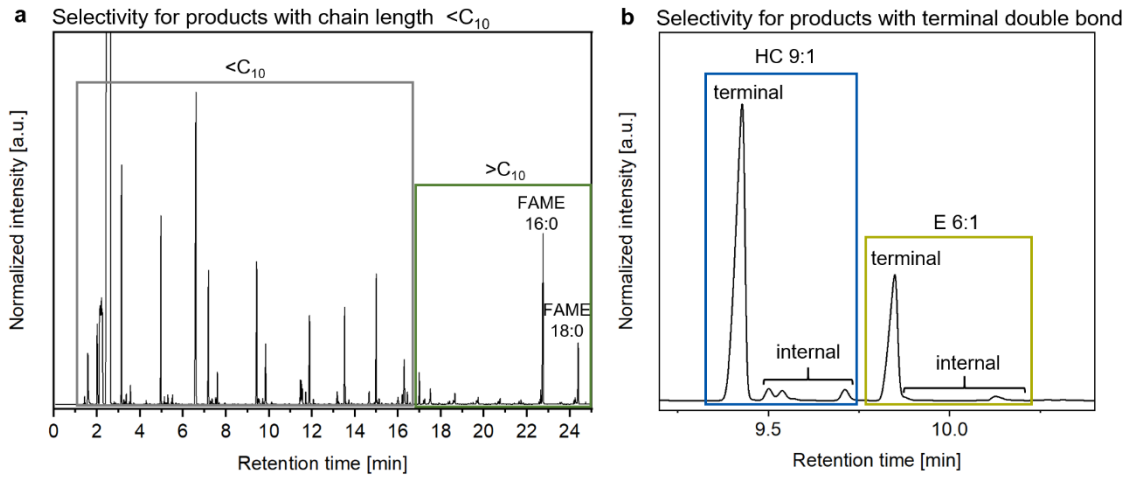

Figure 3.21 Gas chromatograms representing the selectivity for products with chain length $<C_{10}$ (a) and for products with terminal double bonds (b).

The multicatalytic sequential reaction in dichloromethane and MeOH under the same reaction conditions results in a product mixture with a lower selectivity of 55 % for terminal products. This can be explained by a more pronounced deceleration of the double bond isomerization in $scCO_2$, especially in the presence of ethylene, suppressing the simultaneous isomerization and ethenolysis. Thus, the usage of $scCO_2$ as solvent not only facilitates a more environment-friendly process but also a more selective reaction towards terminal products. Within this experiment, a successful reaction sequence was presented leading to all desired products with the expected relative amounts.

3.2.6.2 Olive Oil

Next to HOSO, other commercially available oils containing high amounts of unsaturated fatty acids can be used as renewable feedstock for the presented biorefinery approach. As a first example, olive oil was utilized. It contains, besides high amounts of the monounsaturated fatty acid methyl oleate (FAME 18:1), methyl palmitoleate (FAME 16:1) as well as the polyunsaturated fatty acid methyl linoleate (FAME 18:2). The primary ethenolysis reaction yields, next to decene (HC 10:1) and decenoate (E 10:1), octene (HC 8:1), heptene (HC 7:1) as well as pentadiene (HC 5:2). Their relative amounts depend on the fatty acid composition present in the oil (Figure 3.22 a,b). This results after isomerization and further ethenolysis in a slight shift in the product distribution compared to HOSO.

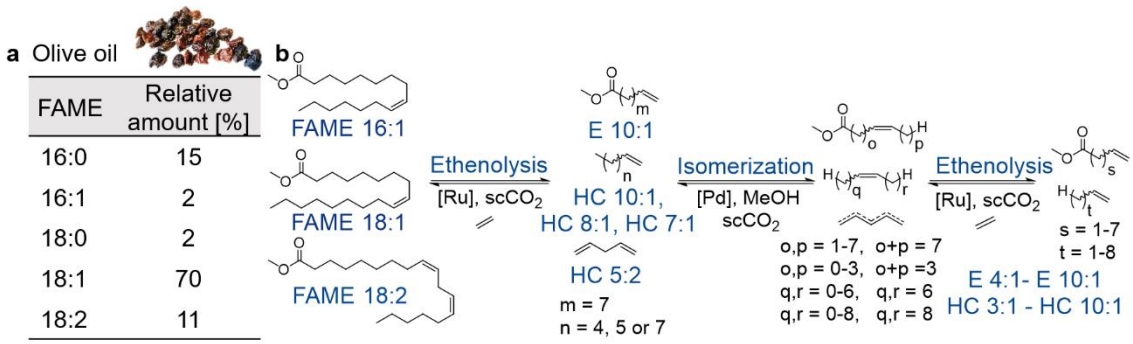

Figure 3.22 a, Tandem reaction sequence of unsaturated fatty acids present in commercial olive oil. b, Fatty acid composition of transesterified commercial olive oil.

Applying optimized reaction conditions found for HOSO (Table 3.6), the primary ethenolysis of transesterified olive oil resulted in a conversion of 70 % for FAME 18:1/ 18:2 with selectivities for ethenolysis products of over 98 %. FAME 16:1 on the other side is converted in 95 % with a selectivity of 99 %.

Table 3.6 Results obtained after the multicatalytic sequential reaction of transesterified HOSO and olive oil.

Substrate	1. Ethenolysis			Isomerization	2. Ethenolysis			
	Conv. [%]		Selec. [%]*		Conv. [%]		Selec. [%]†	Terminal products [%]
HOSO	FAME 18:1	97	97	Close to equilibrium	HC 10:1 E 10:1	96 91	97	92
Olive oil	FAME 18:1/2 FAME 16:1	70 95	98 99	Close to equilibrium	HC 10:1 E 10:1	85 84	93	89

Reaction conditions: (1) ethenolysis 0.06 mol% of UC, 55 °C, 3 bar ethylene pressure, p_{tot}= 250 bar, 6 mL of DCM, 24 h; (2) isomerization 0.4 mol% of [(dtbpx)Pd(OTf)$_2$] per double bond, 85 °C, p_{tot}= 500 bar, 6 mL of DCM, 48 h; (3) ethenolysis 0.4 mol% of UC per double bond, 55 °C, 15 bar ethylene pressure, p_{tot}=450 bar, 6 mL of DCM, 24 h; * with respect to ethenolysis products, †selectivity for products with chain lengths <C_{10}.

The double bond isomerization of the primary ethenolysis products proceeded close to equilibrium (Appendix Table 6.3).[151] Thus, a followed ethenolysis led to all expected products as observed by GC. The conversion of HC 10:1 and E 10:1 in the second ethenolysis was calculated to be 85 % and 84 %, respectively. For all other primary ethenolysis products, the conversions cannot be calculated as they are also formed during the second ethenolysis from other isomers. However, due to an incomplete conversion of FAME 18:2 in the primary ethenolysis, the followed isomerization and ethenolysis led to the formation of higher amounts of products with chain lengths $>C_{10}$. This is reflected in a lower selectivity of 93 % for the desired products C_3 to C_{10}. The amount of terminal products compared to substrates with internal double bonds was calculated to be 89 %, indicating only minor isomerization in the last reaction step of the multicatalytic sequence.

To visualize the actual product distribution obtained by the multicatalytic sequential approach for olive oil, the total amounts of low boiling olefins HC 3:1 to HC 5:1 were calculated, closing the mass balance. For this purpose, the isomer distribution of all primary ethenolysis products present in the multicatalytic sequential process are required (HC 7:1, HC 8:1, HC 10:1, HC 5:2 and E 10:1, Figure 3.22 b). Due to overlapping signals, it is not possible to conclusively determine the isomer distributions of these first ethenolysis products by ^{13}C-NMR spectroscopy directly from the product mixture. Therefore, model compounds of primary ethenolysis products (HC 8:1, HC 7:1 and HC 5:2) were separately isomerized in reference experiments in $scCO_2$ under the same reaction conditions used for the multicatalytic sequential process. The relative amounts of the different isomers were determined by ^{13}C NMR for each compound (see appendix Table 6.1, Table 6.2). A following theoretical ethenolysis that takes the actual ethenolysis conversion of the process into account results in the relative amounts of HC 3:1 to HC 5:1. Note that 1,4-pentadiene HC 5:2, formed in small amounts from ethenolysis of multiple unsaturated fatty acids and its follow-up products (1,3-pentadiene from isomerization, and propylene and butadiene from further ethenolysis) are not considered here. Due to their volatility these compounds evade quantitative detection, and for the same reason they are not considered in evaluation of experimentally observed products distribution by comparison to the theoretical distributions. However, as the ethenolysis of HC 5:2 in organic solvents revealed also only a minor performance, the contribution of HC 5:2 to the theoretical product distribution was excluded. A theoretical complete ethenolysis of all other isomers gives the theoretical product distribution that differs only slightly from HOSO (Figure 3.20).

The product distribution, obtained after the sequential catalysis is comparable to the theoretical product distribution (Figure 3.23). Furthermore, as selectivities for the desired products with chain lengths $<C_{10}$ as well as for terminal unsaturated compounds are high, the implementation of the biorefinery concept to oils containing low amounts of polyunsaturated fatty acids was shown to be possible.

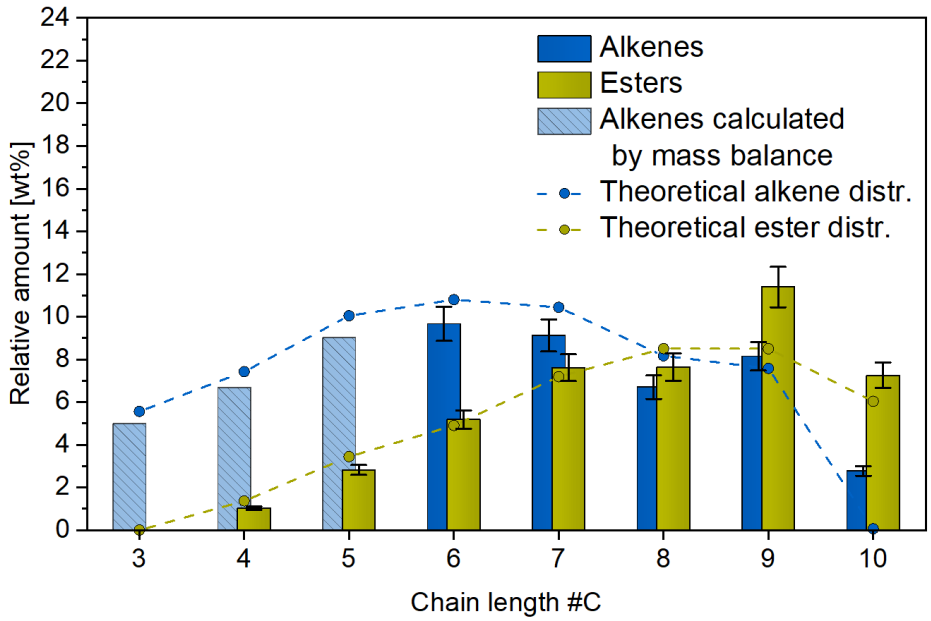

Figure 3.23. Obtained product distribution for alkenes (blue) and unsaturated esters (yellow) after tandem catalysis starting from commercial olive oil. Dashed lines represent the theoretical product distribution (Contribution of HC 5:2 is excluded). Conditions: ethenolysis: 3 mmol substrate, 0.06 mol% of UC, 6 mL of DCM, 55 °C, p_{tot}= 250 bar, 3 bar ethylene pressure, 6 h; isomerization: 0.4 mol% of $[(dtbpx)Pd(OTf)_2]$ pdb, 0.1 mL of MeOH, 5.9 mL of DCM, 85 °C, p_{tot}= 350 bar, 48 h; ethenolysis: 0.4 mol% of UC pdb, 6 mL of DCM, 55 °C, p_{tot}= 450 bar, +15 bar ethylene pressure, 24 h.

3.2.6.3 Soybean Oil

In 2021, around 60 % of the globally produced oilseeds were soybean crops.[3] Next to the extracted soybean oil, organic residues serve as an important animal feed. This makes it a promising renewable resource for the production of industrial relevant intermediates. High oleic sunflower oil has a fatty acid content for the monounsaturated FAME 18:1 of over 90 %. In contrast, soy bean oil consists mainly of polyunsaturated fatty acids including methyl linoleate FAME 18:2 and methyl linolenate FAME 18:3 (Figure 3.24 a,b).

a

FAME	Relative amount [%]
16:0	11
16:1	-
18:0	4
18:1	24
18:2/ 18:3	61

b

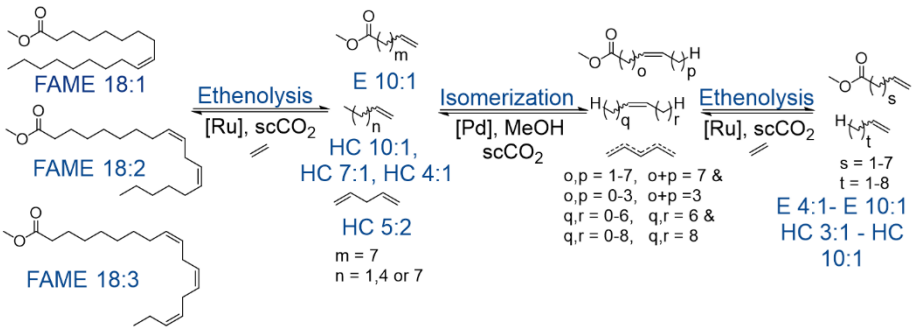

Figure 3.24. a, Fatty acid composition of transesterified commercial soybean oil. b, Tandem reaction sequence of unsaturated fatty acids present in commercial soy bean oil.

This leads to a shift of the product distribution to higher amounts of HC 3:1 to HC 5:1 and lower amounts of HC 7:1 to HC 10:1. Moreover, due to the high polyunsaturated fatty acid content, the transformation of soybean oil in the multicatalytic sequential process is challenging. The polyunsaturated fatty acids and other formed dienes can form stable allylic Pd-complexes with the isomerization catalyst, thereby impeding the double bond isomerization.[154]

Using the same optimized reaction conditions as for HOSO (Table 3.7), the primary ethenolysis of FAME 18:1/18:2/18:3 resulted in a conversion of 96 % with a selectivity for ethenolysis products of 99 %. Even though the isomerization took place to a sufficient degree despite the presence of polyunsaturated compounds, a full isomer equilibrium was not reached (Appendix Table 6.3).[151] This hints at a suppressed isomerization leading to a shift in the isomer distribution as well as after ethenolysis in a shift in the product distribution. This is especially visible for the ester products (Figure 3.25 yellow bars).

Table 3.7 Results obtained after the multicatalytic sequential reaction of transesterified HOSO and soybean oils.

Substrate	1. Ethenolysis			Isomerization	2. Ethenolysis			
	Conv. [%]		Selec. [%]*		Conv. [%]	Selec. [%]†		Terminal products [%]
HOSO	FAME 18:1	97	97	Close to equilibrium	HC 10:1 E 10:1	96 91	97	92
Soybean oil	FAME 18:1/2/3	96	99	Far from equilibrium	HC 10:1 E 10:1	86 83	97	95

Reaction conditions: (1) ethenolysis 0.06 mol% of UC, 55 °C, 3 bar ethylene pressure, p_{tot}= 250 bar, 6 mL of DCM, 24h; (2) isomerization 0.4 mol% of [(dtbpx)Pd(OTf)$_2$] per double bond, 85 °C, p_{tot}= 500 bar, 6 mL of DCM, 48 h; (3) ethenolysis 0.4 mol% of UC per double bond, 55 °C, 15 bar ethylene pressure, p_{tot}=450 bar, 6 mL of DCM, 24 h; * with respect to ethenolysis products †selectivity for products with chain lengths <C_{10}.

The second ethenolysis step proceeded with a conversion for HC 10:1 of 86 % and for E 10:1 of 83 %. The lower conversion compared to HOSO is a result of the incomplete isomerization, as higher amounts of terminal isomers are obtained, impeding a full ethenolysis conversion. Regarding the selectivity for desired products with chain lengths <C_{10} a value of 97 % is achieved.

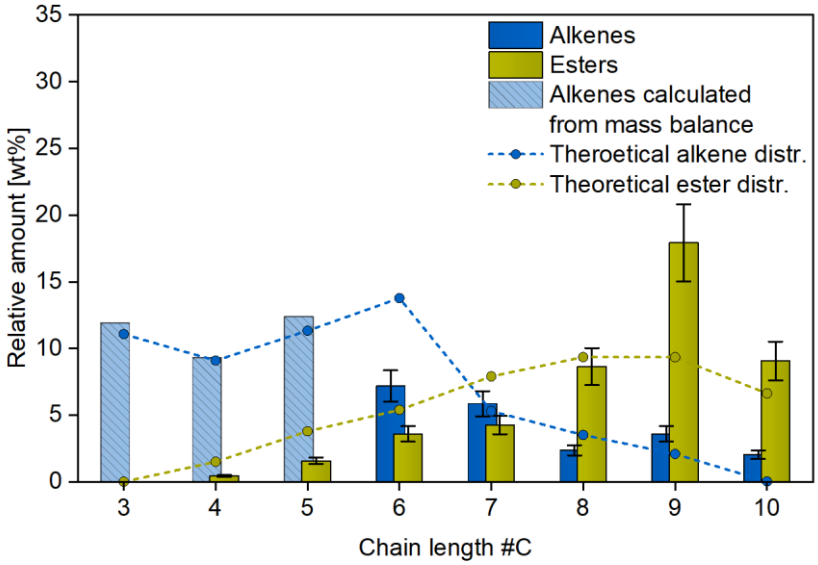

Figure 3.25 Obtained product distribution for alkenes (blue) and unsaturated esters (yellow) after tandem catalysis starting from commercial soybean oil. Dashed lines represent the theoretical product distribution (contribution of HC 5:2 is excluded, 1-butene is assumed to isomerize into a mixture of 93% 2-butene and 7 % of the terminal isomer according to literature values).[155] Conditions: ethenolysis: 3 mmol substrate, 0.06 mol% of UC, 6 mL of DCM, 55 °C, p_{tot}= 250 bar, 3 bar ethylene pressure, 6 h; isomerization: 0.4 mol% of [(dtbpx)Pd(OTf)$_2$] pdb, 0.1 mL of MeOH, 5.9 mL of DCM, 85 °C, p_{tot}= 350 bar, 48 h; ethenolysis: 0.4 mol% of UC pdb, 6 mL DCM, 55 °C, p_{tot}= 450 bar, +15 bar ethylene pressure, 24 h.

In addition, the ratio of terminal products was determined to be 95 %. The enhanced selectivity can be explained as simultaneous isomerizing ethenolysis is almost completely prevented due to the decelerated isomerization in the presence of polyunsaturated compounds.

Even though the obtained product distribution is shifted due to an incomplete isomerization, the general concept of the biorefinery approach is also applicable to oils containing high amounts of polyunsaturated fatty acids. As many renewable oils contain polyunsaturated fatty acids, their successful transformation represents a major advantage and allows for an extension of the approach to a wide range of renewable oils such as promising microalgae feedstocks.[155]

3.2.6.4 Waste Cooking oil

Besides the challenging transformation of polyunsaturated fatty acids in the multicatalytic sequential approach, the presence of other organic compounds and impurities in oils might negatively affect the catalysts performances. Waste cocking oil, for instance, contains various impurities due to the frying processes. In times of food shortage, the usage of waste oils has a high potential as a renewable feedstock. There is no competition with the food industry and at the same time, it avoids the improper disposal of used oils. To analyze the robustness of the biorefinery process towards these impurities, frying oil that had been used three times to prepare fries, was applied (Figure 3.26).

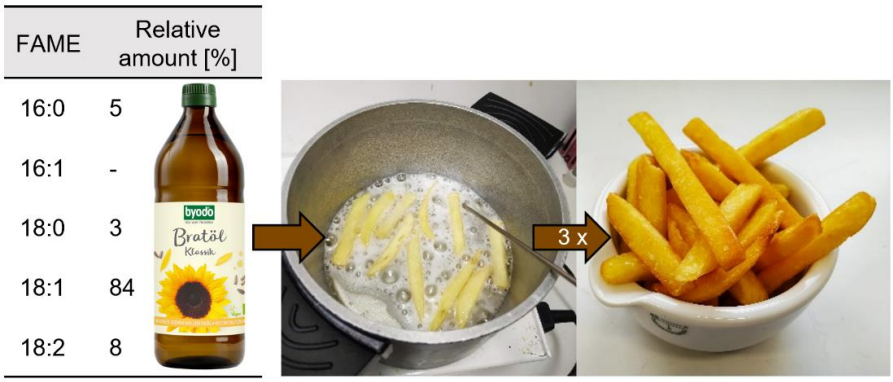

Figure 3.26 Fatty acid composition of cooking oil used for the frying process of fries. [146]

The used commercial frying oil is based on sunflower oil, thus it contains high amounts of FAME 18:1. Nevertheless, in contrast to HOSO, GC analysis of the transesterified oil revealed next to 84 % of FAME 18:1 also 8 % of polyunsaturated fatty acid FAME 18:2 (Figure 3.26). The primary ethenolysis of the multicatalytic sequential process results in a conversion of 84 % for FAME 18:1/FAME 18:2 with a high selectivity of 97 % (Table 3.8).

Table 3.8 Results obtained after the sequential catalysis of transesterified HOSO and waste cooking oil.

Substrate	1. Ethenolysis			Isomerization	2. Ethenolysis			
	Conv. [%]		Selec. [%]*		Conv. [%]		Selec. [%]†	Terminal products [%]
HOSO	FAME 18:1	97	97	Close to equilibrium	HC 10:1 E 10:1	96 91	97	92
Waste cooking oil	FAME 18:1	84	97	Close to equilibrium	HC 10:1 E 10:1	90 85	95	94

Reaction conditions: (1) ethenolysis 0.06 mol% of UC, 55 °C, 3 bar ethylene pressure, p_{tot}= 250 bar, 6 mL of DCM, 24 h; (2) isomerization 0.4 mol% of [(dtbpx)Pd(OTf)$_2$] per double bond, 85 °C, p_{tot}= 500 bar, 6 mL of DCM, 48 h; (3) ethenolysis 0.4 mol% of UC per double bond, 55 °C, 15 bar ethylene pressure, p_{tot}=450 bar, 6 mL of DCM, 24 h; * with respect to ethenolysis products, †selectivity for products with chain lengths <C_{10}.

Compared to HOSO, a drop of 13 % is visible. In addition, a negative impact on the double bond isomerization was also observed, as the obtained isomer distribution is slightly further away from equilibrium (Appendix Table 6.3).[151] This leads after subsequent ethenolysis to a shift in the product distribution (Figure 3.27, blue and yellow bars) compared to the theoretical distribution (Figure 3.27 dashed lines).

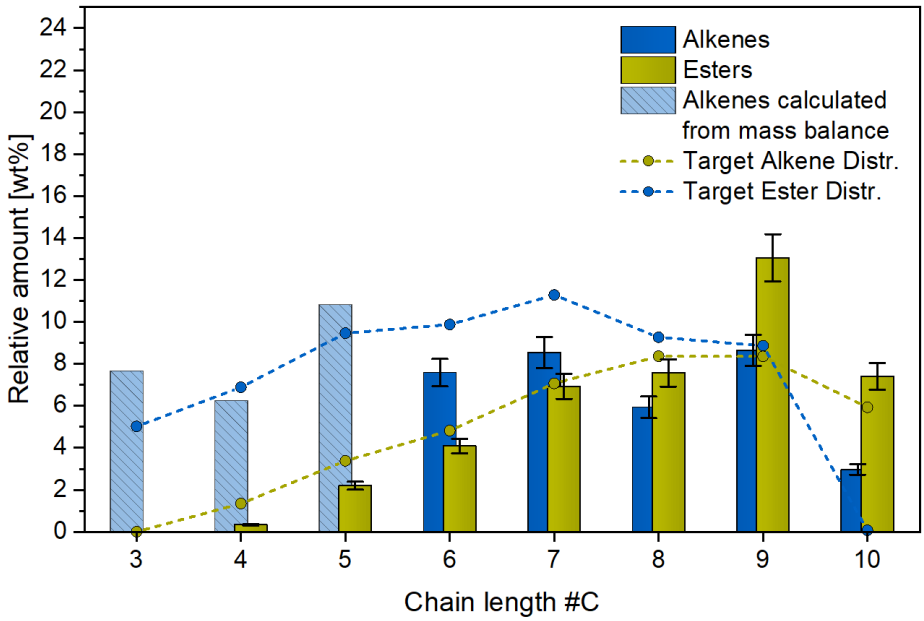

Figure 3.27. Obtained product distribution for alkenes (blue) and unsaturated esters (yellow) after tandem catalysis starting from waste frying oil. Dashed lines represent the theoretical product distribution. Conditions: 3 mmol substrate, 0.06 mol% of UC, 6 mL of DCM, 55°C, p_{tot}= 250 bar, 3 bar ethylene pressure, 24 h; isomerization 0.4 mol% of [(dtbpx)Pd(OTf)$_2$] pdb, 0.1 mL of MeOH, 5.9 mL of DCM, 85 °C, p_{tot}= 350 bar, 48 h; ethenolysis: 0.4 mol% of UC pdb, 6 mL of DCM, 55 °C, p_{tot}= 450 bar, +15 bar ethylene pressure, 24 h.

Higher amounts of olefins HC 3:1, HC 5:1, HC 10:1 and ester E 9:1 are formed as well as lower amounts of olefins HC 6:1 to HC 8:1. For the second ethenolysis a conversion for HC 10:1 was calculated to be 90 % and 85 % for E 10:1. Also in this case, the ethenolysis performance is slightly reduced compared to the reaction starting from HOSO (HC 10:1 96 %, E 10:1 91 %).

This negative influence on the ethenolysis and isomerization performance might originate from the present impurities in the oil. In addition, isomerization might be further affected by the presence of low amounts of polyunsaturated fatty acids, leading to the formation of dienes and therefore to a slowdown of the isomerization reaction.

Due to the decreased conversions in the primary ethenolysis, the higher amounts of remaining FAME 18:1 and FAME 18:2 lead, after isomerization and subsequent ethenolysis, to an increase in products with chain lengths >C_{10}. Thus, the selectivity for products with

chain lengths <C_{10} is slightly lower with 95 % compared to the selectivity of 97 % for HOSO. The ratio of terminal products was determined to be 94 %, showing only minor isomerization in the second ethenolysis step.

Even though the performance of the ethenolysis as well as the isomerization is slightly reduced when waste frying oil is used, the negative effects are limited. The process seems to be robust enough towards these impurities offering an even broader spectrum of possible renewable materials.

3.2.6.5 Model mixture algae oil

In contrast to traditional oilseed crops, microalgae show short harvesting cycles, high growth rates and can deliver up to 20 times more fatty acids per dry weight.[2,14] Moreover, they do not need huge areas of arable land as they can be grown in a range of aquatic habitats including rivers, lakes and even in wastewater and tolerate a wide range of temperatures and pH-values, enabling their growth all over the world. Subsequently, microalgae biomass exhibits a high potential as sustainable source by overcoming the deficiencies of plant based oils. Usually microalgae oil contains next to saturated and monounsaturated fatty acids, unusual fatty acids such as methyl eicosapentaenoate, (FAME 20:5,Figure 3.28 a,b) with five double bonds. This bears a challenge due to the formation of high amounts of dienes in the primary ethenolysis.

a

FAME	Relative amount [%]
14:0	9
16:0	25
16:1	47
18:0	<1
18:1	8
20:5	10

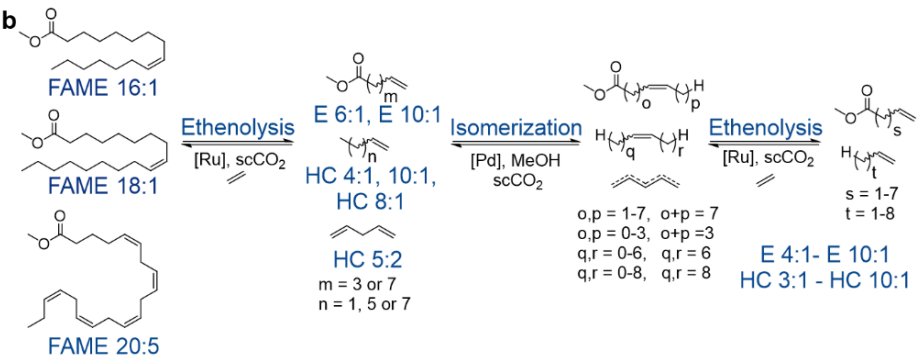

Figure 3.28 a, Fatty acid composition of transesterified artificial microalgae oil.
b, Sequencial reaction sequence of unsaturated fatty acids present in artificial microalgae oil.

In this thesis, the *Phaeodactiylum tricurnutum* species, a unicellular diatom, was used as microalgae feedstock, as it produces relatively large amounts of unsaturated fatty acids.[19] To exclude any adverse effects from additional compounds that are present in the algae oil besides the fatty acids, an artificial fatty acid mixture was used comprising a fatty acid

composition that is present in cultivated *Phaeodactiylum tricurnutum* microalgae (Figure 3.28 a). The performance of the multicatalytic sequential approach using the optimized reaction conditions previously described (Table 3.9), showed for the primary ethenolysis conversions of 98 % for FAME 16:1, 90 % for FAME 18:1 and 96 % for FAME 20:5 with selectivities for ethenolysis products of up to 99 %.

Table 3.9 Results obtained after the sequencial catalysis of transesterified HOSO, soybean oil and artificial microalgae oil.

Substrate	1. Ethenolysis			Isomerization	2. Ethenolysis			
	Conv. [%]		Selec. [%]*		Conv. [%]	Selec. [%]†		Terminal products [%]
HOSO	FAME 18:1	97	97	Close to equilibrium	HC 10:1 E 10:1	96 91	97	92
Soybean oil	FAME 18:1/2/3	96	99	Far from equilibrium	HC 10:1 E 10:1	86 83	97	95
Artificial microalgae oil	FAME 16:1	98	98	Far from equilibrium	HC 10:1 E 10:1	94 91	98	94
	FAME 18:1	90	99					
	FAME20:5	96	98					

Reaction conditions: (1) ethenolysis 0.06 mol% of UC, 55 °C, 3 bar ethylene pressure, p_{tot}= 250 bar, 6 mL of DCM, 24 h; (2) isomerization 0.4 mol% of [(dtbpx)Pd(OTf)$_2$] per double bond, 85 °C, p_{tot}= 500 bar, 6 mL of DCM, 48 h; (3) ethenolysis 0.4 mol% of UC per double bond, 55 °C, 15 bar ethylene pressure, p_{tot}=450 bar, 6 mL of DCM, 24 h; * with respect to ethenolysis products, †selectivity for products with chain lengths <C_{10}.

Due to the present dienes, isomerization is slightly slowed down leading to an isomer distribution that is further away from equilibrium (Appendix Table 6.3).[151] As a consequence, a slight shift in the obtained product distribution (Figure 3.29, blue and yellow bars) compared to the theoretical distribution (Figure 3.29, dashed lines) is observed.

The second ethenolysis resulted in high conversions for HC 10:1 and E 10:1 of 94 % and 91 % respectively. Furthermore, as primary ethenolysis proceeded with high conversions and selectivities for ethenolysis products, the analysis of the product mixture revealed a high selectivity for products with chain lengths <C_{10} of 98 %. Isomerizing ethenolysis is barely observed, leading to high selectivities for terminal products with 94 %. This proves that the multicatalytic sequential approach is also applicable to fatty acid mixtures containing FAME 20:5, allowing for a catalytic upgrading of promising micro algae feedstocks.

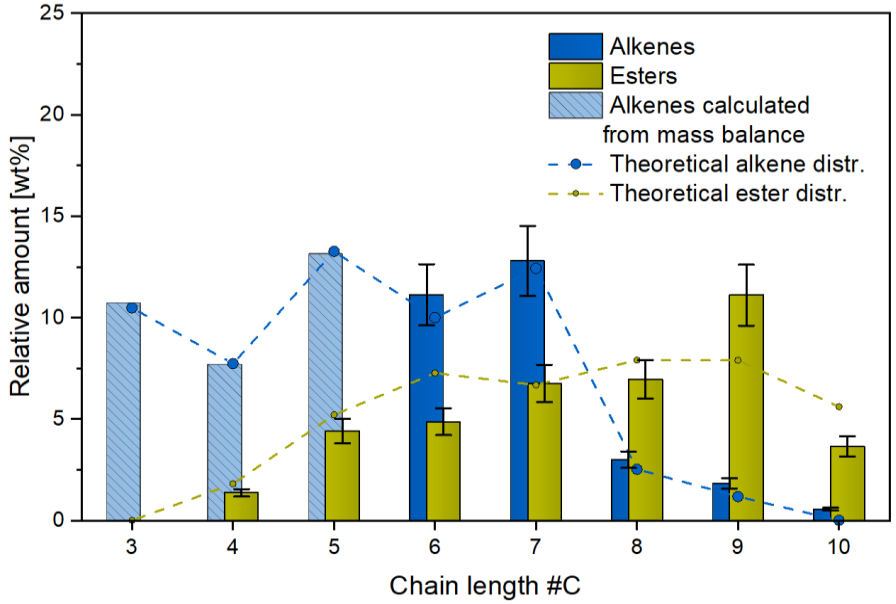

Figure 3.29 Obtained product distribution for alkenes (blue) and unsaturated esters (yellow) after tandem catalysis starting from an artificial microalgae oil. Dashed lines represent the theoretical product distribution (contribution of HC 5:2 is excluded, 1-butene is assumed to isomerize into a mixture of 93% 2-butene and 7 % of the terminal isomer according to literature values). Conditions: 3 mmol substrate, 0.06 mol% of UC, 6 mL of DCM, 55°C, p_{tot}= 250 bar, 3 bar ethylene pressure, 24 h; isomerization 0.4 mol% of [(dtbpx)Pd(OTf)$_2$] pdb, 0.1 mL of MeOH, 5.9 mL of DCM, 85 °C, p_{tot}= 350 bar, 48 h; ethenolysis: 0.4 mol% of UC pdb, 6 mL of DCM, 55 °C, p_{tot}= 450 bar, +15 bar ethylene pressure, 24 h.

3.2.7 Extraction and catalysis of renewable feedstocks

To get closer to a straight-forward industrial process, it is desired to use renewable raw materials such as sunflower seeds, olives and microalgae as starting material. This is especially relevant for the transformation of microalgae oil, which contains high amounts of unsaturated fatty acids and is not commercially available. Here, the cultivation of the desired microalgae species and a subsequent oil extraction is required. In this work, sunflower seeds, olives and microalgae biomass were used as raw materials. In a first step, the oils were isolated by extraction. In contrast to industrially used extraction processes such as organic solvent extraction or cold pressing, extraction by means of $scCO_2$ shows several advantages. It provides higher lipid selectivities and avoids the use of toxic and environmentally unfriendly organic solvents. It also prevents a tedious purification process after extraction since the carbon dioxide simply evaporates. Thus, $scCO_2$ as medium allows for an efficient and environmentally friendly combination of extraction and catalytic upgrading of the raw material and is therefore used in this work.

3.2.7.1 High Oleic Sunflower Seeds

Initially, the combined process of oil extraction and sequential catalysis was analyzed for high oleic sunflower seeds. For oil extraction, the sunflower seeds were hulled, cut into small pieces and placed in a nylon bag into the extraction vessel (Figure 3.30 a). At extraction flow rates of 6.5 mL/min, a pressure of 400 bar and a temperature of 60 °C, around 40 % of the contained oil was extracted from the seeds (around 50 wt% of the seeds correspond to oil, Figure 3.30 b). By increasing the pressure and temperature to 500 bar and 70 °C, the extraction yield was increased to 90 %. At the same time, the fatty acid composition remained constant with a ratio of 92 % for FAME 18:1. This fatty acid composition is in accordance with contents found in the commercial high oleic sunflower oil (Figure 3.30 c).

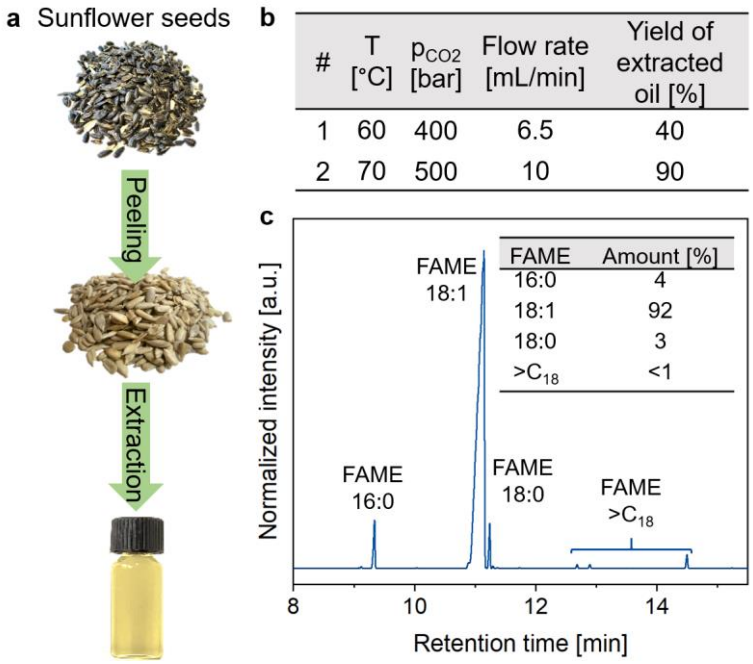

Figure 3.30. a, Procedure for the extraction of sunflower from seeds by $scCO_2$. b, Table showing the reaction conditions for the extraction process in $scCO_2$. c, Gas chromatogram showing the fatty acid composition of the extracted sunflower oil.[146]

The extracted oil was transesterified to allow for a direct analysis of all products by GC measurements and it was subsequently applied to the multicatalytic sequential process. The same reaction conditions as for commercial oils were used. The primary ethenolysis yielded a conversion of 98 % with a selectivity for ethenolysis products of 99 % (Table 3.10Table 3.10).

Table 3.10 Results obtained after the sequential catalysis of transesterified HOSO and extracted sunflower oil.

Substrate	1. Ethenolysis			Isomerization	2. Ethenolysis			
	Conv. [%]		Selec [%]*		Conv. [%]		Selec. [%]†	Terminal products [%]
HOSO	FAME 18:1	97	97	Close to equilibrium	HC 10:1 E 10:1	96 91	97	92
Extracted sunflower oil	FAME 18:1	98	99	Close to equilibrium	HC 10:1 E 10:1	91 98	98	90

Reaction conditions: (1) ethenolysis 0.06 mol% of UC, 55 °C, 3 bar ethylene pressure, p_{tot}= 250 bar, 6 mL of DCM, 24 h; (2) isomerization 0.4 mol% of $[(dtbpx)Pd(OTf)_2]$ per double bond, 85 °C, p_{tot}= 500 bar, 6 mL of DCM, 48 h; (3) ethenolysis 0.4 mol% of UC per double bond, 55 °C, 15 bar ethylene pressure, p_{tot}=450 bar, 6 mL of DCM, 24 h; * with respect to ethenolysis products, †selectivity for products with chain lengths $<C_{10}$.

The isomerization proceeded close to equilibrium (Appendix Table 6.3).[151] For the subsequent ethenolysis reaction, a conversion of 91 % for HC 10:1 and 86 % for E 10:1 was found. The selectivity for products with chain lengths $<C_{10}$ was calculated to be 98 %, originating from the high conversions and selectivities in the primary ethenolysis step. In addition, the selectivity for terminal products was determined to be 90 %.

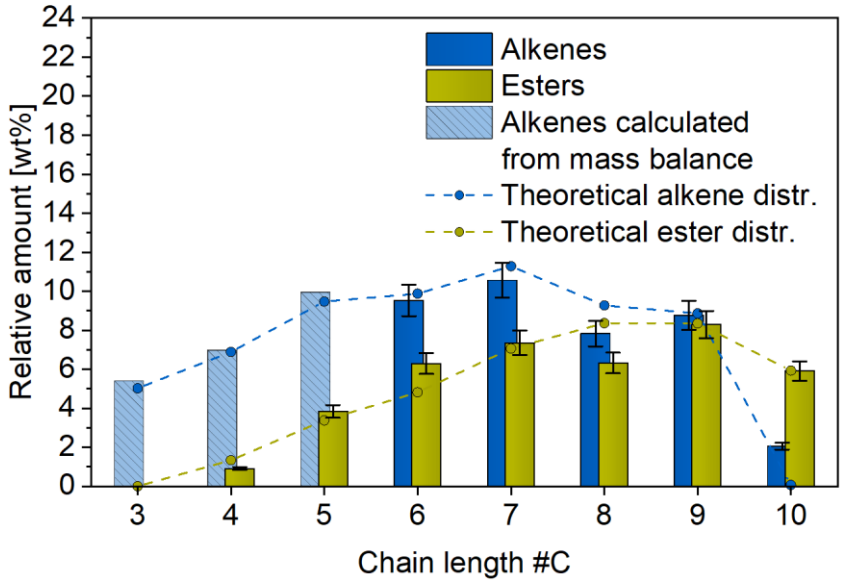

Figure 3.31 Obtained product distribution for alkenes (blue) and unsaturated esters (yellow) after tandem catalysis starting from extracted sunflower oil. Dashed lines represent the theoretical product distribution. Conditions: 3 mmol substrate, 0.06 mol% of UC, 6 mL of DCM, 55°C, p_{tot}= 250 bar, 3 bar ethylene pressure, 24 h; isomerization 0.4 mol% of [(dtbpx)Pd(OTf)$_2$] pdb, 0.1 mL of MeOH, 5.9 mL of DCM, 85 °C, p_{tot}= 350 bar, 48 h; ethenolysis: 0.4 mol% of UC pdb, 6 mL of DCM, 55 °C, p_{tot}= 450 bar, +15 bar ethylene pressure, 24 h.

These results are comparable to obtained values for HOSO and led to a product distribution (Figure 3.31, blue and yellow bars) that is close to the theoretical distribution (Figure 3.31, dashed lines). This illustrates an efficient biorefinery process starting from the raw material sunflower seeds.

3.2.7.2 Black Olives

In a further experiment, black olives were used in a consecutive extraction and refining process (Figure 3.32 a). Using the same extraction conditions as for the sunflower seeds, an extraction yield of around 50 % was reached (Figure 3.32 b). In contrast to sunflower seeds, olives contain only 35 wt% oil and a high water content of 55 wt%. The lower extraction yield is probably the result of the high water content in the olives as higher moister contents are reported to create a barrier to mass transfer when the raw material is subjected to $scCO_2$ extraction.[156] The fatty acid composition was analyzed by GC revealing similar compositions in comparison to commercial olive oil (Figure 3.32 c).

a

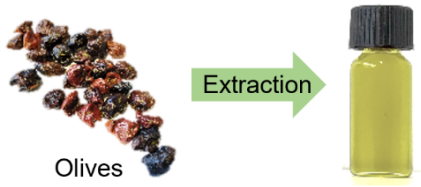

b

#	T [°C]	p_{CO2} [bar]	Flow rate [mL/min]	Yield of extracted oil [%]
1	70	500	10	50

c

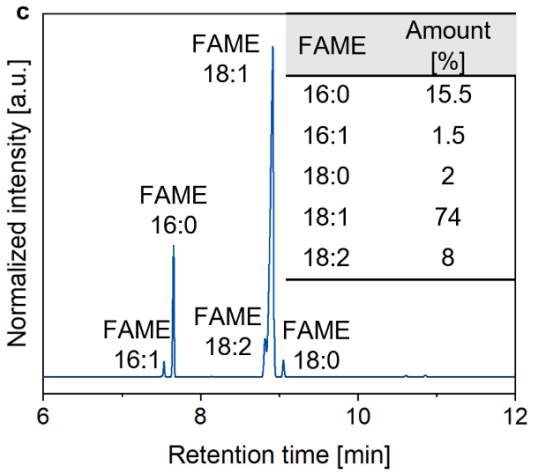

FAME	Amount [%]
16:0	15.5
16:1	1.5
18:0	2
18:1	74
18:2	8

Figure 3.32. a, Picture of black olives and the extracted oil using $scCO_2$ as extraction medium. b, Table showing extraction conditions and yield c, Gas chromatogram showing the fatty acid composition of the extracted olive oil.[146]

Using the extracted olive oil, the primary ethenolysis of the multicatalytic sequential process led to a high conversion for FAME 18:1/18:2 of 98 % with a selectivity for ethenolysis products of 99 %. Moreover, FAME 16:1 was converted to 91 % with a selectivity of 98 % (Table 3.11). In contrast, the present FAME 18:1/18:2 in commercial olive oil was only converted to 70 %. An increased performance was also visible in the second ethenolysis of the sequential process, leading for HC 10:1 and E 10:1 with conversions of 91 and 89 %, respectively (85 % and 84 % for commercial olive oil).

As described, extraction by means of $scCO_2$ is known to yield oils with a higher selectivity for fatty acids. Thus, the higher ethenolysis performance for $scCO_2$-extracted olive oil might originate from lower amounts of undesired organic impurities in the oil. Compared to the multicatalytic sequential process of commercial olive oil, the isomerization of the extracted oil led to an isomer distribution that was further away from equilibrium (Appendix Table 6.3).[151]

Table 3.11 Results obtained after the sequential catalysis of transesterified and extracted olive oil.

Substrate	1. Ethenolysis			Isomerization	2. Ethenolysis			
	Conv. [%]		Selec. [%]*		Conv. [%]		Selec. [%]†	Terminal products [%]
Olive oil	FAME 18:1/2	70	98	Close to equil.	HC 10:1	85	93	89
	FAME 16:1	95	99		E 10:1	84		
Extracted olive oil	FAME 18:1/2	98	99	Far from equil.	HC 10:1	91	98	96
	FAME 16:1	91	98		E 10:1	89		

Reaction conditions: (1) ethenolysis 0.06 mol% of UC, 55 °C, 3 bar ethylene pressure, p_{tot}= 250 bar, 6 mL of DCM, 24 h; (2) isomerization 0.4 mol% of [(dtbpx)Pd(OTf)$_2$] per double bond, 85 °C, p_{tot}= 500 bar, 6 mL of DCM, 48 h; (3) ethenolysis 0.4 mol% of UC per double bond, 55 °C, 15 bar ethylene pressure, p_{tot}= 450 bar, 6 mL of DCM, 24 h; * with respect to ethenolysis products, †selectivity for products with chain lengths <C_{10}.

As a consequence, a subsequent ethenolysis leads to a shift in the product distribution (Figure 3.33 blue and yellow bars) in contrast to the theoretical distribution (Figure 3.33 dashed lines). This is especially visible for alkenes HC 6:1 to HC 8:1 and esters E 9:1 to E 10:1. Nevertheless, the selectivity for products with chain lengths <C_{10} was determined to be 98 %. Moreover, the selectivity for terminal products was high with 96 %.

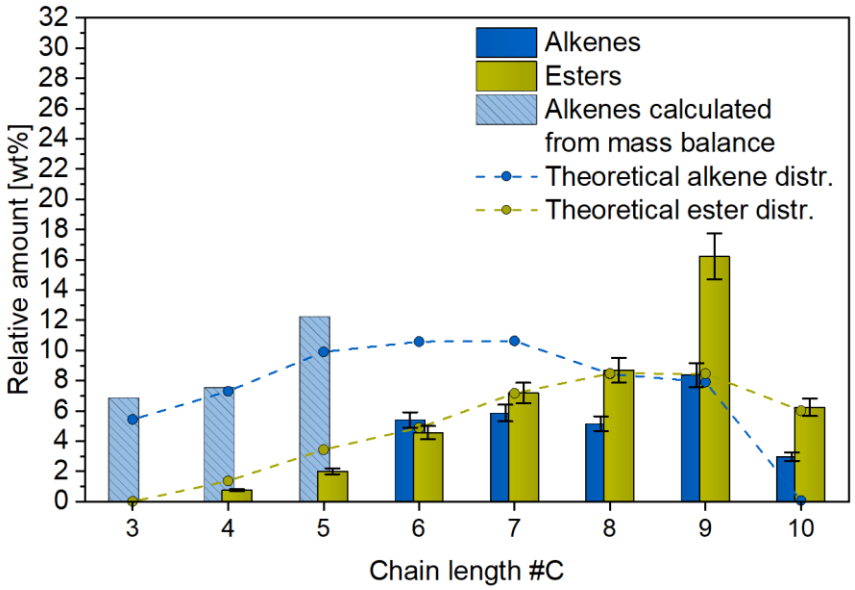

Figure 3.33 Obtained product distribution for alkenes (blue) and unsaturated esters (yellow) after tandem catalysis starting from extracted olive oil. Dashed lines represent the theoretical product distribution (contribution of HC 5:2 is excluded, 1-butene is assumed to isomerize into a mixture of 93 % 2-butene and 7 % of the terminal isomer according to literature values). Conditions: ethenolysis: 3 mmol substrate, 0.06 mol% of UC, 6 mL of DCM, 55 °C, p_{tot}= 250 bar, 3 bar ethylene pressure, 24 h; isomerization: 0.4 mol% of [(dtbpx)Pd(OTf)$_2$] pdb, 0.1 mL of MeOH, 5.9 mL of DCM, 85 °C, p_{tot}= 350 bar, 48 h; ethenolysis: 0.4 mol% of UC pdb, 6 mL of DCM, 55 °C, p_{tot}= 450 bar, +15 bar ethylene pressure, 24 h.

In summary, aside from a slight shift in the product distribution, the transformation of the extracted olive oil to the desired terminal low chain olefins and unsaturated esters was successful. This illustrates a possible consecutive extraction and upgrading of olives in $scCO_2$.

3.2.7.3 Microalgae *Phaeodactylum tricornutum*

To explore the full potential of the biorefinery concept for microalgae feedstocks, the cultivation, harvest and extraction of microalgae is necessary (Figure 3.34 a). Due to their high content of unsaturated fatty acids and its robustness, the microalgae *Phaeodactylum tricornutum* was used for this purpose (Figure 3.34 a).[19]

The microalgae were grown in f2 medium at 18 °C with a permanent light intensity of 55-65 µmol/m²/s and harvested by centrifugation. After pretreatment by ultra-sonication, the microalgae were freeze-dried. The extraction of the green powder at 90 °C and 620 bar, using a CO_2 flow rate of 10 mL/min, resulted in a yield of 17 wt % for crude algae oil. This extraction yield is in the same range as published extraction yields obtained with $scCO_2$. In addition, the composition of the oil, as determined *via* GC after transesterification with methanol, agrees with expected values (Figure 3.34 b).[19]

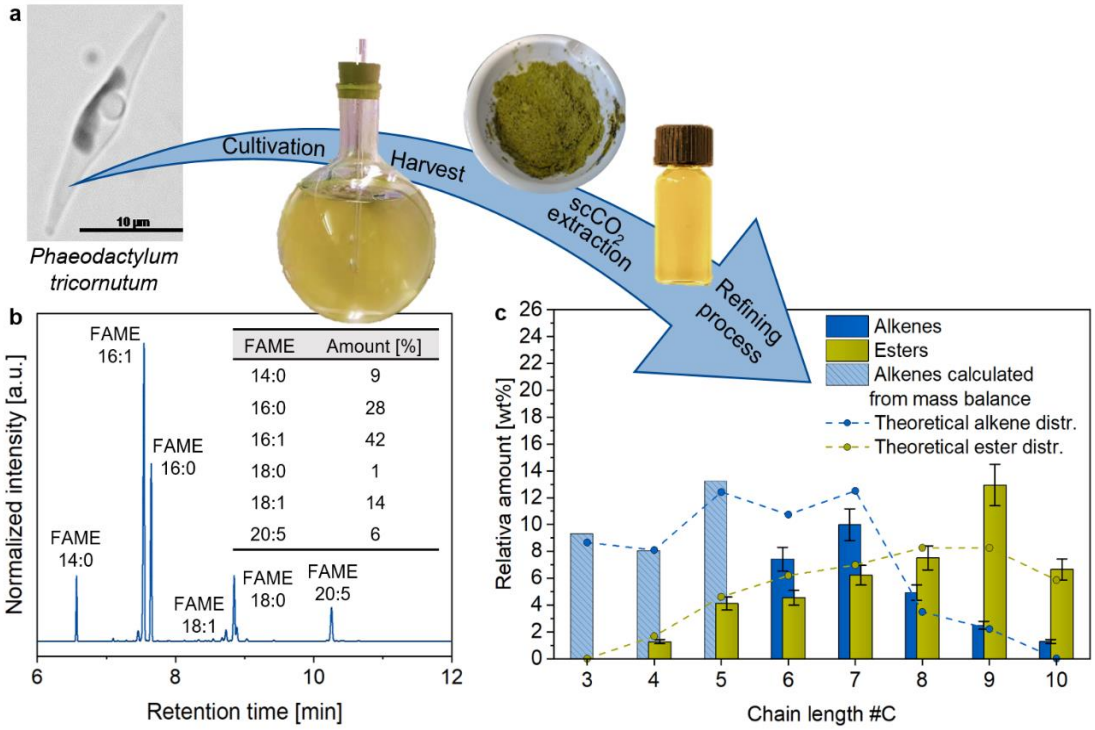

Figure 3.34. a, Schematic representation of the biorefinery process starting from Phaeodactylum tricornutum biomass b, Gas chromatogram with the fatty acid composition of extracted microalgae oil c, obtained product distribution for alkenes (blue) and unsaturated esters (yellow) of extracted microalgae oil after tandem catalysis. Dashed lines represent the theoretical product distribution (contribution of HC 5:2 is excluded, 1-butene is assumed to isomerize into a mixture of 93 % 2-butene and 7 % of the terminal isomer according to literature values) Conditions: ethenolysis: 3 mmol substrate, 0.06 mol% of UC, 6 mL of DCM, 55 °C, p_{tot}= 250 bar, 3 bar ethylene pressure, 24 h; isomerization: 0.4 mol% of [(dtbpx)Pd(OTf)$_2$] pdb, 0.1 mL of MeOH, 5.9 mL of DCM, 85 °C, p_{tot}= 350 bar, 48 h; ethenolysis: 0.4 mol% of UC pdb, 6 mL of DCM, 55 °C, p_{tot}= 450 bar, +15 bar ethylene pressure, 24 h. [146]

The transesterified microalgae oil was subjected to the multicatalytic sequential process. The primary ethenolysis resulted for FAME 16:1, FAME 18:1 as well as FAME 20:5 in comparable conversions (98 %, 96 %, 96 %, Table 3.12) as observed for artificial mixture microalgae oil (98 %, 90 % and 96 %). Thus, other extracted compounds in the oil such as pigments seem to have no influence on the ethenolysis performance.

Table 3.12 Results obtained after the sequenctial catalysis of artificial microalgae oil and extracted microalgae oil.

Substrate	1. Ethenolysis			Isomerization	2. Ethenolysis			
	Conv. [%]		Selec. [%]*		Conv. [%]	Selec. [%]†		Terminal products [%]
Artificial microalgae oil	FAME 16:1	98	98	Far from equilibrium	HC 10:1	94	98	94
	FAME 18:1	90	99		E 10:1	91		
	FAME20:5	96	98					
Extracted microalgae oil	FAME 16:1	98	99	Far from equilibrium	HC 10:1	84	98	90
	FAME 18:1	96	94		E 10:1	83		
	FAME20:5	96	99					

Reaction conditions: (1) ethenolysis 0.06 mol% of UC, 55 °C, 3 bar ethylene pressure, p_{tot}= 250 bar, 6 mL of DCM, 24 h; (2) isomerization 0.4 mol% of [(dtbpx)Pd(OTf)$_2$] per double bond, 85 °C, p_{tot}= 500 bar, 6 mL of DCM, 48 h; (3) ethenolysis 0.4 mol% of UC per double bond, 55 °C, 15 bar ethylene pressure, p_{tot}=450 bar, 6 mL of DCM, 24 h; * with respect to ethenolysis products, †selectivity for products with chain lengths <C_{10}.

In contrast, the isomerization revealed a slightly lower performance even though lower amounts of polyunsaturated fatty acids were present compared to the artificial algae oil (3.1 mmol double bond per 1 g oil *vs* 3.8 mmol). This led, due to higher amounts of terminal isomers, to a lower conversion for HC 10:1 and E 10:1 of 84 %, respectively, and to a shift in the product distribution (Figure 3.34 c). For products with chain lengths <C_{10} a selectivity of 98 % was found which can be explained by the high obtained conversions and selectivities in the primary ethenolysis. In addition, 90 % of the products have terminal double bonds proving that extensive simultaneous isomerization and ethenolysis is prevented in the last step of the multicatalytic sequential process. This illustrates a general compatibility of the promising renewable feedstock microalgae in the multicatalytic sequential approach enabling the transformation of various microalgae species into the desired short chain linear olefin and unsaturated ester products.

3.3 Conclusion

Ethenolysis represents a powerful tool for the catalytic upgrading of fatty acids from renewable resources, such as plant and microalgae oils, to terminal unsaturated products. Especially short chain linear alpha olefins are of great interest in the chemical industry as they serve as valuable intermediates for the production of sought-after polymers, plasticizers, lubricants and fuels. However, starting from renewable lipids, the product scope is limited due to the prescribed fatty acid chain lengths found in nature. In this work, a broadening of the product scope to short chain terminal olefins and unsaturated esters in the C_3 to C_{10} regime was demonstrated. This was accomplished by a catalytic multicatalytic sequential process comprising of two ethenolysis steps and a double bond isomerization in between.

The one-pod reaction sequence was performed in a custom-built high pressure semi-batch reactor system, allowing for the use of supercritical carbon dioxide ($scCO_2$) as environmentally friendly reaction medium. Since ruthenium-alkylidene metathesis catalysts are known to be compatible with fatty acids and $scCO_2$, state-of-the-art Hoveyda-Grubbs type catalysts as well as Ru-alkylidene catalysts with cyclic alkyl amino carbene ligands (CAAC) were screened for ethenolysis of transesterified high oleic sunflower oil (HOSO) in $scCO_2$. Conversions and selectivities achieved with the CAAC-substituted 'Ultracat' catalyst (UC) stand out. Under optimized reaction conditions (10 ppm of commercial UC, 10 bar ethylene, p_{total} = 450 bar, 55 °C, 6 h), the ethenolysis proceeded with a turnover number (TON) of up to 78 000 and selectivities of over 97 %. This catalyst performance is on par with reported data in neat substrates, illustrating the excellent suitability of UC for the ethenolysis of fatty acid esters in $scCO_2$ as a medium. It could be further shown that the ethenolysis performance was only slightly reduced in the presence of low amounts of MeOH, required for the activation of the isomerization catalyst [(dtbpx)Pd(OTf)$_2$]. Moreover, the negative impact on the ethenolysis performance in the presence of the Pd-isomerization catalyst was shown to be minimal at sufficiently high catalyst loadings of 0.06 mol%. In the combined process of ethenolysis-isomerization-ethenolysis, the transformation of HOSO into desired α-olefins and unsaturated esters with chain lengths of C_3 to C_{10} was demonstrated with high conversions and selectivities of over 91 % in both ethenolysis steps (Table 3.13). Moreover, a high selectivity for terminal products as well as for chain lengths $<C_{10}$ of up to 97 % was reached resulting in a product distribution that was comparable to a

calculated theoretical distribution (assuming full conversions in ethenolysis and isomerization into equilibrium).

The application of the process to other oils such as olive, soybean oil and waste frying oil was also successfully demonstrated. Ethenolysis revealed high performances even in the presence of impurities from frying processes. Moreover, selectivities for terminal products with chain lengths $<C_{10}$ reached in all cases values > 94 %. However, for oils containing polyunsaturated fatty acids, such as soybean and microalgae oil, a slight shift in product distribution compared to the theoretical distribution is observed. This is a result of a decelerated isomerization in the presence of polyunsaturated compounds due to the formation of allylic Pd-complexes, preventing isomerization to equilibrium.

Table 3.13 Table showing results from the sequential catalysis of all used transesterified oils.

Substrate	1. Ethenolysis			Isomerization	2. Ethenolysis			
	Conv. [%]		Selec [%]*		Conv. [%]		Selec [%]†	Terminal products [%]
HOSO	FAME 18:1	97	97	Close to equil.	HC 10:1 E 10:1	96 91	97	92
Olive oil	FAME 18:1/2 FAME 16:1	70 95	98 99	Close to equil.	HC 10:1 E 10:1	85 84	93	89
Soybean oil	FAME 18:1/2/3	96	99	Far from equilibrium	HC 10:1 E 10:1	86 83	97	95
Waste cooking oil	FAME 18:1	84	97	Close to equil.	HC 10:1 E 10:1	90 85	95	94
Artificial microalgae oil	FAME 16:1 FAME 18:1 FAME20:5	98 90 96	98 99 98	Far from equil.	HC 10:1 E 10:1	94 91	98	94
Extracted sunflower oil	FAME 18:1	98	99	Close to equil.	HC 10:1 E 10:1	91 98	98	90
Extracted olive oil	FAME 18:1/2 FAME 16:1	98 91	99 98	Far from equil.	HC 10:1 E 10:1	91 89	98	96
Extracted microalgae oil	FAME 16:1 FAME 18:1 FAME20:5	98 96 96	99 94 99	Far from equil.	HC 10:1 E 10:1	84 83	98	90

Reaction conditions: (1) ethenolysis 0.06 mol% of UC, 55 °C, 3 bar ethylene, p_{tot}= 250 bar, 6 mL of DCM, 24 h; (2) isomerization 0.4 mol% of [(dtbpx)Pd(OTf)$_2$] per double bond, 85 °C, p_{tot}= 500 bar, 6 mL of DCM, 48 h; (3) ethenolysis 0.4 mol% of UC per double bond, 55 °C, 15 bar ethylene, p_{tot}=450 bar, 6 mL of DCM, 24 h; * with respect to ethenolysis products †selectivity for products with chain lengths $<C_{10}$.

For an even more straight-forward biorefinery process, the raw materials sunflower seeds, olives and microalgae biomass were utilized directly in a combined extraction and catalysis in $scCO_2$. Extracted oils from sunflower seeds and olives, using $scCO_2$ as extraction medium, show comparable fatty acid compositions as commercial oils and led in the subsequent multicatalytic sequential process to similar catalytic performances. Especially the utilization of microalgae oil as renewable feedstock is desired, since this feedstock show advantages over traditional food crops, including remarkably high lipid contents and growth rates as well as a possible cultivation on non-arable land.[2] The consecutive extraction of cultivated *Phaeodactylum tricornutum* microalgae and catalytic upgrading *via* the biorefinery process in $scCO_2$ was demonstrated and resulted in the expected products with only a small shift in product distribution. This illustrates a good compatibility of the presented concept with the multi-component microalgae mixture, containing next to lipids other organic structures such as pigments. Supercritical carbon dioxide, used as an environmentally benign solvent was found to also promote the high selectivity of the process. The additional benefit of simplifying the overall biomass-to-product process by harmonizing the solvent used for biomass extraction and for sequential catalysis is an additional benefit for a low emission and efficient procedure

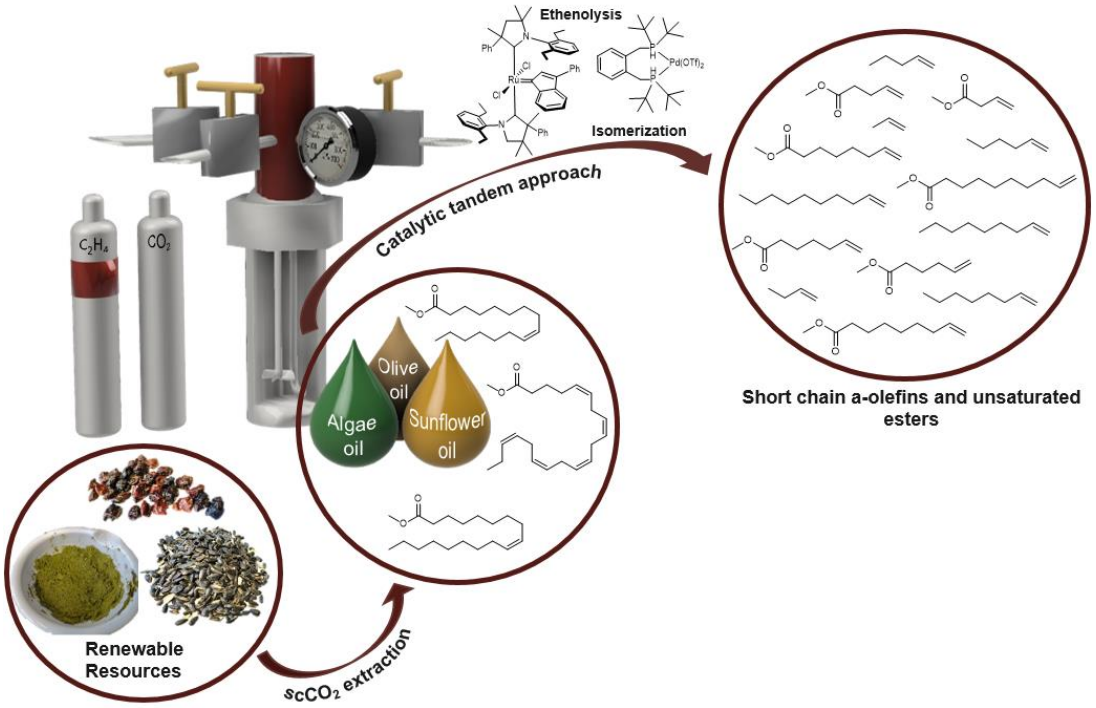

Figure 3.35. Schematic representation of the bio-refinery concept comprising of the extraction of renewable fatty acids and a one pod sequential catalysis in $scCO_2$ to valuable short chain α-olefins and unsaturated esters.

In summary, the multicatalytic sequential process shows a high variability for different renewable oils and a high robustness towards polyunsaturated fatty acids as well as impurities. The final products originate for the largest part (approx. 80 wt%) from the natural oil feedstock and only around 20 wt.-% are derived from the ethylene co-reagent. The latter can also be generated on a renewable basis from bioethanol effectively. Concerning the product chain length distributions, it is notable that our approach offers the possibility of fully adjusting these to a given demand by partial feeding of the products after downstream separation back into the process. The terminal unsaturated ester products, accounting for one fourth of the output in addition to the 1-olefin major products, are valuable precursors for dicarboxylates, used amongst others as monomers for polyesters and polyamides.

3.4 Experimental Section

3.4.1 Nuclear Magnetic Resonance – NMR

NMR spectra were recorded in deuterated solvents on a Bruker Avance III 400 MHz spectrometer. ^{1}H NMR and ^{13}C NMR spectra were referenced to residual protonated solvent signals. Acquired data was processed and analyzed using MestReNova software (version 14.1.0-24037)

3.4.2 Gas Chromatography – GC

GC analysis was performed on a Perkin-Elmer Clarus 690 gas chromatograph, equipped with a Perkin Elmer Elite 5 column (30 m x 0.25 µm x 0.25 µm; Dipenyl- 95% Dimethylpolysiloxane) and a flame ionization detector. For the analysis of single ethenolysis experiments method A was used with an injection volume of the automatic sampler of 1 µl. In this case, the sample was injected at 300 °C and detected at 320 °C. The initial temperature of 50 °C was maintained for 1 min before heating to 280 °C with a heating rate of 10 °C min^{-1}. The final temperature was kept isothermal at 280°C for 5 min. For product mixtures containing low boiling olefins which arise from the multicatalytic sequential biorefinery process, a low temperature method B was used. Here the injection volume of the automatic sampler was set to 1 µl and the sample was injected at 300 °C and detected at 320 °C. In the beginning the oven was cooled by liquid CO_2 to 5 °C which was maintained for 1 min before heating to 80 °C with a heating rate of 8 °C min^{-1} and further to 230 °C with a heating rate of 10 °C min^{-1}. The final temperature of 300 °C was reached with a heating rate of 22 °C min^{-1} and was kept isothermal for 4 min. Peaks were assigned *via* enrichment experiments with genuine samples.

All peaks in the chromatogram were corrected with response factors which were determined as an average of three measurements against dodecane.

Table 5.1: Response factors of fatty acids and their self-metathesis and ethenolysis products.

Name	Abbreviation	Molar response factor	Weight response factor
Methyl myristate	FAME 14:0	1.23	0.86
Methyl palmitate	FAME 16:0	1.39	0.89
Methyl palmitoleate	FAME 16:1	1.43	0.91
Methyl oleate	FAME 18:1	1.58	0.93
Methyl linoleate	FAME 18:2	1.62 †	0.94
Methyl eicosapentaenoate	FAME 20:5	1.78	0.97
Propylene	HC 3:1	0.24	0.98
1-Butene	HC 4:1	0.33	0.97
1-Pentene	HC 5:1	0.4	0.97
1-Hexene	HC 6:1	0.47	0.96
1-Hepene	HC 7:1	0.59	1.04
1-Octene	HC 8:1	0.74	1.10
1-Nonene	HC 9:1	0.81	1.05
1-Decene	HC 10:1	0.88	0.99
9-Octadecene	HC 18:1	1.59	1.08
Methyl-3-butenoate	E 4:1	0.26	0.59
Methyl-4-pentenoate	E 5:1	0.35 †	0.61
Methyl-5-hexenoate	E 6:1	0.49	0.65
Methyl-6-heptenoate	E 7:1	0.54 †	0.67
Methyl-7-octenoate	E 8:1	0.64 †	0.68
Methyl-8-nonenoate	E 9:1	0.68	0.70
Methyl-9-decenoate	E 10:1	0.83	0.74

† Derived from comparable compounds

3.4.3 General Considerations

All manipulations of air and moisture sensitive compounds were conducted under an inert gas atmosphere (nitrogen) using standard glovebox or Schlenk techniques. Dichloromethane was distilled from CaH_2 prior to use and stored under an inert atmosphere. Methanol was distilled over Mg under a nitrogen atmosphere and stored over molecular sieves. Carbon dioxide (N 4.5 and N 5.5 grade) was purchased from Lindegas (Pullach, Germany) and used with a dip-tube tank as received. Ethylene (N 3.5 and N 4.5 grade) was supplied by Air Liquide (Düsseldorf, Germany) and used as received. Calibration gas containing 3 mol% of propylene, 1-butene and 1-pentene was delivered from Linde electronics. Trans esterified sunflower oil (Dakolub MB9001; contains only fatty acid methyl esters and no glycerol) as well as high oleic sunflower seeds were kindly donated by DAKO AG (Wiesentheid, Germany). Cooking oil (Bratöl klassik) was purchased from byodo (Cologne, Germany) and black dried olives were purchased from LaSelva (Gräfelfing, Germany). Olive oil (Fillipo Berio) as well as soybean oil (sojola) were bought in a local supermarket. The UltraCat was supplied by Apeiron (Wrocław, Poland) as well as synthesized according to the literature procedure.[64] Hoveyda Grubbs 1st and 2nd generation catalysts as well as methyl 2-decenoate and ethyl vinyl ether were purchased from Merck (Darmstadt, Germany). [(dtbpx)Pd(OTf)$_2$] and the Hoveyda-type UltraCat were synthesized according to a reported procedure and available in the group.[64] Methyl myristate, methyl palmitate, methyl palmitoleate, methyl oleate and methyl eicosapentaenoate were purchased from Nu-Check Prep, Inc. (Elysian, USA) and served as model mixture of microalgae oil. All oils were transesterified using 1 % H_2SO_4 in methanol at 50 °C for 24 h prior to use. Deuterated solvents were purchased by Eurisotop (Saarbrücken, Germany).

3.4.4 High Pressure Equipment

The supercritical fluid extractor SFX-110W setup as well as additional supercritical fluid pumps and HPLC pumps of the reactor setup were purchased from Supercriticial Fluid Technologies, Inc. (Newark (Delaware), USA). The high-pressure ethylene pump was purchased from Teledyne ISCO (Lincoln, USA). The high-pressure reactor vessel equipped with stirrer and inlet/outlet valves as well as the heating jacket were obtained from Premex Solutions GmbH (Lyss, Switzerland). High Pressure Tubing, hand valves and check valves were purchased from Hy-Lok D Vetriebs GmbH (Oyten, Germany). Remote control *via* LabVision as well as the control cabinet was installed by Hi-Tec Zang (Herzogenrath,

Germany). The connected reactor set-up was placed on a customized table made by the scientific workshop of the University of Konstanz.

3.4.5 Cultivation and Harvesting of Microalgae

The used microalgae strain is a single clone colony of Phaeodactylum tricornutum UTEX 646 (wild type 4) and was cultivated in f2-medium[157] on shakers at 20 °C and light intensities of 55-65 µmol/m²/s at a day-night rhythm of 16/8. Precultures in 500 mL flasks were cultivated under these conditions for 5-6 days and one culture was used to inoculate one 10 L round bottle flask. Six of those 10 L flasks were cultivated for 7-8 weeks at 18 °C in permanent light of 30-40 µmol m^{-2} s^{-1} and aerated with ambient air through a sterile filter. Cells were harvested by centrifugation with a Sorvall RC 6 centrifuge with a Contifuge® Stratos with a titanium rotor (5000 g, 4 °C) from Hereaus (Hanau, Germany) and pre-concentrated samples were harvested with an Allegra 25R centrifuge (5000 g, 10 min at 4 °C) from Beckman coulter (Brea, USA). To enhance extraction yields, the wet algae were pre-treated by ultrasonication for 10 min with an on/off pulse of 10 s and amplitude of 60 %, using an ultrasound homogenizer HD3200 from Bandelin (Berlin, Germany) with a KE76 sonotrode. After freeze-drying, microalgae were crushed mechanically with a pestle and mortar.

3.4.6 Extraction of Lipids

The extraction setup system (Figure 3.36) is equipped with a high-pressure piston pump, which is fed with liquid CO_2 from a dip-tube tank and allows for pressurization of the system with CO_2 up to 700 bar. In addition, a 100 mL vessel was used as extraction compartment which is located inside an oven. The temperature of the oven as well as of the valves can be adjusted by a temperature control panel. The volume of the vessel could be further reduced and adjusted by addition of glass beads. The microalgae powder was placed in a 25-micron mesh nylon bag and positioned in the 100 mL stainless steel extraction vessel with filter disks at both openings. The vessel was connected to the CO_2 line and pressurized to 620 bar and heated to 90 °C. The extraction material was soaked for 15 min and subsequently liquid CO_2 with a flow rate of 10 mL/min was employed for further 30 min. The soaking and flow extraction were each repeated four times. The extract was collected behind the backpressure valve, the CO_2 evaporating upon expansion. Extraction of sunflower kernels as well as of olives was performed using the same procedure but a pressure of 500 bar and a temperature of 70°C.

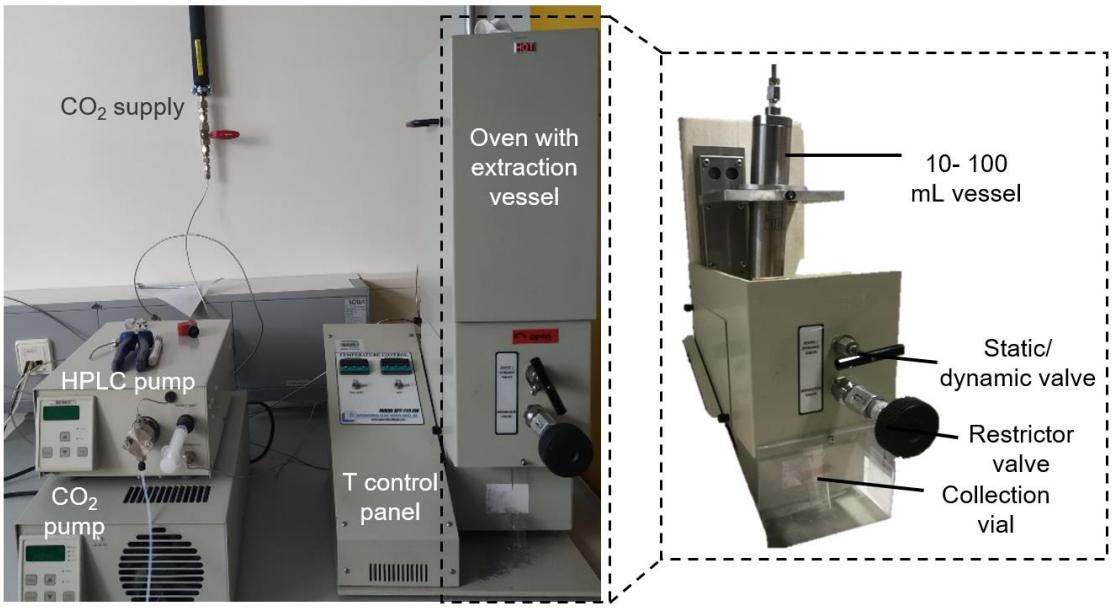

Figure 3.36. $scCO_2$ - extraction apparatus comprising of liquid CO_2 pump, HPLC pump and oven with extraction vessel.[146]

3.4.7 General Procedure for Ethenolysis in $scCO_2$

Transesterified high oleic sunflower oil (1 mL, 3 mmol) was placed in a 100 mL stainless steel high-pressure vessel and degassed. The syringe pump and ethylene tubes were rinsed with ethylene. While stirring, the reactor was initially pressurized with 10 or 20 bar of ethylene and then with CO_2 at 26 °C, respectively. The temperature was increased to 55 °C leading to a total pressure of 450 bar. In a glovebox, the catalyst was weighed into an 8 ml vial and dissolved in 6 mL of DCM (0.005 eq to CO_2). When the set temperature was reached, the catalyst solution was pumped with a flow rate of 6 mL/min by an HPLC pump into the reactor vessel. To end the reaction, the reaction mixture was quenched by venting and bubbling the gas stream through a solution of ethyl vinyl ether (35 eq.) in DCM. Conversions and selectivities were determined by gas chromatography.

3.4.8 General Procedure for Isomerizing Ethenolysis in $scCO_2$

1 mL of the transesterified oil was placed in the 100 mL stainless steel reactor and degassed. The syringe pump and ethylene tubes were rinsed with ethylene. While stirring, the reactor was pressurized with 10 bar of ethylene and subsequently with CO_2 at 26 °C. The temperature was increased to 55°C leading to a total pressure of 350 bar. In a glovebox, the isomerization catalysts was weighed into 8 ml vials and dissolved in 0.5 mL of MeOH and 5.5 mL of DCM. When the set temperature was reached, the catalyst solution was pumped with a flow rate of 6 mL/min by an HPLC pump into the reactor. After the indicated reaction time, the ethenolysis catalyst was dissolved in 6 mL of DCM and pumped with a flow rate of 6 mL/min by the HPLC pump into the vessel, starting the ethenolysis reaction. To end the reaction, the reaction mixture was quenched by venting and bubbling the gas stream through a solution of ethyl vinyl ether (35 eq.) in DCM. The conversions, selectivities as well as the product distributions were determined by gas chromatography.

3.4.9 General Procedure for the Multicatalytic Sequential Catalysis of Ethenolysis - Isomerization - Ethenolysis in $scCO_2$

The first ethenolysis step was performed as described in 3.4.7. After the indicated reaction time, the isomerization catalyst was dissolved in 0.1 mL of MeOH and 5.9 mL of DCM and pumped with a flow rate of 6 mL/min by the HPLC pump into the vessel, starting the double bond isomerization before the temperature was increased to 85 °C. After 48 h, additional 15 bar of ethylene and a second charge of ethenolysis catalyst dissolved in 6 mL of DCM were added to the reaction mixture which was stirred for additional 24 h. The reaction was quenched by venting and bubbling the gas stream through a dry ice cooled mixture of ethyl vinyl ether (35 eq.) and DCM. The conversions, selectivities as well as the product distributions were determined by gas chromatography.

3.4.10 General Procedure for Frying of Potato Chips

80 mL of transesterified frying oil were heated to 160°C in a steel pot. Three portions of potato chips were fried for around 5 min in the same oil in a row. The waste oil was used without further purification in the biorefinery sequence.

4 Flow System for Consecutive Ethenolysis and Isomerization

4.1 Introduction

The utilization of olefin metathesis reactions for the transformation of seed oil-based feedstocks into valuable raw materials plays an important role in academia and in the chemical industry. Several homogeneous olefin metathesis catalysts were analyzed in batch solution processes, including the self-metathesis of methyl oleate[60] and its cross metathesis with short olefins such as butene and ethylene[116]. These reactions provide access to intermediates for the production of polymers, surfactants and lubricants.

As naturally occurring feedstocks show limited fatty acid chain lengths, the product scope obtained by self-metathesis and ethenolysis is restricted. Gooßen *et al*. reported on the expansion of the product range by a combined olefin metathesis and double bond isomerization, resulting in a defined distribution of C_3 to C_{22} olefins and unsaturated esters, which can be used as biodiesel.[85] Especially short chain α-olefins and unsaturated esters are highly interesting intermediates for the chemical and polymer industry. Thus, the transformation of renewable fatty acids into these valuable compounds is desired. As described in chapter 3, the implementation of a sequential process, comprising a reaction sequence of ethenolysis-isomerization-ethenolysis gives access to desired α-olefins in the C_3 to C_{10} regime.

From an industrial point of view, high-throughput techniques such as continuous flow processes are more desirable compared to batch processes. They provide low catalyst wastage, facile automation, good reproducibility and low maintenance costs.[158] In this context, the utilization of homogeneous olefin metathesis catalysts come to its limits. On the contrary, immobilized olefin metathesis catalysts can resolve this issue. Through a covalent linkage of homogeneous catalysts to a solid support such as silica materials, flow reactions are facilitated. This reaction mode comes further along with the prevention of catalyst contaminations in the desired product and allows for catalyst recovery and reuse, providing a cost-efficient process. To combine advantages of continuous flow processes with

the here presented multicatalytic sequential concept, the utilization of immobilized olefin metathesis- and isomerization- catalysts is desired. (Figure 4.1).

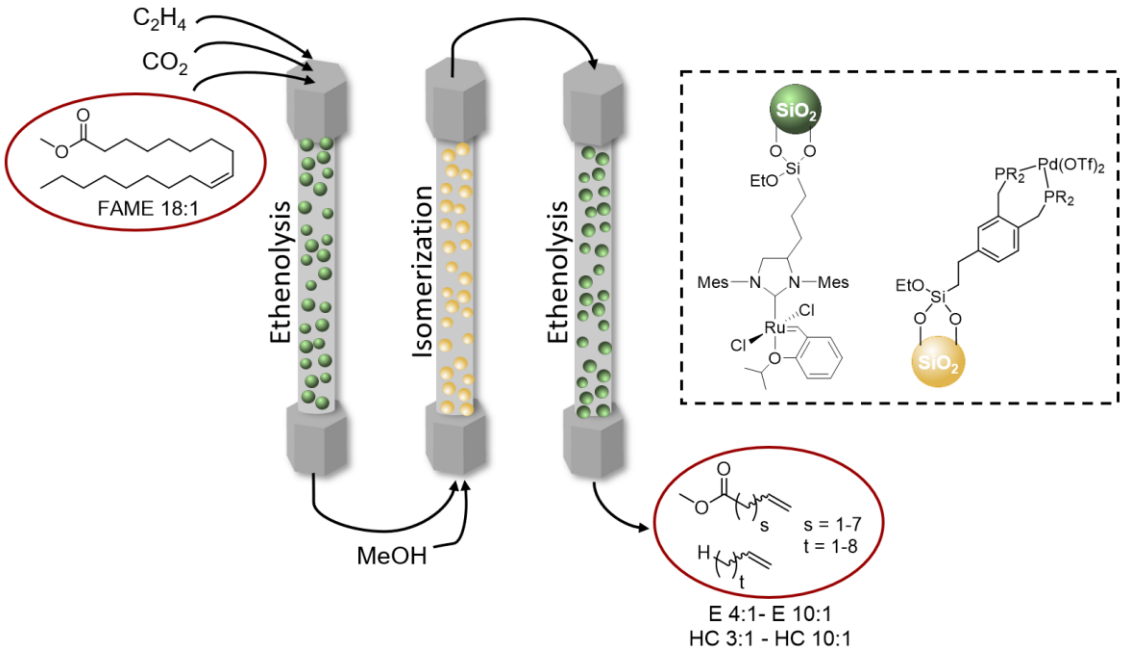

Figure 4.1 Schematic representation of the three-step continuous flow biorefinery process towards short chain α-olefins and unsaturated esters.

This chapter focusses on the examination of the performance and stability of an immobilized Hoveyda-Grubbs-type catalyst in the olefin metathesis of fatty acids under continuous flow conditions to form the basis for the aimed high throughput multicatalytic sequential process. Next to organic solvents, the utilization of the environmentally friendly reaction medium supercritical carbon dioxide ($scCO_2$) is used since it facilitates an easy removal from the product mixture. In addition, it allows for a simplification of the overall biomass to product process as $scCO_2$ is particularly well suited to selectively extract lipids from biomass.

4.2 Results and Discussion

4.2.1 Synthesis of the Immobilized Olefin Metathesis Catalyst

Silica materials are due to their high surface areas as well as due to their high chemical, thermal and mechanical stability promising support materials for the immobilization of homogenous catalysts.[98,159] To enable a covalent linkage of a homogeneous catalyst precursor to the silica material, a modification is necessary. In this work, a literature known procedure for the synthesis of an immobilized Hoveyda Grubbs 2nd generation type catalyst (HGII, Scheme 4.1 (7)), bearing a triethoxysilyl-linker was used.[160] Due to its already established synthesis procedure as well as its good activity in the ethenolysis of methyl oleate in batch reactions, analyzed in previous work, it represents a promising catalytic system for the use in continuous flow applications.[56, 161]

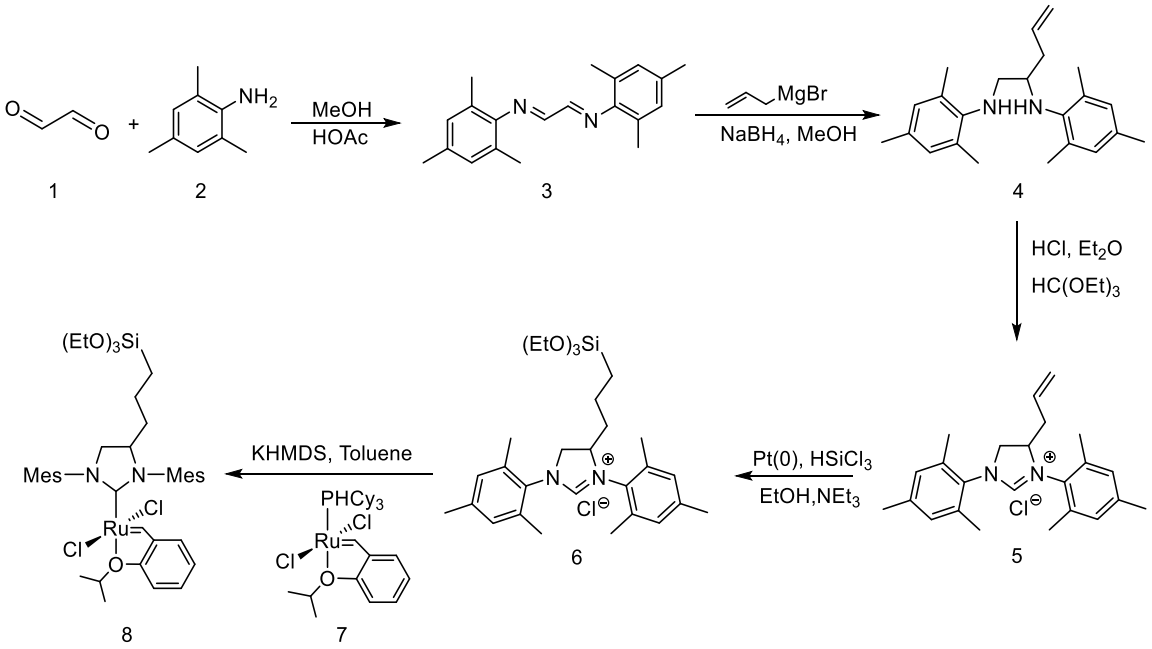

Scheme 4.1. Proposed synthesis route for the preparation of the modified Hoveyda Grubbs-type catalyst 8.

Through the four-step synthesis approach, the modified N-heterocyclic carbene (NHC) ligand 6 was obtained with yields comparable to reported values (see chapter 4.4.4 to 4.4.9).[160,161] The last crucial step including the ligand exchange of the phosphine ligand of catalyst precursor 7 with the modified NHC ligand 6, proceeded with conversions of 55 % when CuCl was added to the reaction mixture. CuCl is reported to be an effective phosphine scavenger preventing undesired side reactions and increasing reaction yields.[162]

To yield the desired immobilized catalyst HGII-SiO_2, a subsequent condensation of the modified catalyst precursor 8 onto silica was performed (Scheme 4.2). Spherical particles with a size in the range of 45 to 70 µm and a surface area of 450 to 550 m^2/g were used. The spherical shape allows for a tighter packing of the material into a fixed bed reactor typically used for continuous flow applications. With an immobilization temperature of 40 °C for 48 h, Ru contents between 0.12 and 0.48 wt% were detected by inductively coupled plasma optical emission spectroscopy (ICP-OES) measurements, depending on the relative used silica amount.

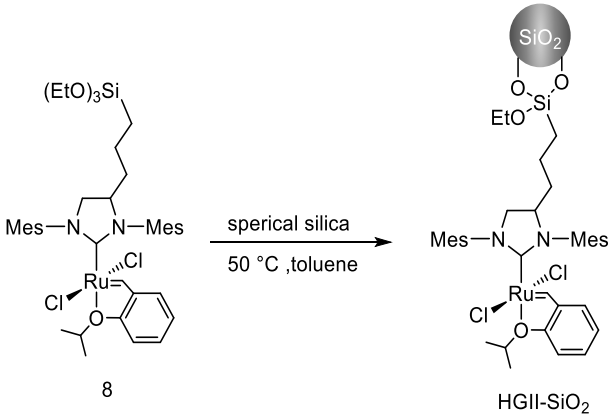

Scheme 4.2 Immobilization of the modified HGII catalyst 8 onto spherical silica.

4.2.2 Continuous Flow Self-metathesis of Methyl Oleate in Organic Solvents

The self-metathesis of oleo chemicals such as methyl oleate (FAME 18:1) or high oleic sunflower oil (HOSO, > 90 % of FAME 18:1) is of importance in the polymer chemistry.[163,164] It provides access to the valuable substrates dimethyl 1,18-octa-9-decene (DE 18:1) and 9-octadecene (HC 18:1, Scheme 4.3). As reported by Mol *et al.*, the self-metathesis of FAME 18:1 is an equilibrium reaction resulting in a mixture of FAME 18:1, DE 18:1 and HC 18:1 in a ratio of 2:1:1, respectively.[165]

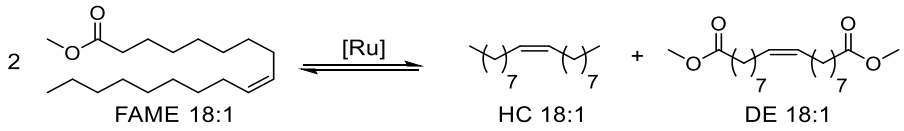

Scheme 4.3 Equilibrium reaction of the self-metathesis of methyl oleate.

In previous work, the performance of the immobilized catalyst precursor HGII-SiO_2 was analyzed in the self-metathesis of transesterified high oleic sunflower oil (HOSO, 92.5 % methyl oleate) as model substrate in a batch reaction.[161] At a catalyst loading of 0.04 mol% the maximum conversion of 50 % was reached in toluene as solvent. However, as batch reactions show in general limited turnover numbers, the implementation of the immobilized catalyst HGII-SiO_2 to continuous flow processes is desired. To allow for a comparison of the catalyst performance obtained in batch reactions, the continuous flow self-metathesis of HOSO was also performed in the solvent toluene. Reaction conditions were initially screened under a cyclic continuous flow mode to save resources such as solvent and substrate. An appropriate reaction set-up was designed to allow for a cyclic continuous flow self-metathesis (Figure 4.2 a). As a reaction vessel an HPLC column was used, filled with the immobilized catalyst (Figure 4.2 a, b). The reaction temperature was controlled by a column oven. To enable a constant flow of substrate solution, an HPLC pump was used. The product mixture was collected after the column and fed back to the system for several cycles (Figure 4.2 a). The conversion of the self-metathesis reaction was monitored by frequent sampling and analysis of the cycled reaction mixture by GC.

To find optimal conditions for a high catalytic performance, temperatures and substrate concentrations were varied at a constant flow of 1 mL/min (corresponds to a retention time of ~2 min, Figure 4.2 b, Table 4.1).

Table 4.1. Reaction conditions for cyclic continuous flow experiments in the self-metathesis of transesterified HOSO in toluene.

Entry	$c_{Substrate}$ [mol/L]	T [°C]	Conversion [%]*
1	0.13	rt	33
2	0.13	60	41
3	0.13	80	16
4	0.065	60	44

Reaction conditions: 0.24 mg Ru, 1 mL/min flow rate, *determined by gas chromatography.

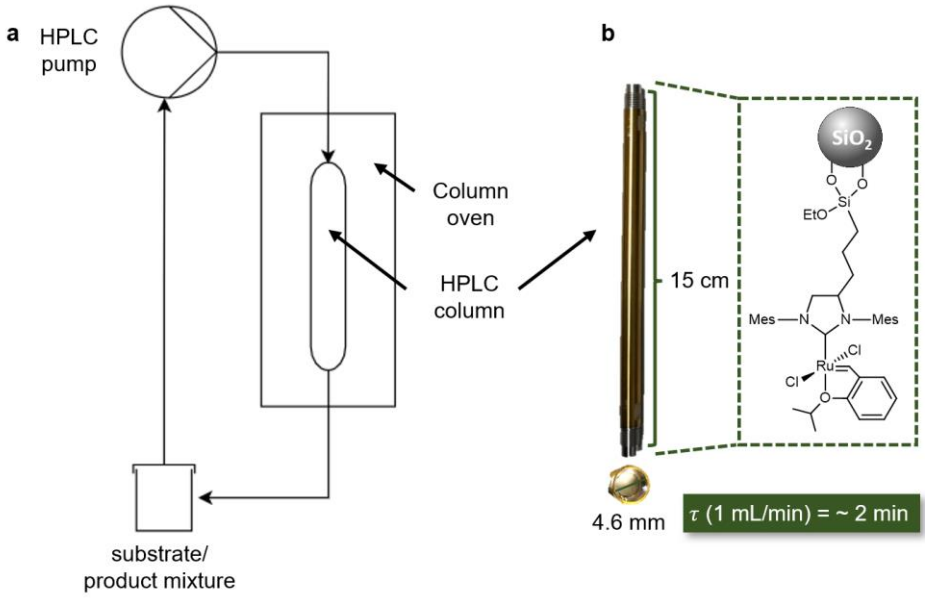

Figure 4.2 a, Technical drawing of the cyclic continuous flow set-up. b, size of the used HPLC column leading to a retention time of about 2 min when a flow rate of 1 mL/min is applied.

At room temperature a maximum conversion of 33 % was reached after 22 h (Table 4.1, entry 1). At elevated temperatures of 60 °C, a conversion of 41 % was observed after 3 h (Table 4.1, entry 2, Figure 4.3 a). A further increase in temperature to 80 °C led to a decreased catalytic performance as a significantly lower conversion of 16 % is monitored after 3 h (Table 4.1, entry 3). This hints at a catalyst deactivation at too high temperatures.

To analyze the influence of the substrate concentration on the catalytic performance, the concentration was lowered to 0.065 mol/L and a cyclic flow process was performed at 60 °C. Under these conditions, a slight increase in the conversion to 44 % is observed, illustrating an only minor impact of the substrate concentration on the performance of the catalyst at a flow rate of 1 mL/min.

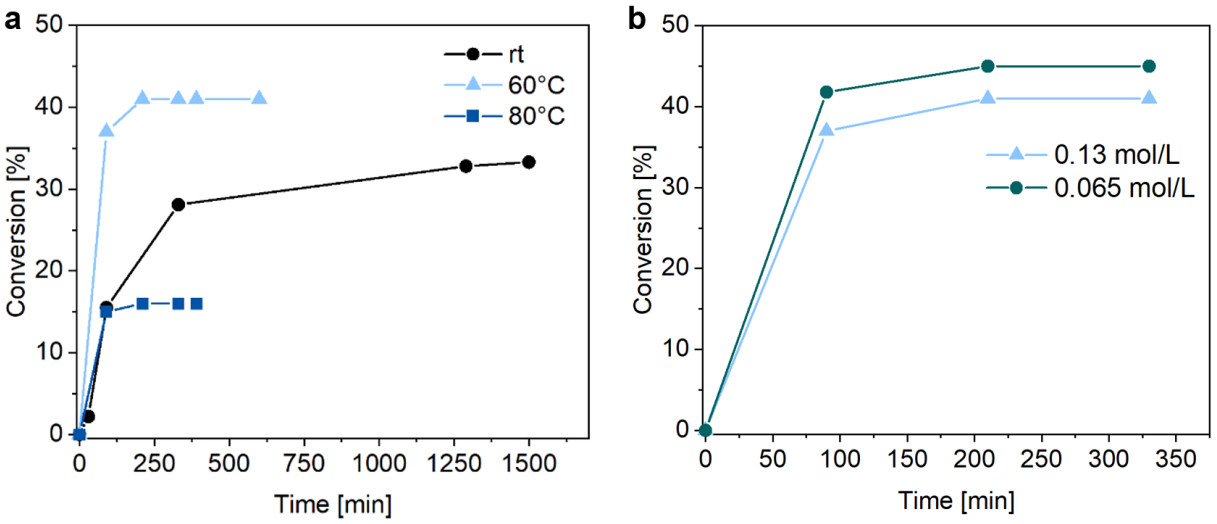

Figure 4.3. a, Depicted time conversion plots of the cyclic continuous flow self-metathesis of transesterified HOSO in toluene at different temperatures a (Table 4.1 entry 1 to 3) and substrate concentrations b (Table 4.1 entry 2 & 4).

In summary, conversions close to the maximum equilibrium conversion of 50 % are reached. This indicated a good suitability of toluene as solvent. However, toluene is toxic and has a negative impact on the environment as well as on health and safety. Thus, a more environmentally friendly solvent is desired that is also suited for olefin metathesis reactions. The organic solvents ethyl acetate and ethanol show only a low negative impact on the environment and health. In addition, it is reported that the self-metathesis of unsaturated esters performed in ethyl acetate reaches equilibrium conversions of 50 % when the Hoveyda-Grubbs 2nd generation type catalyst is used.[66,166] With respect to the aimed multicatalytic sequential process of ethenolysis-isomerization-ethenolysis under continuous flow conditions, the utilization of ethanol is of special relevance as the isomerization catalyst needs an alcohol source for its activation. Therefore, the performance in the cyclic self-metathesis was analyzed using ethyl acetate as well as ethanol as solvent (Table 4.2).

Table 4.2. Reaction conditions for cyclic continuous flow experiments in the self-metathesis of transesterified HOSO in different organic solvents.

Entry	solvent	T [°C]	Conversion [%]*
1	Toluene	rt	33
2	Ethyl acetate	rt	33
3	Ethanol	rt	2
4	Toluene	60	41
5	Ethyl acetate	60	47

Reaction conditions: 0.24 mg Ru, $c_{Substrate}$ = 0.13 mol/L, 1 mL/min flow rate, * determined by gas chromatography

In ethyl acetate, a maximum conversion of 33 % is reached at room temperature. The catalytic activity is comparable to that in toluene (Table 4.2, entry 1 & 2, Figure 4.4 a). In contrast, the use of ethanol resulted in low conversions of 2 % even after 7 h (Table 4.2, entry 3). The low observed performance hints at a catalyst decomposition in the presence of ethanol. With Grubbs olefin metathesis catalysts, alcohols have been frequently reported to produce side products or lead to a degradation of the catalyst. This is why ethyl acetate was used for further experiments.

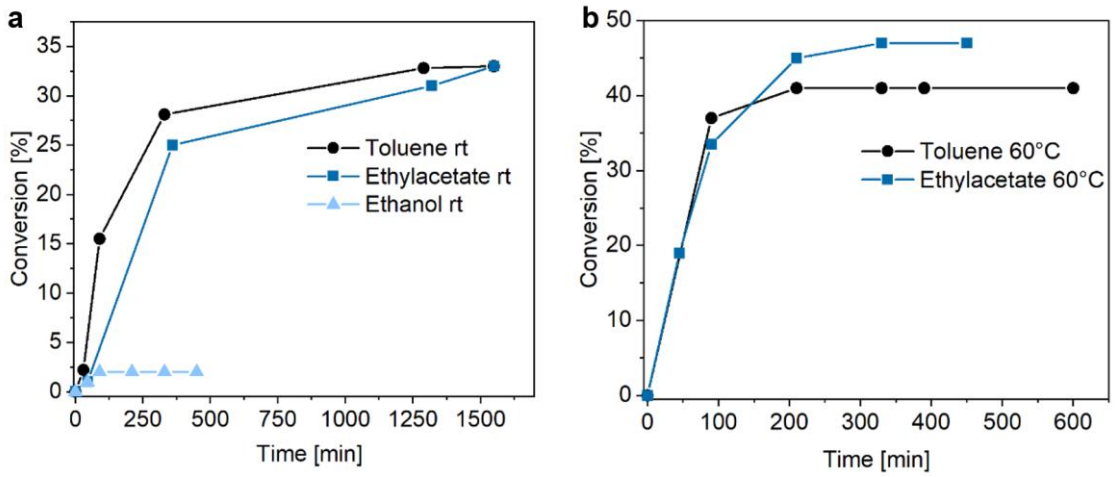

Figure 4.4. a, Time conversion plot of the cyclic continuous flow self-metathesis of transesterified HOSO in different organic solvents and b, of toluene and ethyl acetate at 60 °C.

By increasing the reaction temperature to 60 °C, an improved conversion of 47 % is reached with ethyl acetate as a solvent (Table 4.2 entry 5, Figure 4.4 b). Compared to the obtained conversion in toluene (41 %, Table 4.2 entry 4) an even higher catalytic performance is observed. Whereas at room temperature, the maximum conversion of 33 % is reached after 20 h, at elevated temperatures of 60 °C a reaction time of 200 min is sufficient to almost end

up in equilibrium conversions of 47 % (theoretical 50 %). This illustrates a much faster reaction at higher temperatures and is coherent with observations made in toluene (Figure 4.3 a). In summary, the greener solvent ethyl acetate represents a good alternative to toluene and the catalytic performance is superior in ethyl acetate.

By cycling the substrate solution, a maximal turnover number (TON), which is defined by the amount of formed product using a certain amount of catalyst, (conversion · $n_{substrate}/n_{catalyst}$) of 1030 was reached. Under batch conditions, TON of up to 1200 are reported for the immobilized catalyst HGII-SiO_2.[161] On the contrary, a non-cyclical continuous flow reaction might increase the catalytic productivity and allows for a closer insight into the catalyst stability over a certain period of time. Thus, a continuous flow reaction was performed by constantly pumping fresh substrate solution through the column. The conversions were directly measured by analyzing the product mixture that passed through the column after a specific time (Table 4.3, Figure 4.5 a).

Table 4.3. Reaction conditions for continuous flow experiments in the self-metathesis of transesterified HOSO in ethyl acetate.

Entry	Ru [mg]	T [°C]	$c_{Substrate}$ [mol/L]	Flow rate [mL/min]	Residence time [sec]	Remark
1	0.24	60	0.15	1 to 0.3	114 to 380	-
2	0.24	60	0.15	0.3	380	-
3	0.48	60	0.15	0.6	190	-
4	0.48	45	0.15	0.4	285	-
5	0.48	45	0.15	0.4	285	Dried ethyl acetate 99.9%
6	0.48	45	0.2*	0.4	285	Nylon filter, Ethyl acetate 99.9%

A substrate concentration of 0.15 mol/L at a temperature of 60 °C and an initial flow rate of 1 mL/min resulted in conversions lower than 5 % (Table 4.3 entry 1, Figure 4.5 b, entry 1). By decreasing the flow rate during the flow process of this reaction to 0.3 mL/min, the conversion increases to the equilibrium conversion of 50 %. However, the conversion drops over a period of 4 h to around 10 %. Using an initial flow rate of 0.3 mL/min, the maximum conversion of 50 % was directly reached at the beginning of the process (Table 4.3 entry 2, Figure 4.5 b entry 2). However, a similar decrease in catalytic activity over time is visible leading to low conversions of around 5 % after 5 h.

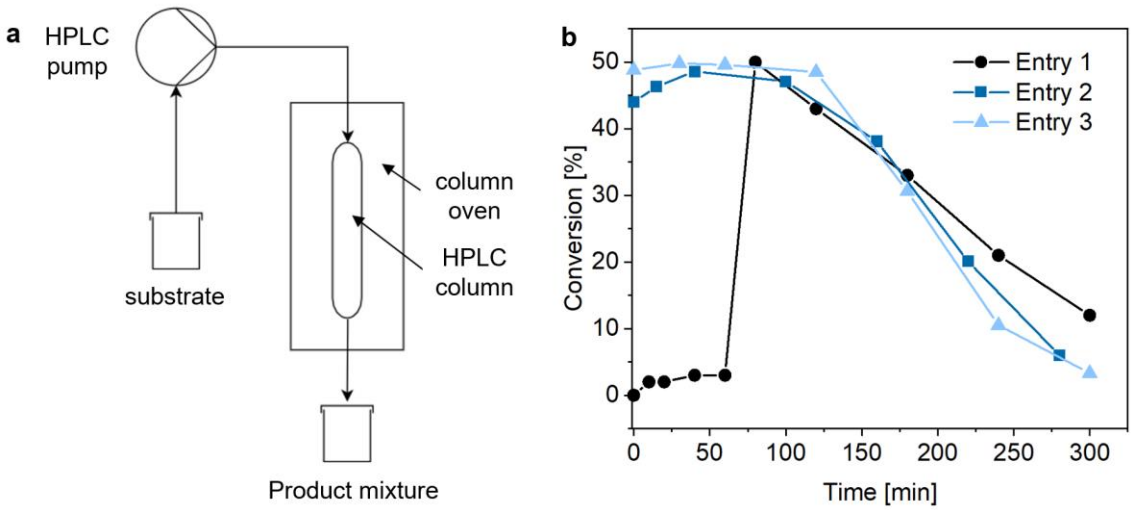

Figure 4.5 a, Technical drawing of the continuous flow set-up b, Time conversion plot of the continuous flow self-metathesis of transesterified HOSO in ethyl acetate (Table 4.3., entry 1 to 3).

By doubling the catalyst amount and flow rate, a comparable reaction profile was observed, illustrating the reproducibility of the process (Table 4.3 entry 3). The decline in conversions over time might originate from catalyst deactivation processes. From cyclic reactions at elevated temperatures of 80 °C in toluene, a negative impact on the catalytic stability was already shown. To get a closer look into the influence of the temperature on the catalyst stability, the temperature was reduced from 60 °C to 45 °C (Table 4.3 entry 4). Under these conditions, the equilibrium conversion of 50 % is only reached after 30 min hinting at an initial low reaction rate (Figure 4.6, entry 4).

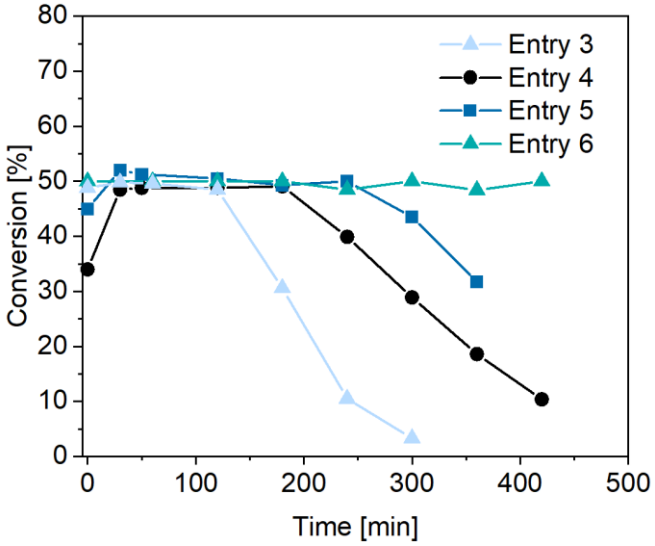

Figure 4.6. a, Time conversion plot of the continuous flow self-metathesis of transesterified HOSO in ethyl acetate (Table 4.3 entry 3 to 7).

Such a short induction periode has been reported in the self-metathesis of HOSO at 45 °C using HGII-SiO_2 under batch conditions.[161] Nevertheless, the conversion is constant over a total period of 3 h and decreases to 30 % over a period of 5 h. Thus, the catalytic stability seems to be enhanced at 45 °C, probably due to less or slower catalyst deactivation.

Impurities represent a possible parameter contributing to deactivation processes. Examples are water and other organic compounds present in organic solvents. To investigate their impact on the catalyst stability, high purity grade ethyl acetate was used which additionally was dried prior to use (99.9 % purity, Table 4.3 entry 5). Under these conditions, a further improvement in the catalytic performance is observed. The conversion is stable over 4 h. Nevertheless, the conversion still decreases to around 30 % after 6 h. This indicates that organic impurities and water have an impact on the catalytic stability.

In addition, small silica particles are found in the product mixture, hinting at a loss of immobilized catalyst through the column frit. This was underlined by scanning electron microscopy measurements (SEM), showing particles with sizes below 1 µm in diameter (Figure 4.7). The original silica material has a particle size of 3.5 to 5 µm. This means that the particles are probably crushed during stirring in the immobilization process. With a pore size of 2 µm for the column frit, the smaller particles can move through the frit. Next to deactivation processes, the loss of silica particles bearing active catalyst results in an intensified decrease in catalytic activity.

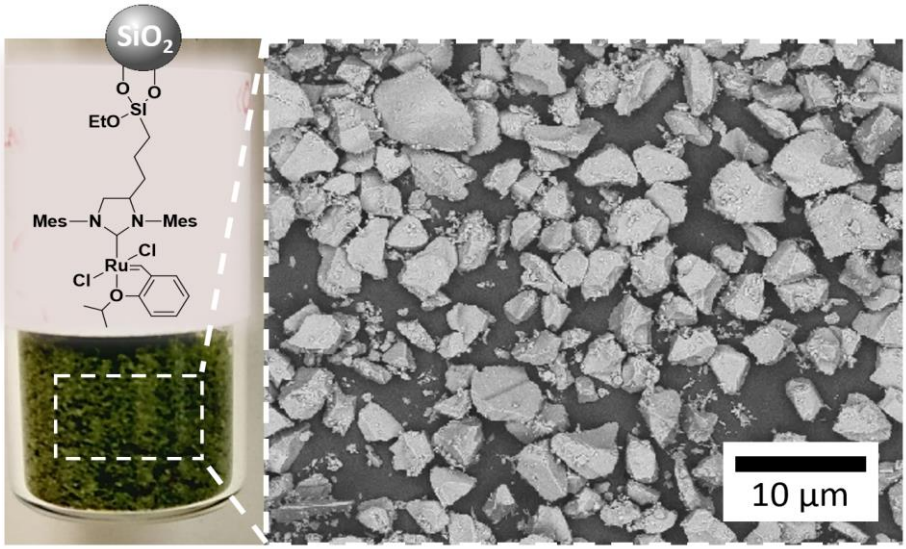

Figure 4.7 SEM image of immobilized silica material.

The analysis of the product mixture by inductively coupled plasma optical emission spectrometry (ICP-OES) showed that up to 20 % of the used Ru content was lost during the continuous flow process. This loss might be due to the observed leakage of immobilized silica material. However, additional leaching processes of homogeneous species might also contribute to the total found Ru content. To investigate the main origin for the loss in Ru on the column, a continuous flow experiment installing a nylon filter with a pore size of 0.45 µm at the column ends was conducted (Table 4.3 entry 6). This prevents the leakage of small, immobilized catalyst particles. Under these conditions, the conversion stayed stable over the whole flow process during 7 h even at a slightly higher methyl oleate concentration of 0.2 mol/L. This might indicate that homogenous catalyst leaching is not relevant. Thus, the main reason for the decreased conversions over time is the loss of small crushed immobilized catalyst particles. This was further confirmed by analyzing the product mixture by ICP-OES revealing a Ru content of only 3 % when the nylon filter is used. This indicates a stable linkage of the functionalized homogenous catalyst on the silica material.

The performance of a split test further supported this statement (Figure 4.8). After 4 h of constant flow, 1 mL of the product mixture was collected and 0.2 mL of methyl oleate was added. The mixture was split into two samples (Figure 4.8 sample 1 & sample 2). Sample 1 was quenched with ethyl vinyl ether and its conversion was calculated by GC (33 %). Sample 2 was stirred at 45 °C for 2 h to investigate if there is a possible increase in conversion due to leached homogenous catalyst.

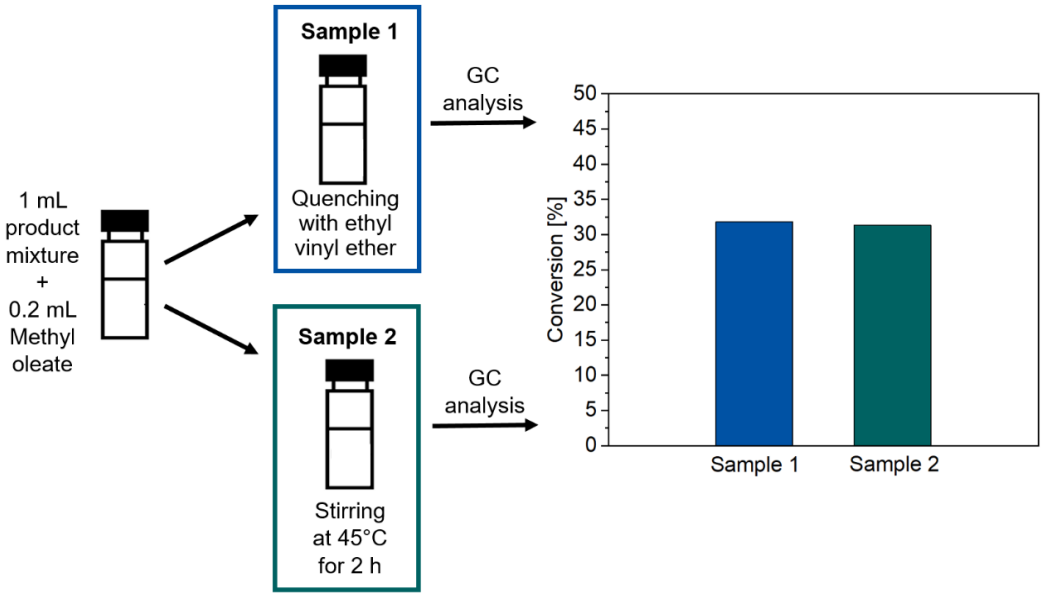

Figure 4.8 Split test procedure to analyze possible leaching processes which would result in an increased in conversion in sample 2.

Determination of the conversion of sample 2 by GC reveals the same conversion of 33 % as for sample 1. There is no increase in conversion underlining that no significant leaching of the immobilized catalyst is taking place.

Under the described optimized reaction conditions (Table 4.3 entry 6), a maximum TON of 3030 is reached, which is almost 3 times higher than reported TONs under batch conditions in toluene (1200). As the conversions are still at equilibrium after 7 h, the reaction time was increased to 10 h, still resulting in equilibrium conversion of 50 %. No loss in catalytic activity over the whole period is observed. Thus, an even higher TON of around 5000 is achieved (Figure 4.9).

Cabrera *et al.* reported on the utilization of a non-covalently bonded Hoveyda Grubbs catalyst onto silica material in the continuous flow self-metathesis of methyl oleate.[122] They reported a maximum TON of 2475 with a Ru loss of 12 to 19 %. In contrast, the covalently linked HGII-SiO_2 catalyst used in this work shows TONs that are twice as high with only minor Ru leaching as low as 3 %. These results illustrate a good suitability of the immobilized catalyst HGII-SiO_2 for continuous flow applications in the self-metathesis of methyl oleate.

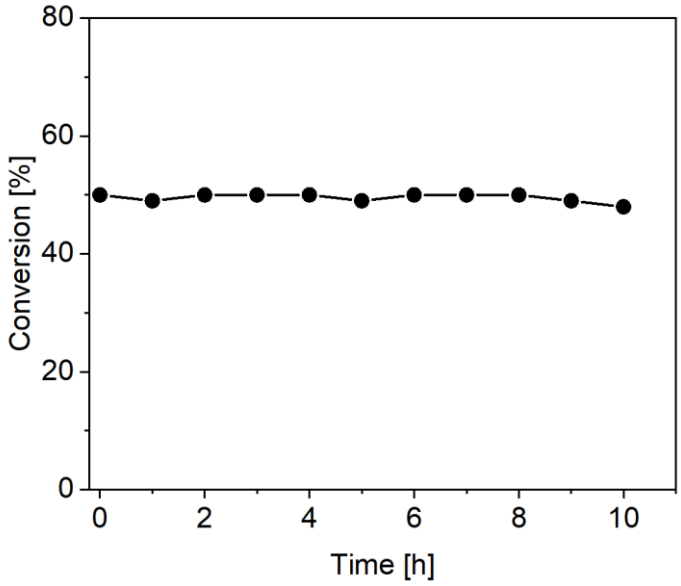

Figure 4.9 Time conversion plot of the continuous flow self-metathesis of methyl oleate in ethyl acetate using a nylon filter over the course of 10 h.

4.2.3 Continuous Flow Self-metathesis of Methyl Oleate in $scCO_2$

Towards a more sustainable process for the upgrading of renewable feedstocks, one important aspect is the replacement of volatile organic solvents as they are often toxic, flammable and have a negative impact on the environment. Moreover, for downstream processing their isolation from the reaction mixture to get access to the desired pure products and their disposal are important cost factors. Compressed carbon dioxide gained in importance as green replacement for such organic solvents as it is relatively cheap, environmentally friendly and non-toxic.[167] In addition, $scCO_2$ is easy removable and the mild critical parameters of 31 °C and 74 bar allow for the catalysis with thermal sensible substrates and catalysts.[20]

As homogeneous Hoveyda Grubbs-type catalysts are known to be active in $scCO_2$ [142], a continuous flow process using its immobilized version in the green solvent $scCO_2$ is desirable. However, to dissolve substrates like fatty acids, high CO_2 densities are required, which is why a high reaction pressure needs to be applied. For this reason, a high-pressure reactor system was constructed to allow for the continuous flow of transesterified HOSO in $scCO_2$ at pressures up to 500 bar (Figure 4.10).

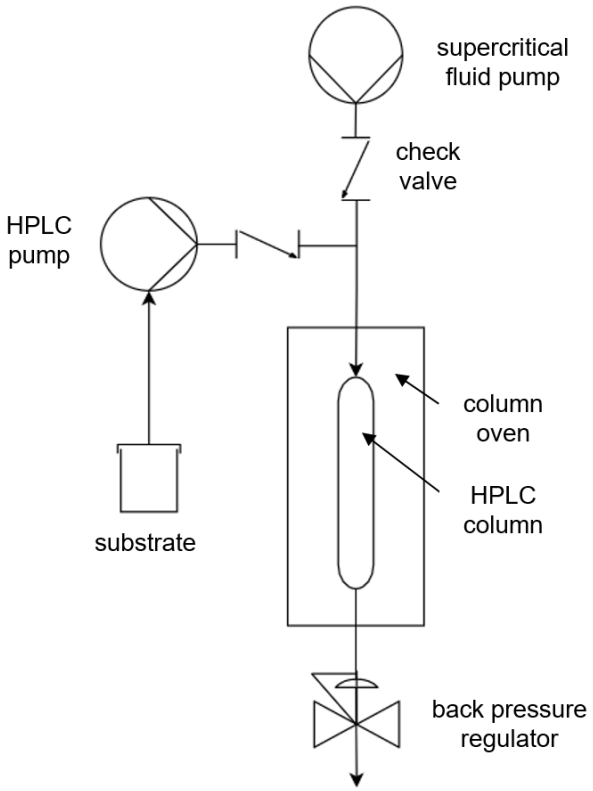

Figure 4.10 Technical drawing of the high-pressure continuous flow set-up for the self-metathesis of HOSO in $scCO_2$.

As reaction vessel, an HPLC column with integrated frit was used which was placed in a column oven to allow for the adjustment of the reaction temperature. A supercritical fluid pump was connected to the reactor system. It facilitates the delivery of liquid CO_2 into the reactor set-up and allows for the pressurization up to 700 bar.

By pressurizing the reactor setup with liquid CO_2 to 500 bar at a minimum temperature of 31 °C, a supercritical medium is obtained. An integrated fine-tuned valve at the end of the reactor system allows for the controlled release of the CO_2 reaction mixture and enables a continuous flow under increased pressures. As the continuous flow self-metathesis of transesterified HOSO in ethyl acetate was found to be stable at 45 °C, first experiments were performed in a solvent mixture of $scCO_2$ and ethyl acetate at 45 °C (Table 4.4).

Table 4.4 Used reaction conditions for continuous flow experiments in the self-metathesis of HOSO in $scCO_2$.

Entry	Ru [mg]	T [°C]	p [bar]	ρ_{CO2} [g·cm^{-3}]	$c_{substrate}$ [mol/L]	Flow rate MO [mL/min]	Flow rate CO_2 [mL/min]
1	0.34	45	350	0.92	0.7	0.3	1.5
2	0.34	45	350	0.92	0.7	0.15	0.3
3	0.34	45	450	0.96	0.7	0.15	0.3
4	0.34	45	450	0.96	2.6	0.01	0.3
5	0.34	40	500	0.99	Pure MO	0.01	0.2
6	0.34	35	500	1.00	Pure MO	0.01	0.2

A solution of HOSO in ethyl acetate with a concentration of 0.7 mol/L was pumped with a flow rate of 0.3 mL/min into the reactor system. In addition, CO_2 is delivered at a total pressure of 350 bar with a flow rate of 1.5 mL/min (Table 4.4 entry 1). Under these conditions, only low conversions < 10 % were reached. This hints at a too high total flow rate resulting in an insufficient retention time of the substrate on the column. By decreasing the flow of the HOSO solution as well as of CO_2 to 0.15 mL/min and 0.3 mL/min, respectively, the equilibrium conversion of 50 % was reached irrespective of whether 350 bar or 450 bar were used (Table 4.4 entry 2 & 3, Figure 4.12).

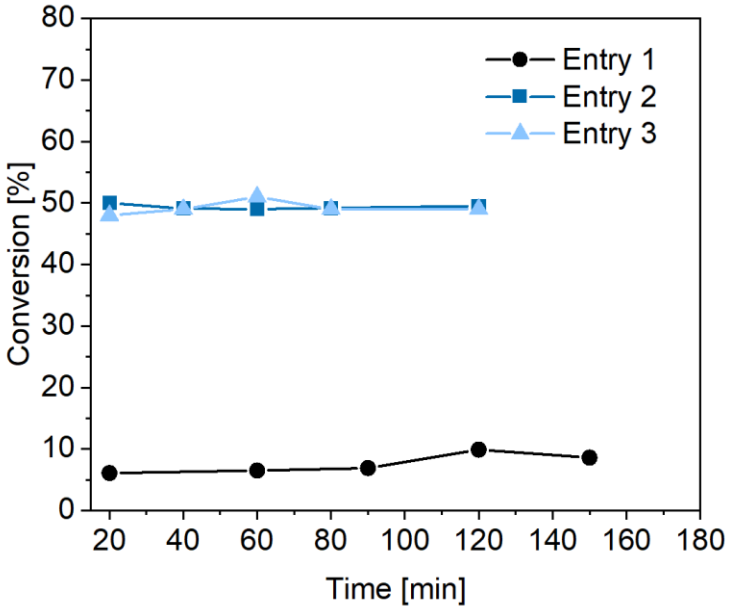

Figure 4.12 Depicted time conversion plot of the continuous flow self-metathesis of HOSO using $scCO_2$ and ethyl acetate as reaction medium with reaction conditions described in Table 4.4 entry 1 to 3.

To get closer to a continuous flow process using solely $scCO_2$ as a reaction medium, the substrate concentration in ethyl acetate was increased to 2.6 mol/L. Even with a lower flow rate for the substrate solution of 0.01 mL/min, thus a higher CO_2 concentration, the equilibrium conversion was only reached after 1.5 h. This suggests a slow dissolving of HOSO at higher CO_2 concentrations (Table 4.4 entry 4, Figure 4.11).

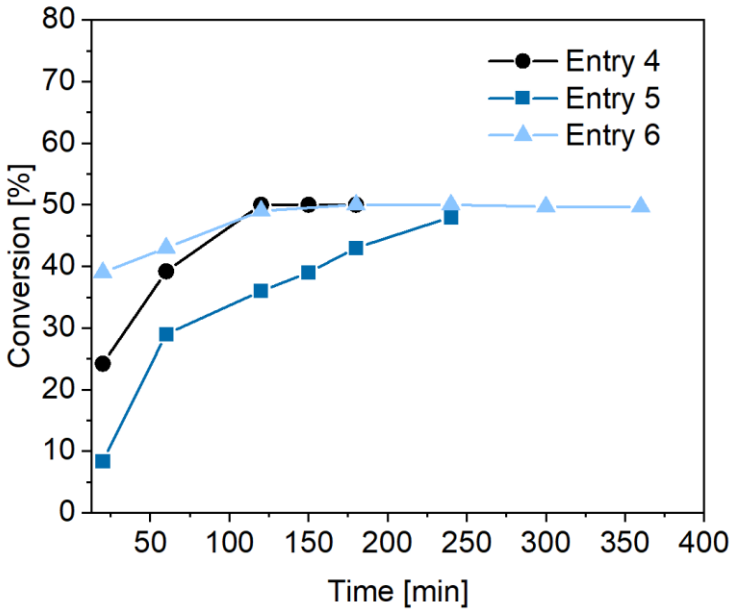

Figure 4.11 Time conversion plot of the continuous flow self-metathesis of HOSO in $scCO_2$ with reaction conditions described in Table 4.4 entry 4 to 6.

As the solubility of methyl oleate is increased in $scCO_2$ at higher CO_2 densities, the temperature was decreased to 40 °C and the pressure increased to 500 bar to reach a sufficient solubility when pure HOSO in $scCO_2$ is used (Table 4.4 entry 5).

Even tough under these conditions, the continuous flow with pure HOSO led to a maximum conversion of around 45 %, it took even longer to reach this value. By a further decrease in temperature to 35 °C, leading to an even higher CO_2 density of around 1 $g \cdot cm^{-3}$, a higher initial conversion of 40 % was observed which reached equilibrium after 2 h and stayed constant over a total period of 6 h (Table 4.4 entry 6, Figure 4.11 entry 6).

Here, a stable continuous flow self-metathesis of HOSO in $scCO_2$ as reaction medium is presented leading to a TON of > 2000. As no decline in catalytic activity is observed it is assumed that even higher TONs can be achieved. Moreover, ICP-OES analysis of the product mixture revealed a Ru loss of around 2 %, indicating that no significant catalyst leaching was occurring in the presence of $scCO_2$ as medium. To our knowledge, this is the first reported example of a continuous flow self-metathesis of methyl oleate performed in the environmentally friendly medium $scCO_2$. These results built the basis for a green and efficient catalytic high throughput self-metathesis of renewable fatty acids.

4.2.4 Continuous Flow Ethenolysis of Methyl Oleate

Ethenolysis is a very powerful tool to transform renewable lipids into terminal olefins and unsaturated esters. However, the product scope is restrained by the variety of occurring fatty acids in nature. To expand the range of possible products, the combination of ethenolysis and double bond isomerization represents a promising approach. Gooßen *et al*. reported on a simultaneous isomerizing ethenolysis of rapeseed oil to get access to olefins, monoesters as well as diesters with a carbon chain length in the range of C_3 to C_{23}.[85] As short chain terminal products are of special interest in the chemical industry, a synthesis route for their production from renewable oils is desired. Within this work a new concept of a consecutive ethenolysis, isomerization and additional ethenolysis in $scCO_2$ under batch conditions is described (chapter 3.2). It allows for the upgrading of fatty acids from renewable oils into α-olefins and terminal unsaturated esters in the C_3 to C_{10} regime. From an industrial point of view, the performance of the multicatalytic sequential process under continuous flow conditions is desired as it lowers maintenance costs and facilitates recycling and reuse of the catalyst. Thus, a continuous flow process in sCO_2, using an immobilized catalysts is aimed.

To form the basis for such a continuous flow biorefinery process, the continuous flow ethenolysis of fatty acids using the immobilized catalyst HGII-SiO_2 is investigated. Analysis was focused on catalyst performance and stability. Transesterified HOSO, containing 92.5 % of the fatty acid methyl oleate (FAME 18:1) was used as model substrate. The ethenolysis of FAME 18:1 result in the terminal products methyl 9-decenoate (E 10:1) and 1-decene (HC 10:1) as well as in the side products dimethyl 1,18-octa-9-decene (DE 18:1) and 9-octadecene (HC 18:1) *via* self-metathesis (Scheme 4.4).

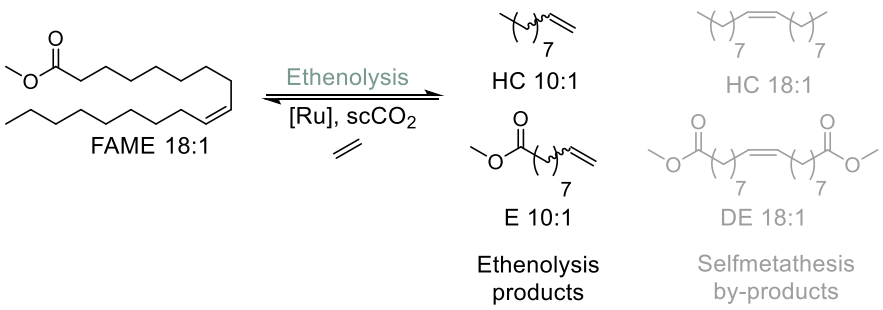

Scheme 4.4 Reaction scheme of an ethenolysis reaction of methyl oleate (FAME 18:1) with possible self-metathesis by-product formation.

To allow for a continuous flow ethenolysis using $scCO_2$ as reaction medium, a reactor set-up was designed allowing for the use of high pressures up to 700 bar (Figure 4.13). As already described for continuous flow reactions in the self-metathesis of HOSO (chapter 4.2.3), the immobilized catalyst is filled into an HPLC column which is fixed in a column oven to adjust reaction temperatures. Ethylene and CO_2 are delivered by a syringe pump and supercritical fluid pump, respectively. The substrate is pumped by an HPLC pump. To allow for a sufficient mixing of ethylene, CO_2 and the substrate, a static mixer is used.

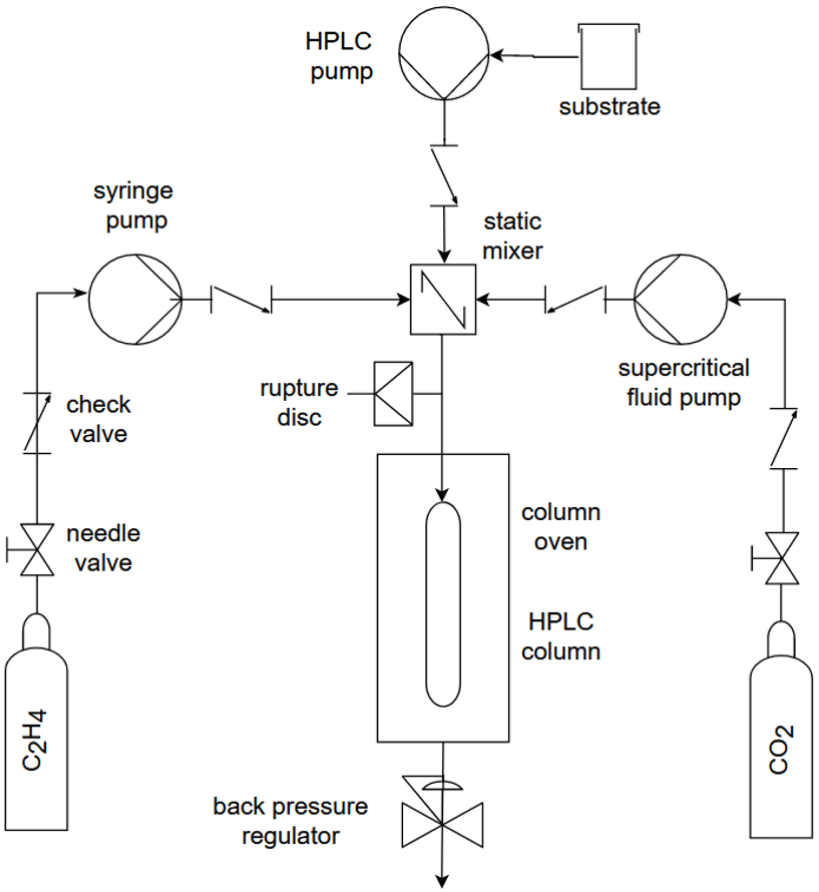

Figure 4.13 Technical drawing of the continuous flow set-up for the ethenolysis of HOSO in $scCO_2$.

To reach a constant flow of the $scCO_2$ mixture, a back pressure regulator is inserted allowing for a controlled release of the product mixture while a set pressure is held. Conversions and selectivities of the product mixture are periodically determined by GC measurements to obtain a reaction profile. First ethenolysis experiments were conducted at pressures of 500 bar, temperatures of 45 °C and a CO_2 flow of 0.2 mL/min (Table 4.5).

Table 4.5 Reaction conditions in continuous flow ethenolysis experiments of HOSO in $scCO_2$.

Entry	Ru [mg]	T [°C]	p [bar]	Flow rate HOSO [mL/min]	Flow rate CO_2 [mL/min]	Flow rate C_2H_4 [mL/min]
1	0.36	45	500	0.03	0.2	0.08
2	0.85	45	500	0.02	0.2	0.04

CO_2 density: 0.98 g·cm^{-3}

Using a total Ru content of 0.36 mg in the packed column at a substrate flow rate of 0.03 mL/min and an ethylene flow rate of 0.08 mL/min, low conversions under 10 % were reached over a period of time of 300 min (Table 4.5 entry 1, Figure 4.14 entry 1). The high ethylene flow led to a maximum selectivity for ethenolysis products of 60 % after 40 min. However, a fast decline in selectivity as well as in conversion is observed after 60 min.

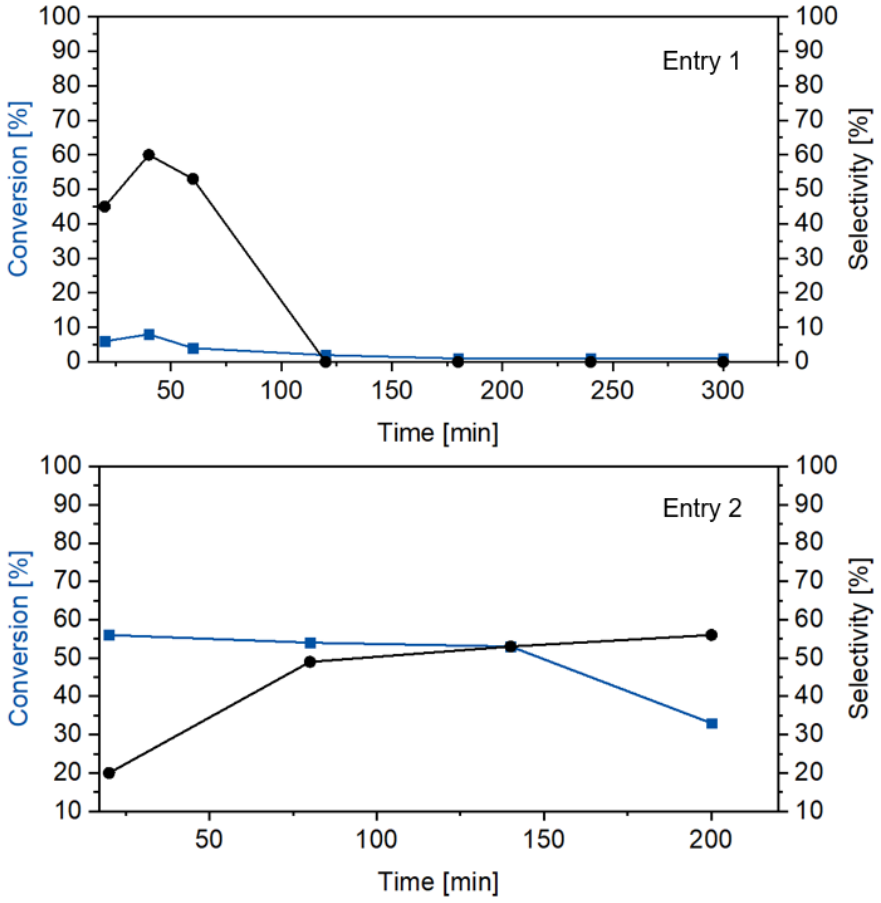

Figure 4.14 Depicted time conversion plot of the continuous flow ethenolysis of HOSO in a $scCO_2$ reaction medium under reaction conditions described in Table 4.5 entry 1 & 2.

The low conversions over time might be the origin of too high substrate flow rates leading to an overload of the column. A further reason might be too high ethylene flow rates facilitating deactivation of the catalyst. Thus, both flow rates were reduced to 0.02 and 0.04 mL/min, respectively and a higher catalyst loading of 0.85 mg of Ru was used to enhance the catalyst performance (Table 4.5 entry 2, Figure 4.14 entry 2). Within these reaction parameters, a maximum conversion of around 55 % was obtained after 20 min, which stayed constant over 140 min until it decreased to 35 %. Therefore, the lower flow rates and higher catalyst loadings resulted in an enhanced catalytic activity. However, the maximum selectivity for ethenolysis of around 60 % was only slowly reached after 200 min, hinting at an inconstant ethylene flow or an initial pour mixing of the ethylene in $scCO_2$.

To enable a more efficient mixing of the ethylene with $scCO_2$ and the substrate, the reactor set-up was modified. By pumping liquid CO_2 into the 100 mL cylinder of the syringe pump, filled with a defined amount of ethylene, a mixture of CO_2 and ethylene was prepared prior to the start of the continuous flow process (Figure 4.15). As a result, a constant flow with a defined ratio of ethylene to CO_2 is applied.

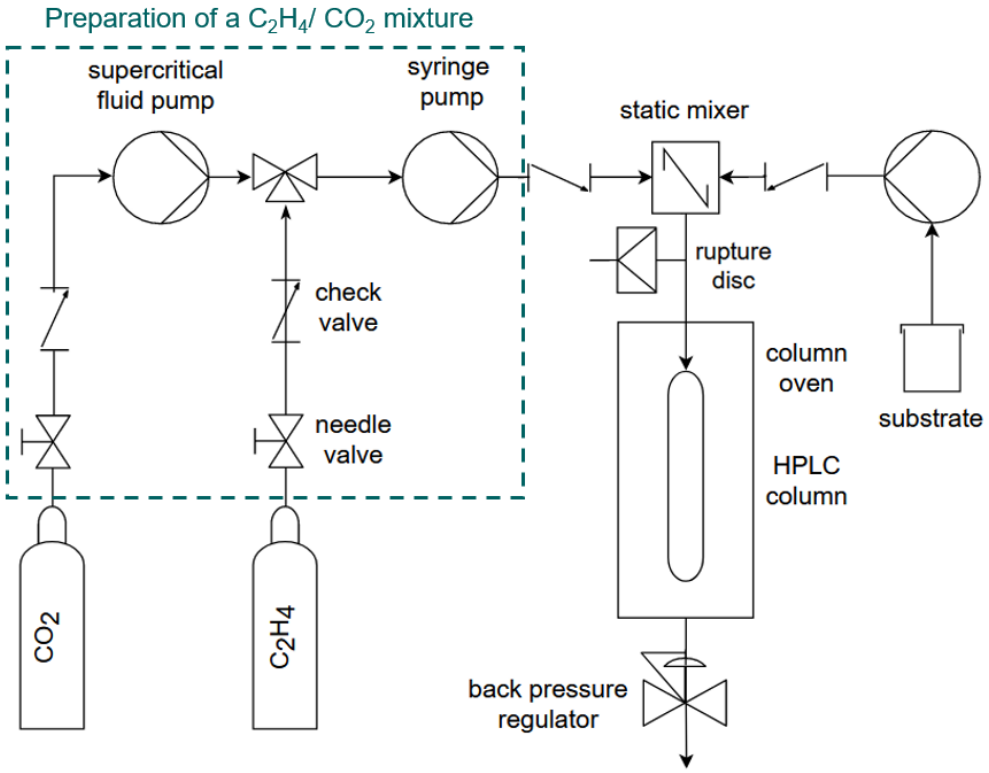

Figure 4.15 Technical drawing of the modified high pressure continuous flow set-up for ethenolysis of HOSO in $scCO_2$ and picture section of the constructed reactor.

With the modified reactor set-up, the catalytic activity and stability in the ethenolysis of HOSO was investigated (Table 4.6). In a first attempt, a gas mixture was prepared that corresponded to 5 equivalents of ethylene to the substrate when a flow rate of HOSO of 0.02 mL/min and of 0.2 mL/min for the C_2H_4/CO_2 mixture was applied (Table 4.6, entry 1). By varying the temperature from 40 to 50 °C, conversions and selectivities for ethenolysis products were determined over the whole flow process.

Table 4.6 Reaction conditions of continuous flow ethenolysis of HOSO in $scCO_2$ using a modified reactor set-up.

Entry	Ru [mg]	T [°C]	Flow rate MO [mL/min]	Eq. C_2H_4 to HOSO	Flow rate C_2H_4/ CO_2 [mL/min]	Additive	TON
1	0.36	40-50	0.02	5	0.2	-	270
2	0.36	40	0.02	7.5	0.2	-	170
3	0.6	40	0.01	12	0.1	-	250
4	0.72	40	0.01	9	0.1	-	550
5	0.9	40	0.01*	9	0.1	-	650
6	0.9	40	0.01*	9	0.1	10 vol% Ethyl acetate	370
7	0.9	40	0.01*	9	0.1†	5 mol% 2-Isopropoxy-styrene	340

*GC grade methyl oleate was used and pumped before pressurization up to the static mixer to reduce contact time of ethylene with the catalyst, † CO_2 5.5 grade was used. p_{tot}= 500 bar, CO_2 density: 0.99 g·cm^{-3}.

At a reaction temperature of 40 °C, an initial conversion of 30 % is obtained with a selectivity of around 60 %. As the selectivity reaches its maximum value right from the beginning of the reaction, it suggests a positive influence of the constant flow of a defined mixture of ethylene and CO_2 on the catalyst performance. The conversions and selectivities decrease after 180 min to values of 2 and 30 %, respectively, when the temperature is increased after 30 min and 120 min to 45 °C and 50 °C (Figure 4.16, entry 1).

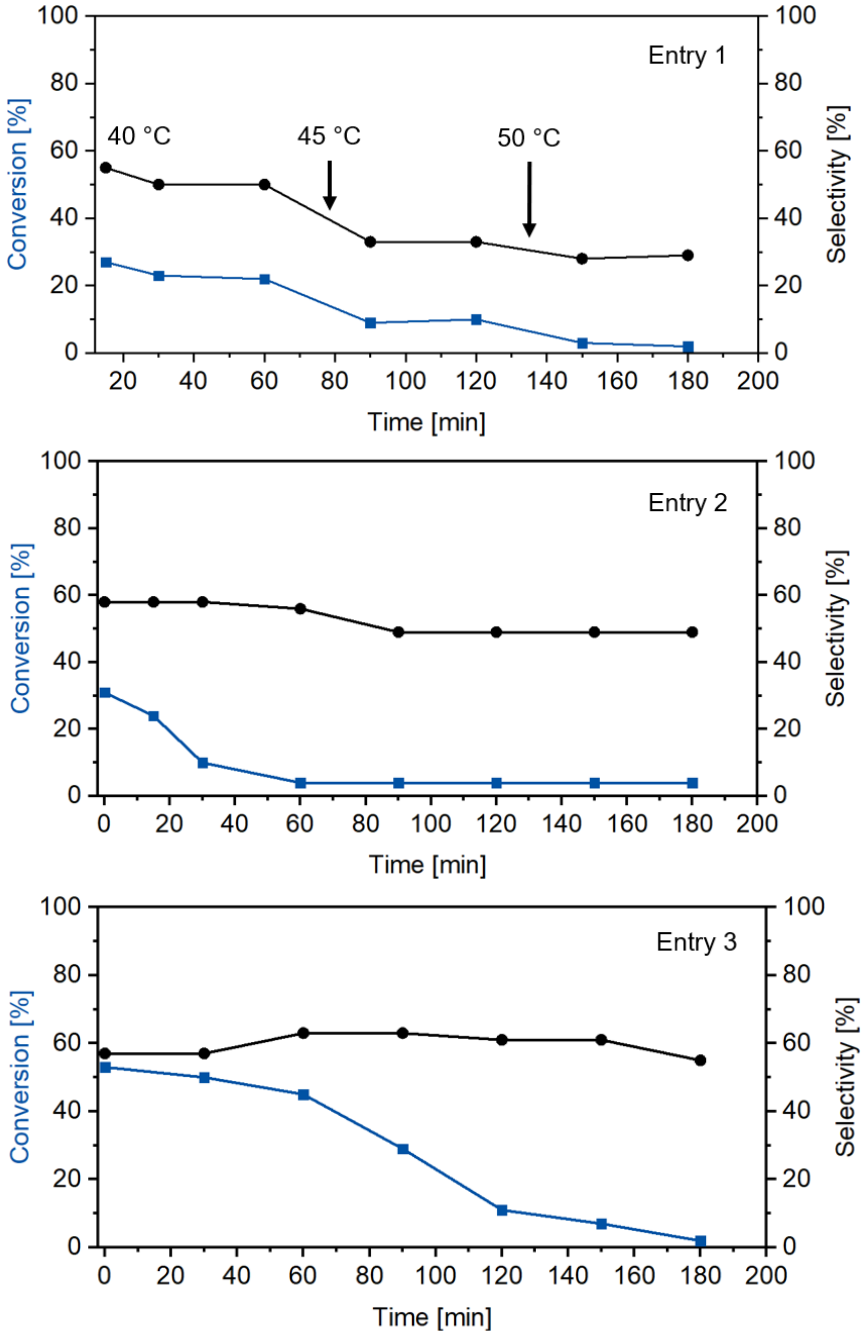

Figure 4.16 Depicted time conversion plot of the continuous flow ethenolysis of HOSO in a $scCO_2$ reaction medium under reaction conditions described in Table 4.6, entry 1 to 3.

Compared to that, at a constant temperature of 40 °C and higher ethylene equivalents of 7.5, the selectivity stays relatively constant (around 55 %) over the whole flow process (Figure 4.16, entry 2). This hints at a higher preference for the self-metathesis side reaction at higher temperatures and lower ethylene pressures. The conversions decrease in both cases to a minimum conversion < 5 %. Even though the conversion is slightly higher for the use of 7.5 equivalents of ethylene, the decline proceeds faster and reaches already after 60 min its minimum. The origin of this fast decrease might be catalyst deactivation as during

ethenolysis unstable methylidene complexes are formed, undergoing rapid decomposition processes. With the use of higher ethylene amounts, deactivation can proceed even more pronounced.

To improve the catalyst performance, a higher catalyst amount of 0.6 mg Ru as well as reduced flow rates for HOSO and the ethylene/CO_2 mixture of 0.01 mL/min and 0.1 mL/min, respectively, were used (Figure 4.16, entry 3). At the same time, the amount of ethylene was further increased to 12 equivalents to analyze the impact of ethylene amounts on the catalyst stability more closely. The higher Ru loading and lower flow rates led even in the presence of higher amounts of ethylene to an increased conversion of 53 %. The conversion stayed relatively constant over a period of 60 min until a fast decrease to 2 % is observed. Compared to the reaction before (Figure 4.16, entry 2), the decline in conversion is slower hinting at a prolonged catalyst stability under these conditions. Thus, the increased catalyst loading in combination with lower flow rates seem to have a higher influence on the catalyst performance than the higher ethylene pressures, which are known to facilitate catalyst deactivation.[149]

At 7.5 equivalents of ethylene, a relatively constant selectivity of around 55 % was reached. As at 12 equivalents of ethylene the selectivity was only slightly increased to around 60 %, for further reactions 9 equivalents of ethylene were used to prevent possible deactivation processes. With a further increase in catalyst loading to 0.72 mg of Ru, an enhanced conversion of 60 % was observed. With a ratio of substrate to ethylene of 1:9, the highest observed selectivity of 80 % is reached (Table 4.6 & Figure 4.17, entry 4).

In addition, the catalyst performance was relatively constant over a period of 180 min and the conversion is only decreasing slowly to 37 % over a period of 260 min. Under these conditions, a TON of about 550 was observed. Thus, with the modified reaction conditions a more stable catalyst performance was reached. However, even higher conversions and TONs are desired. To further improve the catalyst performance, possible impurities in the reactor system were eliminated by the use of CO_2 with a higher purity (99.9995 % instead of 99.995 %) as well as pure methyl oleate (99.9 %) instead of HOSO (Table 4.6, entry 5).

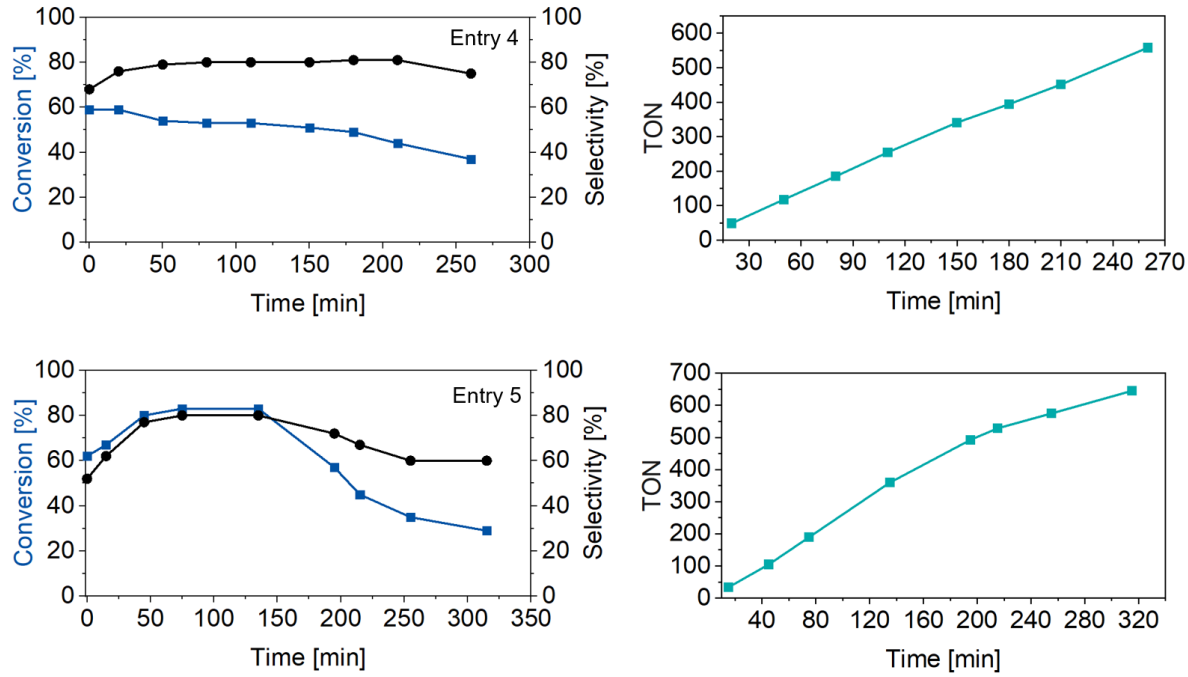

Figure 4.17 Depicted time conversion plot (left) and TON (right) of the continuous flow ethenolysis of HOSO in a $scCO_2$ under reaction conditions described in Table 5.6, entry 4 & 5.

In addition, the reaction was performed using 0.9 mg of Ru. As described by the group of Apesteguia, a diminished conversion of the ethenolysis of methyl oleate was observed, when a non-covalently immobilized HGII catalyst is exposed to ethylene before the addition of methyl oleate.[121] Therefore, the contact time of ethylene with the immobilized catalyst was reduced by pumping the methyl oleate up to the static mixer. By doing so, the catalyst has direct contact with ethylene as well as methyl oleate when the reactor system is pressurized with the CO_2/ethylene mixture. Upon pressurization of the reactor, the methyl oleate passes relatively quickly through the column leading to a slow initial increase of the conversion (Figure 4.17 entry 5). After a period of 75 min, the maximum conversion of 83 % was reached which resulted in a slightly increased TON of 650. The maximum observed selectivity was with values of 80 % comparable to the reaction using 0.72 mg of Ru. With a higher catalyst loading as well as high purity grad methyl oleate and CO_2, a higher performance over 140 min was reached. However, still a fast decline in conversion and selectivity was observed. After 320 min, a minimum conversion of around 30 % with a selectivity for ethenolysis products of 60 % was reached.

In a further step, the effect of additives such as a co-solvent or stabilizing ligands was investigated (Table 4.6, entry 6 & 7). As ethyl acetate was shown to be a good solvent for the continuous flow self-metathesis of HOSO, 10 vol% was added to the substrate. At otherwise same reaction conditions, a maximum conversion of 90 % was already reached after 30 min, indicating a better solubility of the substrate which facilitates a faster reaction in the column. Nevertheless, after 60 min of flow, a fast decrease in conversion was observed resulting in a minimum conversion of around 10 % after 270 min. The better solubility might in this case not only lead to a more efficient catalyst performance but also to a faster decomposition of the catalytic species leading to a reduced TON of 370 (Figure 4.18, entry 6). Even though dried and degassed ethyl acetate was used, remaining impurities might have a negative impact on the catalyst stability. Thus, the use of pure $scCO_2$ seems to have a positive influence on the catalyst stability.

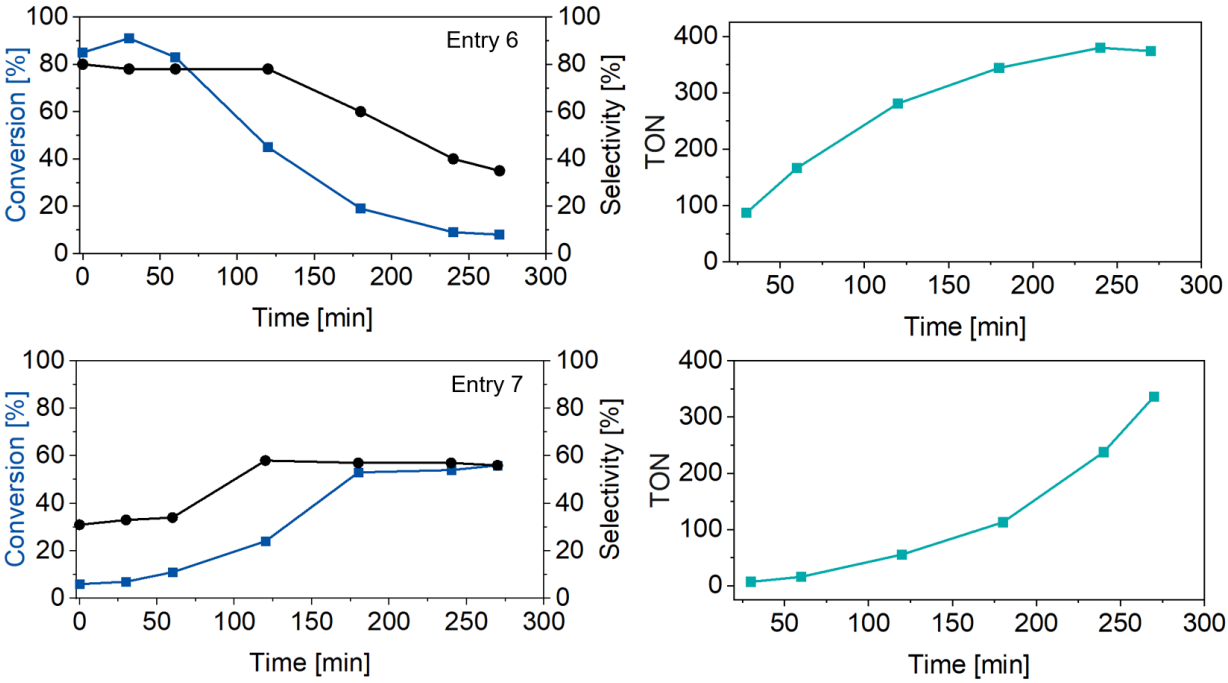

Figure 4.18 Depicted time conversion plot (left) and TON (right) of the continuous flow ethenolysis of HOSO in a $scCO_2$ under reaction conditions described in Table 5.6 entry 6 & 7.

As reported in literature, the addition of 2-Isopropoxy-styrene enables the stabilization of the active catalyst.[168] By the addition of 5 mol% of 2-Isopropoxy-styrene ligand, a slow increase of conversion up to 55 % and a TON of 340 is observed after 180 min (Figure 4.18, entry 7). This hints at a decelerated ethenolysis reaction, resulting in an insufficient retention time of the substrate on the column.

As described in previous investigations, the highest observed TON in the ethenolysis of HOSO under batch conditions with 0.4 mol % of the immobilized catalyst HGII-SiO_2, was around 150 with a conversion of 60 %. By applying 0.17 mol% of the catalyst to a flow process, a maximum conversion of 80 % was reached resulting in an increased TON of 650. Under batch conditions, a maximum selectivity for ethenolysis products of 50 % is reached. In contrast, the flow process in $scCO_2$ resulted even at lower catalyst loadings in an enhanced maximum selectivity of 80 %. Nevertheless, the decrease in conversion over time hints at catalyst decomposition processes, representing a limiting factor in the continuous flow process.

4.2.5 Sequential Conversion of Methyl Oleate under Continuous Flow Mode

Compared to a single ethenolysis reaction of fatty acids, their transformation by a sequence of ethenolysis-isomerization-ethenolysis allows for a broadening of the product scope. As discussed in chapter 3.2.6, within this approach the synthesis of industrial relevant terminal alkenes is possible. For the realization of the biorefinery approach under continuous flow conditions, the reactor-set up was complemented as depicted in Figure 4.19. Two further HPLC columns were installed that serve as reaction vessels for the double bond isomerization and a second ethenolysis reaction. A second ethylene pump was implemented to allow for an additional ethylene flow in the second ethenolysis step as well as an HPLC pump, facilitating the delivery of MeOH for the activation of the isomerization catalyst. Due to deactivation reactions, MeOH was found to have a negative influence on the ethenolysis performance (refer to chapter 3.2.3). To prevent the contact of high amounts of MeOH with the immobilized ethenolysis catalyst, molecular sieve (4A powder) was used as MeOH-scavenger which was packed in a column and installed after the isomerization column.

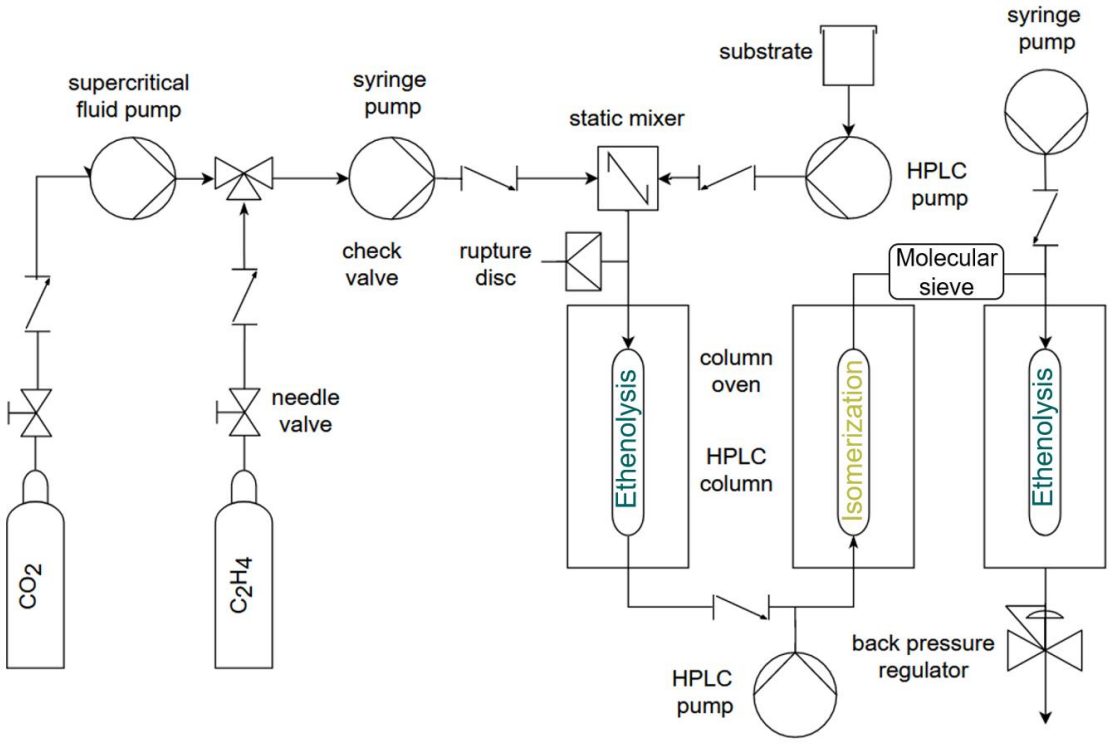

Figure 4.19 Technical drawing of the continuous flow set-up for the tandem process of ethenolysis-isomerization-ethenolysis of methyl oleate in $scCO_2$.

The multicatalytic sequential reaction was performed with methyl oleate as model renewable feedstock. Initially, optimized reaction conditions from single ethenolysis and isomerization reactions[151] were used (Table 4.7, entry 1).

Table 4.7 Sequential catalysis of ethenolysis-isomerization-ethenolysis in continuous flow mode using $scCO_2$ as reaction medium.

Entry	1st column	2nd column		3rd column		Remark
	Ru [mg]	Pd [mg]	MeOH flow [mL/min]	Ru [mg]	Ethylene flow rate [mL/min]	
1	0.85	0.36	0.01	1	-	
2	3.2	1	0.02	3.6	-	bypass
3	3.2	1	0.02	3.6	0.03	bypass

Reaction conditions: 400 bar, $T_{ethenolysis}$ = 40 °C, $T_{isomerization}$ = 85 °C, 0.01 mL/min MO, 0.1 mL/min CO_2, 9 eq. ethylene to MO.

Under these conditions a total maximum conversion of 45 % is observed. The main products are primary ethenolysis (HC 10:1 and E 10:1) and self-metathesis (HC 18:1 and DE 18:1) products (Figure 4.20). The selectivity for ethenolysis products was determined to be 57 %. The conversion and selectivity stayed relatively constant over 1 h.

Even though isomerization of the primary ethenolysis products was observed, no products <C_{10} were formed, assuming no conversion in the second ethenolysis step. This might originate from catalyst deactivation by ethylene as well as MeOH. However, small amounts of products with chain lengths > C_{10} are present in the product mixture, hinting at the occurrence of self-metathesis of isomerized methyl oleate as well as of primary ethenolysis (HC 10:1 and E 10:1) and self-metathesis (HC 18:1 and DE 18:1) products. As the major products are primary ethenolysis and self-metathesis products of methyl oleate, prevention of fast deactivation of the ethenolysis catalyst in the last column is desired.

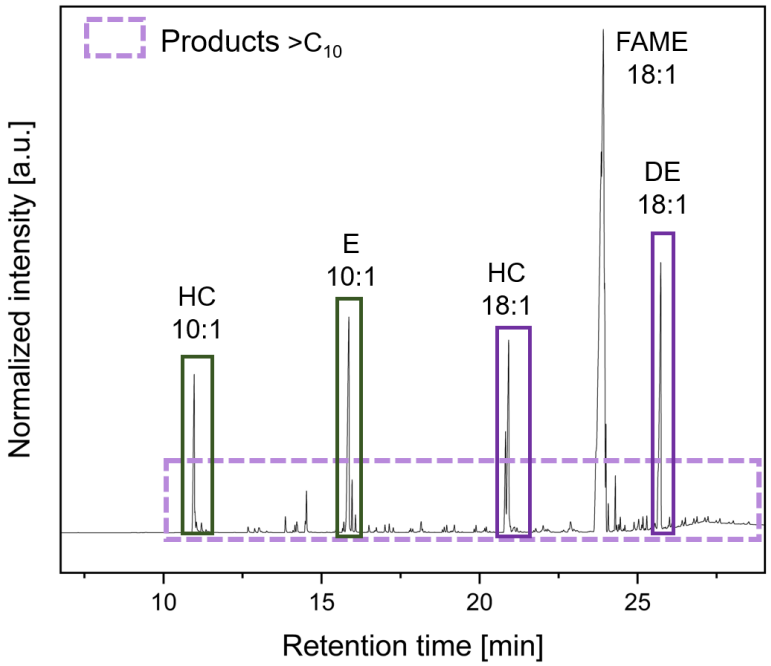

Figure 4.20 Gas chromatogram of the product mixture after sequential continuous flow catalysis of methyl oleate (Table 4.7. entry 1)

To prevent catalyst deactivation by too high amounts of ethylene and MeOH, the contact time with the immobilized metathesis catalyst in the last column was minimized. This was achieved by bypassing the reaction mixture after the isomerization column to an additional outlet until the formed products from the first two steps reached the end of the isomerization column. For this purpose, a second back pressure regulator was installed (Figure 4.22 (1)). In addition, the catalyst loading was increased to counteract a fast catalyst deactivation (Table 4.7, entry 2).

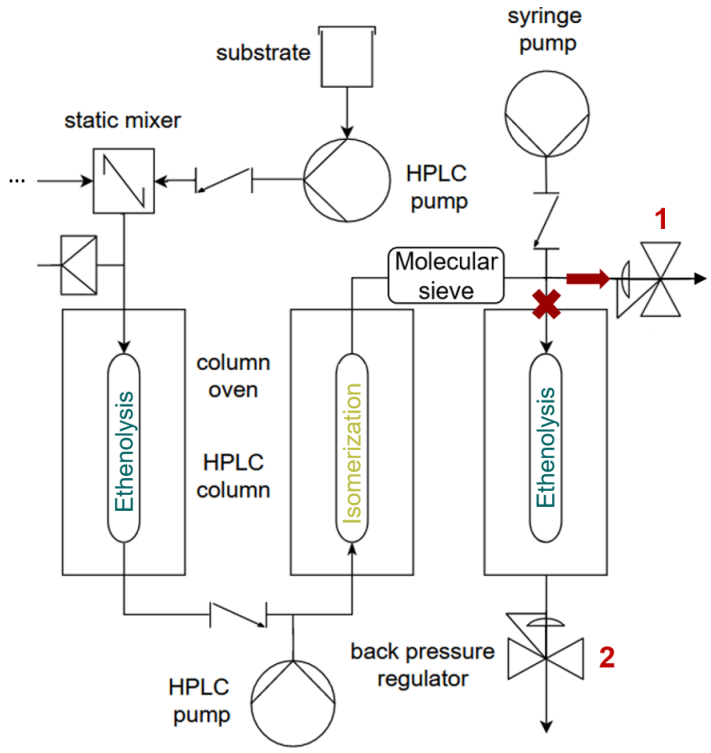

Figure 4.22 Adjusted reactor set-up with bypass.

The gas chromatogram of a sample of the product mixture revealed a conversion for the primary ethenolysis of 16 % with a selectivity for ethenolysis products of 32 %. In addition, isomerization took place, however, equilibrium was not reached. From that moment, backpressure regulator 1 was closed and backpressure regulator 2 was opened to allow the flow of the reaction mixture through the second ethenolysis column. Samples were taken and analyzed by GC over 150 min showing a maximum total conversion of methyl oleate of 16 % (Figure 4.21 a).

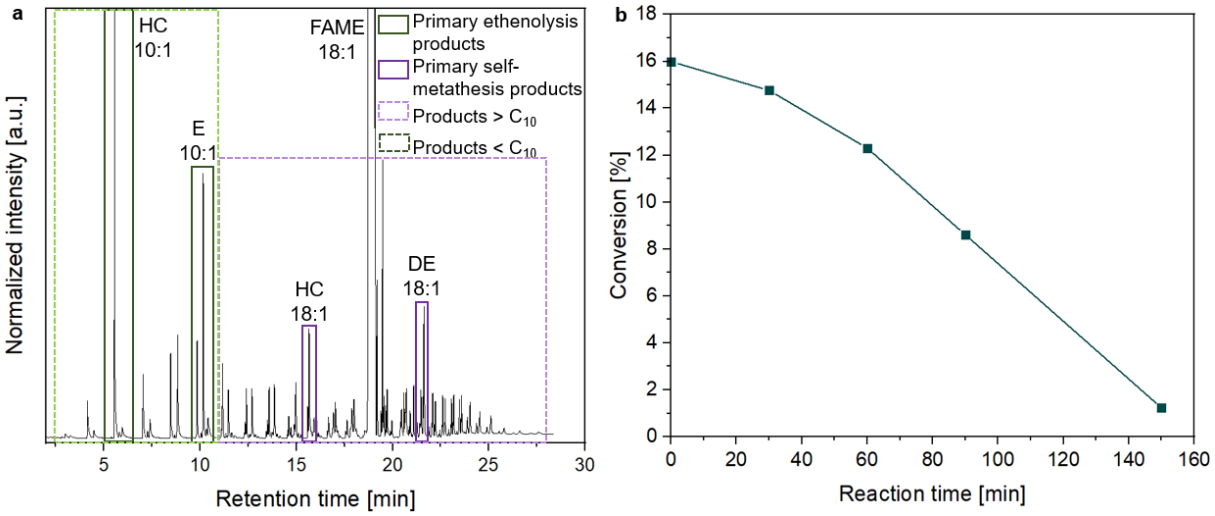

Figure 4.21 a, Gas chromatogram of the product mixture after sequential continuous flow catalysis of methyl oleate. b, Time-conversion plot of the sequential catalytic flow process (Table 4.7, entry 2).

However, a fast decrease in conversion was observed resulting in a conversion of <1 % after 150 min (Figure 4.21 b). The fast decline in catalyst activity was observed in previous continuous flow ethenolysis experiments hinting at catalyst deactivation processes by ethylene as well as alcohols (refer to chapter 4.2.2 & 4.2.3). Whereas the conversion constantly decreased over time, the obtained product distribution remained almost constant (Figure 4.23 a). The product mixture comprises products with chain lengths in the range of C_6 to C_{27}. As already visible from the determined selectivity in the primary ethenolysis, self-metathesis took place to a high extent. This is the reason why after isomerization and further ethenolysis and self-metathesis not only the desired products in the regime of C_3 to C_{10} are obtained but also longer chain lengths up to C_{27}.

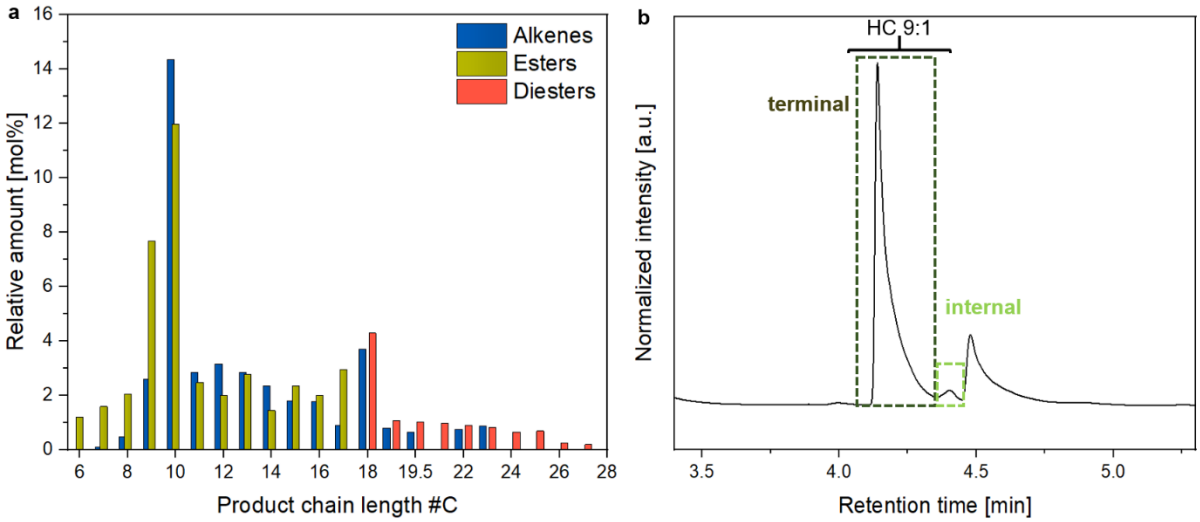

Figure 4.23 a, Product distribution of the catalytic sequence of ethenolysis-isomerization-ethenolysis under continuous flow conditions. b, Signals for terminal and internal alkene isomers of HC 9:1.

A closer look into the product distribution reveals that the primary ethenolysis products HC 10:1 and E 10:1 account for the largest proportion. This reflects the incomplete isomerization as well as incomplete second ethenolysis. The selectivity for detected products $<C_{10}$ is determined to be 43 %. However, alkene products with chain lengths of C_3 to C_6 are not detected by GC due to their fast evaporation from the product mixture resulting in the underestimation of the value. This further leads to an inaccuracy in the product distribution. The selectivity for terminal alkenes and esters with chain length $<C_{10}$ is calculated to be 98 % indicating that they are formed by ethenolysis (Figure 4.23 b). As the self-metathesis side reaction was also occurring in the second ethenolysis to a relatively high extent too low ethylene amounts or insufficient mixing of ethylene with the reaction mixture can be assumed.

For this reason, additional ethylene was delivered by a syringe pump with a flow rate of 0.03 mL/min into the last column (Table 4.7, entry 3). In this experiment, the primary ethenolysis proceeded with a conversion of 38 % and a selectivity for ethenolysis products of 50 %. Even though the total initial conversion of methyl oleate was higher with 27 %, an even stronger decrease in conversion over 150 min to <1 % was observed. This indicates an even faster deactivation of the ethenolysis catalyst in the presence of higher ethylene amounts. This results in higher amounts of primary ethenolysis and self-metathesis products in the product mixture. The selectivity for products $<C_{10}$ was determined to be 42 % which is comparable to the previous experiment. Moreover, they show a selectivity for terminal double bonds of 97 %. Nevertheless, as even lower amounts of products $<C_{10}$ were formed, additional ethylene seem to have a negative impact on the outcome of the product distribution.

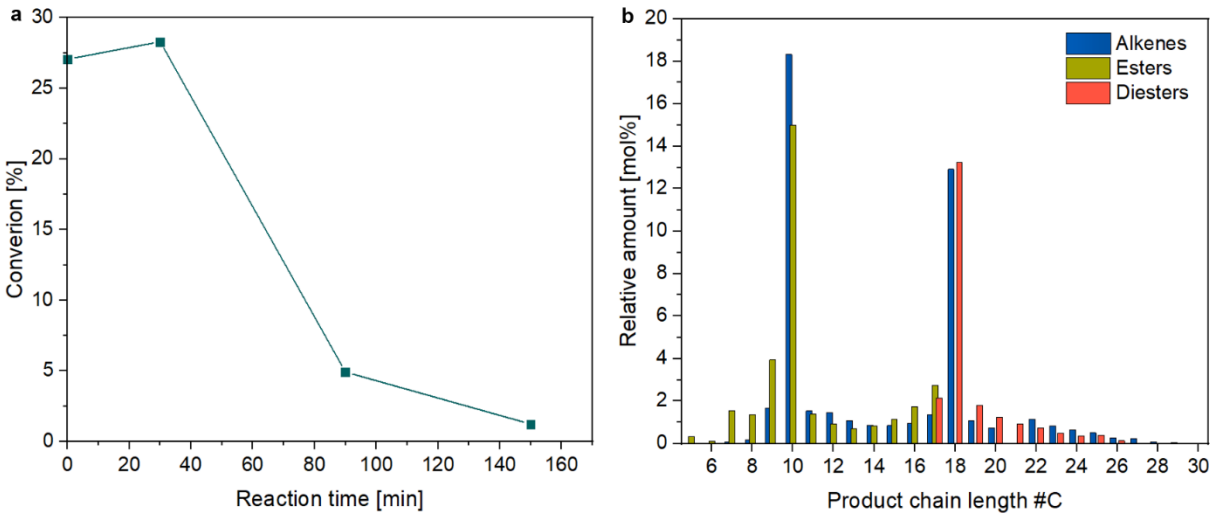

Figure 4.24 a, Time-conversion plot of the sequential catalytic flow process (Table 4.7, entry 2). b, Product distribution of the catalytic sequence of ethenolysis-isomerization-ethenolysis under continuous flow conditions.

Within these experiments, the principle of the concept could be demonstrated, however, resulting in a broad product distribution with high amounts for products with chain length $>C_{10}$. Thus, further improvements in the reaction conditions as well as catalyst performances are necessary. As catalyst deactivation processes represented the main issue, the utilization of a more stable ethenolysis catalyst is desirable. A possible suitable catalyst could be a ruthenium precursor bearing a cyclic alkyl amino carbene ligand as they provide a higher stability and activity in the presence of ethylene. However, the synthesis of a modified UC catalyst for a possible immobilization onto silica materials represents a big challenge and has not been published so far.

4.3 Conclusion

Olefin metathesis of oleo feedstocks is a promising procedure to get access to valuable intermediates such as 1-decene (HC 10:1), methyl-9-decenoate (E 10:1) and dimethyl 9-octadecenedioate (DE 18:1). For industrial applications, homogeneous catalysis comes to its limit, as costly catalyst separation from the product mixture is required and continuous flow processes are impeded. To address this problem, the self-metathesis and ethenolysis of transesterified high oleic sunflower oil (HOSO) in a continuous flow process was demonstrated, using a literature known immobilized HGII-type catalyst. In a continuous flow self-metathesis of HOSO, a stable process was reached, showing full equilibrium conversions over 10 h without loss of catalytic activity. Notably, ethyl acetate, featuring a lower negative impact on health and environment compared to usual olefin-metathesis solvents such as toluene, dichloromethane and cyclohexane, could be used, still providing a high catalytic activity and stability (Figure 4.25, left side).

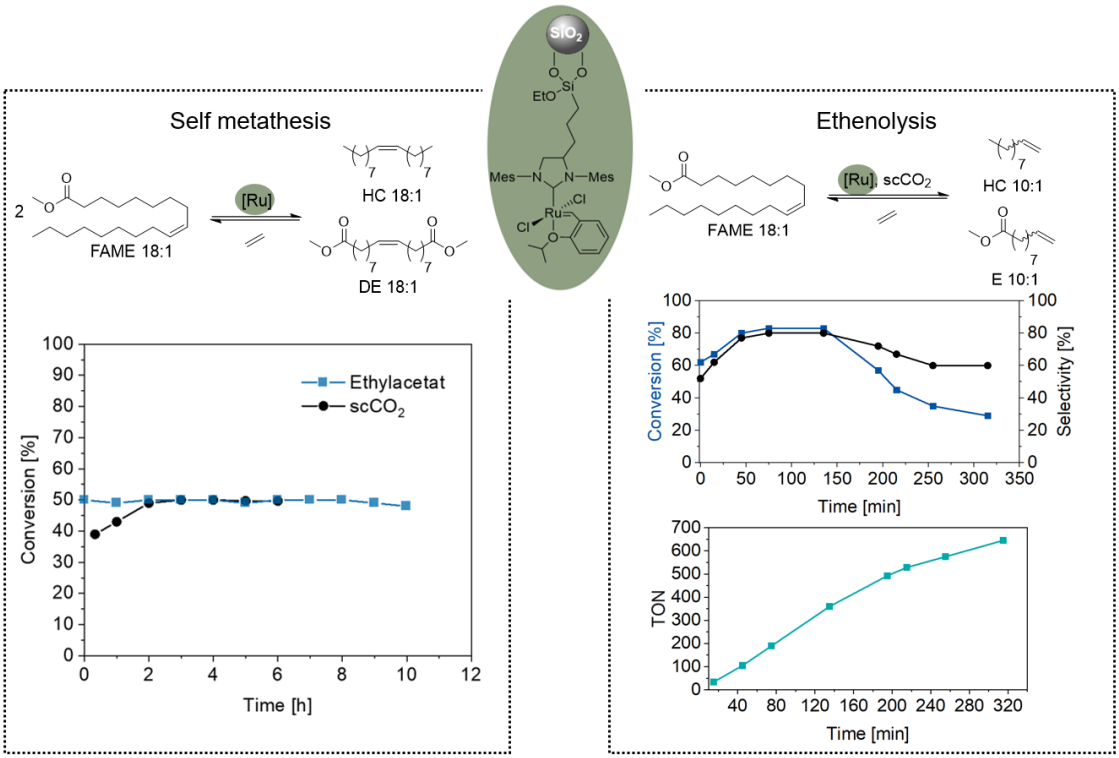

Figure 4.25 Overview of results from continuous flow self-metathesis and ethenolysis of HOSO.

Catalyst leaching was only observed in negligible amounts (3 % of the used Ru amount), preventing a tedious purification of the product. Moreover, a successful self-metathesis under continuous flow conditions could be performed with the even greener medium super critical carbon dioxide ($scCO_2$).

Also in this case, high catalyst stability was observed as the maximum equilibrium conversion was reached over a period of 6 h without loss in catalytic activity. The product mixture revealed only minor amounts of Ru (2 % of the used Ru amount), illustrating a stable covalent linkage of the modified HGII catalyst to the solid support in $scCO_2$. Especially, the obtained ethenolysis products HC 10:1 and E 10:1 are valuable intermediates, allowing for the production of polymers and surfactants.

The implementation of the immobilized catalyst in the ethenolysis of methyl oleate in $scCO_2$ led to maximum conversions and selectivities for ethenolysis of over 80 % (Figure 4.25, right side). As reported for homogeneous HGII catalysts, catalyst deactivation due to the formation of unstable methylene species was observed, resulting in a diminished catalyst stability over several hours. Nevertheless, increased TONs compared to the ethenolysis of the immobilized catalyst under batch conditions could be reached.

A combined continuous flow process of ethenolysis-isomerization-ethenolysis revealed the limitations of the immobilized HGII-SiO2 catalyst. Here, catalyst deactivation processes were even intensified in the second ethenolysis step due to the utilization of alcohols, required for the activation of the isomerization catalyst. This resulted in a product mixture comprising mainly primary ethenolysis and self-metathesis products as well as products with chain lengths up to C_{27}.

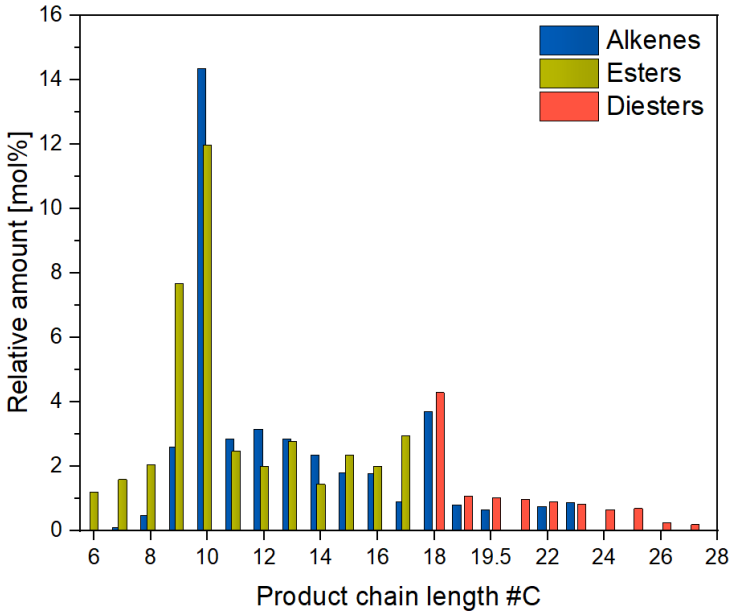

Figure 4.26 Product distribution of the catalytic sequence of ethenolysis-isomerization-ethenolysis under continuous flow conditions

In summary, these results illustrate a possible concept of a continuous flow process involving ethenolysis and isomerization. However, the compatibility of the used immobilized ethenolysis catalyst with methanol as well as ethylene needs to be improved in order to successfully implement the multicatalytic sequential concept. One possibility would be to use a more stable catalyst precursor bearing a cyclic alkyl amino carbene ligand such as the UltraCat (refer to chapter 3.2.2). However, its synthesis for a possible immobilization onto silica materials represents a big challenge and has not been published so far.

4.4 Materials and Methods

All manipulations of air and moisture sensitive compounds were conducted under an inert gas atmosphere (nitrogen) using standard glovebox or Schlenk techniques. Solvents were dried under an inert atmosphere as follows: Dichloromethane was distilled from CaH_2 prior to use. Et_2O was dried by passing through columns equipped with copper catalyst/molecular sieve 3 Å. THF was distilled from sodium / benzophenone and MeOH from magnesium turnings. All dry solvents were stored under an inert atmosphere over molecular sieves. Carbon dioxide (N 4.5 grade) was purchased from Lindegas (Pullach, Germany) and used with a dip-tube tank as received. Ethylene (N3.5 and N 4.5 grade) was supplied by Air Liquide (Düsseldorf, Germany) and used as received. Transesterified sunflower oil (Dakolub MB9001, contains only fatty acid methyl esters and no glycerol) was kindly donated by DAKO AG (Wiesentheid, Germany) and. Ethyl vinyl ether, Hoveda-Grubbs first generation catalyst, Pt(0)-1,3-divinyl-1,1,3,3-tetramethyldisiloxane complex solution in poly[dimethylsiloxan], potassium bis(trimethylsilyl)amide (KHMDS), tichlorosilane, glyoxal, 2,4,6-trimethylaniline, allyl magnesiumbromide, sodium borohydride, triethylorthoformate, $HSiCl_3$, $MgSO_4$ and deuterated chloroform $CDCl_3$ for NMR spectroscopy were provided by Sigma Aldrich (Darmstadt, Germany). All other deuterated solvents were supplied by Eurisotop (Saarbrücken, Germany) and stored over 3 Å molecular sieves without further purification. All commercial chemicals were used as received unless otherwise noted. Flash column chromatography of organic compounds was performed using silica gel 60 (230–400 mesh) from Macherey-Nagel (Düren, Germany). Spherical silica gel (pore volume 0.9 cm^3, surface area 450-55 m^2/g) was used for grafting of Ru-complexes and supplied by Sigma Aldrich. Prior to immobilization, the silica was dried under vacuum at 200 °C for 70 h. Ruthenium contents on silica materials as well as in solutions were analyzed by Mikroanalytisches Labor Kolbe using ICP-OES.

4.4.1 Nuclear Magnetic Resonance – NMR

NMR spectra were recorded in deuterated solvents on a Bruker Avance III 400 MHz spectrometer. ^1H NMR and ^{13}C NMR spectra were referenced to residual protonated solvent signals. Acquired data was processed and analyzed using MestReNova software (version 14.1.0-24037)

4.4.2 Gas Chromatography – GC

GC analysis was performed on a Perkin-Elmer Clarus 690 gas chromatograph, equipped with a Perkin Elmer Elite 5 column (30 m x 0.25 µm x 0.25 µm; Dipenyl- 95% Dimethylpolysiloxane) and a flame ionization detector. For the analysis of single ethenolysis experiments method A was used with an injection volume of the automatic sampler of 1 µl. In this case, the sample was injected at 300 °C and detected at 320 °C. The initial temperature of 50 °C was maintained for 1 min before heating to 280 °C with a heating rate of 10 °C min^{-1}. The final temperature was kept isothermal at 280°C for 5 min. For product mixtures containing low boiling olefins which arise from the multicatalytic sequential biorefinery process, a low temperature method B was used. Here the injection volume of the automatic sampler was set to 1 µl and the sample was injected at 300 °C and detected at 320 °C. In the beginning the oven was cooled by liquid CO_2 to 5 °C which was maintained for 1 min before heating to 80 °C with a heating rate of 8 °C min^{-1} and further to 230 °C with a heating rate of 10 °C min^{-1}. The final temperature of 300 °C was reached with a heating rate of 22 °C min^{-1} and was kept isothermal for 4 min. Peaks were assigned *via* enrichment experiments with genuine samples.

All peaks in the chromatogram were corrected with response factors which were determined as an average of three measurements against dodecane.

4.4.3 High Pressure Equipment

The supercritical fluid pumps were purchased from Supercriticial Fluid Technologies, Inc. (Newark (Delaware), USA) and the HPLC pump from Knauer (Berlin, Germany). The high pressure ethylene pump was purchased from Teledyne ISCO (Lincoln, USA) and high pressure tubing and check valves were purchased from Hy-Lok D Vetriebs GmbH (Oyten, Germany). HPLC tubing and fittings were delivered by Restek (Bad Homburg vor der Höhe, Germany) and column ovens were bought from Schambeck SFD GmbH (Bad Honnef, Germany). The dome loaded back pressure regulator was purchased from Pressure Control Solutions (Veenendaal, Netherlands) and the static mixer from ERC GmbH (Riemerling, Germany). The customized table as well as the aluminum heating block was made by the scientific workshop of the University of Konstanz.

4.4.4 Synthesis of Triethoxysilyl-Functionalized Catalyst 8

Catalyst **8** was synthesized using a literature known procedure published by Grubbs and co-workers, which is described in the following.[104]

4.4.5 Synthesis of N¹,N²-Dimesitylethane-1,2-diimine (3)

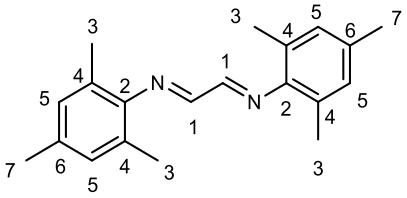

M= 292.43 g/mol

In a dried 500 mL round-bottom flask 11 ml (97 mmol) of glyoxal were dissolved in a mixture of 100 mL of isopropanol and 200 of mL water at 0 °C. Subsequently, 31 mL (212.4 mmol, 2.2 eq.) of 2,4,6-trimethylaniline were added dropwise leading to the formation of a yellow precipitate. The reaction mixture was stirred for 72 h at room temperature. After the precipitate was filtered through a frit it was washed with 150 mL of water, four times with 100 ml of hexane and finally with 150 mL of acetone. The yellow solid was dried under vacuum to obtain the desired product in 76 % yield (20.6 g, 70.2 mmol).

^{1}H NMR (400 MHz, $CDCl_3$, 25 °C): δ [ppm] = 8.10 (s, 2H, H-1), 6.92 (s, 4H, H-5), 2.29 (s, 6H, H-7), 2.18 (s, 12H, H-3).

^{13}C {^{1}H} NMR (100 MHz, $CDCl_3$, 25 °C): δ [ppm] = 163.62 (C-1), 148.34 (C-2), 134.12 (C-6), 129.46 (C-5), 126.76 (C-4), 20.88 (C-7), 18.4 (C-3).

4.4.6 Synthesis of N¹,N²-Dimesitylpentene-1,2-diamine (4)

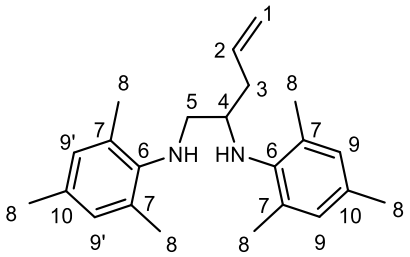

M= 336.52 g/mol

In a dried 500 mL round-bottom flask, a solution of 1 g (3.45 mmol) of bisimine (**3**) in 100 mL of dry THF was prepared. The solution was cooled by means of an ice/acetone bath to -78 °C and subsequently 4.5 mL of allyl magnesium bromide (1.0 M in Et_2O, 3.46 mmol) were

added slowly. While stirring for 1 h the reaction mixture was warmed up to room temperature. After addition of 80 mL of methanol an excess of sodium borohydride (0.80 g, 21.15 mmol) was added in 2 portions - the first portion in the beginning and the second portion after 30 min. The reaction mixture was stirred for 2 h at room temperature and finally quenched by addition of saturated aqueous NH_4Cl solution. The organic layers were separated in a separatory funnel and the aqueous phase was washed three times with 50 mL of Et_2O. The combined organic layers were extracted with water, brine and dried over $MgSO_4$. After removal of the solvents a yellow-brownish oil was obtained which was purified by column chromatography using pentane/Et_2O (20/1). A yellow oil was obtained (0.852 g, 2.53 mmol, 73 %).

^{1}H NMR (400 MHz, C_6D_6, 25 ◦C): δ [ppm] = 6.81 (s, 2H, H-9'), 6.76 (s, 2H, H-9), 5.60-5.68 (m, 1H, H-2), 4.91-4.96 (m, 2H, H-1), 3.50-3.56 (m, 1H, H-4), 3.14 (dd, J = 12.1 Hz, 4.6 Hz, 1H, H-5), 2.75 (dd, J = 12.1 Hz, 6.7 Hz, 1H, H-5), 2.18-2.23 (m, 18H, H-8), 2.94-2.06 (m, 2H, H-3).

^{13}C {^{1}H} NMR (100 MHz, C_6D_6, 25 ◦C): δ [ppm] = 144.18- 142.18 (C-6), 135.7 (C-2), 131.35-129.28 (C-7,9,9',10), 117.20 (C-1), 57.33 (C-4), 52.73(C-5), 38.43 (C-3), 20.80 (C-10), 20.74- 18.58 (C-8).

4.4.7 Synthesis of 4-allyl-1,3-Dimesityldihydroimidazolium chloride (5)

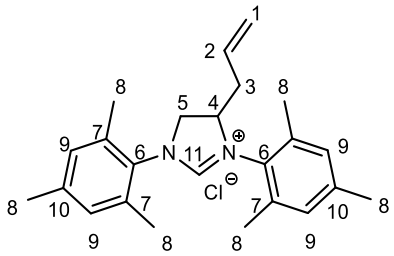

M= 382.98 g/mol

In a 250 mL dried round-bottom flask, 2.0 g (5.94 mmol) of diamine (**4**) was dissolved in 40 mL of dried Et_2O and cooled by means of an ice bath to 0 °C. Subsequently, 3.6 mL of a 2 M HCl solution in Et_2O was added to the reaction mixture leading to the precipitation of the diamine hydrochloride salt. The solid was filtered, washed with 40 mL of Et_2O and finally dried in a round-bottom flask under vacuum. After 12.5 mL (75 mmol, 12.6 eq.) of triethylorthoformate were added *via* syringe, the reaction mixture was stirred for 16 hours at 110 °C. The mixture was cooled to room temperature and after removal of the volatiles the brown solid was washed with 40 mL of Et_2O, 15 mL of EtOAc and finally with 15 mL of

pentane. The solvents were removed under reduced pressure and an off-white solid in 79 % yield was obtained (1.8 g, 4.7 mmol).

^{1}H NMR (400 MHz, C_6D_6, 25 ◦C): δ [ppm] = 10.75 (s, 1H, H-11), 7.03 (s, 4H, H-9), 5.67-5.57 (m, 1H, H-2), 5.24-5.18 (m, 2H, H-1), 4.84-4.76 (m, 1H, H-4), 4.44 (t, J = 11.5 Hz, 4.6 Hz, 1H, H-5), 3.96 (dd, J = 12.1 Hz, 7.9 Hz, 1H, H-5), 2.63-2.48 (m, 2H, H-3), 2.48-2.2.33 (m, 18H, H-8).

^{13}C {^{1}H} NMR (100 MHz, C_6D_6, 25 ◦C): δ [ppm] = 161.73 (C-11), 141.08-140.95 (C-6), 135.59 (C-2), 131.29-129.55 (C-7,9,10), 120.65 (C-1), 63.40 (C-4), 56.32 (C-5), 37.44 (C-3), 21.36-18.80 (C-8).

4.4.8 Synthesis of 1,3–Dimesityl-4-(3-triethoxysilyl)propyl)-dihydro-imida- zolium chloride (6)

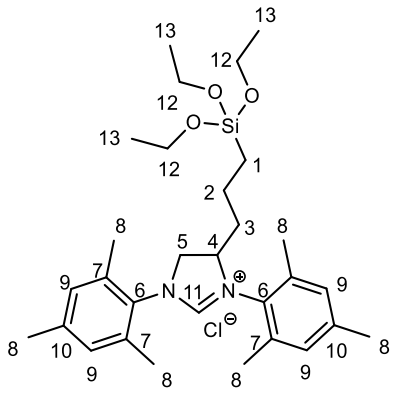

M= 546.25 g/mol

In a dried 50 mL round-bottom flask 1 g (2.62 mmol) of **5** was dissolved in 20 mL of dry CH_2Cl_2. 10 mL of $HSiCl_3$ (99 mmol, 38 eq.) was added dropwise to the solution and then 2 mL of Pt(0)-1,3-divinyl1,1,3,3-tetramethyldisiloxane complex solution (0.05 M in poly[dimethylsiloxan], 3.8 mol%) were added. After refluxing the reaction mixture for 18 h it was cooled to room temperature and the volatiles were removed under vacuum to get rid of the excess of trichlorosilane. Subsequently, the residue was dissolved in 10 mL of CH_2Cl_2 and cooled to 0°C. 10 mL of a 1/1 solution of EtOH/NEt_3 were added *via* syringe resulting in the formation of a cloudy precipitate which disappeared when the reaction mixture was warmed to room temperature. After 2 h of stirring, the volatiles were removed and the crude product was purified by column chromatography using 10 % of ethanol in CH_2Cl_2 to yield 69 % of the desired product (0.99 g, 1.81 mmol).

^{1}H NMR (400 MHz, CD_2Cl_2, 25 °C): δ [ppm] = 10.65 (s, 1H, H-11), 7.03 (s, 4H, H-9), 4.67-4.61(m, 1H, H-4), 4.43 (t, J = 11.4 Hz, 4.6 Hz, 1H, H-5), 3.93-3.89 (m, 1H, H-5), 3.97 (q, J = 7 Hz, 6H, H-12), 2.45-2.40 (m, 18H, H-8), 1.86-1.79 (m, 2H, H-3), 1.43-1.36 (m, 2H, H-2), 1.14 (t, J = 7 Hz, 9H, H-13) 0.59 (t, J= 8 Hz, 2H, H-1).

^{13}C {^{1}H} NMR (100 MHz, CD_2Cl_2, 25 °C): δ [ppm] = 161.71 (C-11), 141.18-129.74 (C-6,7,9,10), 64.33 (C-4), 58.93 (C-12), 57.13 (C-5), 36.12 (C-3), 20.82-19.35 (C-8), 18.86 (C-2), 18.06 (C-13), 10.63 (C-1).

4.4.9 Synthesis of [$RuCl_2$ (1,3-dimesityl-4-(3-triethoxy silyl) propyl)-dihydro-imidazol-2-ylidene) (=CH–*o*-^{i}PrO–Ph)] (8)

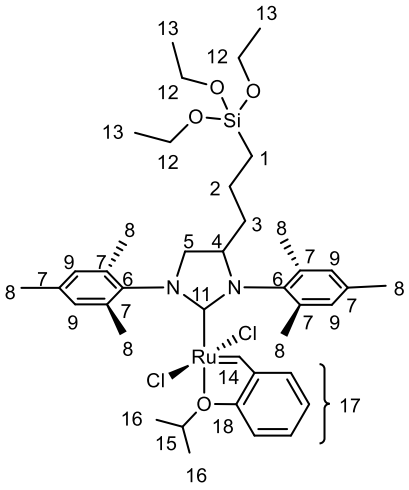

M= 831.98 g/mol

In a glove box, 518 mg (0.7 mmol) of **6** was dissolved in 20 mL of toluene and 208 mg (1.04 mmol, 1.1 eq.) of KHMDS were added while stirring at room temperature. After 10 min the suspension turned homogeneous and was added after 1 h of stirring to a mixture of 500 mg (0.82 mmol) of Hoveyda-Grubbs first-generation catalyst **7** in 15 mL of toluene. The flask was removed from the dry box and stirred at reflux for 2 h under inert gas. After the addition of 1.69 mmol of CuCl the reaction mixture was refluxed for another 2 h. The crude product was purified by column chromatography using 10/1 hexane/EtOAc to yield 390 mg (0.50 mmol, 55 %) of **20** as a dark green sticky solid. The solid was lyophilized from toluene to obtain a green powder.

^{1}H NMR (400 MHz, CD_2Cl_2, 25 °C): δ [ppm] = 16.46 (s, 1H, H14), 7.59-7.55 (m, 1H, H-17), 7.09-7.04 (m, 4H, H-9), 6.97-6.81 (m, 3H, H-17), 4.87 (septet, J = 6 Hz, 1H, H-15), 4.49-4.43 (m, 1H, H-4), 4.18 (t, J = 10.2 Hz, 1H, H-5), 3.86 (t , J = 10.1 Hz, 1H, H-5), 3.74 (q, J = 7 Hz, 6H, H-12),

2.47-2.37 (m, 18H, H-8), 1.83-1.68 (m, 2H, H-3), 1.28-1.22 (m, 2H, H-2), 1.24 (d, J= 6 Hz, 6H, H-16), 1.19 (t, J = 7 Hz, 9H, H-13), 0.56 (t, J = 8 Hz, 2H, H-1).

^{13}C {^{1}H} NMR (100 MHz, CD_2Cl_2, 25 ◦C): δ [ppm] = 296.5 (C-14), 212.33 (C-11), 152.51 (C-18), 145.83 (C-17), 129.98 (C-9), 122.84- 113.50 (C-6,7,10,17), 75.63 (C-15), 64.85 (C-4), 58.84 (C-12), 58.45 (C-5), 37.51 (C-3), 30.68 (C2), 21.46 (C-8,16), 20.38 (C-13), 18.66 (C-2), 10.94 (C-1).

4.4.10 Synthesis of Hybrid Silica Material HGII-SiO_2

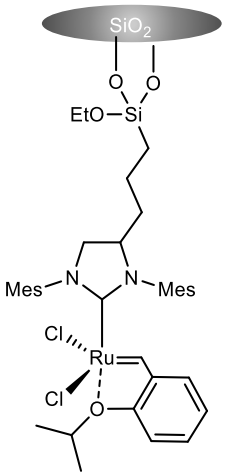

100 mg (0.12 mmol) of catalyst precursor **20** were dissolved in 5 mL of toluene. This solution was added to 1.2 g of spherical silica. To ensure a complete transfer, the vial containing the catalyst solution was washed twice with 2 mL of toluene and finally the reaction mixture was mixed by a shaker for 48 h at 40 °C. After filtration through a fritted disc extraction thimble the silica-supported catalyst was placed into a soxhlet extraction apparatus and extracted under nitrogen with CH_2Cl_2 for 48 h. The light green silica material was dried under vacuum for 24 h and ruthenium contents were determined by ICP-OES.

4.4.11 Continuous flow self-metathesis in organic solvents

A solution of methyl oleate in toluene or ethyl acetate was prepared. The HPLC column was densely packed with the immobilized catalyst and connected to the HPLC tubes. After the column was fixed at the column oven holder, the oven was heated to the desired temperature. The reaction was started by pumping the substrate solution with a chosen flow rate through the HPLC column. The product mixture was either recycled to the substrate mixture or collected after passing the HPLC column. Reaction progress was monitored over time by gas chromatography to determine conversions.

4.4.12 Continuous flow self-metathesis in $scCO_2$

The HPLC column was densely packed with the immobilized catalyst, connected to the HPLC tubes and fixed at the column oven holder, followed by heating to the desired temperature. The dome loaded back pressure regulator was set to an opening pressure of 500 bar by means of the $scCO_2$ pump. The reactor system was pressurized with $scCO_2$ using the liquid CO_2 pump. When the desired pressure was reached, a flow rate was set leading to increased pressures in the system and thus to the opening of the back pressure regulator. The reaction was started by pumping the substrate with a chosen flow rate through the HPLC column. After a certain time, product samples were collected and analyzed by gas chromatography to determine conversions.

4.4.13 Continuous flow Ethenolysis in $scCO_2$

Methyl oleate was pumped up to the static mixer. After the HPLC column was densely packed with the immobilized catalyst and connected to the HPLC tubes, the column was fixed at the column oven holder and the oven as well as the aluminum block were heated to the desired temperature. The cylinder of the ethylene pump, containing a volume of 100 mL, was filled with the desired pressure of ethylene. Subsequently, liquid CO_2 was pressurized into the cylinder until 500 bar were reached to get a mixture of both substances. At the same time, the dome loaded back pressure regulator was set to an opening pressure of 500 bar by means of a $scCO_2$ pump. When the set pressures and temperatures were reached, the syringe pump was started in continuous flow mode with a flow rate of 5 mL/min to pressurize the whole reactor system to 500 bar. At a pressure of 490 bar the flow rate was set to 0.1 mL/min. When the pressure exceeded 500 bar, the back pressure regulator opened and methyl oleate was pumped into the system by a HPLC pump with 0.01 mL/min. The reaction progress was monitored by gas chromatography.

4.4.14 Split test

After 4 h of constant flow, a 1 mL sample of the product mixture was collected. Then 0.1 mL of methyl oleate was added and half of the mixture was quenched with ethyl vinyl ether to determine the current conversion of the mixture. The other half was stirred for further 2 h at 45°C and the conversion was calculated by gas chromatography. In case of a negligible catalyst leaching, both conversions show similar results.

4.4.15 Multicatalytic Sequential Continuous flow Process in CO_2

For a sequential flow process of ethenolysis-isomerization-ethenolysis, reaction set-up was prepared as described in 4.4.13. Additionally, two further columns were filled with the isomerization catalyst and the ethenolysis catalyst, respectively. Moreover, MeOH was pumped by a HPLC pump into the second column to activate the isomerization catalyst. In order to prevent deactivation in the second ethenolysis due to the presence of high amounts of MeOH, a column filled will molecular sieves was placed right after the column filled with the isomerization catalyst. For the analysis of the product mixture samples were analyzed by gas chromatography.

5 CONCLUSIVE SUMMARY

Due to the world-wide increasing demand for fossil fuel-based chemicals such as polymers and specialty chemicals, renewable raw materials gained in importance. Especially unsaturated lipids, present in various renewable feedstocks, are due to their chemical structure well suited for a catalytic upgrading to industrial relevant intermediates. Food crops including sunflowers, soybeans and rapeseeds play an essential role as lipid source as cultivation and extraction procedures are already established. Microalgae biomass on the other side represent an even more promising raw material as they show some advantages over traditional lipid sources. They can be grown in salt or brackish water, preventing the need for huge agricultural land and therefor the competition with the food industry. Moreover, they show high growing rates and reach lipid contents of up to 70 % of their dry weight.

So far, research focusses on the transformation of plant and microalgae oil to biodiesel. However, this defunctionalization of the lipids to hydrocarbons does not exploit the full potential of the chemical structure of the lipids. A catalytic upgrading to highly relevant industrial intermediates would be more valuable. Whereas the transformation of renewable lipids to aromatic compounds is of an advanced stage, the access to industrial relevant olefinic products is still challenging. In particular, short chain linear α-olefins are of interest, since they serve as basic building block for the synthesis of detergents, plasticizers, lubricants as well as various polymers. In industry, they are produced with a production value of over one million tons per year by the petroleum-based "Shell Higher Olefin Process". Thus, the development of an alternative synthesis route, starting from renewable resources would be of great significance.

Within the scope of this work, a biorefinery concept is presented, transforming renewable plant oils and microalgae oil to short chain α-olefins as well as terminal unsaturated esters (C_3 to C_{10}). This is performed by a catalytic sequence of ethenolysis- double bond isomerization – ethenolysis in the environmentally friendly medium supercritical carbon dioxide ($scCO_2$) and is investigated in a semi-batch process as well as in a continuous flow mode.

As a sufficient solubility of lipids in $scCO_2$ is only present at high CO_2 densities and thus at high pressures, for the realization of the semi-batch process in $scCO_2$, soluble homogeneous catalysts are used in a specially constructed high-pressure reactor (Figure 5.1). Through a controlled addition of catalyst solutions under CO_2 pressure, the desired catalytic reaction sequence is facilitated in a one-pot reaction. This work focusses on the analysis and optimization of the ethenolysis reactions in the biorefinery approach. In an initial step, the performance of a single ethenolysis reaction of transesterified high oleic sunflower oil (HOSO) in $scCO_2$ was investigated to find suited reaction conditions. During catalyst screening the ruthenium-based metathesis catalyst UltraCat (UC) showed a remarkable high catalytic activity in $scCO_2$ with a turnover number (TON) of 78 000 and a selectivity of 97 % at a catalyst loading of 10 ppm. This hints at a good solubility of UC in $scCO_2$. Further investigations revealed a negative impact of the palladium-based isomerization catalyst as well as of methanol, required for its activation, on the ethenolysis performance. Nevertheless, the usage of the minimal required amount of 0.1 mL methanol and the increase of the catalyst loading of UC to 0.06 mol% results in high conversions and selectivities over 90 %. This illustrates an excellent suitability of UC for the targeted bio refinery approach.

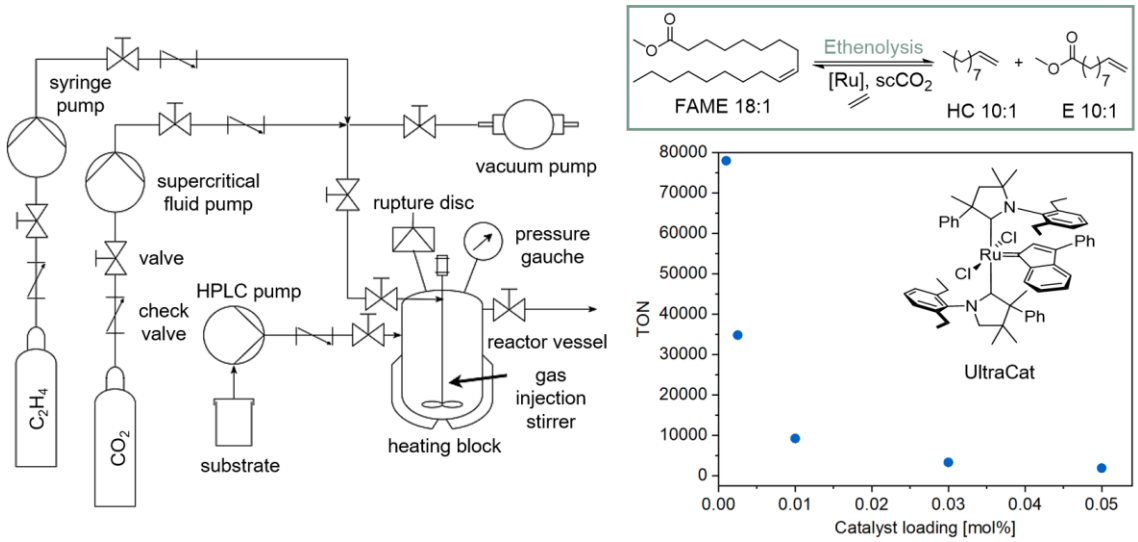

Figure 5.1 Ethenolysis of transesterified HOSO in $scCO_2$ using UC in a semi-batch solution process.

Based on these findings, the sequential catalysis of transesterified HOSO was explored. Under optimized reaction conditions, a successful transformation of the fatty acids to short chain α-olefins and terminal unsaturated esters was reached. In both ethenolysis steps, high conversions and selectivities of over 90% were obtained (Table 5.1). Moreover, the double bond isomerization of the primary ethenolysis products resulted in isomer distributions close to equilibrium. This was reflected in the obtained product distribution, showing

relative product amounts comparable to theoretical calculated values (Figure 5.2). The high selectivities for products with chain lengths <C_{10} of over 97 % as well as for terminal products of 92 % were particularly remarkable (Table 5.1). In this context, the usage of $scCO_2$ instead of MeOH as reaction medium showed an increased selectivity for terminal products, originating from a more effective prevention of undesired simultaneous isomerizing ethenolysis in $scCO_2$. This represents a key factor for the access to short chain α-olefins with high selectivities by this biorefinery approach.

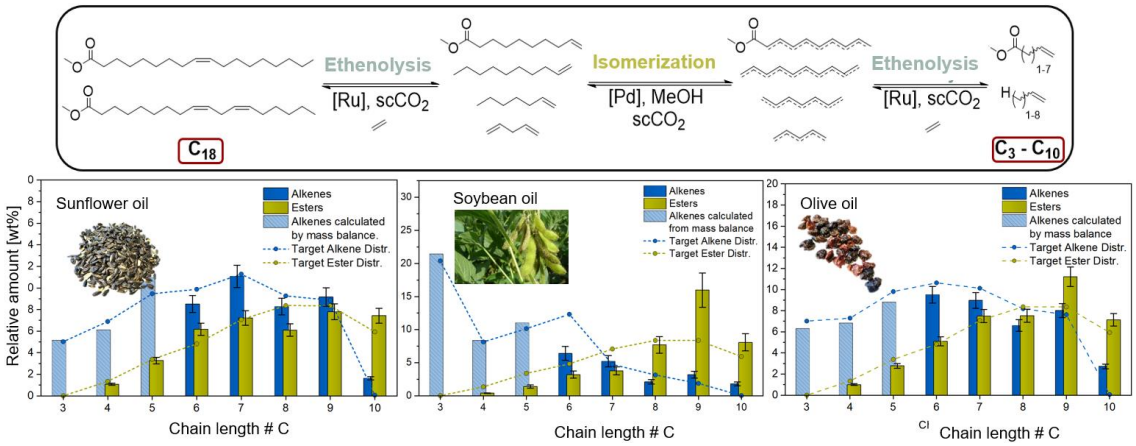

Figure 5.2 Concept and results for the catalytic biorefinery approach for various renewable oils.

Furthermore, the implementation of the concept to other plant oils containing higher amounts of polyunsaturated fatty acids such as olive and soybean oil was successfully shown. High selectivities of over 95 % for terminal products with chain lengths between C3 to C10 were reached, however, also a slight shift of the product distribution as a consequence of a decelerated isomerization was observed. The reason for that can be found in the high polyunsaturated fatty acid content in these oils, impeding double bond isomerization through coordination to the palladium-catalyst.

The robustness of the approach was further explored by applying used frying oil. For this purpose, transesterified HOSO was used several times for the frying of potato chips and subsequently applied to the multicatalytic sequential concept. Next to a slightly reduced activity in ethenolysis, probably due to the present impurities in the oil, the expected product distribution with high selectivities for the desired terminal products of 94 % is reached (Table 5.1).

Table 5.1 Results obtained after the multicatalytic sequential reaction of several substrates.

Substrate	1. Ethenolysis			Isomerization	2. Ethenolysis			
	Conv. [%]		Selec. [%]*		Conv. [%]	Selec. [%]†		Terminal products [%]
HOSO	FAME 18:1	97	97	Close to equilibrium	HC 10:1 E 10:1	96 91	97	92
Olive oil	FAME 18:1/2 FAME 16:1	70 95	98 99	Close to equilibrium	HC 10:1 E 10:1	85 84	93	89
Soybean oil	FAME 18:1/2/3	96	99	Far from equilibrium	HC 10:1 E 10:1	86 83	97	95
Waste cooking oil	FAME 18:1	84	97	Close to equilibrium	HC 10:1 E 10:1	90 85	95	94
Extracted sunflower oil	FAME 18:1	98	99	Close to equilibrium	HC 10:1 E 10:1	91 98	98	90
Extracted olive oil	FAME 18:1/2 FAME 16:1	98 91	99 98	Far from equilibrium	HC 10:1 E 10:1	91 89	98	96
Extracted microalgae oil	FAME 16:1 FAME 18:1 FAME20:5	98 96 96	99 94 99	Far from equilibrium	HC 10:1 E 10:1	84 83	98	90

To reach an even more straight-forward process, extraction of the lipids directly from the raw material was performed prior to sequential catalysis. This is especially important for microalgae lipids as these are not commercially available yet. For the sequence of extraction and catalysis, $scCO_2$ was used as extraction as well as reaction medium. Compared to other industrially used extraction media, scCO2 reveals the advantage of a high lipid selectivity of the extract and allows for its direct utilization for catalytic reactions without the need for tedious separation and purification processes. This was illustrated for sunflower seeds and olives which resulted in product distributions with selectivities for terminal products comparable to the commercially available oils.

For the upgrading of microalgae, the unicellular species *Phaeodactylum tricornutum* is used as lipid source since these algae exhibit a high robustness as well as high contents of unsaturated fatty acids. The $scCO_2$ extracted microalgae showed lipid contents similar to reported values in literature. The subsequent catalytic transformation of the transesterified lipids was also in this case possible, leading to high selectivities of over 90 % for the desired terminal products (Figure 5.3).

Thus, the used catalysts revealed a good compatibility with the multicomponent system, containing, besides lipids, other organic structures such as pigments. Within these results, a successful implementation of the new biorefinery concept could be clearly illustrated for several renewable plant oils as well as microalgae oil.

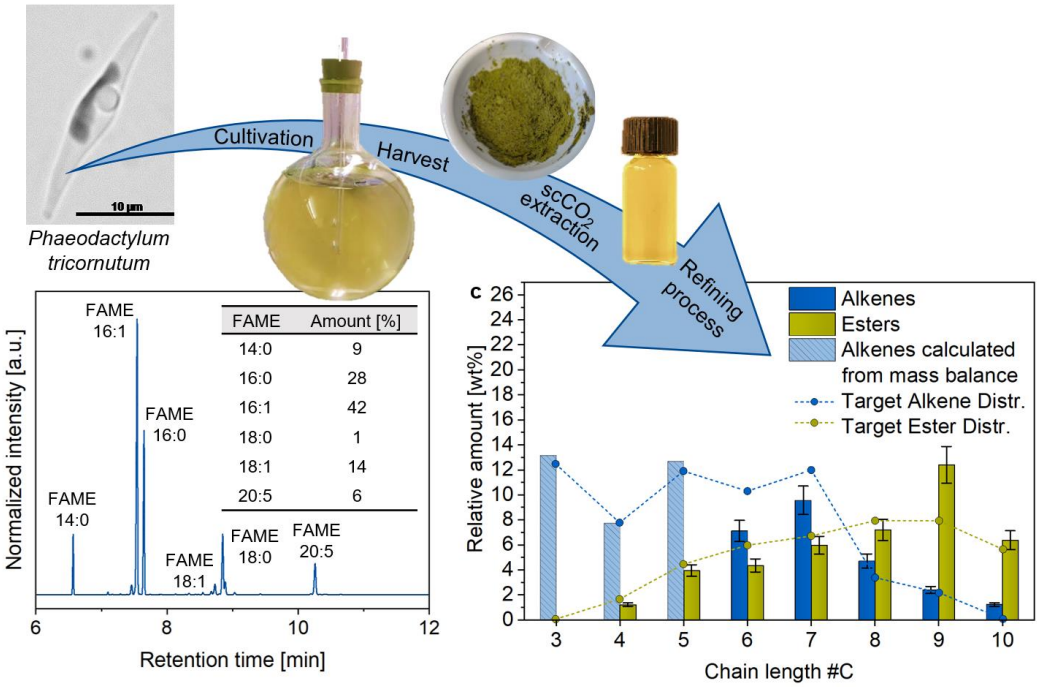

Figure 5.3 Consecutive extraction and catalytic upgrading of microalgae oil using $scCO_2$ as medium.

In a second approach, the biorefinery approach is analyzed in a continuous flow process. Continuous flow processes are commonly more a cost effective compared to batch processes. The utilization of immobilized homogeneous catalysts allows for the realization of such a flow process and comes along with several additional advantages including a simple catalyst separation and its recycling. Within this work, a literature known modified Hoveyda-Grubbs catalyst, covalently linked to silica materials *via* a triethoxysilyl linker, was used. To investigate its activity in ethenolysis of fatty acids and its stability under flow conditions, the self-metathesis of methyl oleate was performed in first experiments. A high stability and activity of the catalyst was observed leading to equilibrium conversions of 50 % over a constant flow period of up to 10 h. Organic solvents such as ethyl acetate as well as the green alternative $scCO_2$ were compatible in the continuous flow self-metathesis (Figure 5.4). The obtained products, analyzed by inductively coupled plasma optical emission spectrometry, revealed in both cases only low amounts of ruthenium which indicates a strong covalent binding of the catalyst to the silica material allowing for a stable process.

Continuous flow ethenolysis was further analyzed in $scCO_2$ showing under optimized conditions a maximum conversion and selectivities for ethenolysis products of 80 %. In contrast to the self-metathesis, the immobilized catalysts exhibits a reduced stability, probably originating from catalyst deactivation. This represents a well-known issue in homogeneous cross-metathesis with ethylene due to the formation of unstable methylidene species that tend to undergo deactivation pathways.

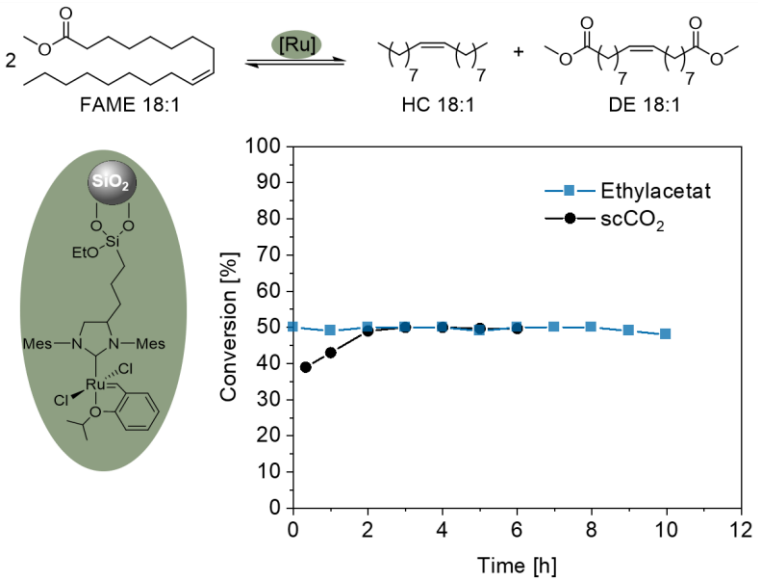

Figure 5.4 Continuous flow self-metathesis of methyl oleate in ethyl acetate and $scCO_2$.

The same behavior is observed in the multicatalytic sequential process of ethenolysis-isomerization-ethenolysis, leading only partially to the desired products. Here, the primary ethenolysis and self-metathesis products were formed as well as products with chain length up to C_{27}.

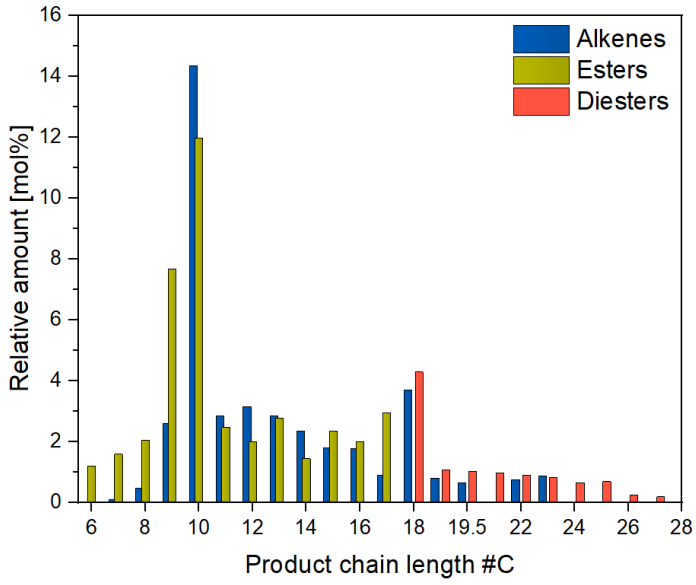

Figure 5.5 Product distribution obtained after sequential continuous flow process

To reach a more stable process, the usage of ruthenium catalysts bearing a cyclic alkyl amino carbene ligand could be of advantage. As shown in the homogeneous batch process, they provide higher activity in the presence of ethylene. However, the synthesis of a modified UC catalyst for a possible immobilization onto silica materials represents a big challenge and has not been published so far.

6 APPENDIX

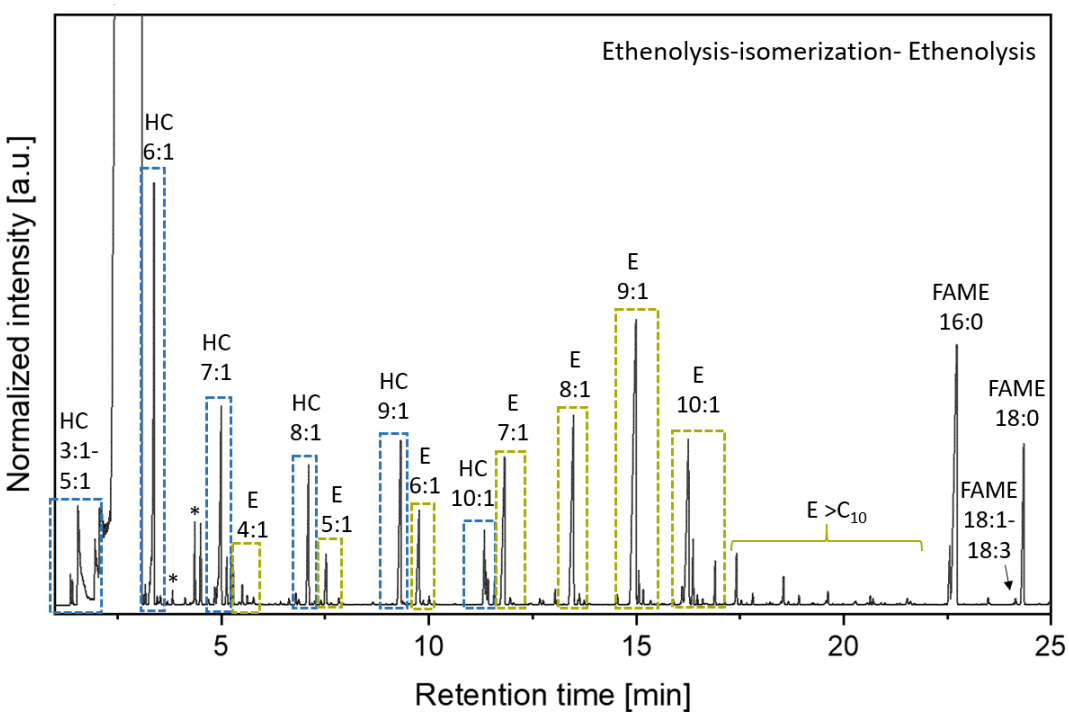

Figure 5.2 Typical gas chromatogram of transesterified HOSO and waste oil after ethenolysis and isomerization.

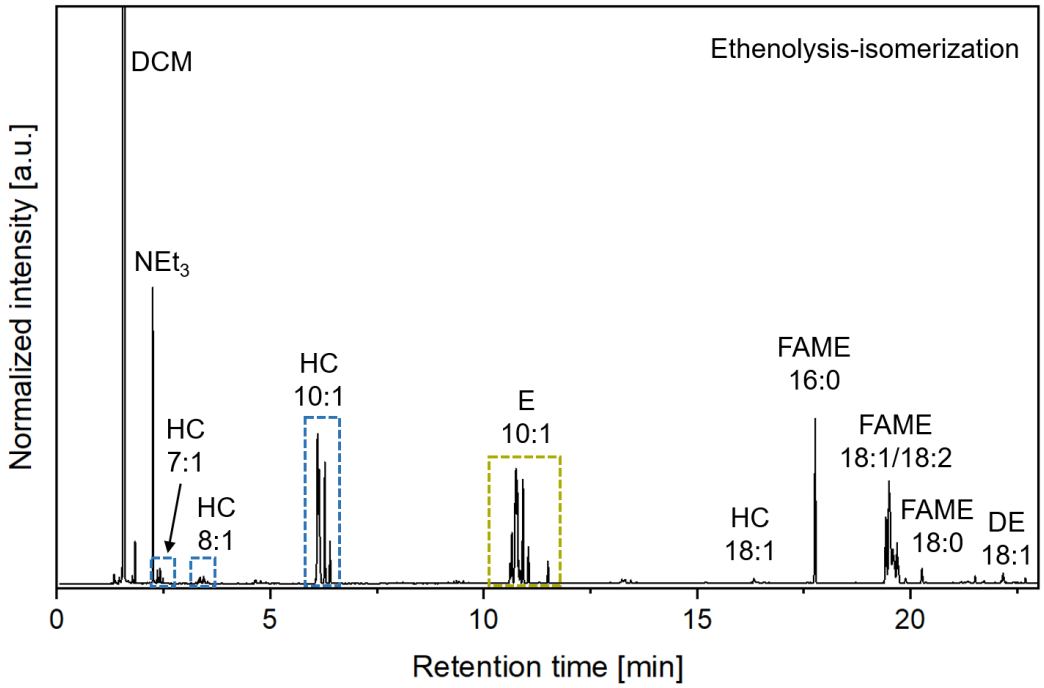

Figure 5.2 Typical gas chromatogram of transesterified olive oil after ethenolysis and isomerization.

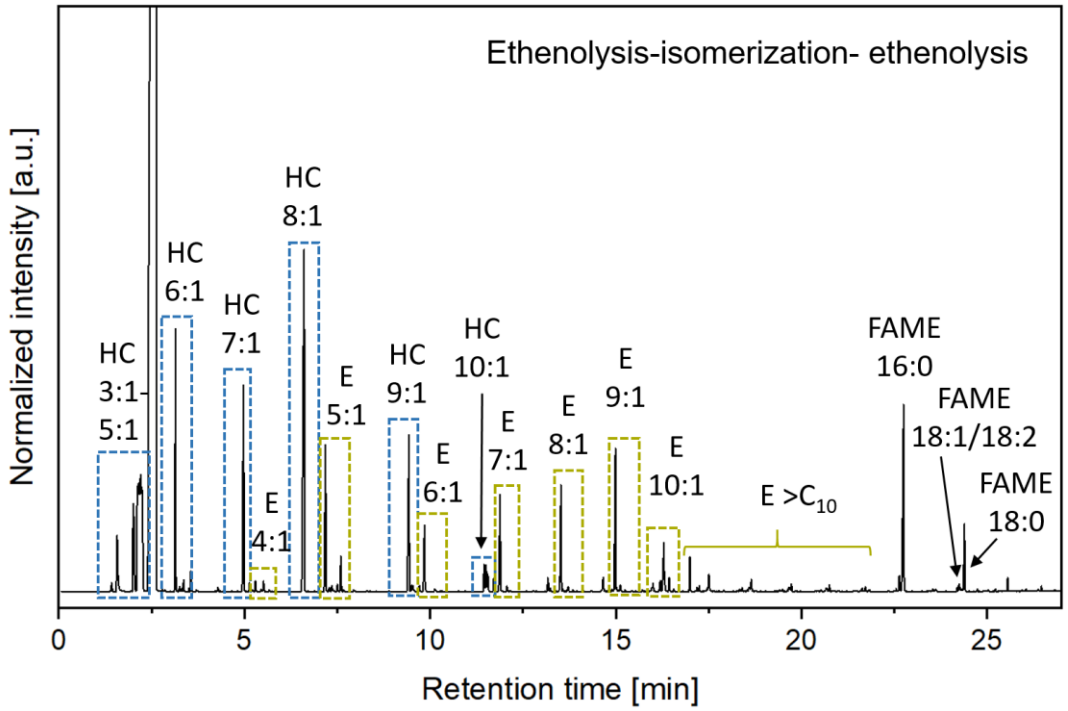

Figure 6.4 Typical gas chromatogram of transesterified olive oil after the tandem process.

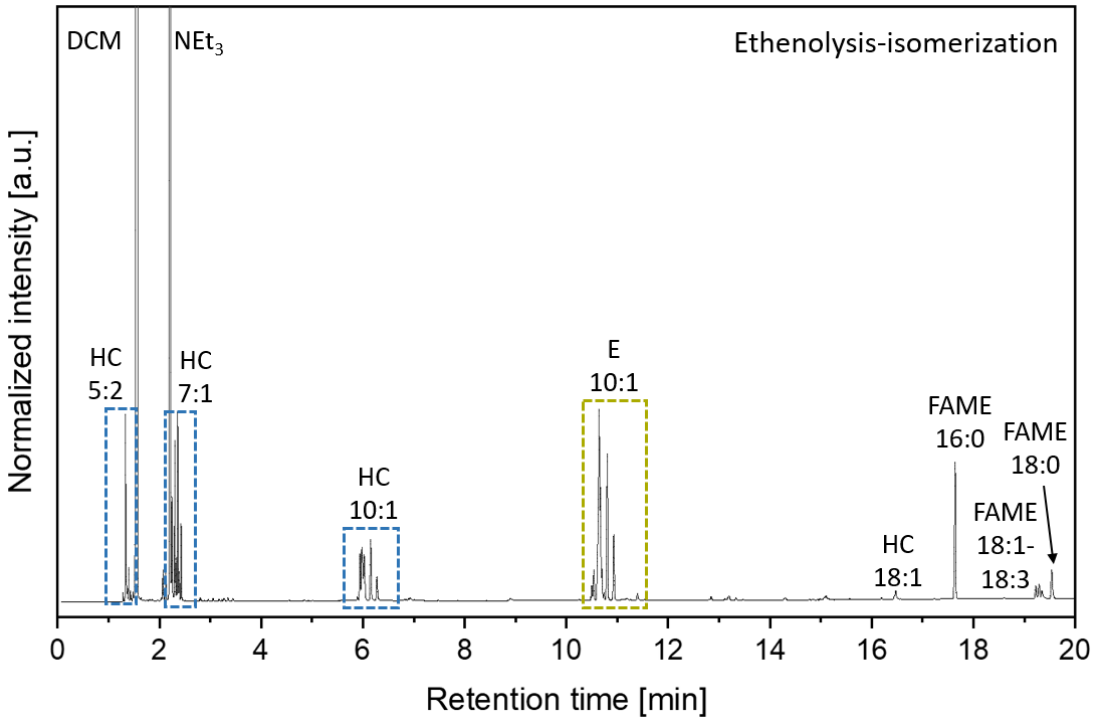

Figure 6.4 Typical gas chromatogram of transesterified soybean oil after ethenolysis and isomerization.

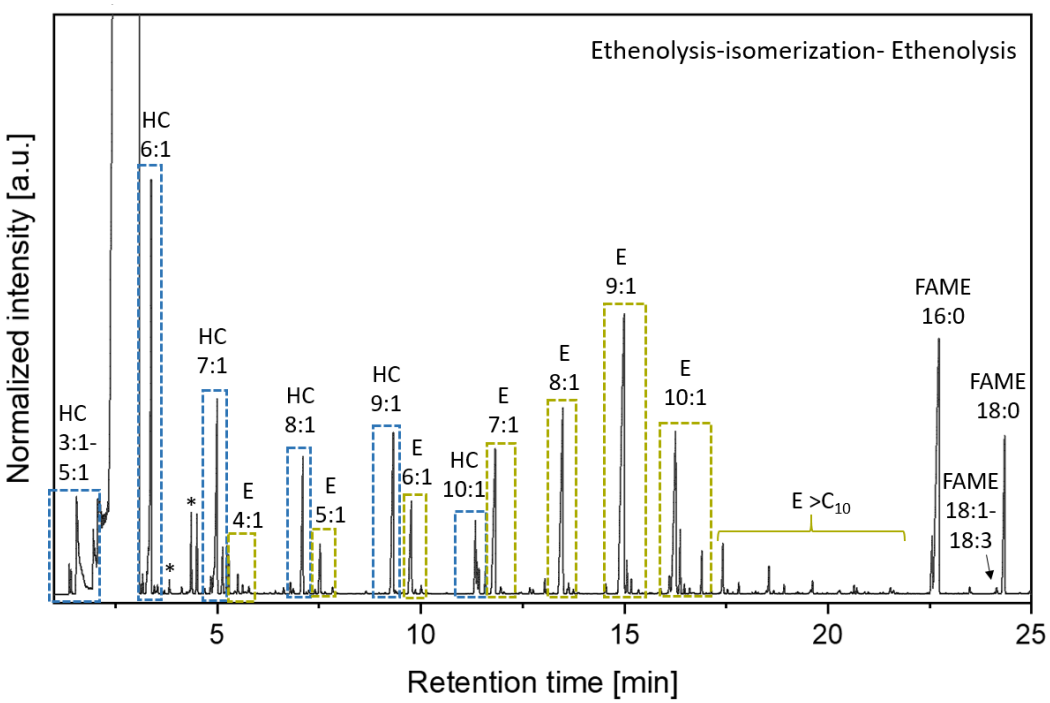

Figure 6.6 Typical gas chromatogram of transesterified soybean oil after the tandem process.

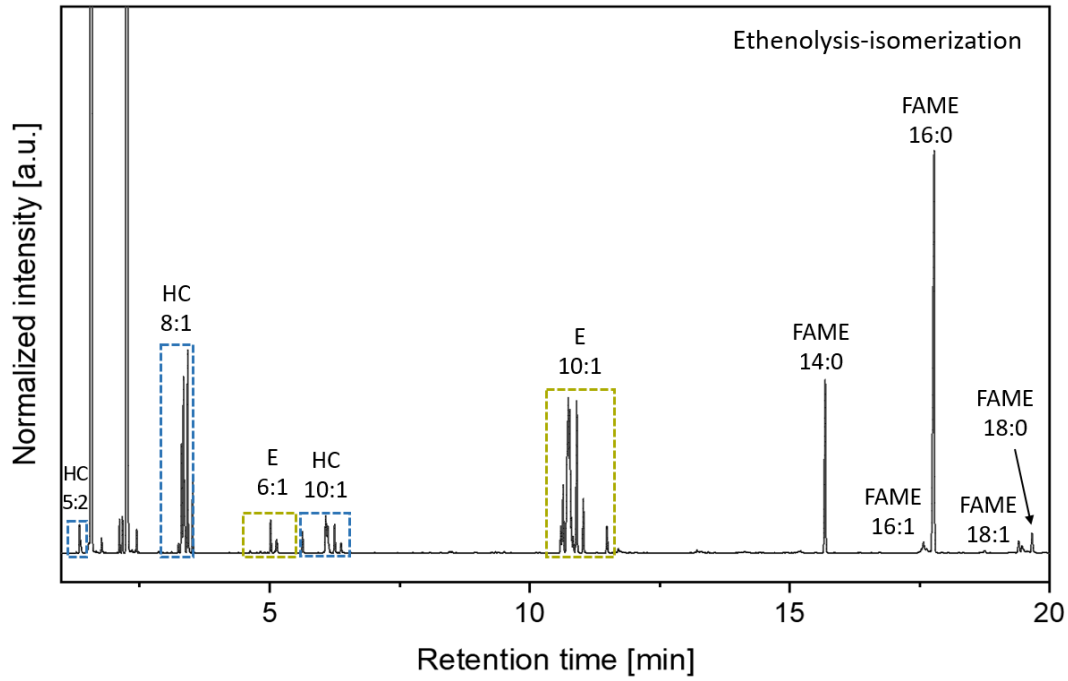

Figure 6.6 Typical gas chromatogram of transesterified microalgae oil after ethenolysis and isomerization.

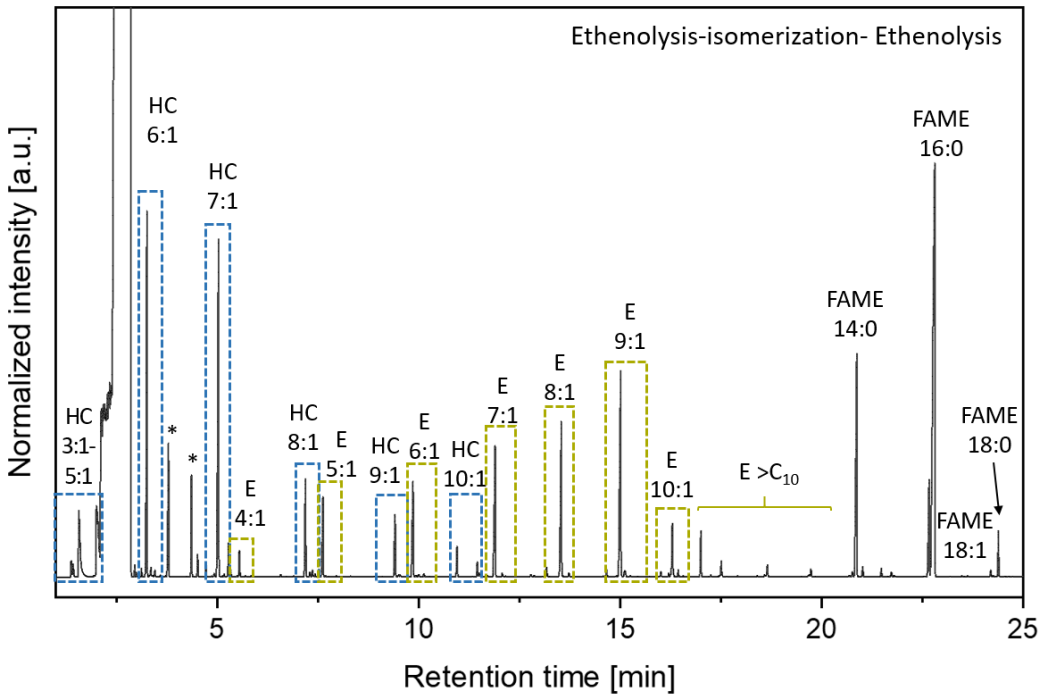

Figure 6.7 Typical gas chromatogram of transesterified microalgae oil after the tandem process.

Table 6.1 Obtained decene and methyl decenoate isomer distribution from isomerization with [(dabpx)Pd(OPFBS)$_2$] in supercritical carbon dioxide (500 bar, 85 °C, 3 bar ethylene) and reference values for isomerization in methanol.[151]

	Positional Isomers of decene and methyl decenoate							
Decene	1	2	3	4	5			
MeOH NMR [mol%]	0.18 ± 0.03	26.49 ± 3.74	26.11 ±3.69	32.16 ± 4.55	15.04 ± 2.13			
CO_2 NMR [mol%]	0.19 ± 0.02	25.63 ± 3.62	22.64 ± 3.20	36.48 ± 5.16	15.06 ± 2.13			
Methyl decenoate	2	3	4	5	6	7	8	9
MeOH NMR [mol%]	12.02± 1.69	5.05 ± 0.71	11.17 ± 1.58	14.18 ± 2.00	18.75 ± 2.65	20.19 ± 2.85	18.51 ± 2.62	0.12± 0.02
CO_2 NMR [mol%]	7.07± 1.00	2.26± 0.32	10.74± 1.52	16.83± 2.38	20.08± 2.84	20.86± 2.95	22.07± 3.12	0.07± 0.01

Reaction conditions in $scCO_2$: 3 mmol 1-decene substrate, 3 mmol methyl dec-9-enoate substrate, V_{DCM} = 5.9 mL, V_{MeOH} = 0.1 mL, p_{total} = 500 bar CO_2, $p_{ethylene}$ = 3 bar, 0.4 mol % [(dabpx)Pd(OPFBS)$_2$] per double bond, 85 °C, t = 48 h. Reaction conditions in methanol: 3 mmol substrate, 6 mL MeOH, 0.4 mol % [(dtbpx)Pd(OTf)$_2$] per double bond, 85 °C, 48 h. Errors given assuming an error of 10 % in ^{13}C NMR integration.

Table 6.2 Obtained isomer distributions for heptene (HC 7:1), octene (HC 8:1) and methyl hexenoate (E 6:1) after isomerization in MeOH and supercritical carbon dioxide for the calculation of the theoretical product distribution and the theoretical amounts of HC 3:1 to HC 5:1, respectively. For butene (HC 4:1) an isomer distribution is assumed as described in literature.[151, 155]

Heptene	**Positional Isomers**		
	1	**2**	**3**
MeOH exp. NMR [mol%]	0.42 ± 0.04	54.24 ± 5.37	45.33 ± 4.49
CO_2 exp. NMR [mol%]	1.56 ± 0.15	53.13 ± 5.23	45.31 ± 4.49
Octene	**1**	**2**	**3**	**4**
MeOH exp. NMR [mol%]	0.28 ± 0.03	40.51 ± 4.01	33.71 ± 3.34	25.50 ± 2.52
CO_2 exp. NMR [mol%]	0.29 ± 0.03	39.24 ± 3.88	36.04 ± 3.57	24.42 ± 2.42
Methyl hexenoate	**2**	**3**	**4**	**5**
MeOH exp. NMR [mol%]	47.39 ± 4.69	13.32 ± 1.22	39.81 ± 3.94	0.47 ± 0.05
CO_2 exp. NMR [mol%]	42.91 ± 4.25	13.37 ± 1.36	42.92 ± 4.25	0.43 ± 0.04

Reaction conditions in methanol: 3 mmol terminal olefin substrate, 6 mL MeOH, 0.4 mol % [(dtbpx)Pd(OTf)$_2$] per double bond, 85 °C, 48 h. Reaction conditions in scCO_2: 3 mmol pure isomer, V_{DCM} = 5.9 mL, V_{MeOH} = 0.1 mL, p_{total} = 500 bar CO_2, $p_{ethylene}$ = 3 bar, 0.4 mol % [(dtbpx)Pd(OTf)$_2$] per double bond, 85 °C, t = 48 h.

Table 6.3 Values for isomers obtained after isomerization in the sequential conversion of several substrates in $scCO_2$ as well as of single reference compounds in equilibrium at 85 °C.

Substrate	Isomers				
	1-decene	methyl 2-decenoate	1-octene	1-heptene	Methyl 2 hexenoate
Single reference compound isomerized at 85°C in MeOH	0.18	12.02	0.28	0.42	47.4
HOSO[1]	0.76	10.9	-	-	-
Olive oil[1]	2	3.7	3.4	1	
Soybean oil[2]	17.3	1.23	-	14.18	-
Waste oil[1]	1	1.92	-	-	-
Artificial microalgae oil[2]	1	3.4	1.47	-	38.07
Extracted Sunflower oil[1]	0.2	6.9	-	-	-
Extracted olive oil[1]	3.1	1.66	3.2	1.8	-
Extracted microalgae oil[2]	8.5	1.46	7.8	-	16.5

Reaction conditions: (1) ethenolysis 0.06 mol% of **UC**, 55°C, 3 bar ethylene, p_{total} = 250 bar, 6 mL of DCM, V_{total} = 100 mL, 24 h; (2) isomerization 0.4 mol% of $[(dtbpx)Pd(OTf)_2]$ per double bond, 85 °C, p_{total} = 500 bar, 5.9 mL of DCM, 0.1 mL of MeOH, V_{total} = 100 mL, [1] 24 h, [2] 48 h.

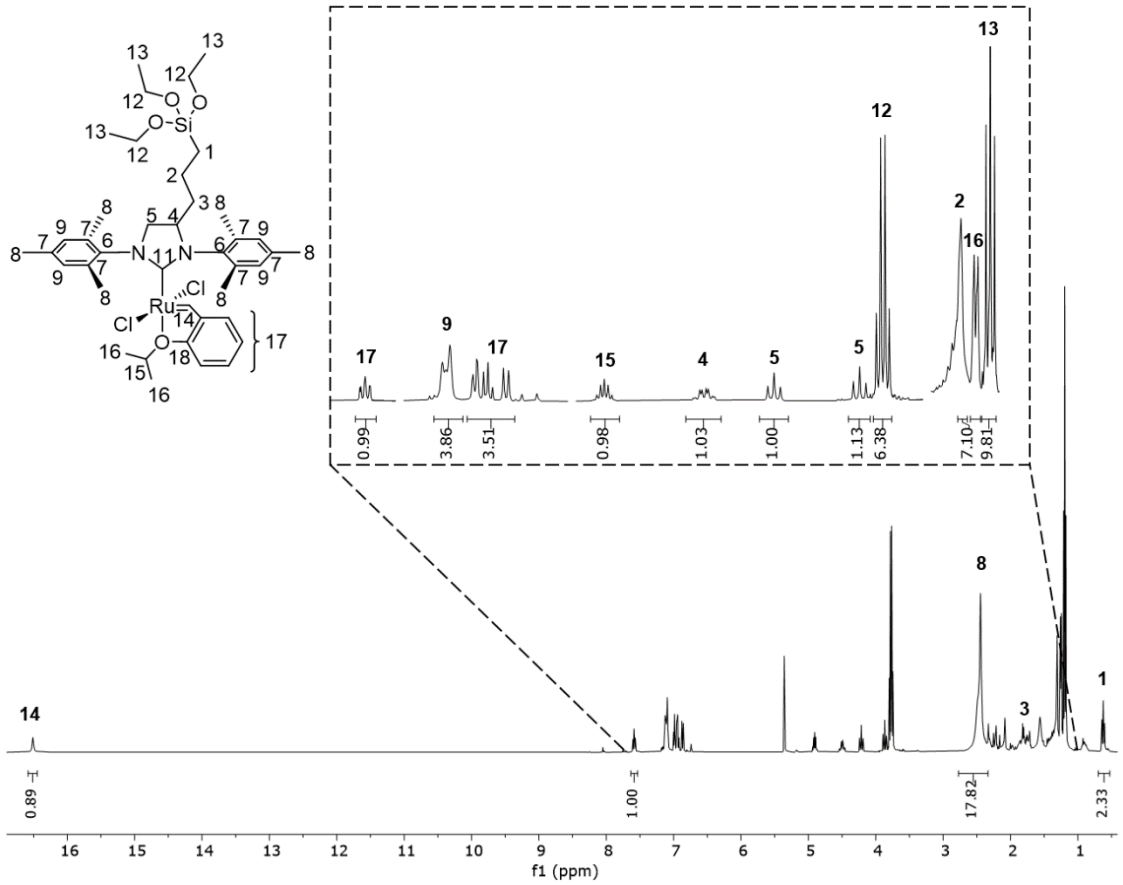

Figure 6.8 ^{1}H NMR spectrum (CD_2Cl_2, 400 MHz, 25 °C) of [$RuCl_2$ (1,3-dimesityl-4-(3-triethoxy silyl) propyl)-dihydro-imidazol-2-ylidene) (=CH–o- ^{i}PrO–Ph)] (**8**).

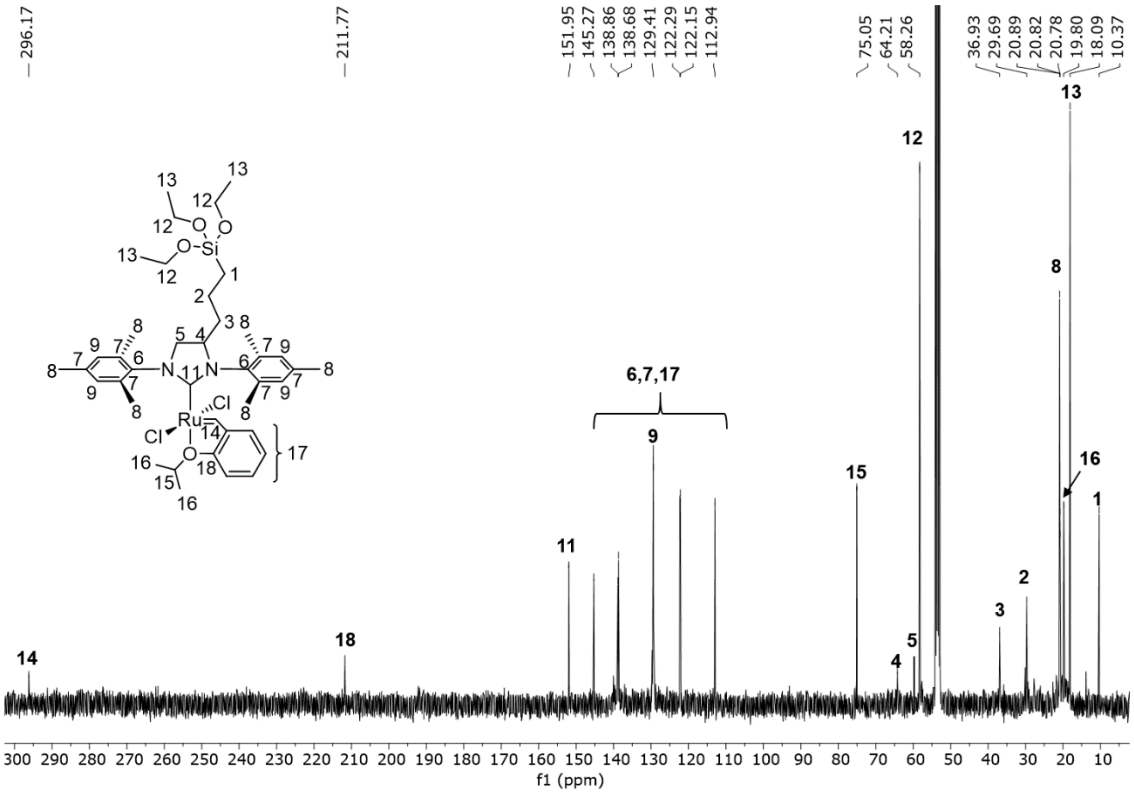

Figure 6.9 ^{13}C-NMR (100 MHz, CD_2Cl_2, 25 °C) spectrum of [$RuCl_2$ (1,3-dimesityl-4-(3-triethoxy silyl) propyl)-dihydro-imidazol-2-ylidene) (=CH–o- ^{i}PrO–Ph)] (**8**).

7 REFERENCES

[1] Aravanis A. M., Goodall B. L., Mendez, M., Pyle J. L., Moreno J. E., Methods and systems for biofuel production. US 2010/0297749 A1, 2010/04/19, (2010).

[2] Chisti, Y. Biodiesel from microalgae. *Biotechnol. Ad.* **25**, 294-306, (2007).

[3] UFOP. Report on global market supply 2020/2021 (2021).

[4] Roesle, P. *et al.* Mechanistic features of isomerizing alkoxycarbonylation of methyl oleate. *J. Am. Chem. Soc.* **134**, 17696-17703, (2012).

[5] Chikkali, S. & Mecking, S. Refining of plant oils to chemicals by olefin metathesis. *Angew. Chem. Int. Ed.***51**, 5802-5808 (2012).

[6] Alves, A. Q. *et al.* The fatty acid composition of vegetable oils and their potential use in wound Care. *Adv. Skin Wound Care* **32**, 1-8, (2019).

[7] Ackman, R. G., Retson, M. E., Gallay, L. R. & Vandenheuvel, F. A. Ozonolysis if unsaturated fatty acids. *Can. J. Chem.* **39**, 1956-1963, (1961).

[8] Cohen, S. A. Elevance Biorefinery Pilot Plant, Newton, IA. (United States, 2017).

[9] FAO and UNEP. 2007. The State of Food and Agriculture: Food and Agriculture Organization New York, NY, USA.

[10] Arca, M. *et al.*, *J. Am. Oil Chem. Soc.*, **89**, 987-994, Exhibit 1058 in Syntroleum v. Neste IPR2013-00178, (2012).

[11] Yongmanitchai, W. & Ward, O. P. Growth of and omega-3 fatty acid production by Phaeodactylum tricornutum under different culture conditions. *Applied and Environmental Microbiology* **57**, 419-425, (1991).

[12] Metting, F. B. Biodiversity and application of microalgae. *J. Ind. Microbiol.* **17**, 477-489, (1996).

[13] Hess, S. K., Lepetit, B., Kroth, P. G. & Mecking, S. Production of chemicals from microalgae lipids – status and perspectives. . *Eur. J. Lipid Sci. Technol.* **120**, 1700152, (2018).

[14] Halim, R., Danquah, M. K. & Webley, P. A. Extraction of oil from microalgae for biodiesel production: A review. *Biotechnol. Adv.* **30**, 709-732, (2012).

[15] Mata, T. M., Martins, A. A. & Caetano, N. S. Microalgae for biodiesel production and other applications: A review. *Renew. Sust. Energ. Rev.* **14**, 217-232, (2010).

[16] Aravanis, A. M. Goodall, B. L., Mendez M., Pyle, L. L., Moreno, J. E. US2010/0297749 A1, Sapphire Engergy (2010).

[17] Ratledge, C. Microbial oils: an introductory overview of current status and future prospects. *OCL* **20**, D602 (2013).

[18] Usui, N. & Ikenouchi, M. The biological CO_2 fixation and utilization project by RITE(1) - Highly-effective photobioreactor system. *Energy Convers. Manage.* **38**, 487-S492, (1997).

[19] Tonon, T., Harvey, D., Larson, T. R. & Graham, I. A. Long chain polyunsaturated fatty acid production and partitioning to triacylglycerols in four microalgae. *Phytochemistry* **61**, 15-24, (2002).

[20] Zimmerer, J., Pingen, D., Hess, S. K., Koengeter, T. & Mecking, S. Integrated extraction and catalytic upgrading of microalgae lipids in supercritical carbon dioxide. *Green Chem.* **21**, 2428-2435, (2019).

[21] Daboussi, F. *et al.* Genome engineering empowers the diatom Phaeodactylum tricornutum for biotechnology. *Nat. Commun.* **5**, 3831, (2014).

[22] Xue, J. *et al.* Genetic improvement of the microalga Phaeodactylum tricornutum for boosting neutral lipid accumulation. *Metab. Eng.* **27**, 1-9, (2015).

[23] Hamilton, M. L., Haslam, R. P., Napier, J. A. & Sayanova, O. Metabolic engineering of Phaeodactylum tricornutum for the enhanced accumulation of omega-3 long chain polyunsaturated fatty acids. *Metab. Eng.* **22**, 3-9, (2014).

[24] Bowler, C. *et al.* The Phaeodactylum genome reveals the evolutionary history of diatom genomes. *Nature* **456**, 239-244, (2008).

[25] K. Chojnacka, F.J. Marquez-RochaKinetic and stoichiometric relationships of the energy and carbon metabolism in the culture of microalgae. *Biotechnology* **3** , 21-34, (2004)

[26] Gouveia, L., Marques, A. E., da Silva, T. L. & Reis, A. Neochloris oleabundans UTEX #1185: a suitable renewable lipid source for biofuel production. *J. Ind. Microbiol. Biotech.* **36**, 821-826, (2009).

[27] Illman, A. M., Scragg, A. H. & Shales, S. W. Increase in Chlorella strains calorific values when grown in low nitrogen medium. *Enzyme Microb. Technol.* **27**, 631-635, (2000).

[28] Huang, G., Chen, F., Wei, D., Zhang, X. & Chen, G. Biodiesel production by microalgal biotechnology. *Appl. Energy* **87**, 38-46, (2010).

[29] Rosello Sastre, R. & Posten, C. Die vielfältige Anwendung von Mikroalgen als nachwachsende Rohstoffe. *Chem. Ing. Tech.* **82**, 1925-1939, (2010).

[30] Brennan, L. & Owende, P. Biofuels from microalgae—A review of technologies for production, processing, and extractions of biofuels and co-products. *Renew. Sust. Energ. Rev.* **14**, 557-577, (2010).

[31] Pulz, O. Photobioreactors: production systems for phototrophic microorganisms. *Appl. Microbiol. Biotech.* **57**, 287-293, (2001).

[32] Wijffels, R. H. & Barbosa, M. J. An outlook on microalgal biofuels. *Science* **329**, 796-799, (2010).

[33] Dassey, A. J. & Theegala, C. S. Harvesting economics and strategies using centrifugation for cost effective separation of microalgae cells for biodiesel applications. *Bioresour. Technol.* **128**, 241-245, (2013).

[34] Folch, J., Ascoli, I., Lees, M., Meath, J. A. & Le, B. N. Preparation of lipide extracts from brain tissue. *J. Biol. Chem.* **191**, 833-841 (1951).

[35] Bligh, E. G. & Dyer, W. J. A rapid method of total lipid extraction and purification. *Can. J. Biochem. Physiol.* **37**, 911-917, (1959).

[36] Dakubu, S. Cell inactivation by ultrasound. *Biotechno.l Bioeng.* **18**, 465-471, (1976).

[37] Chisti, Y.; Moo-Young, M., Disruption of microbial cells for intracellular products. *Enzyme Microb. Technol.* **8**, 194-204 (1986).

[38] Lorenzen, J. *et al.* Extraction of microalgae derived lipids with supercritical carbon dioxide in an industrial relevant pilot plant. *Bioprocess Biosyst. Eng.* **40**, 911-918, (2017).

[39] Aliev, A. M. & Abdulagatov, I. M. The study of microalgae Nannochloropsis salina fatty acid composition of the extracts using different techniques. SCF vs conventional extraction. *J. Mol. Liq.* **239**, 96-100, (2017).

[40] Mendes, R. L. *et al.* Supercritical CO_2 extraction of carotenoids and other lipids from Chlorella vulgaris. *Food Chem.* **53**, 99-103, (1995).

[41] Jenkins, R. W. *et al.* Cross-Metathesis of Microbial Oils for the Production of Advanced Biofuels and Chemicals. *ACS Sustainable Chem. Eng.* **3**, 1526-1535, (2015).

[42] Philipp, R. *et al.* Synthetic Polyester from Algae Oil. *Angew. Chem. Int. Ed.* **53**, 6800-6804, (2014).

[43] Pingen, D., Klinkenberg, N. & Mecking, S. Single-Step Catalytic Upgrading of Microalgae Biomass. *ACS Sustainable Chem. Eng.* **6**, 11219-11221, (2018).

[44] Hess, S. K. *et al.* Valorization of Unconventional Lipids from Microalgae or Tall Oil via a Selective Dual Catalysis One-Pot Approach. *J. Am. Chem. Soc.* **139**, 13487-13491, (2017).

[45] Nelson, D. J., Manzini, S., Urbina-Blanco, C. A. & Nolan, S. P. Key processes in ruthenium-catalysed olefin metathesis. *Chem. Commun*. **50**, 10355-10375, (2014).

[46] Rouhi, A. M. *Chem. Eng. News*, **80**, 34-38 (2002).

[47] Hérisson, P. J. L. & Chauvin, Y. Catalyse de transformation des oléfines par les complexes du tungstène. II. Télomérisation des oléfines cycliques en présence d'oléfines acycliques. *Macromol. Chem. Phys.* **141**, 161-176 (1971).

[48] Van Dam, P. B., Mittelmeijer, M. C. & Boelhouwer, C. Metathesis of unsaturated fatty acid esters by a homogeneous tungsten hexachloride-tetramethyltin catalyst. *J. Chem. Soc., Chem. Commun.*, **22**, 1221-1222 (1972).

[49] Schaverien, C. J., Dewan, J. C. & Schrock, R. R. Multiple metal-carbon bonds. 43. Well-characterized, highly active, Lewis acid free olefin metathesis catalysts. *J. Am. Chem. Soc.* **108**, 2771-2773, (1986).

[50] H., G. R. Olefin-Metathesis Catalysts for the Preparation of Molecules and Materials (Nobel Lecture). *Angew. Chem. Int. Ed.* **45**, 3760-3765, (2006).

[51] Vougioukalakis, G. C. & Grubbs, R. H. Ruthenium-Based Heterocyclic Carbene-Coordinated Olefin Metathesis Catalysts. *Chem. Rev.* **110**, 1746-1787, (2010).

[52] Dinger, M. B. & Mol, J. C. High Turnover Numbers with Ruthenium-Based Metathesis Catalysts. *Adv. Syn. & Catal.* **344**, 671-677 (2002).

[53] Rybak, A. & Meier, M. A. R. Cross-metathesis of oleyl alcohol with methyl acrylate: optimization of reaction conditions and comparison of their environmental impact. *Green Chem.* **10**, 1099-1104, (2008).

[54] Miao, X. et al. Alkylidene-Ruthenium-Tin Catalysts for the Formation of Fatty Nitriles and Esters via Cross-Metathesis of Plant Oil Derivatives. *Organometallics* **29**, 5257-5262, (2010).

[55] Malacea, R. *et al.* Renewable materials as precursors of linear nitrile-acid derivatives via cross-metathesis of fatty esters and acids with acrylonitrile and fumaronitrile. *Green Chem.* **11**, 152-155, (2009).

[56] Schrodi, Y. *et al.* Ruthenium Olefin Metathesis Catalysts for the Ethenolysis of Renewable Feedstocks. *Clean* **36**, 669-673, (2008).

[57] Ngo, H. L., Jones, K. & Foglia, T. A. Metathesis of unsaturated fatty acids: Synthesis of long-chain unsaturated-α,ω-dicarboxylic acids. *J. Am. Oil Chem. Soc.* **83**, 629-634, (2006).

[58] Mol, J. C. Metathesis in Oleochemistry. *Braz. Chem. Soc.* **9**, 1 (1998).

[59] Marx, V. M. *et al.* Cyclic Alkyl Amino Carbene (CAAC) Ruthenium Complexes as Remarkably Active Catalysts for Ethenolysis. *Angew. Chem. Int. Ed.* **54**, 1919-1923, (2015).

[60] Burdett, K. A. *et al.* Renewable Monomer Feedstocks via Olefin Metathesis: Fundamental Mechanistic Studies of Methyl Oleate Ethenolysis with the First-Generation Grubbs Catalyst. *Organometallics* **23**, 2027-2047, (2004).

[61] Ulman, M. & Grubbs, R. H. Ruthenium Carbene-Based Olefin Metathesis Initiators: Catalyst Decomposition and Longevity. *J. Org. Chem.* **64**, 7202-7207, (1999).

[62] Marinescu, S. C., Schrock, R. R., Müller, P. & Hoveyda, A. H. Ethenolysis Reactions Catalyzed by Imido Alkylidene Monoaryloxide Monopyrrolide (MAP) Complexes of Molybdenum. *J. Am. Chem. Soc.* **131**, 10840-10841, (2009).

[63] Nickel, A. *et al.* A Highly Efficient Olefin Metathesis Process for the Synthesis of Terminal Alkenes from Fatty Acid Esters. *Top. Catal.* **55**, 518-523, (2012).

[64] Gawin, R., Kozakiewicz, A., Guńka, P. A., Dąbrowski, P. & Skowerski, K. Bis(Cyclic Alkyl Amino Carbene) Ruthenium Complexes: A Versatile, Highly Efficient Tool for Olefin Metathesis. *Angew. Chem. Int. Ed.* **56**, 981-986, (2017).

[65] Malacea, R. *et al.* Renewable materials as precursors of linear nitrile-acid derivatives via cross-metathesis of fatty esters and acids with acrylonitrile and fumaronitrile. *Green Chem.* **11**, 152-155, (2009).

[66] Miao, X., Malacea, R., Fischmeister, C., Bruneau, C. & Dixneuf, P. H. Ruthenium-alkylidene catalysed cross-metathesis of fatty acid derivatives with acrylonitrile and methyl acrylate: a key step toward long-chain bifunctional and amino acid compounds. *Green Chem.* **13**, 2911-2919, (2011).

[67] Rybak, A. & Meier, M. A. R. Cross-metathesis of fatty acid derivatives with methyl acrylate: renewable raw materials for the chemical industry. *Green Chem.* **9**, 1356-1361, (2007).

[68] Jacobs, T., Rybak, A. & Meier, M. A. R. Cross-metathesis reactions of allyl chloride with fatty acid methyl esters: Efficient synthesis of α,ω-difunctional chemical intermediates from renewable raw materials. *Appl. Catal. A* **353**, 32-35, (2009).

[69] Behr, A., Westfechtel, A. *Chem. Ing. Technol.* **79** 621–636 (2007).

[70] Witt, T., Häußler, M., Kulpa, S. & Mecking, S. Chain Multiplication of Fatty Acids to Precise Telechelic Polyethylene. *Angew. Chem. Int. Ed.* **56**, 7589-7594, (2017).

[71] Mol, J. C. Industrial applications of olefin metathesis. J. Mol. Cat. A **213**, 39-45, (2004).

[72] Cohen, S. A. Elevance Biorefinery Pilot Plant, Newton, IA. (United States, 2017).

[73] Fogg, D. E. & dos Santos, E. N. Tandem catalysis: a taxonomy and illustrative review. *Coord. Chem. Rev.* **248**, 2365-2379, (2004).

[74] Louie, J., Bielawski, C. W. & Grubbs, R. H. Tandem Catalysis: The Sequential Mediation of Olefin Metathesis, Hydrogenation, and Hydrogen Transfer with Single-Component Ru Complexes. *J. Am. Chem. Soc* .**123**, 11312-11313, (2001).

[75] Bielawski, C. W., Louie, J. & Grubbs, R. H. Tandem Catalysis: Three Mechanistically Distinct Reactions from a Single Ruthenium Complex. *J. Am. Chem. Soc.* **122**, 12872-12873, (2000).

[76] Lutz, E. F. Shell higher olefins process. *J. Chem. Ed.* **63**, 202, (1986).

[77] Freitas, R., & Gum, C.R. *Chem. Eng. Prog.* **75**, 73 (1979).

[78] Ferreira, L. A., Sokolovicz, Y. C. A., Couto, J. L. & Schrekker, H. S. Tandem olefin isomerization/metathesis and volatiles capture: Accessing light olefin blends and broadening the scope to higher olefins. *Mol. Catal.* **460**, 36-39, (2018).

[79] Ohlmann, D. M. *et al.* Isomerizing Olefin Metathesis as a Strategy To Access Defined Distributions of Unsaturated Compounds from Fatty Acids. *J. Am. Chem. Soc.* **134**, 13716-13729 (2012).

[80] Pollini, J., Pankau, W. M. & Gooßen, L. J. Isomerizing Olefin Metathesis. *Chem. Eur. J.* **25**, 7416-7425, (2019).

[81] Porri, L.; Diversi., P.; Lucherini, A.; Rossi, R. *Makromol. Chem.* **176**, 3121–3125 (1975).

[82] France, M. B., Feldman, J. & Grubbs, R. H. An iridium-based catalyst system for metathesis/isomerization of acyclic olefins, including methyl oleate. *Chem. Commun.* 1307-1308, (1994).

[83] Consorti, C. S., Aydos, G. L. P. & Dupont, J. Tandem isomerisation–metathesis catalytic processes of linear olefins in ionic liquid biphasic system. *Chem. Commun.* **46**, 9058-9060, (2010).

[84] Mamone, P., Grünberg, M. F., Fromm, A., Khan, B. A. & Gooßen, L. J. [Pd(μ-Br)(PtBu3)]2 as a Highly Active Isomerization Catalyst: Synthesis of Enol Esters from Allylic Esters. *Org. Lett.***14**, 3716-3719, (2012).

[85]Pfister, K. F., Baader, S., Baader, M., Berndt, S. & Goossen, L. J. Biofuel by isomerizing metathesis of rapeseed oil esters with (bio)ethylene for use in contemporary diesel engines. *Sci. Adv.* **3**, (2017).

[86] Yu, M. *et al.* Synthesis of macrocyclic natural products by catalyst-controlled stereoselective ring-closing metathesis. *Nature* **479**, 88-93, (2011).

[87] Wallace, D. J. *et al.* A double ring closing metathesis reaction in the rapid, enantioselective synthesis of NK-1 receptor antagonists. *Org. Lett.* **3**, 671-674, (2001).

[88] Pugh, C. & Schrock, R. R. Synthesis of side-chain liquid crystal polymers by living ring-opening metathesis polymerization. 3. Influence of molecular weight, interconnecting unit, and substituent on the mesomorphic behavior of polymers with laterally attached mesogens. *Macromolecules* **25**, 6593-6604, (1992).

[89] Hafner, A., Mühlebach, A. & van der Schaaf, P. A. One-Component Catalysts for Thermal and Photoinduced Ring Opening Metathesis Polymerization. *Angew. Chem. Int. Ed.* **36**, 2121-2124, (1997).

[90] Hoveyda, A. H., Malcolmson, S. J., Meek, S. J. & Zhugralin, A. R. Catalytic Enantioselective Olefin Metathesis in Natural Product Synthesis. Chiral Metal-Based Complexes that Deliver High Enantioselectivity and More. *Angew. Chem. Int. Ed.* **49**, 34-44, (2010).

[91] Jas, G. & Kirschning, A. Continuous Flow Techniques in Organic Synthesis. *Chem. Eur. J.* **9**, 5708-5723, (2003).

[92] Kirschning, A. *et al.* Homo- and heterogeneous Ru-based metathesis catalysts in cross-metathesis of 15-allylestrone—towards 17β-hydroxysteroid dehydrogenase type 1 inhibitors. *Tetrahedron Lett.* **49**, 3019-3022, (2008).

[93] Schürer, S. C., Gessler, S., Buschmann, N. & Blechert, S. Synthesis and Application of a Permanently Immobilized Olefin-Metathesis Catalyst. *Angew. Chem. In.t Ed.* **39**, 3898-3901, (2000).

[94] Zaman, S. & Abell, A. D. A robust and recyclable ruthenium catalyst immobilised on polyethylene glycol. *Tetrahedron Lett.* **50**, 5340-5343, (2009).

[95] Elias, X., Pleixats, R. & Wong Chi Man, M. Hybrid silica materials derived from Hoveyda–Grubbs ruthenium carbenes. Electronic effects of the nitro group on the activity and recyclability as diene and enyne metathesis catalysts. *Tetrahedron* **64**, 6770-6781, (2008).

[96] Lim, J., Seong Lee, S. & Ying, J. Y. Mesoporous silica-supported catalysts for metathesis: application to a circulating flow reactor. *Chem. Commun.* **46**, (2010).

[97] Krause, J. O., Lubbad, S., Nuyken, O. & Buchmeiser, M. R. Monolith- and Silica-Supported Carboxylate-Based Grubbs–Herrmann-Type Metathesis Catalysts. *Adv. Synth. Catal.* **345**, 996-1004, (2003).

[98] Chabanas, M., Copéret, C. & Basset, J.-M. Re-Based Heterogeneous Catalysts for Olefin Metathesis Prepared by Surface Organometallic Chemistry: Reactivity and Selectivity. *Chem. Eur. J.* **9**, 971-975, (2003).

[99] Alothman, ZA Review: Fundamental Aspects of Silicate Mesoporous Materials. *Materials* **5**, 2874-2902 (2012).

[100] Liang, L.; Jian-lin, S., A Highly Active and Reusable Heterogeneous Ruthenium Catalyst for Olefin Metathesis. *Adv. Synth. Catal.* **347** , 1745-1749 (2005).

[101] Dewaele, A.; Van Berlo, B.; Dijkmans, J.; Jacobs, P. A.; Sels, B. F., Immobilized Grubbs catalysts on mesoporous silica materials: insight into support characteristics and their impact on catalytic activity and product selectivity. *Catal. Sci. Technol*, **6**, 2580-2597, (2016).

[102] Yasmin, T.; Müller, K., Synthesis and surface modification of mesoporous mcm-41 silica materials. *J. Chromatogr.*, **1217**, 3362-3374, (2010).

[103] Dewaele, A.; Van Berlo, B.; Dijkmans, J.; Jacobs, P. A.; Sels, B. F., Immobilized Grubbs catalysts on mesoporous silica materials: insight into support characteristics and their impact on catalytic activity and product selectivity. *Catal. Sci. Technol*, **6**, 2580-2597, (2016).

[104] Allen, D. P., Van Wingerden, M. M. & Grubbs, R. H. Well-Defined Silica-Supported Olefin Metathesis Catalysts. *Organic Lett.* **11**, 1261-1264, (2009).

[105] Van Berlo, B., Houthoofd, K., Sels, B. F. & Jacobs, P. A. *Adv. Synth. Catal.* **350**, 1949-1953, (2008).

[106] Yang, H.; Ma, Z.; Wang, Y.; Wang, Y.; Fang, L., Hoveyda-Grubbs catalyst confined in the nanocages of SBA-1: enhanced recyclability for olefin metathesis. *Chem. Commun.*, **46**, 8659-8661, (2010).

[107] Dewaele, A., Van Berlo, B., Dijkmans, J., Jacobs, P. A. & Sels, B. F. Immobilized Grubbs catalysts on mesoporous silica materials: insight into support characteristics and their impact on catalytic activity and product selectivity. *Catal. Sci. Technol.* **6**, 2580-2597, (2016).

[108] Balcar, H., Shinde, T., Žilková, N. & Bastl, Z. Hoveyda–Grubbs type metathesis catalyst immobilized on mesoporous molecular sieves MCM-41 and SBA-15. *Beilstein J. Org. Chem.* 7, 22-28, (2011).

[109] Kingsbury, J. S. *et al.* Immobilization of Olefin Metathesis Catalysts on Monolithic Sol–Gel: Practical, Efficient, and Easily Recyclable Catalysts for Organic and Combinatorial Synthesis. *Angew. Chem., Int. Ed.* **40**, 4251-4256, (2001).

[110] Fischer, D. & Blechert, S. Highly Active Silica Gel-Supported Metathesis (Pre)Catalysts. *Synfacts* **2005**, 0216-0216 (2005).

[111] Xavier, E., Roser, P., Chi, M. M. W. & E., M. J. J. Hybrid-Bridged Silsesquioxane as Recyclable Metathesis Catalyst Derived from a Bis-Silylated Hoveyda-Type Ligand. *Adv. Synth. Catal.* **348**, 751-762, (2006).

[112] Hoveyda, A. H. *et al.* Ru complexes bearing bidentate carbenes: from innocent curiosity to uniquely effective catalysts for olefin metathesis. *Org. Biomol. Chem.* **2**, 8-23, (2004).

[113] Kingsbury, J. S., Harrity, J. P. A., Bonitatebus, P. J. & Hoveyda, A. H. A Recyclable Ru-Based Metathesis Catalyst. *J Am. Chem. Soc.* **121**, 791-799, (1999).

[114] Marciniec, B., Rogalski, S., Potrzebowski, M. J. & Pietraszuk, C. Ruthenium Carbene Siloxide Complexes Immobilized on Silica: Synthesis and Catalytic Activity in Olefin Metathesis. *ChemCatChem.* **3**, 904-910, (2011).

[115] Bek, D., Žilková, N., Dědeček, J., Sedláček, J. & Balcar, H. SBA-15 Immobilized Ruthenium Carbenes as Catalysts for Ring Closing Metathesis and Ring Opening Metathesis Polymerization. *Top. Catal.* **53**, 200-209, (2010).

[116] Thomas, W., J., K. F., Wolfgang, H., Dieter, G. & A., H. W. Highly Active Ruthenium Catalysts for Olefin Metathesis: The Synergy of N-Heterocyclic Carbenes and Coordinatively Labile Ligands. *Angew. Chem. Int. Ed.* **38**, 2416-2419, (1999).

[117] Monge-Marcet, A., Pleixats, R., Cattoën, X. & Wong Chi Man, M. Sol–gel immobilized Hoveyda–Grubbs complex through the NHC ligand: A recyclable metathesis catalyst. *J. Mol. Catal. Chem.* **357**, 59-66, (2012).

[118] Monge-Marcet, A., Pleixats, R., Cattoën, X. & Wong Chi Man, M. Catalytic applications of recyclable silica immobilized NHC–ruthenium complexes. *Tetrahedron* **69**, 341-348, (2013).

[119] Iyad, K. *et al.* Tailored Ru-NHC Heterogeneous Catalysts for Alkene Metathesis. *Chem. Eur. J.* **15**, 11820-11823, (2009).

[120] Zelin, J., Trasarti, A. F. & Apesteguía, C. R. Self-metathesis of methyl oleate on silica-supported Hoveyda–Grubbs catalysts. *Catal. Commun.* **42**, 84-88, (2013).

[121] Nieres, P. D., Zelin, J., Trasarti, A. F. & Apesteguía, C. R. Heterogeneous catalysis for valorisation of vegetable oils via metathesis reactions: ethenolysis of methyl oleate. *Catal. Sci. Technol.* **6**, 6561-6568, (2016).

[122] Cabrera, J. *et al.* Linker-Free, Silica-Bound Olefin-Metathesis Catalysts: Applications in Heterogeneous Catalysis. *Chem. Eur. J.* **18**, 14717-14724, (2012).

[123] Cagniard de la Tour, C., Expos´e de quelques r´esultats obtenu par l'action combin´ee de lachaleur et de la compression sur certains liquides, tels que l'eau, l'alcool, l'´ether sulfurique et l'essence de p´etrole rectifi´ee, *Ann. Chim. Phys*. **21**, 127-132, (1822).

[124] Plotted with data from Angus, S.; Armstrong, B.; de Reuck, K.M., International Thermodynamic Tables of the Fluid State - 3 Carbon Dioxide, Pergamon, New York, 1976.

[125] Gupta RB, Shim JJ. Solubility in supercritical carbon dioxide. Boca Raton: CRC Press; 2006.

[126] Knez, Ž. Škerget, M. Phase equilibria of the vitamins D2, D3 and K3 in binary systems with CO_2 and propane. *J. Supercrit. Fluids* **20**, 131-144, (2001).

[127] Knez, Ž., Škerget, M. & Rizvi, S.H. , Separation, extraction and concentration processes in the food, beverage and nutraceutical industries, Woodhead Publishing, Cambridge (2010), pp. 3-38

[128] Capuzzo, A., Maffei, M. E. & Occhipinti, A. Supercritical Fluid Extraction of Plant Flavors and Fragrances. *Molecules* **18**, 7194-7238 (2013).

[129] Sovilj, M.N., Nikolovski, B.G. & Spasojević, M.D. *Maced. J. Chem. Chem. Eng*., **30**, 197-220 (2011).

[130] Marr, R., Gamse, T. Use of supercritical fluids for different processes including new developments-a review. *Chem. Eng. Process.* **39**, 19-28 (2000).

[131] Capuzzo A., Maffei M.E., Occhipinti A. Supercritical fluid extraction of plant flavors and fragrances. *Molecules* **18**, 194-238 (2013).

[132] Stahl, E., Quirin, K.W. & Gerard, D. Verdichtete Gase zur Exstraktion und Raffination Springer, Berlin (1987)

[133] Crampon, C.; Boutin, O.; Badens, E., Supercritical Carbon Dioxide Extraction of Molecules of Interest from Microalgae and Seaweeds. *Ind. Eng. Chem. Res.*, **50**, 8941-8953 (2011).

[134] Taylor, S.L., Eller, F.J. & King, J.W. Food Research International, comparison of oil and fat content in oilseeds and ground beef-using supercritical fluid ex traction and related analytical techniques. **30**, 365-370 (1997),

[135] Santana, A., Jesus, S., Larrayoz, M. A. & Filho, R. M. Supercritical Carbon Dioxide Extraction of Algal Lipids for the Biodiesel Production. *Procedia Engineering* **42**, 1755-1761, (2012).

[136] Machado, B. A. S., Pereira, C. G., Nunes, S. B., Padilha, F. F., Umsza-Guez, M. A., Supercritical Fluid Extraction Using CO_2: Main Applications and Future Perspectives. *Sep. Sci. Technol.*, **48**, 2741-2760 (2013).

[137] Tommasi, E. *et al.* Enhanced and Selective Lipid Extraction from the Microalga P. tricornutum by Dimethyl Carbonate and Supercritical CO2 Using Deep Eutectic Solvents and Microwaves as Pretreatment. *ACS Sustainable Chem. Eng.* **5**, 8316-8322, (2017).

[138] Mendes, R. L., Coelho, J. P., Fernandes, H. L., Marrucho, I. J., Cabral, J. M. S., Novais, J. M., Palavra, A. F., Applications of supercritical CO_2 extraction to microalgae and plants. *J . Chem. Tech. Biotechnol.*, **62**, 53-59 (1995).

[139] Mouahid, A., Crampon, C., Toudji, S.-A. A., Badens, E., Supercritical CO_2 extraction of neutral lipids from microalgae: Experiments and modelling. *J. Supercrit. Fluids*, **77**, 7-16 (2013).

[140] Zimmerer, J., Pingen, D., Hess, S. K., Koengeter, T. & Mecking, S. Integrated extraction and catalytic upgrading of microalgae lipids in supercritical carbon dioxide. *Green Chem.* **21**, 2428-2435, (2019).

[141] Mistele, C. D., Thorp, H. H. & Desimone, J. M. Ring-Opening Metathesis Polymerizations in Carbon Dioxide. J. Macromol. Sci. **33**, 953-960, (1996).

[142] Fürstner, A. *et al.* Olefin Metathesis in Supercritical Carbon Dioxide. *J. Am. Chem. Soc.* **123**, 9000-9006, (2001).

[143] Fürstner, A., Koch, D., Langemann, K., Leitner, W. & Six, C. Olefin Metathesis in Compressed Carbon Dioxide. *Angew. Chem. Int. Ed.* **36**, 2466-2469, (1997).

[144] Martín, R., Murruzzu, C., Pericàs, M. A. & Riera, A. General Approach to Glycosidase Inhibitors. Enantioselective Synthesis of Deoxymannojirimycin and Swainsonine. *J. Org. Chem.* **70**, 2325-2328, (2005).

[145] Song, J. *et al.* Effect of Phase Behavior on the Ethenolysis of Ethyl Oleate in Compressed CO_2. *The J. Phys. Chem.* B **113**, 2810-2814, (2009).

[146] de Roo, S., Einsiedler, F., Mecking, S., Catalytic Biorefining of Natural Oils to Basic Olefinic Building Blocks of Proven Chemical Valorization Schemes *Angew. Chem. Int. Ed.* **2023**, 62, e202219222.

[147] Gunstone, F.D. The Chemistry of Oils and Fats: sources, composition, properties, and uses. Blackwell Publishing, Oxford, 288 (2004).

[148] Liong, K. K., Foster, N. R. & Ting, S. S. T. Solubility of fatty acid esters in supercritical carbon dioxide. *Ind. Eng. Chem. Res.* **31**, 400-404, (1992).

[149] Nascimento, D. L. & Fogg, D. E. Origin of the Breakthrough Productivity of Ruthenium–Cyclic Alkyl Amino Carbene Catalysts in Olefin Metathesis. *J. Am. Chem. Soc.* **141**, 19236-19240, (2019).

[150] Gawin, R., Kozakiewicz, A., Guńka, P. A., Dąbrowski, P. & Skowerski, K. Bis(Cyclic Alkyl Amino Carbene) Ruthenium Complexes: A Versatile, Highly Efficient Tool for Olefin Metathesis. *Angew. Chem. Int. Ed.* **56**, 981-986 (2017).

[151] Einsiedler, F., A Biorefinery Approach to Short Chain Olefins from Plant Oils by a Multicatalytic Sequence Comprising Olefin Isomerization (doctoral dissertation), University of Konstanz.

[152] Roesle, P. *et al.* Mechanistic Features of Isomerizing Alkoxycarbonylation of Methyl Oleate. *J. Am. Chem. Soc.* **134**, 17696-17703, (2012).

[153] Trnka, T. M. et al. Synthesis and Activity of Ruthenium Alkylidene Complexes Coordinated with Phosphine and N-Heterocyclic Carbene Ligands. *J. Am. Chem. Soc.* **125**, 2546-2558, (2003).

[154] Roesle, P. The mechanism of the isomerizing alkoxycarbonylation of plant oils (doctoral dissertation), University of Konstanz, (2015).

[155] Twigg, G. H. & Rideal, E. K. The catalytic isomerization of buten-1. *Proceedings of the Royal Society of London. Series A. Math. Phys. Sci.,* **178**, 106-117 (1941)

[156] Tirado, D. F., Fuente, E. d. l. & Calvo, L. A selective extraction of hydroxytyrosol rich olive oil from alperujo. *J. Food Eng.* **263**, 409-416, (2019).

[157] Guillard, R. R. L., in Culture of Marine Invertebrate Animals: Proceedings — 1st Conference on Culture of Marine Invertebrate Animals Greenport, Springer US, Boston, MA, 29-60 (1975).

[158] Jas, G. & Kirschning, A. Continuous Flow Techniques in Organic Synthesis. *Chem. Eur. J.* **9**, 5708-5723, (2003).

[159] Krause, J. O., Lubbad, S., Nuyken, O. & Buchmeiser, M. R. Monolith- and Silica-Supported Carboxylate-Based Grubbs–Herrmann-Type Metathesis Catalysts. *Adv. Synth. & Catal.* **345**, 996-1004, (2003).

[160] Allen, D. P., Van Wingerden, M. M. & Grubbs, R. H. Well-Defined Silica-Supported Olefin Metathesis Catalysts. *Org. Lett.* **11**, (2009).

[161] Kulpa, S. Immobilized Olefin-metathesis Catalysts for the Conversion of Renewable Raw Materials (Master thesis), University of Konstanz, (2018).

[162] Bieniek, M., Michrowska, A., Gułajski, Ł. & Grela, K. A Practical Larger Scale Preparation of Second-Generation Hoveyda-Type Catalysts. *Organometallics* **26**, 1096-1099, (2007).

[163] Behr, A., Westfechtel, A. & Pérez Gomes, J. Catalytic Processes for the Technical Use of Natural Fats and Oils. *Chem. Eng. Technol.* **31**, 700-714, (2008).

[164] Rybak, A., Fokou, P. A. & Meier, M. A. R. Metathesis as a versatile tool in oleochemistry. *Eur. J. Lipid Sci. Technol.* **110**, 797-804, (2008).

[165] Mol, J. C. Metathesis of unsaturated fatty acid esters and fatty oils. *J. Mol. Catal.* **90**, 185-199, (1994).

[166] Skowerski, K., Białecki, J., Tracz, A. & Olszewski, T. K. An attempt to provide an environmentally friendly solvent selection guide for olefin metathesis. *Green Chem.* **16**, 1125-1130, (2014).

[167] Leitner, W. Supercritical Carbon Dioxide as a Green Reaction Medium for Catalysis. *Acc. Chem. Res.* **35**, 746-756, (2002).

[168] Kingsbury, J. S., Harrity, J. P. A., Bonitatebus, P. J. & Hoveyda, A. H. A Recyclable Ru-Based Metathesis Catalyst. *J. Am. Chem. Soc.* **121**, 791-799, (1999).